Photochemical Reactions of Intra- and Intermolecularly Hydrogen Bonded Compounds

Masashi IKEGAMI

A dissertation submitted to the Doctoral Program
in Chemistry, the University of Tsukuba
in partial fulfillment of the requirements
for the degree of Doctor of Philosophy in Science

January 2002

Preface

The present work is a collection of the studies during my graduate course from 1997 to 2002 at University of Tsukuba, supervised by Professor Tatsuo Arai. The main subject of this thesis is the investigation of photochemical reaction of intra- and intermolecularly hydrogen bonded compounds.

I wish to express my deep gratitude to Professor Tatsuo Arai for his guidance, encouragement, discussion and advice throughout the course of this study and for giving me many opportunities to give a talk in domestic and international conference. I am delighted to have spent my graduate course under Professor Tatsuo Arai.

I am grateful to Dr. Ritsuko Nagahata for her kind help in ESI-MS spectroscopy.

Thanks are also due to all the stuffs, guests, graduates and undergraduates of the laboratory, especially due to Dr. Kiminori Maeda, Dr. Yuji Kaneko, Dr. Yasuo Norikane, and Dr. Yanyan Yang.

Lastly, I would express my sincere gratitude to my family.

Masashi IKEGAMI

January 2002

Contents

General Introduction 1

Chapter 1

Photoisomerization of 2-(2-(2-Pyrrolyl)ethenyl)benzoxazole and 2-(2-(2-Pyrrolyl)ethenyl)benzothiazole

Abstract 14

Introduction 15

Experimental 16

Results 19

Discussion 25

Conclusion 27

References and Notes 28

Tables and Figures 30

Chapter 2

Photoinduced Intramolecular Hydrogen Atom Transfer in 2-(2-Hydroxy -phenyl)benzoxazole and 2-(2-Hydroxyphenyl)benzothiazole

Abstract 42

Introduction 43

Experimental 44

Results 45

Discussion 51

Conclusion 55

References and Notes 56

Tables and Figures 58

Chapter 3

Photochromism and Thermochromism of Hydrogen Bonded Schiff Bases

Abstract 68

Introduction 69

Experimental 70

Results 71

Discussion 74

Conclusion 76

References 77

Tables and Figures 78

Chapter 4

Photochromism of Hemiindigo Compounds Having Intramolecular Hydrogen Bonding

Abstract 94

Introduction 95

Experimental 96

Results 98

Discussion 104

Conclusion 111

References 112

Tables and Figures 114

Chapter 5

Study on Triplet State Behaviors of Pyrrole-2-carboxyaldehyde and Its Related Compounds

Abstract 127

Introduction 128

Experimental 129

Results 130

Discussion 136

Conclusion 140

References 141

Tables and Figures 143

Chapter 6

Excimer or Exciplex Formation and Energy Transfer of Aromatic Compounds Linked by Intermolecular Quadruple Hydrogen Bonding

Abstract 158

Introduction 159

Results 165

Discussion 173

Conclusion 178

Experiment 178

References 190

Tables and Figures 192

General Introduction

Hydrogen bonding plays an important role in constructing the double helical structure of DNA and highly-ordered structure of proteins.[1] In addition, hydrogen bonding is expected to be useful in constructing supramolecular structure because of its association character in directional and selective way.[2,3] Practically, the molecular systems having multiple hydrogen bond can be used as building blocks for supramolecular structure.[4-14] Furthermore, hydrogen bonding is of importance in enzymatic reaction from the point of view of the substrate specificity.[1,2] Chemical properties can also be strongly affected by hydrogen bonding.

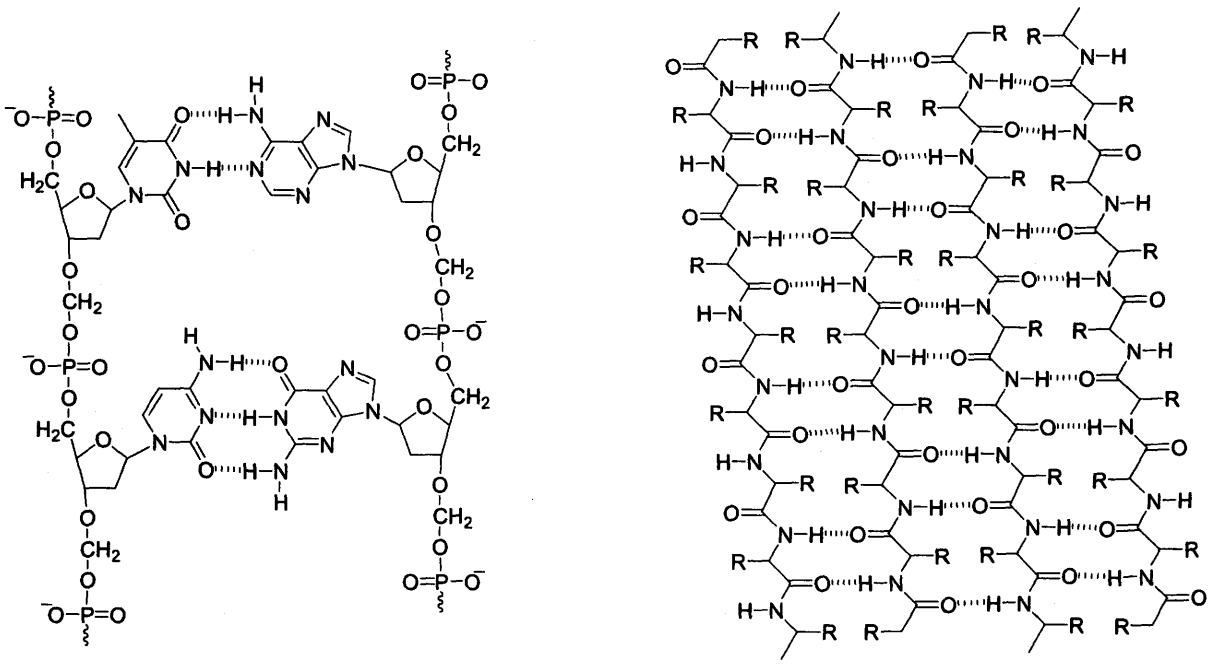

Scheme 1. The base pair of DNA (left) and β-sheet structure in protein (right).

First of all, hydrogen bonding in photodynamic therapy for jaundice of new-born infants will be discussed. Bilirubin is the degradation product of the hemoglobin and has NH group and carboxyl group capable to form hydrogen bonding. However, bilirubin can not be dissolved in water and is hydrophobic because the hydrophilic parts in bilirubin form intramolecular hydrogen bonding. Usually, bilirubin is esterified by a glucuronyl transferase enzyme in the liver to give the hydrophilic derivatives to go out. However, in case that the function of the liver of a new-born baby is underdeveloped, bilirubin is accumulated in the tissues and brings about jaundice.

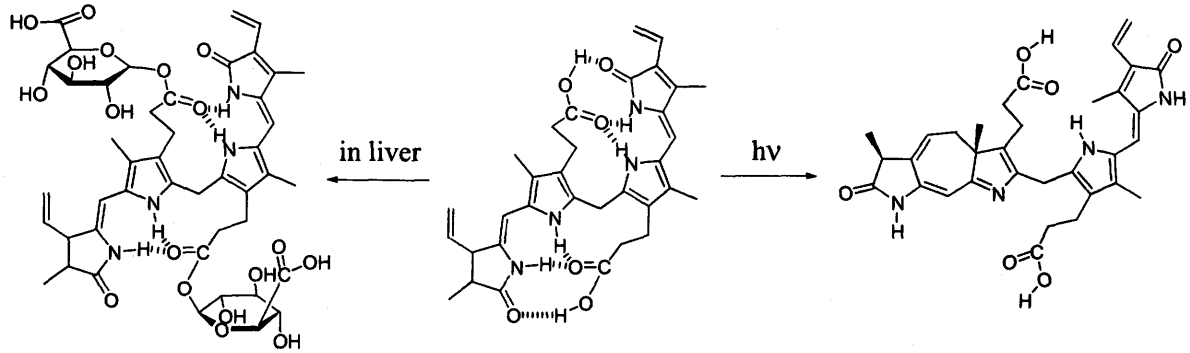

Scheme 2.

Photodynamic therapy is one of the medical treatments for jaundice of new-born infants. On irradiation with light from violet to blue to the skin, bilirubin underwent photoisomerization of a C=C double bond followed by photocyclization to give a more hydrophilic isomer. Thus, the light irradiation changes the property of bilirubin from hydrophobic to hydrophilic.[15,16]

Hydrogen bonding is also important in some photochemical reaction. For example, excited state double proton transfer reaction occurs in 7-azaindole.[17-23] 7-Azaindole has both donor and acceptor for hydrogen

bonding in one molecule, therefore the hydrogen bonded dimer was formed in non-polar solvent. 7-Azaindole dimer underwent excited state double proton transfer on photoirradiation to give tautomer exhibiting the blue fluorescence.

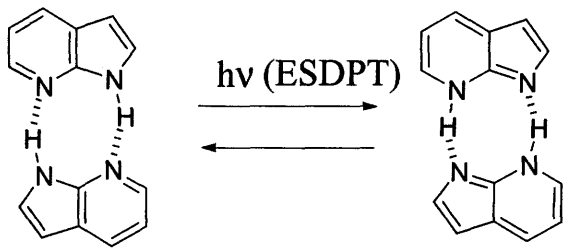

Scheme 3. Excited state double proton transfer (ESDPT) of 7-azaindole.

Hydrogen atom or proton transfer reaction in the intermolecularly hydrogen bonded system can be applied for proton relay system and control of degradation and formation of hydrogen bonded polymer.[2] One of the examples of proton relay system was shown in Scheme 4.[24] The proton or hydrogen atom transfer reaction in the solid state can cause phase transition and is applied for memory devices.[2]

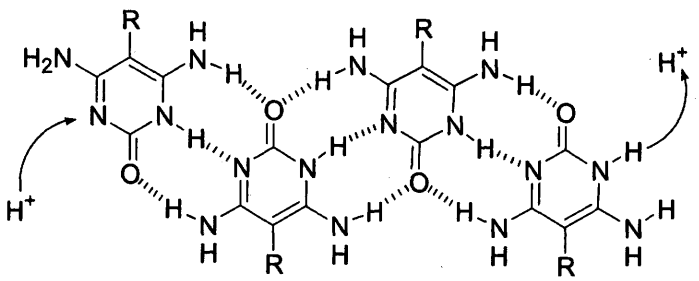

Scheme 4.

Excited state intramolecular hydrogen atom or proton transfer reaction (ESIPT) also took place in some intramolecularly hydrogen bonded compounds. For example, methyl salicylate and 3-hydroxyflavone exhibited fluorescence at

longer wavelength due to the occurrence of ESIPT, and the proton transfer mechanism was extensively investigated by transient spectroscopic techniques.[25-29]

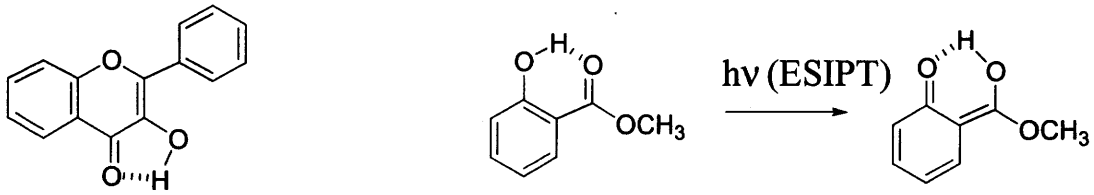

3-Hydroxyflavone Methyl salicylate

Scheme 5.

Intramolecular hydrogen atom transfer reaction can play an important role in photochromism of some compounds. For example, salicylideneaniline derivatives are well known to exhibit photochromism in crystalline state and the application to the photochromic memory has received much attention.[30-36] Recently, the tautomer form of salicylideneaniline was observed by X-ray crystallography and was assigned to the photochromic form.[32-34] However, the properties of photochromism of salicylideneaniline in solution is still uncertain.

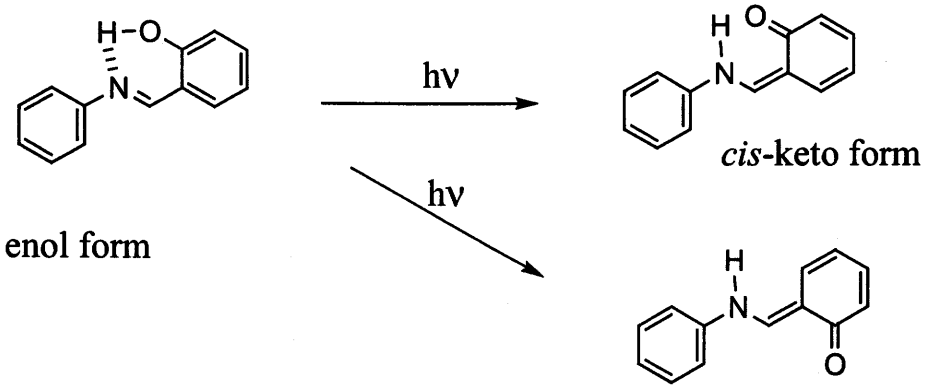

enol form *cis*-keto form

N-Salicylideneaniline *trans*-keto form

Scheme 6.

From the view point of control of chemical reaction by the hydrogen bonding, the effect of intramolecular hydrogen bonding on the photochemical behaviors has been investigated.[37-44] Thus, Hydrogen bonding affected the photochemical isomerization mode of the aromatic olefin. For example, the olefin having pyrrole ring and pyridine ring, 2-(2-(2-pyrrolyl)ethenyl)pyridine, exhibited one-way trans-to-cis photochemical isomerization due to the presence of intramolecular hydrogen bonding in *cis*-form.[40] The *cis*-form also underwent excited state hydrogen atom transfer to give tautomer exhibiting large Stokes shift fluorescence.[40] The hydrogen atom transfer reaction in the excited state and the fast non-radiative deactivation pathway through the intramolecular hydrogen bonding resulted in the one-way isomerization. Furthermore, the absorption maximum of *cis*-form appeared at longer wavelength region than that of *trans*-form indicating that hydrogen bonding be also applied for photochromic compounds.[43]

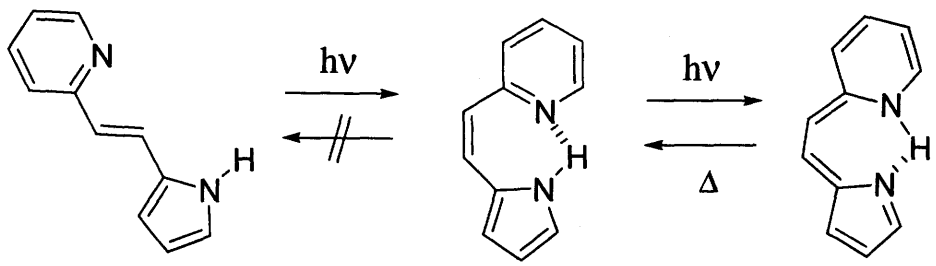

2-(2-(2-Pyrrolyl)ethenyl)pyridine

Scheme 7.

As to the isomerization of aromatic ethene in the triplet excited state, it is reported that the triplet energy of aromatic group on the ethylenic carbon

affects the mode of the isomerization.[45,46] For example, 2-anthrylethenes undergoes photochemical cis-to-trans one-way isomerization.[45,46] *cis*-2'-Hydroxychalcone undergoes intramolecular hydrogen atom transfer in the singlet and the triplet excited state to give the tautomer triplet excited state, which has low triplet energy and one-way cis-to-trans isomerization to the trans isomer in the triplet excited state takes place by the same mechanism of anthrylethene.[47]

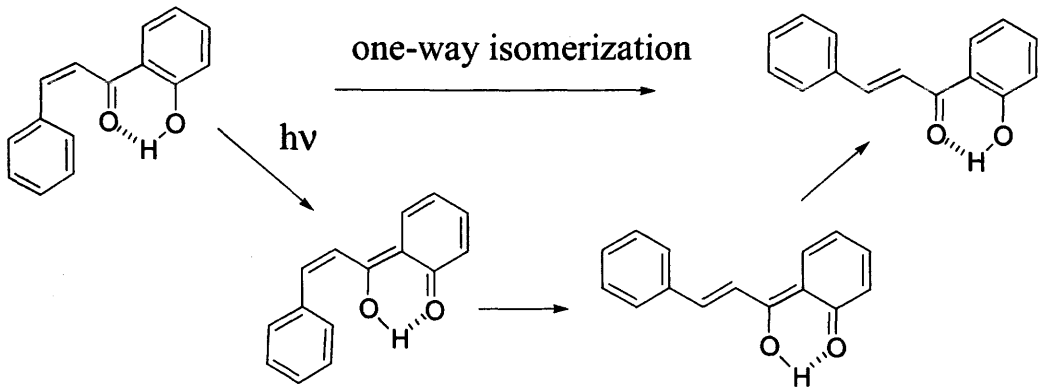

Scheme 8. One-way photoisomerization of 2'-hydroxychalcone

Hydrogen bonding is also expected to be useful in constructing supramolecular structures.[2,3] The control of conformation and association number of intermolecularly hydrogen bonded system by external stimulation have received much attention.[2,10,48] In this respect, photoinduced process to control the molecular weight of the hydrogen bonded assemblies can be applied for photolithography, gel reagent, memory devices and so on.[2] It is also expected that the photochemical reactions could control the polymerization and depolymelization of polymers.[10,48]

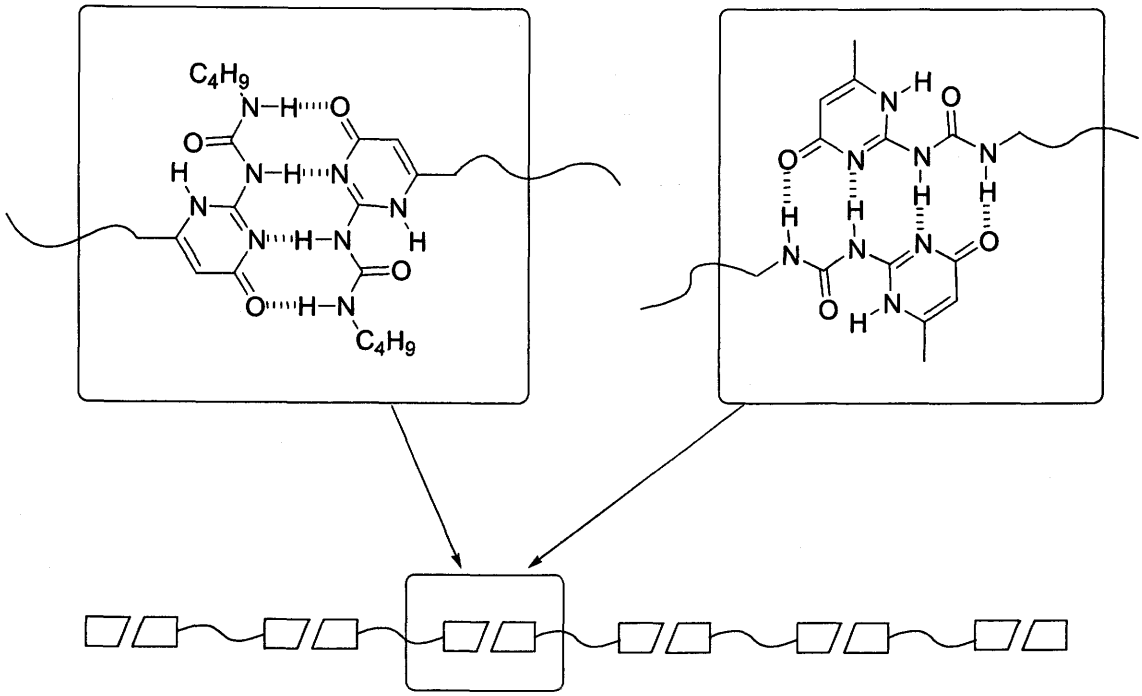

Scheme 9. Hydrogen bonded polymer by quadruple intermolecular hydrogen bonding

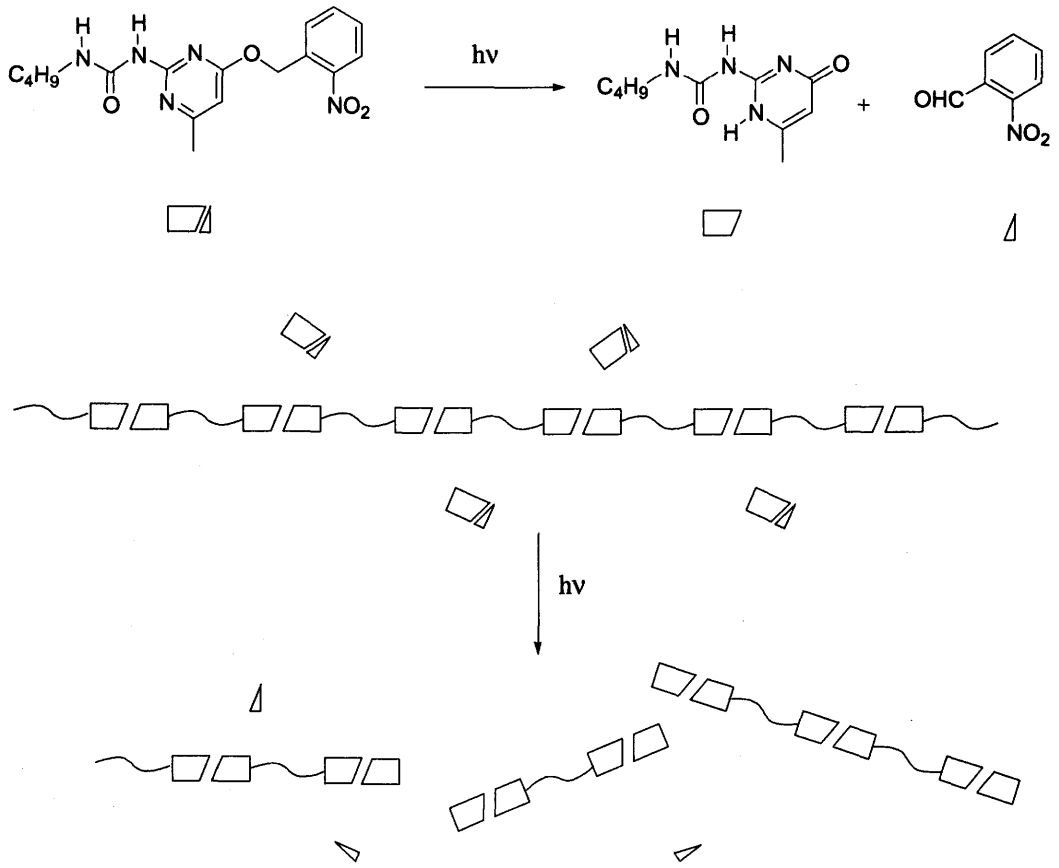

Scheme 10. Change in viscosity induced by photochemical process

The intermolecular hydrogen bonding can be used in photoinduced electron transfer, charge transfer or energy transfer systems.[49] Photoinduced electron transfer reaction has received much attention not only in solution chemistry, but also in heterogeneous systems such as photosynthetic reaction centers and solid state photoresponsive materials.[49,50]

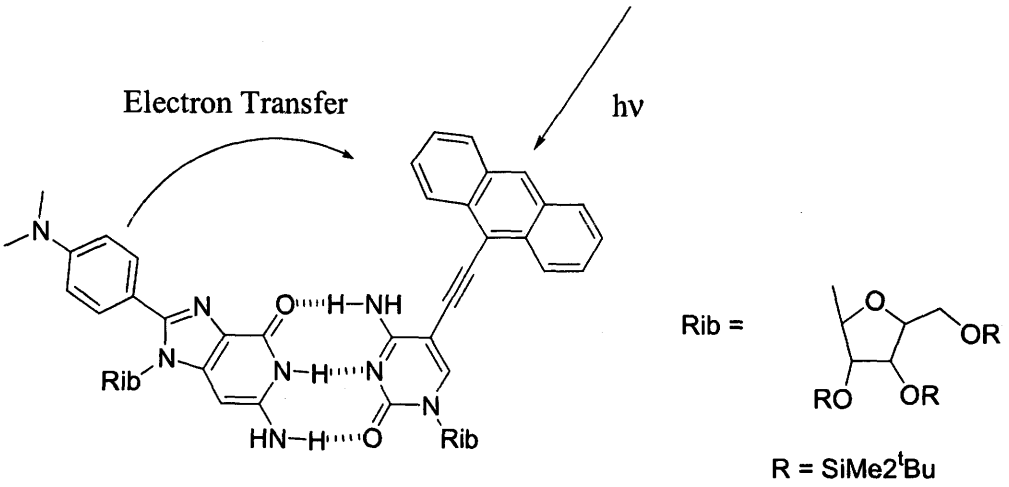

Scheme 11. Photoinduced electoron transfer system in Watoson-Crick base pair

In this thesis, I have studied novel photochemical reaction systems by utilizing the hydrogen bonding.

In chapter 1, 2, and 3, photoisomerization and excited state hydrogen atom transfer of intramolecularly hydrogen bonded compounds were investigated and the mechanism and the potential energy surface have been elucidated.

In chapter 4, photochromic dyes based on intramolecular hydrogen bonding have been studied. It was found that the intramolecular hydrogen bonding plays an important role in construction of photochromic compounds. Furthermore, effects of formyl substituent and temperature on hemiindigo dyes

were investigated. Photochemical behaviors of pyrrole-2-carboxyaldehyde and its related compounds were investigated in connection with this substituent effect and is discussed in Chapter 5.

In Chapter 6, synthesis and excited state behavior of molecular assemblies linked by quadruple intermolecular hydrogen bonding were discussed. The intermolecularly hydrogen bonded compounds exhibit excimer or exciplex formation and efficient energy transfer.

References

1. D. Voet and J. G. Voet , "Biochemistry," John Wiley & Sons (1995).
2. J. M. Lehn, "Supramolecular Chemistry," VCH, Weinheim (1995).
3. L. Brunsveld, B. J. B. Folmer, E. W. Meijer, and R. P. Sijbesma, *Chem. Rev.*, **2001**, *101*, 4071.
4. N. Zimmerman, J. S. Moore, and S. C. Zimmerman, *Chemistry & Industry*, **1998**, 604.
5. P. Terech and R. G. Weiss, *Chem. Rev.*, **1997**, *97*, 3133.
6. N. Kimizuka, T. Kawasaki, K. Hirata, and T. Kunitake, *J. Am. Chem. Soc.*, **1998**, *120*, 4094.
7. C. He, A. M. Donald, A. C. Griffin, T. Waigh, and A. H. Windle, *J. Polym. Sci., Part B: Polym. Phys.*, **1998**, *36*, 1617.
8. H. Kihara, T. Kato, T. Uryu, and J. M. J. Frechet, *Chem. Mater.*, **1998**, *120*, 6761.
9. R. P. Sijbesma, F. H. Beijer, L. Brunsveld, B. J. B. Folmer, J. H. K. Hirschberg, R. G. M. Lange, J. K. L. Lowe, and E. W. Meijer, *Science*, **1997**, 1601.
10. B. J. B. Folmer, E. Cavini, R. P. Sijbesma, and E. W. Meijer, *Chem. Commun.*, **1998**, 1847.
11. F. H. Beijer, R. P. Sijbesma, H. Koojiman, A. L. Spek, and E. W. Meijer, *J. Am. Chem. Soc.*, **1998**, *120*, 6761.
12. B. J. B. Folmer, R. P. Sijbesma, H. Kooijman, A. L. Spek, and E. W. Meijer, *J. Am. Chem. Soc.*, **1999**, *121*, 9001.
13. A, P. H. J. Schenning, P. Jonkheijm, E. Peeters, and E. W. Meijer, *J. Am. Chem. Soc.*, **2001**, *123*, 409.
14. S. H. M. Sontjens, R. P. Sijbesma, M. H. P. van Genderen, and E. W. Meijer,

Macromolecules, **2001**, *34*, 3815.

15. D. A. Lightner and A. F. McDonagh, *Acc. Chem. Res.*, **1984**, *17*, 417.
16. Y. Kanna, T. Arai, and K. Tokumaru, *Bull. Chem. Soc. Jpn.*, **1994**, *67*, 2758; Y. Kanna, T. Arai, and K. Tokumaru, *Bull. Chem. Soc. Jpn.*, **1993**, *66*, 1586; Y. Kanna, T. Arai, and K. Tokumaru, *Bull. Chem. Soc. Jpn.*, **1993**, *66*, 1482.
17. C. Al. Taylor, M. A. El-Byoumi, and M. Kasha, *Proc. Natl. Acad. Sci. USA*, **1969**, *63*, 253.
18. P. T. Chou, C. Y. Wei, C. P. Chang, and C. H. Chiu, *J. Am. Chem. Soc.*, **1995**, *117*, 7259.
19. S. Takeuchi and T. Tahara, *Chem. Phys. Lett.*, **1997**, *277*, 340; S. Takeuchi and T. Tahara, *J. Phys. Chem. A*, **1998**, *102*, 7740.
20. T. Suzuki, U. Okuyama, and T. Ichimura, *J. Phys. Chem. A*, **1997**, *101*, 7047.
21. T. Fiebig, M. Chachisvilis, M. Manger, A. H. Zewail, A. Douhal, O. I. Garcia, and A. D. H. Ayuso, *J. Phys. Chem. A.*, **1999**, *103*, 7419.
22. N. Sarkar, S. Takeuchi, and T. Tahara, *J. Phys. Chem. A.*, **1999**, *103*, 4808.
23. P. T. Chou, C. Y. Wei, G. R. Wu, and W. S. Chen., *J. Am. Chem. Soc.*, **1999**, *121*, 12186.
24. M. C. Etter and G. M. Frankenbach, *Chem. Mater.*, **1989**, *1*, 10; I. Weissbuch, M. Lahav, L. Leiserowitz, G. R. Meredith, and H. Hanherzeele, *Chem. Mater.* **1989**, *1*, 114; S. R. Marder, J. W. Perry, and W. P. Schaefer, *Science*, **1989**, *245*, 626.
25. A. Weller, *Z. Elektrochem.*, **1956**, *60*, 1144.
26. K. Y. Law and J. Shoham, *J. Phys. Chem.*, **1994**, *98*, 3114.
27. J. Catalan and C. Diaz, *J. Phys. Chem.*, **1994**, *98*, 3114.
28. Y. Norikane and T. Arai, *Chem. Lett.*, **1999**, 909.
29. L. L. Premvardhan and L. A. Peteanu, *J. Phys. Chem. A*, **1999**, *103*, 7506.

30. M. D. Cohen, *J. Chem. Soc. (B)*, **1968**, 373.

31. N. Hoshino, T. Inabe, T. Mitani, and Y. Maruyama, *Bull. Chem. Soc. Jpn.* **1988**, *61*, 4207.

32. K. Ogawa, Y. Kasahara, Y. Ohtani, and J. Harada, *J. Am. Chem. Soc.*, **1998**, *120*, 7107.

33. K. Ogawa and T. Fujiwara, *Chem. Lett.*, **1999**, 657.

34. J. Harada, H. Uekusa, and Y. Ohashi, *J. Am. Chem. Soc.*, **1999**, *121*, 5809.

35. T. Kawato, H. Kanatomi, K. Amimoto, H. Koyama, and H. Shigemizu, *Chem. Lett.*, **1999**, 47.

36. T. Kawato, K. Amimoto, H. Maeda, H. Koyama, and H. Kanatomi, *Mol. Cryst. Liq. Cryst.*, **2000**, *345*, 381.

37. F. D. Lewis, B. A. Yoon, T. Arai, T. Iwasaki and K. Tokumaru, *J. Am. Chem. Soc.*, **1994**, *116*, 3171.

38. T. Arai, M. Obi, T. Iwasaki, K. Tokumaru, and F. D. Lewis, *J. Photochem. Photobiol. A: Chem.*, **1995**, *96*, 65.

39. T. Arai, M. Moriyama, and K. Tokumaru, *J. Am. Chem. Soc.*, **1994**, *116*, 3171.

40. M. Obi, H. Sakuragi, and T. Arai, *Chem. Lett.*, **1998**, 169.

41. T. Arai and Y. Hozumi, *Chem. Lett.*, **1998**, 1153.

42. Y. Yang and T. Arai, *Tetrahedron, Lett.*, **1998**, *39*, 2617.

43. T. Arai and M. Ikegami, *Chem. Lett.*, **1999**, 965.

44. M. Ikegami and T. Arai, *J. Chem. Soc. Perkin Trans. 2*, in press.

45. T. Arai, "Molecular and Supramolecular Photochemistry", Vol 3, ed by V. Ramamurthy and K. S. Schanze, Marcel Dekker (1999).

46. T. Arai and K. Tokumaru, *Chem. Rev.*, **1993**, *93*, 23.

47. T. Arai and Y. Norikane, *Chem. Lett.*, **1997**, 339; Y, Norikane, H. Itoh, and T.

Arai, *Chem. Lett.*, **2000**, 1094.

48. M. S. Vollmer, T. D. Clark, C. Steinem, and M. R. Ghadiri., *Angew. Chem. Int. Ed.*, **1999**, *38*, 1598.

49. J. L. Sessler, M. Sathiosatham, C. T. Brown, T. A. Rhodes, and G. Wiederrecht, *J. Am. Chem. Soc.*, **2001**, *123*, 3655.

50. G. J. Kavaronos, "Fundamentals of Photoinduced Electron Transfer," VCH Publishers (1993); G. L. Kavarnos and N. J. Turro, *Chem. Rev.*, **1986**, *86*, 401.

Chapter 1

Photoisomerization of 2-(2-(2-Pyrrolyl)ethenyl)benzoxazole and 2-(2-(2-Pyrrolyl)ethenyl)benzothiazole

Abstract

Hydrogen bonded compounds 2-(2-(2-pyrrolyl)ethenyl)benzoxazole (**4**) and 2-(2-(2-pyrrolyl)ethenyl)benzothiazole (**5**) were synthesized and their photochemical behavior was studied. The cis isomers of **4** and **5** form intramolecular hydrogen bonding as revealed by the ^{1}H-NMR studies. The trans isomers exhibit pale yellow color in solution, but on photoirradiation, the color slightly changes to give yellow due to the change of the absorption spectra. The quantum yield of isomerization of **4** and **5** is considerably high in the range of 0.4-0.6 and is slightly dependent on the solvent properties. On triplet sensitization **4** and **5** gave the T-T absorption spectra with the lifetime of ca. 1 μs in benzene. Since transient absorption spectrum was not observed on direct irradiation of **4** and **5** with 308 nm laser pulse, the cis-trans isomerization on direct irradiation should take place in the excited singlet state. On triplet sensitization **4** and **5** underwent cis-trans isomerization. These results indicate that the intramolecular hydrogen bonding is broken in the singlet excited state as well as in the triplet excited state of *cis*-**4** and *cis*-**5**.

Introduction

In recent years, intramolecular hydrogen atom transfer in 2-(2-hydroxyphenyl)benzoxazole (**1**) and -benzothiazole (**2**) has extensively been investigated by many researchers.[1–8] These molecules underwent intramolecular hydrogen atom transfer to give the tautomer in the excited state exhibiting fluorescence spectra with large Stokes shift. In addition, transient absorption spectra of the tautomer produced by intramolecular hydrogen atom transfer in the singlet excited state have been observed by laser flash photolysis in non-polar solvent.

As to the photoisomerization behavior of hydrogen bonded compounds,[9-15] we have already reported that an olefin with a pyrrole ring and a pyridine ring (**3**) exhibited one-way trans→cis isomerization due to the presence of the intramolecular hydrogen bonding.[12] Furthermore, intramolecular hydrogen atom transfer occurred in the singlet excited state of *cis*-**3** to give the tautomer *cis*-**3'** on photoirradiation, which was revealed by the observation of a fluorescence spectrum with large Stokes shift.[12] In addition, transient absorption spectra due to the tautomer in the ground state were observed by laser flash photolysis.[12,13] Therefore, it will be interesting to study the photochemical behavior of the compounds having isomerizable olefinic part in addition to the hydrogen bonding in **1** and **2**.

We wish to report here the preparation of olefins with a pyrrole ring and a benzoxazole ring (**4**) or a benzothiazole ring (**5**) and the studies of their photoisomerization behavior. The olefins **4** and **5** could undergo cis-trans isomerization as well as intramolecular hydrogen atom transfer and each reaction was expected to control the efficiency and/or the selectivity of the other reaction processes.

Experimental

Materials and solvents

trans-2-(2-(2-(Pyrrolyl)ethenyl)benzoxazole (*trans*-**4**) and -benzothiazole (*trans*-**5**) were prepared by Wittig reaction.[16] Cis isomers were obtained by isomerization of trans isomers on irradiation at 366 nm. Trans and cis isomers were purified with column chromatography on silica gel and recrystallized from benzene and hexane, respectively.

trans-2-(2-(2-(Pyrrolyl)ethenyl)benzoxazole (*trans*-**4**): ^{1}H-NMR($CDCl_3$, 200 MHz) δ (ppm) 6.60 (d, 1H, J = 16.2 Hz; olefinic proton), 7.64 (d, 1H, J = 16.2 Hz; olefinic proton), 6.32 (m, 1H; pyrrole proton), 6.60 (m, 1H; pyrrole proton), 6.95 (m, 1H; pyrrole proton), 7.30 (m, 1H; benzoxazole proton), 7.50 (m, 1H; benzoxazole proton), 7.64 (m, 1H; benzoxazole proton), 8.6 (NH proton). mp = 213-214 °C. Anal Calcd for $C_{13}H_{10}N_2O$: C, 74.27; H, 4.79; N, 13.33; O, 7.61%. Found: C, 74.00; H, 4.84; N, 13.19%.

cis-2-(2-(2-(Pyrrolyl)ethenyl)benzoxazole (*cis*-**4**): ^{1}H-NMR ($CDCl_3$, 200 MHz) δ (ppm) 6.09 (d, J = 13.0 Hz, 1H; olefinic proton), 6.36 (m, 1H; pyrrole H), 6.57 (m, 1H; pyrrole H), 6.83 (d, J = 12.8 Hz, 1H; olefinic proton), 7.17 (m, 1H; pyrrole H), 7.35 (m, 2H; benzoxazole H), 7.49 (m, 1H; benzoxazole H), 7.73 (m, 1H; benzoxazole H), 14.0 ppm (NH proton). mp = 75-76 °C.

trans-2-(2-(2-(Pyrrolyl)ethenyl)benzothiazole (*trans*-**5**) ^{1}H-NMR ($CDCl_3$, 200 MHz) δ (ppm) 6.30 (m, 1H; pyrrole proton), 6.58 (m, 1H; pyrrole proton), 6.94 (d, 1H, J = 16.2 Hz; olefinic proton), 6.95 (m, 1H; pyrrole proton), 7.38 (m, 2H; benzothiazole proton), 7.40 (d, 1H, J=16.2 Hz; olefinic proton), 7.83 (dd, 1H; J = 7.5, 1.2 Hz; benzothiazole proton), 7.92 (dd, 1H; J = 7.5, 1.2; benzothiazole proton), 9.1 (br, NH proton). mp = 198-199°C. Anal Calcd for $C_{13}H_{10}N_2S$: C, 69.00; H, 4.45; N, 12.38; S, 14.17%. Found: C, 68.75; H, 4.45; N, 12.29%.

cis-2-(2-(2-(Pyrrolyl)ethenyl)benzothiazole (*cis*-**5**): ^{1}H-NMR ($CDCl_3$, 200 MHz) δ (ppm) 6.24 (d, J = 12.0 Hz, 1H; olefinic proton), 6.38 (m, 1H; pyrrole proton), 6.56 (m, 1H; pyrrole proton), 6.72 (d, J = 12.0 Hz, 1H; olefinic proton), 7.13 (m, 1H; pyrrole proton), 7.36 (td, 1H; J = 7.3, 1.2 Hz; benzothiazole proton), 7.51 (td, 1H; J = 7.3, 1.2 Hz; benzothiazole proton), 7.85 (dd, J = 7.3, 1.2 Hz, 1H; benzothiazole proton), 8.03 (dd, 1H; J = 7.3, 1.2 Hz, 1H; benzothiazole proton), 14.0 (br, NH proton). mp = 80-81°C.

In spectroscopy, Dotite Spectrosol or Luminasol were used as solvents without further purification.

Measurement

Absorption and fluorescence spectra were measured on a JASCO Ubest-55 and on a Hitachi F-4000 fluorescence spectrometer, respectively.

Laser flash photolyses were performed by using an excimer laser (Lambda Physik LPX-100, 308 nm, 20 ns fwhm) or excimer laser pumped dye laser (Lambda Physik LEXtra-100, 308 nm, 20 ns fwhm and Lambda Physik Scanmate, stilbene 3, 425 nm. 10 ns fwhm) as excitation light sources and a pulsed xenon arc (Ushio UXL-159) was used as a monitoring light source. A photomultiplier (Hamamatsu R-928) and a storage oscilloscope (Iwatsu TS-8123) were used for the detection.

Fluorescence lifetimes were determined with a picosecond laser system consisting of a titanium sapphire laser (Spectra Physics 3900 "Tsunami") operated with a CW Ar^+ laser (Spectra Physics 2060), a frequency doubler (SP-390), a pulse selector (SP-3980; ≈ 2 ps fwhm) and a streak scope (Hamamatsu C4334).

DSC measurement was performed with Seiko DSC-220 and data module SSC-5500H.

Quantum yield of isomerization were determined with 366 nm light from a 400 W high-pressure mercury lamp through UV-35 and U-360 filters. The sample solution was deaerated by bubbling argon and irradiated for 5 - 15 min to keep the conversion within 10%. Light intensity was determined by tris(oxalato)ferrate(III) actinometory.[17] The concentration of each isomer was determined by high performance liquid chromatography through a column (Toso CN-80TS) eluting with ethylacetate / n-hexane = 1 / 9.

Rate constants of acid catalyzed thermal isomerization and equilibrium constant were determined by monitoring absorbance of *trans*-**4**-H^+ in the presence of appropriate amount of 0.1 M HCl (Wako analytical grade). The molar extinction coefficient of *trans*-**4**-H^+ was determined with the concentration of [*trans*-**4**] = 2.0x 10^{-5} M and [HCl] = 1.2x 10^{-2} M.

Results

Absorption and fluorescence spectra

The absorption spectra of **4** and **5** were shown in Figure 1. The molar extinction coefficient at the absorption maximum of *cis*-**4** and *cis*-**5** is smaller than that of *trans*-**4** and *trans*-**5**. The absorption spectrum of *cis*-**4** and *cis*-**5** in benzene is shifted to the longer wavelength region compared to that of *trans*-**4** and *trans*-**5**. Usually, the cis isomers exhibit absorption maximum at shorter wavelength compared to that of the trans isomers, since the aromatic ring and the C=C double bond take almost planar conformation in trans isomers, while the single bonds connecting the aromatic ring and the double bond are twisted by some degrees due to the steric hindrance in cis isomers. The absorption maximum of **5** appeared at longer wavelength than that of **4** by 15 nm and therefore, the singlet excitation energy of **5** is lower than that of **4**.

The unusual red shift of absorption spectra in cis isomers can be explained by the effect of intramolecular hydrogen bonding to increase the conjugation in cis isomers. Actually in ^{1}H-NMR spectra, the signal of the NH proton peak of *cis*-**4** and *trans*-**4** appeared at 14.0 ppm and 8.0 ppm, respectively in $CDCl_3$. The considerable downfield shift of the NH proton signal in *cis*-**4** indicates that *cis*-**4** forms an NH:N intramolecular hydrogen bonding in the ground state.

The difference in charge transfer character between the *cis*- and *trans*-**4** in the excited state may explain the above mentioned observation that *cis*-**4** exhibits absorption spectra at longer wavelength than *trans*-**4**.

The absorption maximum (λ_{max}) of *cis*-**4** does not linearly depend on the solvent polarity and almost the same in all the solvent examined. Thus, λ_{max} in methylcyclohexane and DMSO appeared at 379 nm and the value in acetonitrile (371 nm) and in methanol (373 nm) exhibits at shorter wavelength. These

results indicate that the presence of intramolecular hydrogen bonding in *cis*-**4** in the above solvents.

The absorption maximum of *trans*-**4** shows a red shift with increasing solvent polarity from 356 nm in methylcyclohexane to 368 nm in DMSO. These results show that *trans*-**4** forms intermolecular hydrogen bonding with methanol and DMSO, which may play some role on the behavior of **4** in the singlet excited state. In water, absorption maximum of *cis*-**4** was still slightly red shifted than that of *trans*-**4**. This result indicates that *cis*-**4** forms an intramolecular hydrogen bonding even in water.

The fluorescence spectra of **4** are shown in Figure 2. At room temperature, quantum yield of fluorescence emission of **4** was determined to be $2x\ 10^{-4}$ and $1x\ 10^{-5}$ for *trans*- and *cis*-**4**, respectively, while at 77 K, it was 0.5 for *cis*- and *trans*-**4** in methylcyclohexane. These results indicate that the excited singlet state of *trans*- and *cis*-**4** should deactivate to the ground state by twisting around the double bond resulting in the cis-trans isomerization at room temperature, while at 77 K the fluorescence emission prevails over the isomerization due to the decrease of the rate constant of isomerization in the excited state. In addition, the deactivation through the intramolecular hydrogen bonding in cis isomer seems to be negligible compared to the other deactivation processes such as fluorescence emission. Therefore, intramolecular hydrogen bonding in cis isomer should become weaker or be almost broken in the singlet excited state.

Fluorescence lifetimes of *cis*- and *trans*-**4** were determined to be 2.3 ns and 1.6 ns, respectively in methylcyclohexane and 2.0 and 1.9 ns in ethanol at 77K. Similar fluorescence lifetimes were observed for *cis*- and *trans*-**5** at 77K: 3.2 ns and 1.5 ns in methylcyclohexane and 2.9 and 1.8 ns in ethanol. This also indicates that the intramolecular hydrogen bonding would become weaker in the singlet excited state, and therefore the intramolecular hydrogen bonding could not participate in the deactivation pathways from the singlet excited state.

Differential scanning calorimetry (DSC) in 4

The DSC experiments were performed at different rising temperature (2.5 - 7°C min^{-1}). A typical example was shown in Figure 4. Thus, the energy difference between *cis*- and *trans*-**4** in the ground state was determined to be 5 kcal mol^{-1}. The obtained value means that *cis*-**4** is more stable than *trans*-**4** in 5 kcal mol^{-1}, probably due to the presence of intramolecular hydrogen bonding in *cis*-**4**. In addition, the activation energy of trans-to-cis isomerization was calculated as 33 kcal mol^{-1} by the similar treatment reported by Kissinger.[18]

Quantum yield of isomerization and the photostationary state isomer ratio

The quantum yield of trans→cis isomerization ($\Phi_{t\rightarrow c}$) of **4** is determined to be 0.64 and 0.54 in benzene and methanol and is slightly higher than that of cis→trans isomerization ($\Phi_{c\rightarrow t}$), which is 0.41 and 0.48 in benzene and in methanol, respectively. The quantum yield of isomerization for **5** was determined to be similar to that of **4**. The photostationary state cis-to-trans isomer ratio ([c]/[t])pss of **4** was determined to be 71/29 and 65/35 in benzene and in methanol, respectively. The $([c]/[t])_{pss}$ values for **5** were determined to be 81/19 and 76/24 in benzene and in methanol, respectively. The observed $([c]/[t])_{pss}$ values are quite similar to the values calculated by the combination of the molar extinction coefficient of cis (ε_c) and trans isomers (ε_t) at the excitation wavelength and the quantum yield of isomerization ($([c]/[t])_{pss} = (\varepsilon_t/\varepsilon_c) \times (\Phi_{t\rightarrow c} / \Phi_{c\rightarrow t})$). These values, together with the values determined in acetonitrile are summarized in Table 2. The $\Phi_{c\rightarrow t}$ value is higher, but $\Phi_{t\rightarrow c}$ is lower in polar protic solvent than in less polar solvent. The distortion of conical intersection may explain the above solvent effect.

Triplet sensitized isomerization was performed by biacetyl or Michler's ketone as triplet sensitizers with irradiation at 436 nm or 313 nm from high pressure mercury lamp. On triplet sensitization, both cis-to-trans and trans-to-cis isomerization occurred to give the isomer ratio at the photostationary state to be $([c]/[t])_{pss} = 40 / 60$.

Effect of HCl on the behavior of 4

Absorption spectra of *trans*-**4** in acetonitrile in the presence of HClaq appeared at the longer wavelength region with the maximum at 430 nm compared to the absorption maximum of 356 nm in pure acetonitrile as shown in Figure 5. The concentration of HCl was changed from 1x 10^{-4} M to 1x 10^{-3} M by addition the 1N HCl solution. Thus, the absorbance at 356 nm decreased with the increase of HClaq with the concomitant increase of the absorbance at 430 nm. The isosbestic point appeared at 375 nm and finally, in the presence of 1x 10^{-3} M of HClaq, the absorption spectrum can be assigned to that of the protonated form. On the other hand, the absorption spectrum of *cis*-**4** observed just after the addition of HClaq was identical with that in the absence of HClaq in acetonitrile. The absorption spectra of *cis*-**4** in the presence of HClaq in acetonitrile gradually changed and the absorption maximum shifted from 371 nm to 420 nm during 240 min at 299K (Figure 6).

The ^{1}H-NMR spectra of **4** were observed in methanol-d_4 in the presence of HClaq. The ^{1}H-NMR spectrum of *cis*-**4** in methanol-d_4 did not shift by the addition of 1 drop of 12N HCl, while the peak of ^{1}H-NMR spectrum of *trans*-**4** shifted by addition of HCl. For example, the peak of the olefinic proton of *trans*-**4** shifted from 6.68 and 7.68 ppm to 6.84 and 8.14 ppm, suggesting that protonation took place at the nitrogen atom of benzoxazole ring to give *trans*-**4**-H^+.

As shown in Figure 6, the absorption spectrum observed at 240 min after the addition of HClaq is the same with that of the *trans*-**4** in the presence of HClaq. These results clearly show that the thermal cis-to-trans isomerization of **4** (2.0x 10^{-5} M) occurred in the presence of HClaq (2x 10^{-3} M). The rate constant of cis-to-trans isomerization ($k_{c\rightarrow t}$) was determined to be 4x 10^{-8} s^{-1} at 298K. The $k_{c\rightarrow t}$ value increased with increasing of the temperature (Figure 7). Thus, the temperature effect on the $k_{c\rightarrow t}$ value gave the activation energy (E_a) and preexponential factor (A) of Arrhenius parameter for *cis*-**4**-H^+→*trans*-**4**-H^+ to be 11.9 kcal mol^{-1} and 9.6x 10^4 s^{-1}, respectively.

On 366 nm light irradiation, **4** (2.0x 10^{-5} M) underwent trans-cis isomerization in the presence of HClaq ([HCl] = 2x 10^{-3} M) to give the isomer mixture at the photostationaly state as $([c]/[t])_{pss}$ = 41/59. The addition of HClaq to **4** in acetonitrile did not significantly affect the photoisomerization behavior, since the ratio of the quantum yield of isomerization can be estimated from the ratio of molar extinction coefficient of *cis*- and *trans*-**4** at 366 nm $(\Phi_{t\rightarrow c}/\Phi_{c\rightarrow t}) = ([c]/[t])_{pss} \times (\varepsilon_c/\varepsilon_t)$ = (41/59) x (2.6x 10^4 / 2.0x 10^4) = (0.48/0.52). However, as mentioned above the produced cis isomer underwent isomerization to the trans isomer even in the ground state, when the HClaq was present.

The temperature effect on the absorption spectra of *trans*-**4** ([*trans*-**4**] = 2.0x 10^{-5} M) in the presence of HClaq ([HCl] = 2x 10^{-4} M) are shown in Figure 8. Since the absorbance at 356 nm (non-protonated form) increased with the increase of the temperature with concomitant decrease of the absorbance at 430 nm (protonated form), protonated form favors the low temperature. Thus, the equilibrium constant (K) was estimated to be 8.2x 10^3 M^{-1} (at 298 K), 7.2x 10^3 M^{-1} (at 299K), 5.4x 10^3 M^{-1} (at 301K), and 3.1x 10^3 M^{-1} (at 305K). From these experiments the enthalpy difference ΔH between the neutral *trans*-**4** and the protonated *trans*-**4**-H^+ can be estimated to be 25.5 kcal mol^{-1} by using van't Hoff plot for the temperature effect on the absorption spectra shown in Figure 9.

Under the same acidic condition, fluorescence spectra of *trans*-**4** was observed at longer wavelength region with the emission maximum at 480 nm which is very much shifted to the longer wavelength compared to that of *trans*-**4** in pure acetonitrile as shown in Figure 10. If the entropy difference for the protonation in the ground state could be estimated to be the same as that in the excited singlet state, the pK_a values were estimated from Förster cycle[19] to be 3.9 and 10.6 in the ground state and in the singlet excited state, respectively at 295K. These results suggest that acidity of benzoxazole ring in the excited singlet state was lower than that in the ground state.

Laser flash photolysis

On direct irradiation of **4** and **5** with 308 nm or 425 nm, transient species was not observed.

On triplet sensitization with benzophenone excited by 308 nm excimer laser or with biacetyl excited by 425 nm dye laser, *cis*- and *trans*-**4** gave transient absorption spectra with λ_{max} = 450 nm as shown in Figure 11. Decay profiles monitored at 450 - 800 nm were fitted to the single exponential analysis and the rate constant was determined to be 1.0x 10^6 s^{-1} under argon.

These transients were quenched by oxygen with the rate constant of 4.4x 10^9 M^{-1} s^{-1}. On the basis of the observation of the triplet state with considerably long lifetime and the observed quenching rate constant by oxygen with nearly 1/9 of the diffusion controlled quenching rate constant ((2-3)x10^{10} M^{-1} s^{-1}), the observed transient can be assigned to the trans triplet state.

On benzil sensitization, triplet energy of *cis*- and *trans*-**4** were estimated by determining the quenching rate constant of benzil triplet (E_T = 53.4 kcal mol^{-1})[17] by *cis*- or *trans*-**4**. The quenching rate constants (k_q) are determined to be (1.5 ± 0.1)x 10^9 and (2.4 ± 0.1)x 10^9 M^{-1} s^{-1} for *cis*- and *trans*-**4**, respectively. These values are smaller than that of diffusion controlled rate constant 6.3x 10^9

s^{-1}.[20] Therefore, the energy transfer process should be endothermic process and the triplet energy of **4** can be estimated by eq. 1 [21] to be 54.1 and 53.7 kcal mol^{-1} for *cis*- and *trans*-isomers, respectively.

$$k_q = k_{diff} \exp(-\Delta E_a/RT)/[1+\exp(-\Delta E_a/RT)] \qquad (1)$$

Discussion

Potential energy surface of cis-trans isomerization of 4

In aprotic solvent such as benzene, stabilization energy of *cis*-**4** due to the intramolecular hydrogen bonding was estimated to be 5 kcal mol^{-1} and the activation energy of trans-to-cis isomerization in the ground state was estimated as 33 kcal mol^{-1} by DSC experiments. The singlet excitation energies of *cis*- and *trans*-**4** were obtained to be 69.4 kcal mol^{-1} and 72.4 kcal mol^{-1}, respectively from their absorption and fluorescence spectra.

At room temperature, the quantum yield of fluorescence emission was determined to be 4x 10^{-4} and 4x 10^{-5} for *trans*-**4** and *cis*-**4**, respectively. In addition, no transient absorption spectrum was observed by laser flash photolysis. Furthermore, the sums of quantum yield of isomerization ($\Phi_{t\rightarrow c}$ + $\Phi_{c\rightarrow t}$) for **4** and **5** in all the solvent examined is nearly 1. These results indicate that both *cis*-**4** and *cis*-**5** underwent cis-trans isomerization exclusively from the excited singlet state.

Although *cis*-**4** forms intramolecular hydrogen bonding, the lifetime of fluorescence emission of *cis*-**4** was similar to that of *trans*-**4** in methylcyclohexane and ethanol at 77 K. This also indicates that the intramolecular hydrogen bonding would become weaker in the excited singlet

state, and therefore the intramolecular hydrogen bonding could not participate in the deactivation pathways from the singlet excited state.

cis-**4** and *trans*-**4** gave the same T-T absorption spectra with the same decay constants on triplet sensitization. From the triplet lifetime and the photostationary state isomer composition determined on triplet sensitization, it was found that the equilibration between the trans form and the perpendicular form was established in the excited triplet state. The rate constant of the deactivation from the perpendicular ($^3p^*$) (k_{pd}) and the trans triplet state ($^3t^*$) (k_{td}) could be estimated to be 2x 10^7 s^{-1} and 2x 10^4 s^{-1}, respectively.[22] Thus, the equilibrium constant, K_{tp}, between $^3t^*$ and $^3p^*$ ($[^3p^*]/[^3t^*]$) is estimated as ca. 0.05 from the observed triplet lifetime by using eq. 2, where $^3t^*$ is much more stable than $^3p^*$. On the basis of these results, potential energy surface of isomerization of **4** in benzene was depicted as shown in Figure 12.

$$\tau_T = (1 + K_{tp}) / (K_{tp}k_{pd} + k_{td}) \qquad (2)$$

Photochromic properties

At the photostationary state, the composition of the *cis*-isomers of **4** and **5** was higher in benzene than in methanol. In addition, *cis*-isomers exhibited absorption maximum at longer wavelength region with yellow color compared to the *trans*-isomers. Therefore, by the aid of intramoelcular hydrogen bonding one can extend the absorption spectra of the molecule to the longer wavelength region as observed in the intramolecularly hydrogen bonded compounds *cis*-**4** and *cis*-**5** and can construct photochromic materials by choosing appropriate excitation wavelength. Furthermore, the addition of acid changed the color of the solution and the photochromic behavior, where cis isomers are less stable in the ground state and gradually revert to the trans isomers within several tens to

hundreds minutes. Thus, on photoirradiation one can produce the cis isomers of **4** and **5**, while without light only cis-to-trans isomerization was observed and one can obtain the solution of only the trans isomers in the dark in the presence of acid.

Conclusion

Compounds **4** and **5** forms an intramolecular hydrogen bonding in cis form, and therefore, the absorption spectra of cis isomers shifted to the longer wavelength compared to the trans isomers. In the singlet excited state as well as in the triplet state the intramolecular hydrogen bonding in *cis*-**4** and *cis*-**5** seems to be broken and therefore, the cis-trans isomerization in **4** and **5** efficiently occurs. The cis-to-trans ratio at the photostationaly state $([c]/[t])_{pss}$ was 2.4 and 4.3 for **4** and **5**, respectively in benzene, and deceased in polar protic solvent. The sums of the quantum yield of isomerization were almost nearly 1. Therefore, **4** and **5** would mainly undergo cis-trans isomerization in the excited state without undergoing hydrogen atom transfer to give the tautomer in the excited state.

References

1. J. S. Stephan and K. H. Grellmann, *J. Phys. Chem.*, **1995**, *99*, 10066.
2. W. Al-Soufi, K. H. Grellmann, and B. Nickel, *Chem. Phys. Lett.*, **1990**, *174*, 609.
3. P. T. Chou, W. C. Cooper, J. H. Clements, S. L. Studer, and C. P. Chang, *Chem. Phys. Lett.* **1993**, *216*, 300.
4. P. T. Chou, M. L. Martinez, and S. L. Studer, *Chem. Phys. Lett.*, **1992**, *195*, 586.
5. S. Nagaoka, A. Itoh, K. Mukai, and U. Nagashima, *J. Phys. Chem.*, **1993**, *97*, 11385.
6. M. Itoh and Y. Fujiwara, *J. Am. Chem. Soc.*, **1985**, *107*, 1561.
7. G. Yang, F. Morelet-Savary, Z. Peng, S. Wu, and J. -P, Fouassier, *Chem. Phys. Lett.*, **1996**, *256*, 536.
8. M. Ikegami and T. Arai, *Chem. Lett.*, **2000**, 996.
9. F. D. Lewis, B. A. Yoon, T. Arai, T. Iwasaki, and K. Tokumaru, *J. Am. Chem. Soc.*, **1994**, *116*, 3171.
10. T. Arai, M. Obi, T. Iwasaki, K. Tokumaru, and F. D. Lewis, *J. Photochem. Photobiol. A: Chem.*, **1995**, *96*, 65.
11. T. Arai, M. Moriyama, and K. Tokumaru, *J. Am. Chem. Soc.*, **1994**, *116*, 3171.
12. M. Obi, H. Sakuragi, and T. Arai, *Chem. Lett.*, **1998**, 169.
13. T. Arai and Y. Hozumi, *Chem. Lett.*, **1998**, 1153.
14. Y. Y. Yang and T. Arai, *Tetrahedron, Lett.*, **1998**, *39*, 2617.
15. T. Arai and M. Ikegami, *Chem. Lett.*, **1999**, 965.
16. E. C. Taylar and S. F. Martin, *J. Am. Chem. Soc.*, **1974**, *96*, 8095.
17. "Handbook of Photochemistry," ed by S. L. Murov, I. Carmichal and G. L. Hug, Marcel Dekker, New York (1993).
18. H. E. Kissinger, *Anal. Chem.*, **1957**, *29*, 1702.

19. Th. Förster, *Z. Electrochem.*, **1950**, *54*, 42.
20. Diffusion controlled quenching rate constant was determined by Stern-Volmer analysis for the triplet quenching of benzophenone triplet (E_T = 69 kcal mol^{-1})[17] by naphthalene (E_T = 60 kcal mol^{-1})[17] to be 6.3x 10^9 M^{-1} s^{-1} in benzene at 295K.
21. K. Sandros, *Acta. Chem. Scand.*, **1964**, *18*, 2355.
22. T. Arai and K. Tokumaru, *Chem. Rev.*, **1993**, *93*, 23.

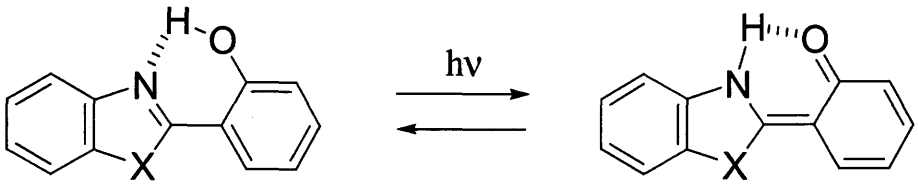

X = O : **1**

S : **2**

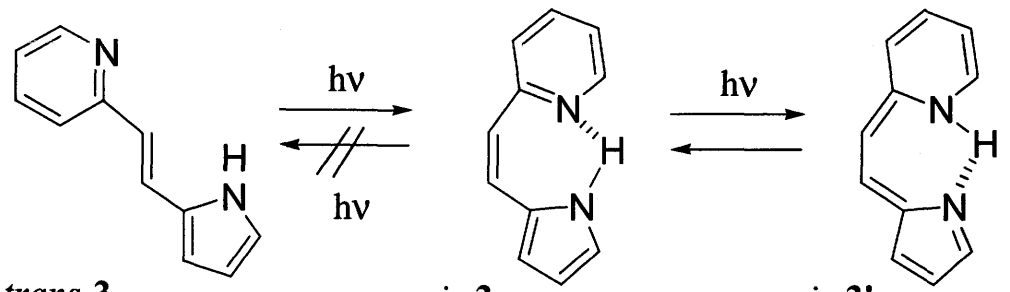

trans-**3** *cis*-**3** *cis*-**3'**

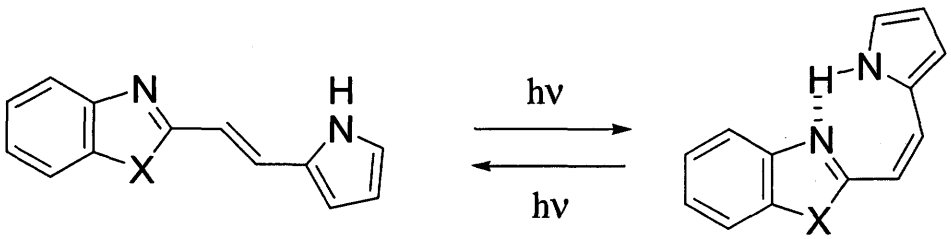

X = O : **4**

S : **5**

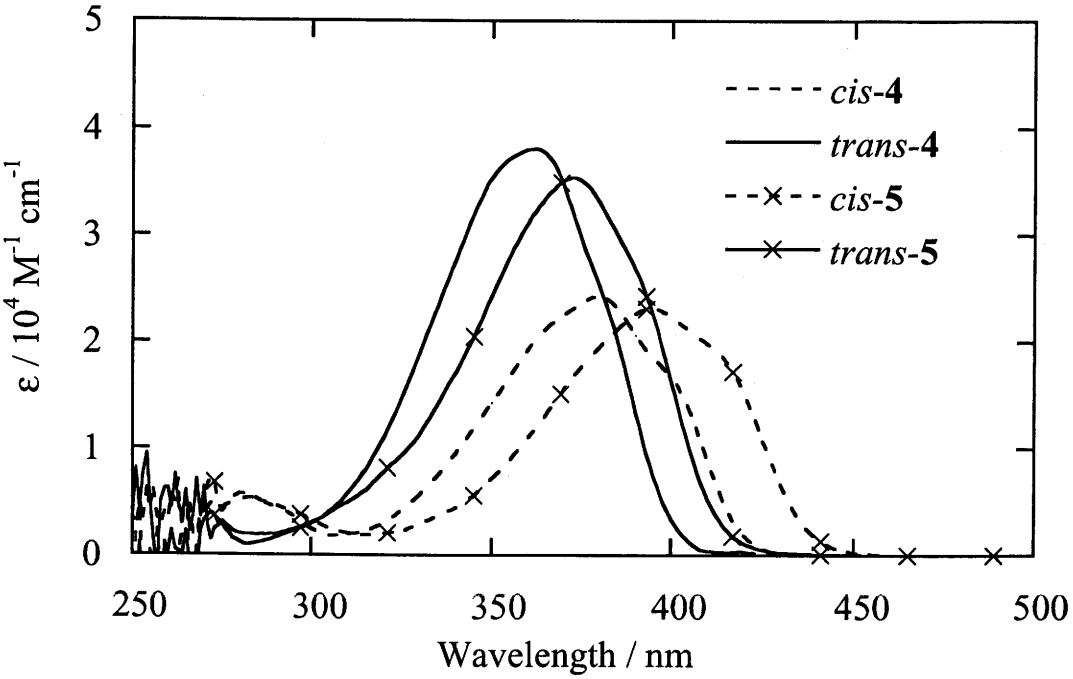

Figure 1. Absorption spectra of **4** and **5** in benzene at room temperature.

Table 1. Molar extinction coefficient of λ_{max} of absorption spectra of **4** and **5**

	$\lambda_{max}{}^{a}$ (ε^{b})			
solvent	*trans*-**4**	*cis*-**4**	*trans*-**5**	*cis*-**5**
methylcyclohexane	356 (4.1)	379 (2.9)	365 (4.4)	394 (2.7)
benzene	362 (3.9)	380 (2.4)	373 (3.5)	394 (2.3)
acetonitrile	356 (4.0)	371 (2.7)	369 (3.6)	386 (2.4)
methanol	363 (4.4)	373 (2.9)	378 (3.4)	388 (2.2)
DMSO	368 (3.5)	379 (2.3)	388 (3.9)	393 (2.6)
water	363	366		

a) in nm b) in 10^4 M^{-1} cm^{-1}

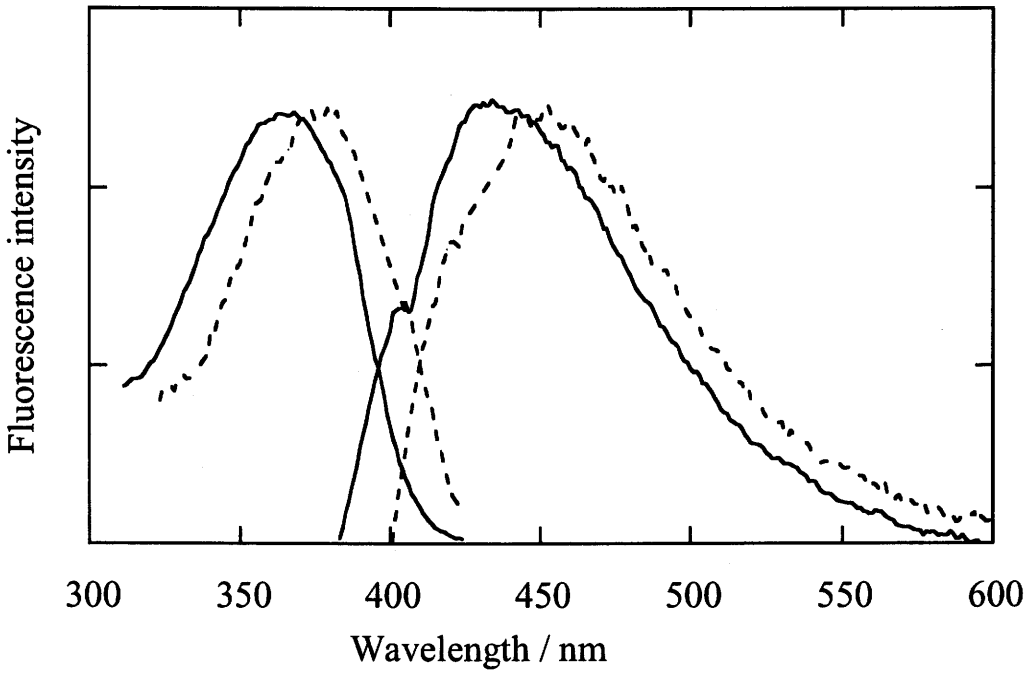

Figure 2. Fluorescence and fluorescence excitation spectra of *trans*-**4** (solid line) and *cis*-**4** (dashed line) in benzene at room temperature.

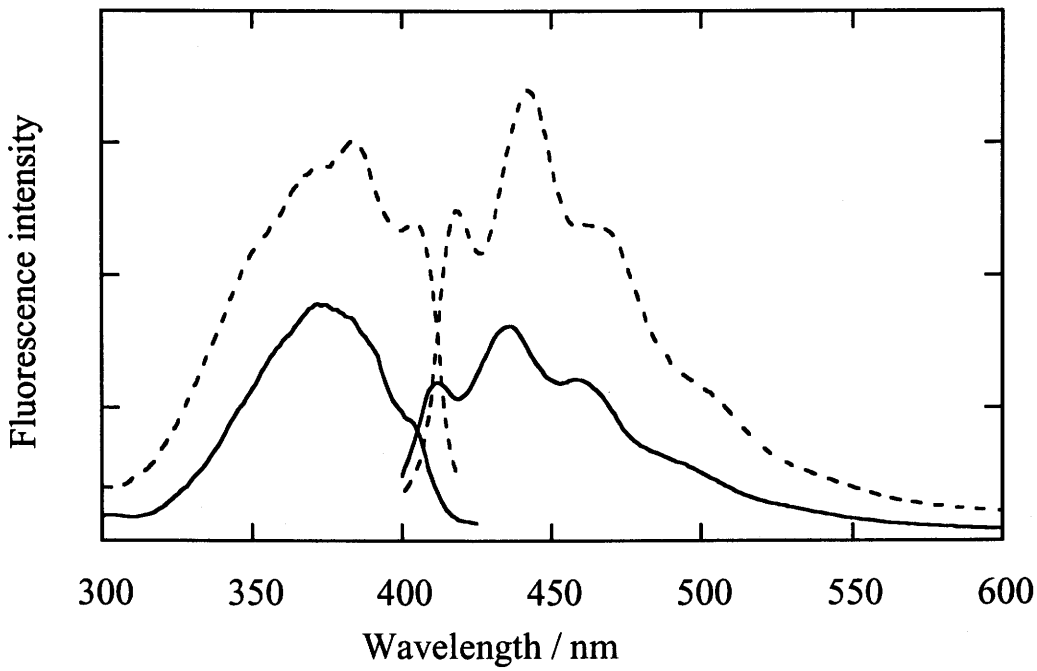

Figure 3. Fluorescence and fluorescence excitation spectra of *trans*-**4** (solid line) and *cis*-**4** (dashed line) in methylcyclohexane at 77K.

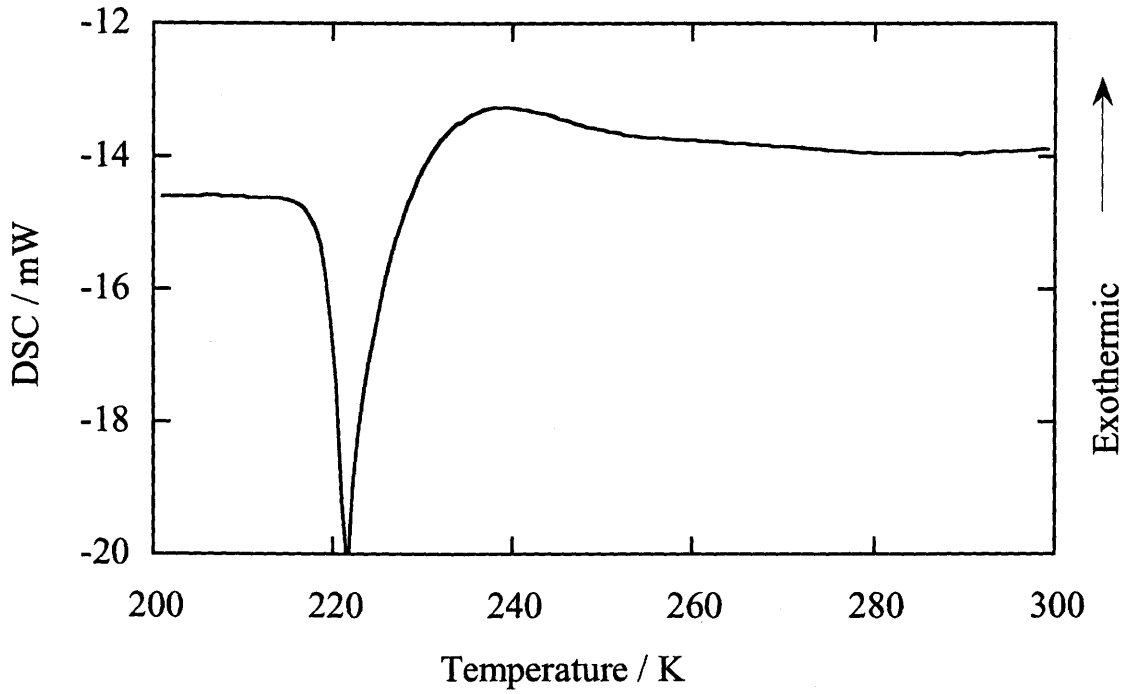

Figure 4. DSC thermogram obtained for *trans*-**4** at rising rate of temperature of 7°C min^{-1}.

Table 2. Quantum yield of isomerization and photostationary state isomer ratio of **4** and **5** determined on irradiation at 366 nm at room temperature.

	solvent	$\Phi_{t\rightarrow c}$	$\Phi_{c\rightarrow t}$	$([c]/[t])_{PSS}$ found	$([c]/[t])_{PSS}$ calcd
	methylcyclohexane			71/29	
4	benzene	0.64	0.41	71/29	73/27
	methanol	0.54	0.48	65/35	63/37
	acetonitrile			70/30	
	benzene	0.71	0.37	81/19	83/17
5	methanol	0.64	0.44	76/24	73/27
	acetonitrile	0.72	0.40	71/29	77/23

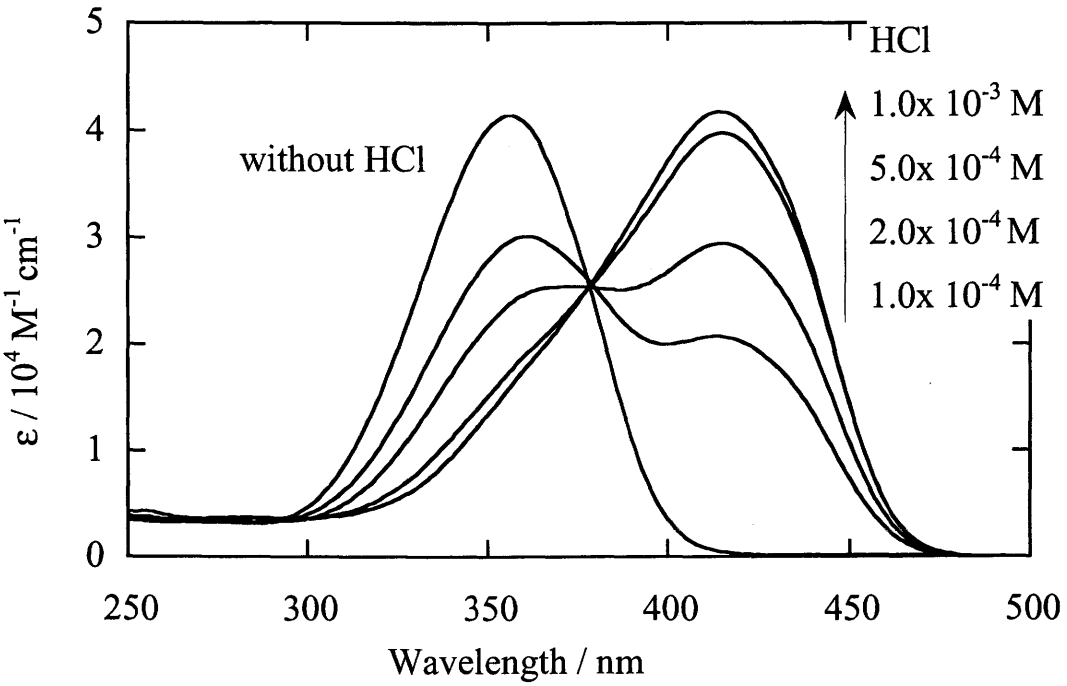

Figure 5. Absorption spectra of *trans*-**4** in the presence of HCl in acetonitrile.

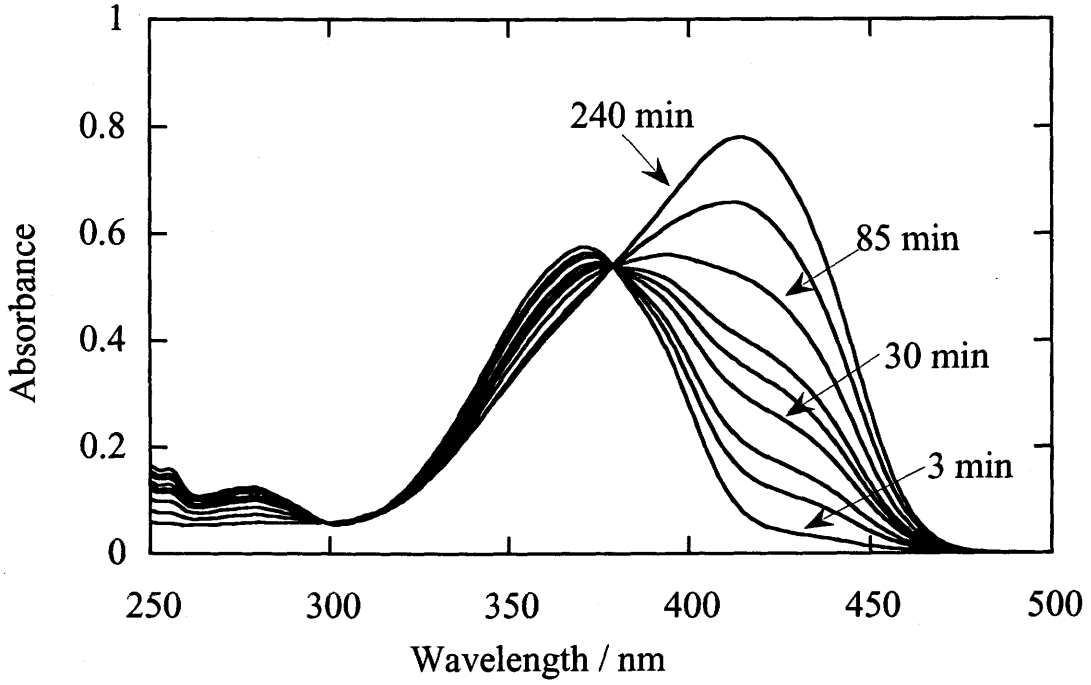

Figure 6. Change of the absorption spectrum of *cis*-**4** (2.0x 10^{-5} M) in the presence of HCl (1.0x 10^{-3} M) at 299K.

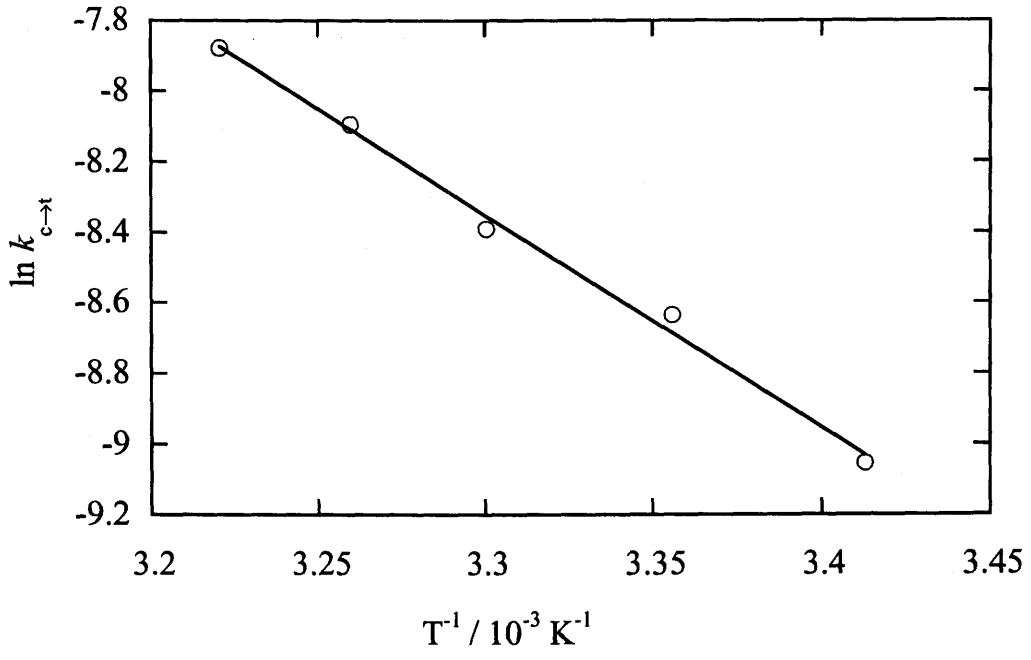

Figure 7. Arrhenius plot for the cis-to-trans thermal isomerization of *cis*-**4** (2.0x 10^{-5} M) in the presence of HCl (1.0x 10^{-3} M).

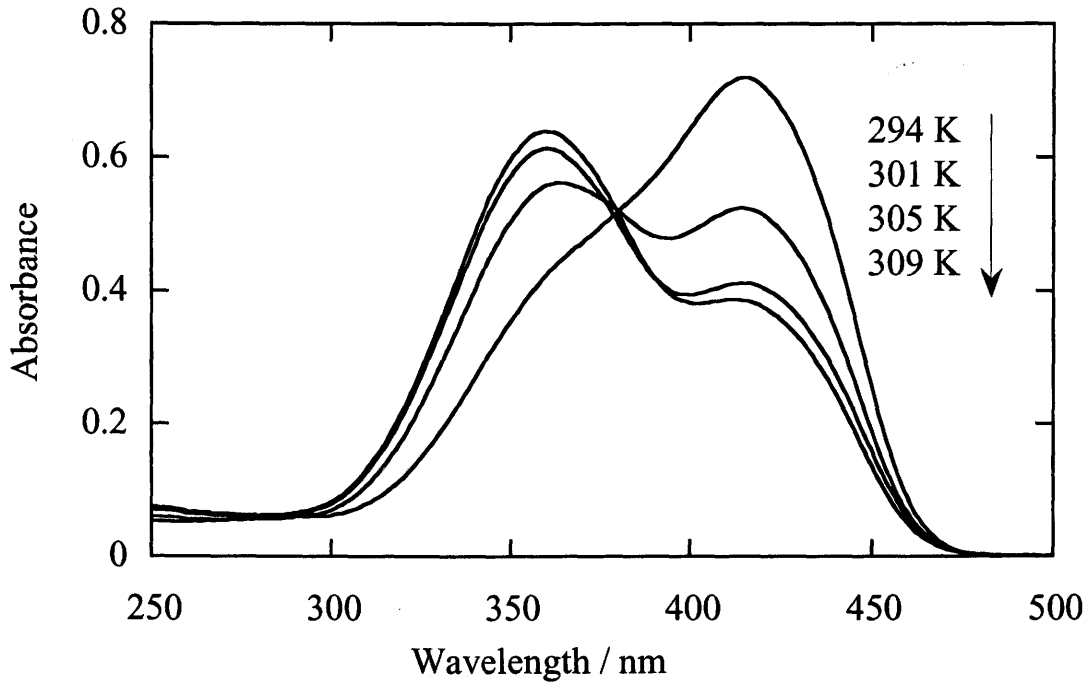

Figure 8. Effect of temperature on the absorption spectrum of *trans*-**4** (2.0×10^{-5} M) in the prescence of HCl (2.0×10^{-4} M) in acetonitrile.

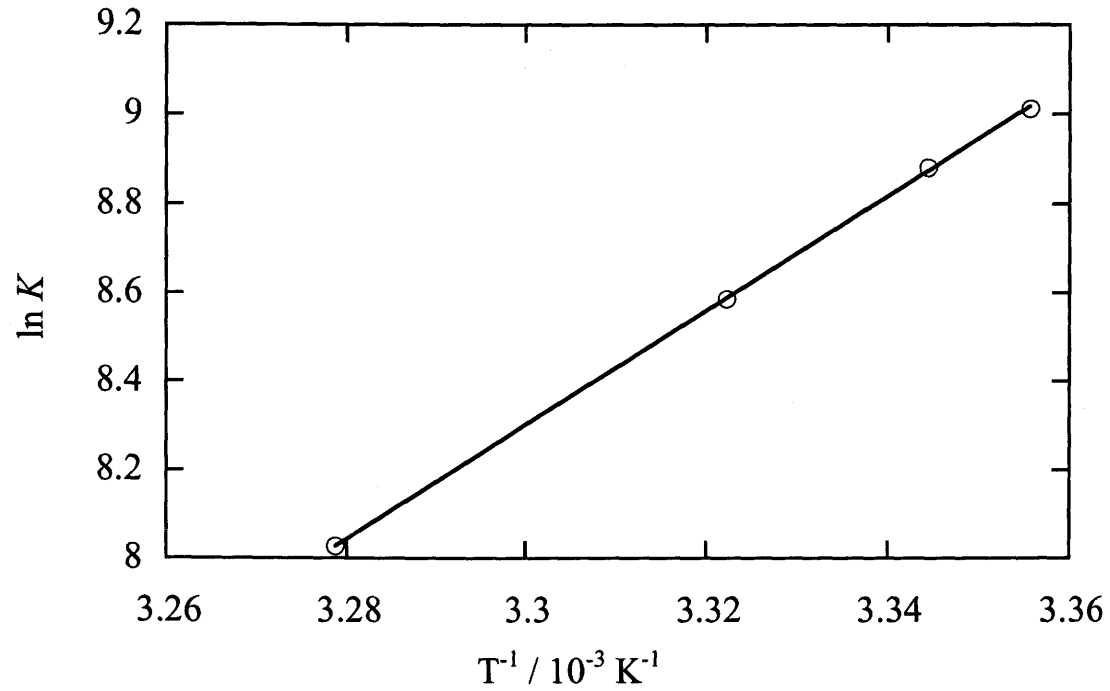

Figure 9. The van't Hoff plot for the equilibrium between *trans*-**4** (2.0x 10^{-5} M) and *trans*-**4**-H^+ in the presence of HCl (2.0x 10^{-4} M) in acetonitrile.

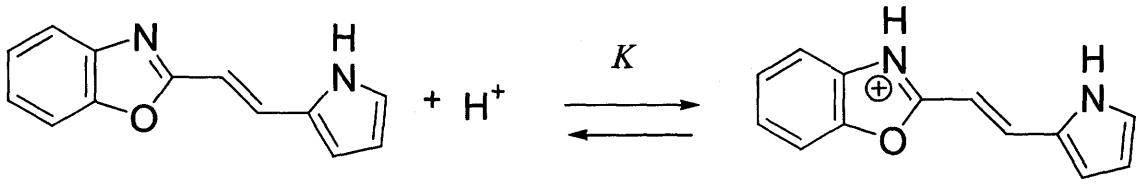

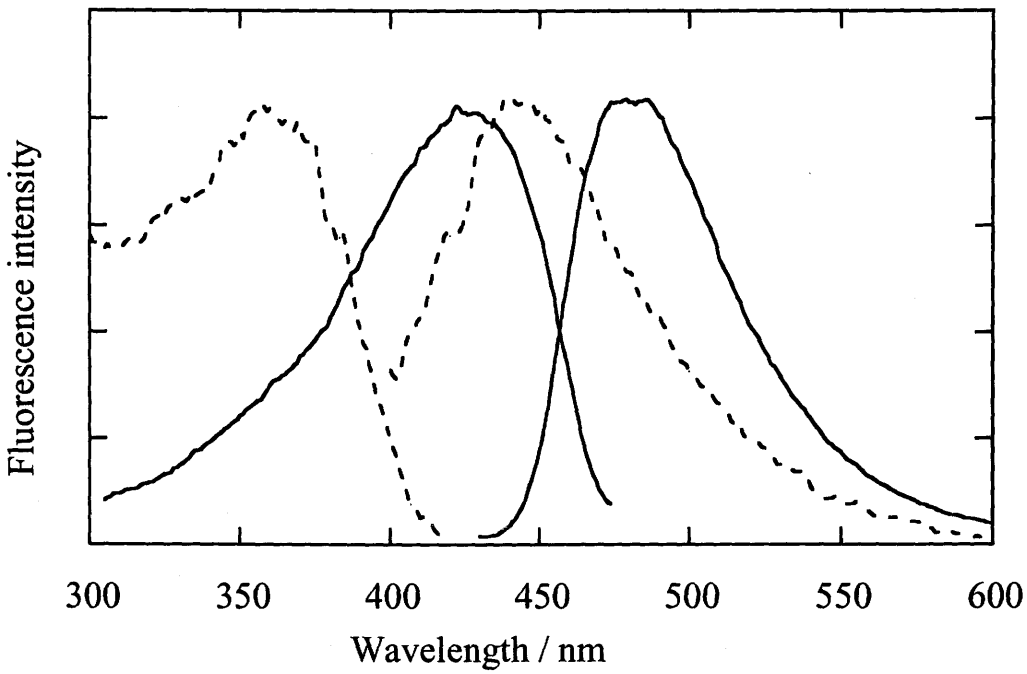

Figure 10. Fluorescence and fluorescence excitation spectra of *trans*-**4** in the absence of HCl (dashed line) in the presence of HCl (1.2×10^{-2} M) in acetonitrile.

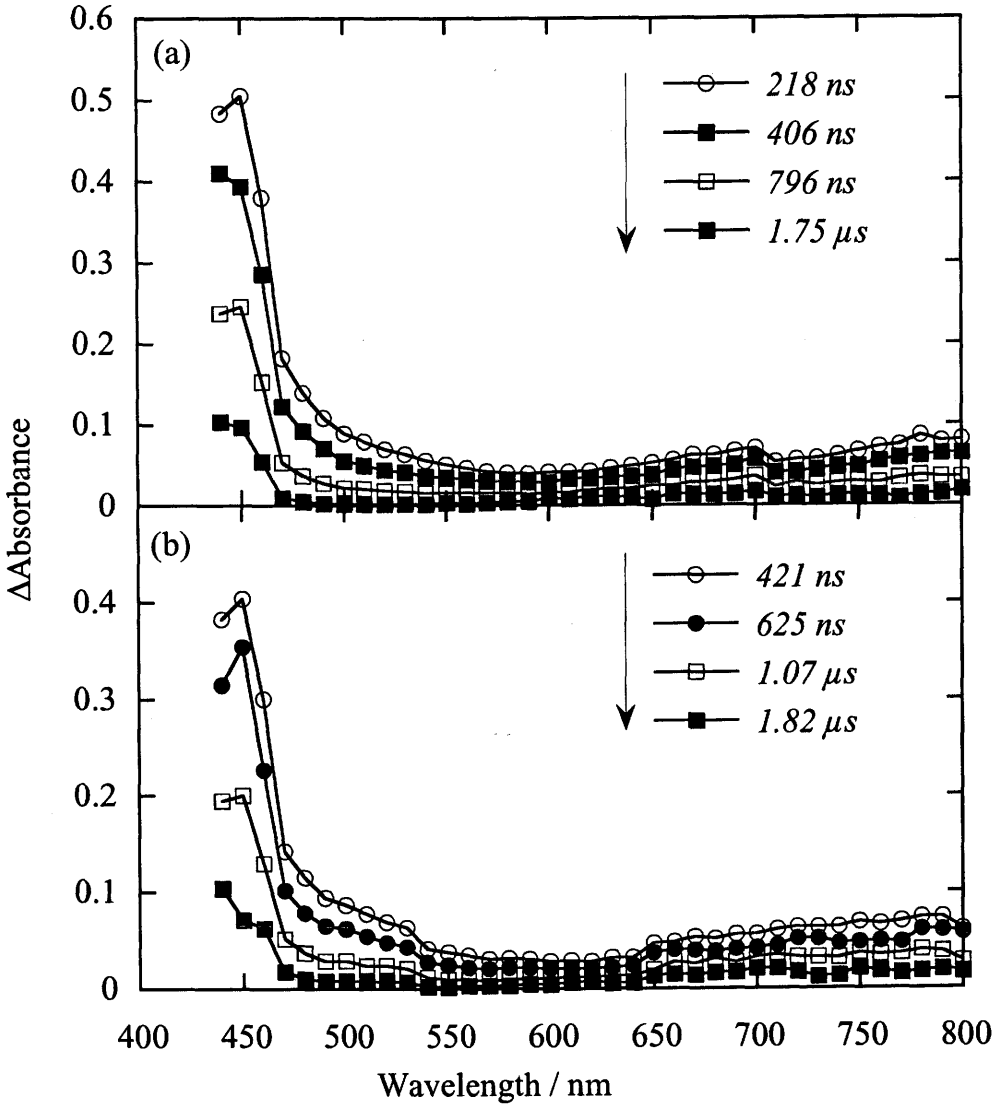

Figure 11. Transient absorption spectra of *trans*-**4** (a) and *cis*-**4** (b) observed on biacetyl sensitization. [**4**] = 2x 10^{-3} M, [biacetyl]=0.07 M in benzene. Excitation wavelength was 425 nm.

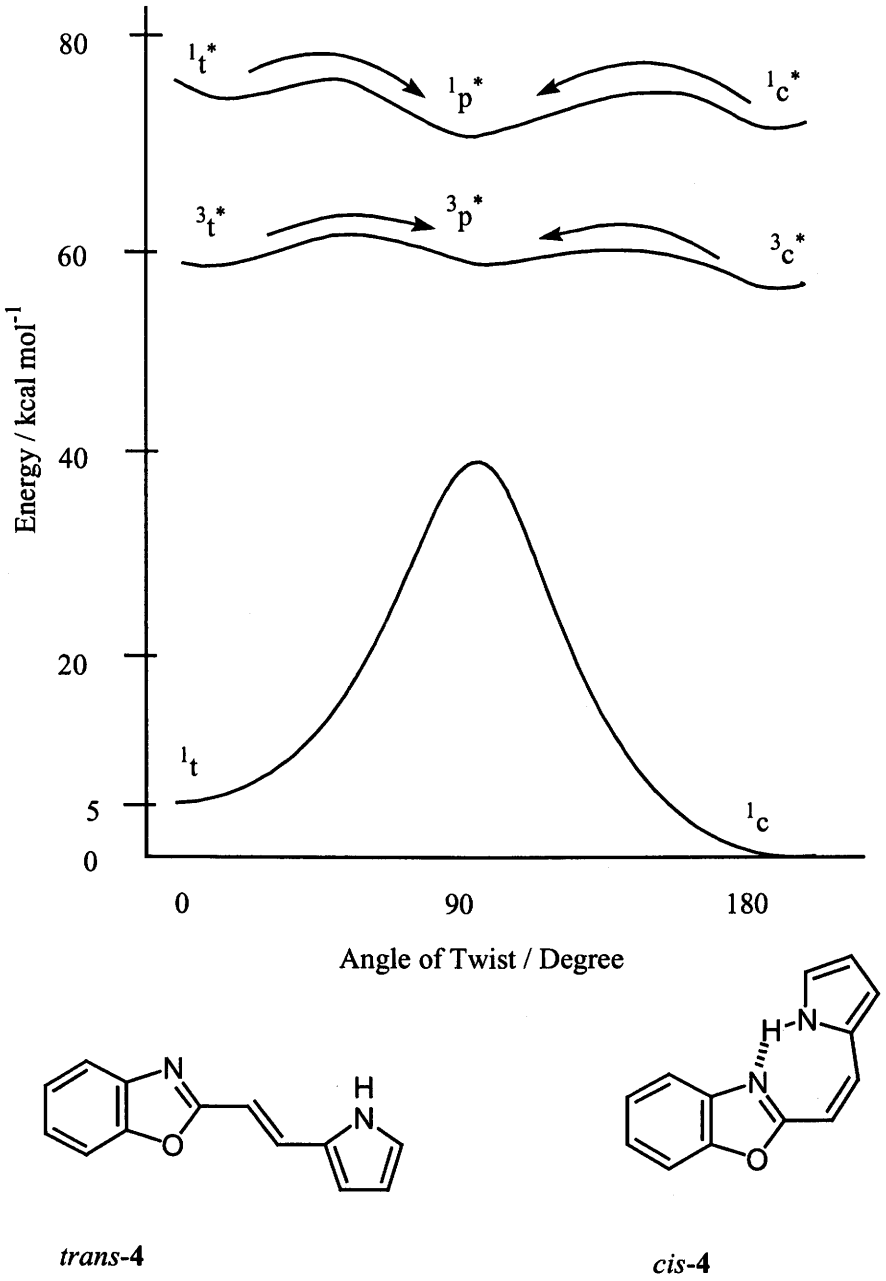

Figure 12. Potential energy surface of isomerization of **4** in benzene.

Chapter 2

Photoinduced Intramolecular Hydrogen Atom Transfer in 2-(2-Hydroxyphenyl)benzoxazole and 2-(2-Hydroxyphenyl)benzothiazole

Abstruct

2-(2-Hydroxyphenyl)benzoxazole and 2-(2-hydoroxyphenyl)benzothia -zole underwent hydrogen atom transfer to give the tautomer in both singlet excited state and triplet excited state. In the singlet excited state, keto form produced by excited state hydrogen atom transfer underwent isomerization around quasi-double bond to give *trans*-keto tautomer. In the triplet excited state, HBO and HBT were equilibrated between *cis*- and *trans*-keto form and the equilibrium constant was determined by triplet sensitization and quenching experiment by using laser flash photolysis in benzene at room temperature. From these results, we have revealed the energy diagram of the hydrogen atom transfer reaction of HBO and HBT both in the singlet excited state and the triplet excited state.

Introduction

The excited state intramolecular proton or hydrogen atom transfer (ESIPT) reaction has received considerable attention from the view point of reaction dynamics and the possibility of the applications of photostabilizers, proton transfer laser, etc.[1-4] The mechanism of ESIPT reaction is usually described by four level scheme involving the singlet excited states of the normal form and the tautomer form and those in the ground state.

The ESIPT reaction of 2-(2-hydroxyphenyl)benzoxazole (HBO) and 2-(2-hydroxyphenyl)benzothiazole (HBT) was extensively investigated.[5-17] HBO and HBT underwent intramolecular hydrogen atom transfer not only in the singlet excited state but also in the triplet excited state.[8,12,13]

In the singlet excited state, HBO and HBT gave tautomer exhibiting fluorescence emission with large Stokes shift, where the maximum wavelength was observed at 500 nm and 520 nm for HBO and HBT, respectively in non-polar solvents. In addition, HBO and HBT exhibited transient absorption spectra with maximum wavelength of 430 and 450 nm, respectively. From the results of TSLIF (two step laser induced fluorescence) and the effect of temperature on the intensity of tautomer emission, the observed transient species in the ground state was assigned to the *trans*-keto form, which was produced by cis-to-trans isomerization of the *cis*-keto form in the singlet excited state.[8,10,14,15]

As to the photochemical behavior in the triplet excited state, HBO exhibited T-T absorption in non polar solvent. In addition, dual phosphorescence spectra were observed in HBO and HBT in cryogenic temperature.[13,15,16] In HBO, the observation of nearly temperature-independent ratio of two phosphorescence was explained by the approximately isoenergetic relation of enol and keto form in the triplet excited state.[13]

However, the potential energy diagram of ESIPT of HBO and HBT at room temperature was still uncertain.

In this study, the equilibrium constant between enol and keto-form in the triplet excited state of HBO and HBT was estimated by laser flash photolysis on triplet sensitization and quenching method. In addition, we synthesized model compound of the tautomer of HBT, and its photochemical behavior was examined. Thus, we can clearly observe the cis-trans isomerization of the keto-form of HBO and HBT in the excited state and can estimate the quantum yield of formation of *trans*-keto form in the ground state. Furthermore, we have revealed the potential energy diagram of hydrogen atom transfer of HBO and HBT.

Experiment

Materials and Solvents

2-(2-Hydroxyphenyl)benzoxazole (HBO) and 2-(2-hydroxyphenyl) -benzothiazole (HBT) were obtained from TCI (Tokyo Kasei) and purified by silica gel column chromatography and recrystilization from ethanol.

2-(2-Methoxyphenyl)benzoxazole (MBO) and 2-(2-methoxyphenyl)-benzothiazole (MBT) were prepared from HBO and HBT by the reaction with dimethylsulfate in dioxane in the presence of aqueous NaOH.

2-Phenylbenzoxazole (BO) and 2-phenylbenzothiazole (BT) were purchased from Aldrich and purified by silica gel column chromatography and recrystilization from ethanol.

6-[*N*-methyl-2(3H)-benzothiazolylidene]cyclohexa-2,4-dieneone (NBT) was synthesized according to a procedure similar to that reported by Nagaoka et

al.[9,18]

In spectroscopy, Dotite Spectrosol or Luminasol were used as solvents without further purification.

Measurement

Absorption and fluorescence spectra were measured on a JASCO Ubest-55 and on a Hitachi F-4000 fluorescence spectrometer, respectively.

Laser flash photolysis was performed by using an eximer laser (Lambda Physik LPX-100, 308 nm, 20 ns fwhm) or excimer laser pumped dye laser (Lambda Physik LEXtra-100, 308 nm, 20 ns fwhm and Lambda Physik Scanmate; Lambda Physik LPX-100, 308 nm, 20 ns fwhm and Lambda Physik FL-4002, 10 ns fwhm). Stilbene 3, DMQ, and QUI were used as laser dyes to obtaind 425 nm, 366 nm, and 399 nm laser pulse, respectively. A pulsed xenon arc (Ushio UXL-159) was used as a monitoring light source.

Results

Absorption and Fluorescence Spectra

Absorption and fluorescence spectra of HBO and HBT in benzene were shown in Figure 3. The quantum yield of the tautomer fluorescence was determined to be 0.02 and 5×10^{-3} in benzene for HBO and HBT, respectively.

The effect of temperature on the quantum yield of fluorescence emission in benzene was examined. Fluorescence quantum yield of the tautomer emission increased with decreasing temperature in benzene from 0.013 at 40°C to 0.035 at 7°C indicating that the deactivation pathway with activation energy exists in the singlet excited state of the tautomer. The temperature effect on the

fluorescence intensity was also reported in some hydrocarbon solvents.[6,17]

Transient Absorption Spectra on Direct Irradiation

HBO and HBT exhibited transient absorption spectra with maximum wavelength of 430 and 450 nm, respectively on 308 nm excitation as shown in Figure 4. The transient absorption spectra of HBO shifted to the shorter wavelength with the time and the maximum wavelength appeared around 400 nm just after the laser pulse, which had lifetime of 2.5 μs at room temperature and was not quenched by oxygen. Therefore, this transient species can be assigned to the tautomer form. We have observed negative temperature effect on the lifetime of this transient in methylcyclohexane as shown in Figure 5. Thus, the lifetime increased with increasing temperature. In addition, the transient absorption with maximum of 360 nm was observed in benzene (Figure 4a), which was assigned to the triplet state by oxygen quenching experiments, where the quenching rate constant was determined to be 3×10^9 M^{-1} s^{-1}. The spectra and the lifetimes of transient absorption were similar to those in other hydrocarbon solvent.[5]

Conformation and absorption spectrum of NBT, a model compound of tautomer

In order to assign the conformation of the model compound NBT, COSY and NOESY spectra were measured in methanol-d_4. The two peaks at 8.05 and 7.67 ppm showed NOE with N-CH_3 proton (4.29 ppm) indicating that NBT exists in trans conformation in the ground state.[18]

The absorption spectrum of *trans*-NBT appeared with the maximum wavelength at 460 nm with molar extinction coefficient of 7000 in benzene as

shown in Figure 6. *trans*-NBT did not give fluorescence emission in benzene at room temperature.

Laser photolysis of NBT

Laser flash photolysis of NBT was performed in benzene. Immediately after excitation with 308 nm laser pulse, the bleaching of the absorption maximum at 460 nm and the intense absorption band at 520 nm were observed as shown in Figure 7. The recovery at 460 nm and the decay at 520 nm gave the same time constant of 110 ns. This result indicates that *trans*-NBT underwent trans-to-cis isomerization photochemically followed by reverse cis-to-trans isomerization thermally in benzene with the time constant of 110 ns.

In addition, we can estimate the molar extinction coefficient at the maximum wavelength to be 7000 for both trans and cis isomers, since the intensity of transient absorption band (510 nm) was just the same as negative intensity of the 460 nm band as shown in Figure 7.

Two Step Laser Excitation of HBO

After we produced the tautomer of HBO by 308 nm laser pulse with laser flash photolysis, the second pulse of 425 nm laser was irradiated with appropriate delay time. In the time profile of transient absorption, we can observe the bleaching of *trans*-keto form at 430 nm, with the concomitant recovery of enol form at 344 nm under argon as shown in Figure 8.

Determination of the quantum yield of formation of the tautomer form

Quantum yield of formation of tautomer form was estimated in benzene by comparing the ΔOD value of the tautomer form of HBO and HBT with ΔOD

of T-T absorption of optically matched benzophenone solution at 308 nm, assuming that the molar extinction coefficient of the tautomer was considered to be the same as that of NBT.[6] The molar extinction coefficient of benzophenone in the triplet excited state at 530 nm was reported to be 7220.[19] Thus, the quantum yield of formation of the tautomer was estimated to be 0.2 and 0.4 for HBO and HBT, respectively at room temperature in benzene.

Transient absorption spectra of BO, BT, MBO, MBT and quantum yield of intersystem crossing

Transient absorption spectra of BO, BT, MBO, and MBT were summarized in Figure 9. The intense band was observed at around 400 nm and the lifetime of transient absorption spectra were determined to be 10 μs under argon atmosphere. The transient absorption spectra were assigned to the enol form, since they could not undergo tautomerization.

The triplet energies of these compounds were estimated by the observation of the triplet energy transfer from sensitizer to quencher. The rate constant (k_q) from Michler's ketone (E_T = 65.8 kcal mol^{-1})[20] to HBO and MBO were 3.7x 10^9 and 3.6x 10^9 M^{-1} s^{-1}, respectively, thus the triplet energy was estimated to be 66 kcal mol^{-1} for both HBO and MBO by using Sandros equation (1),[23] which can be applied in the case that the energy transfer process is isoenergetic or slightly endothermic. The value of ΔE_a was stood for the energy difference between the sensitizer and the quencher and the k_{diff} was 6.3x 10^9 M^{-1} s^{-1} in the case.[12,21,22]

$$k_q = k_{diff} \exp(-\Delta E_a/RT)/[1+\exp(-\Delta E_a/RT)] \quad (1)$$

On the other hand, triplet state of Michler's ketone was quenched by BO, MBT and HBT with diffusion controlled rate constant, however, the lifetime of biacetyl triplet (E_T = 56 kcal mol^{-1})[20] was not affected by BO, MBO and MBT. On the basis of these results, the triplet energy of the enol form of HBT was estimated to be ca. 60 kcal mol^{-1}.

The quantum yields of intersystem crossing (Φ_{isc}) were estimated by comparing ΔOD of T-T absorption spectrum of optically matched solution on benzophenone sensitization (λ_{ex} = 360 nm). The concentration of quencher was 0.01 M and one can expect that triplet energy transfer occurred within the laser pulse of 20 ns. Triplet energies and quantum yields of intersystem crossing were summarized in Table 1.

We should mention here the previously reported arguments about the lack of intersystem crossing for HBT and BT. Both HBO and HBT underwent hydrogen atom transfer to give the *cis*-keto form in the excited singlet state. The *cis*-keto form of HBT did not undergo intersystem crossing to the triplet state,[6] while HBO underwent intersystem crossing to the triplet state. It was reported that only a weak T-T absorption spectrum with a maximum at 420 - 440 nm was detected at room temperature on direct irradiation of BT.[7] Therefore, the lack of intersystem crossing in HBT was explained in connection with the low efficiency of intersystem crossing in BT by the importance of torsional motion around the single bond to the radiationless deactivation.[6,7] However, we observed the T-T absorption spectra (λ_{max}=400 nm) of BT with quantum efficiency as high as 0.6.

Transient absorption spectra of HBO and HBT on triplet sensitization and the quenching rate constant

The transient absorption spectra observed on benzophenone and Michler's ketone sensitization of HBO and HBT on excitation at 366 nm and 390 nm, respectively at room temperature under argon atmosphere in benzene were shown in Figure 7. In this sensitization experiment, the concentration of HBO and HBT was adjusted to 0.01 M and that of benzophenone and Michler's ketone was adjusted to 0.03 and 0.006 M, respectively. In this experimental condition, the triplet energy transfer should take place within the duration of the laser pulse and just after the laser pulse we can observe the triplet state of HBO and HBT. The lifetime of the triplet state was determined to be 7.4 and 7.5 μs for HBO and HBT, respectively under argon atmosphere in benzene. These transient absorption spectra were quenched by oxygen with the rate constant of 3×10^9 M^{-1} s^{-1}.

The spectral profiles of MBO and MBT are similar to those of BO and BT, but the absorption maximum slightly shifted to the longer wavelength and appeared at 420 nm. However, the T-T absorption spectra of HBO and HBT observed on triplet sensitization (Figure 10) are different from those of MBO and MBT (Figure 9) indicating that the observed triplet states for HBO and HBT are not simply the enol triplet, but the mixture of the enol form ($^3E^*$) and the *cis*-keto form ($^3K^*$). The observed transient absorption spectra can be assigned to either the enol form or the *cis*-keto form in the triplet state.

The quenching rate constants for the HBO triplet by *cis*- (E_T=54.3 kcal mol^{-1}) and *trans*-stilbene (E_T=49.2 kcal mol^{-1}) are determined to be 3.3×10^9 M^{-1} s^{-1} and 4.7×10^9 M^{-1} s^{-1}, respectively for HBO. The quenching rate constants for HBT by *cis*- and *trans*-stilbene are 3.2×10^8 M^{-1} s^{-1} and 1.7×10^9 M^{-1} s^{-1},

respectively and are lower than the values for HBO.

Discussion

Photochemistry of NBT, as a model compound of HBT.

The result of laser flash photolysis of NBT (Figure 7) indicates that *trans*-NBT underwent photochemical trans-to-cis isomerization followed by reverse cis-to-trans isomerization thermally in benzene with the time constant of 110 ns.

In addition, we can estimate the molar extinction coefficient of NBT at the maximum wavelength to be 7000 for both trans and cis isomers, since the intensity of transient absorption band (510 nm) was just the same as negative intensity of the 460 nm band as shown in Figure 7. The absorption maximum of *cis*-NBT appeared at 510 nm which is longer than that of *trans*-NBT by 50 nm, probably due to the change of conjugation character of N-CH_3 group between *trans*- and *cis*-NBT. In *trans*-keto form, the N atom of N-CH_3 group has sp^3 character, and non bonding electron of N atom could not participate in conjugation of π orbital. On the other hand, in *cis*-keto form, N-CH_3 may have sp^2 like character due to the steric hindrance to extend the π conjugation. This hypothesis was suggested by preliminary PM3 calculation.

Potential energy surface of isomerization of *trans*-NBT was shown in Figure 11. The absorption spectrum of the ground state transients observed on laser excitation appeared at 460 nm (Figure 4) is quite similar to that of *trans*-NBT. These results strongly indicate that HBT gave the *trans*-keto form by excited state hydrogen atom transfer in the singlet excited state followed by cis-to-trans isomerization.

Conformation of the tautomer

Since the absorption maximum of *trans*-NBT, the model compound of *trans*-keto form was observed at 460 nm and was shorter than that of *cis*-NBT, the transient observed on laser excitation of HBT (Figure 4b) with the maximum at 460 nm was reasonably assigned to *trans*-keto form. We can also assign the 430 nm transient observed for HBO (Figure 4a) to the *trans*-keto form of HBO. Two step laser excitation also support the assignment of the transient species to the *trans*-keto form in the ground state. The *cis*-keto form could not be observed since fast reverse hydrogen atom transfer can take place within our time resolution of 20 ns in *cis*-keto form due to the presence of an intramolecular hydrogen bonding. The quantum yield of *trans*-keto tautomer formation was thus estimated to be 0.2 and 0.4 for HBO and HBT, respectively.

Equilibrium constant between enol form and cis-keto form in the triplet excited state

We can estimate the equilibrium constant (K=[^{3}K*]/[^{3}E*]) by measuring the rate constant of energy transfer from the transient species to several quenchers.

The triplet energies of the enol form and the *cis*-keto form for HBO are estimated to be 63.8 and 50.0 kcal mol^{-1} and those for HBT are estimated to be 59.3 and 49.2 kcal mol^{-1}, respectively from the phosphorescence spectra as shown in Table 1. Thus, the triplet energies of the enol form of HBO and HBT are higher than those of *cis*- and *trans*-stilbene, while those of the *cis*-keto form are comparable to the triplet energy of *trans*-stilbene.

The observed quenching rate constants of HBT triplet by *trans*-stilbene

(k_q = 1.7x 10^9 M^{-1} s^{-1}) as well as *cis*-stilbene (k_q = 0.32x 10^9 M^{-1} s^{-1}) were smaller than the diffusion controlled rate constant, while the values for HBO are nearly 1/2 of the diffusion controlled rate constant (k_{diff}=6.3x 10^9 M^{-1} s^{-1}). Since *cis*-stilbene can quench the triplet enol form with nearly the diffusion controlled rate constant, but can scarcely quench the triplet *cis*-keto form, we can estimate the equilibrium constant between the enol form and the *cis*-keto form (K=[$^3K^*$]/[$^3E^*$]) by using equation 2. Thus, K is estimated to be 0.91 and 20 for HBO and HBT, respectively.

$$k_q=k_{diff}[^3E^*]/([^3E^*]+[^3K^*])=k_{diff}/(1+K) \qquad (2)$$

Potential energy surfaces of hydrogen atom transfer of HBO and HBT

HBO and HBT exhibited fluorescence spectra with large Stokes shift of 10000 cm^{-1}, which were assigned to the tautomer produced by hydrogen atom transfer in the singlet excited state. In addition, the transient absorption spectra with maximum wavelength of 430 nm and 450 nm were observed, respectively in benzene. Fluorescence quantum yield of the tautomer emission increased with decreasing temperature. This result indicated that the deactivation pathway with activation energy exists in the singlet excited state of the tautomer, therefore *trans*-keto form would undergo trans-to-cis isomerization to give *cis*-keto form.

As to the deactivation from the triplet state, one can expect the cis-trans isomerization of the cis-keto form to give the *trans*-keto form as well as in the singlet excited state. If the *trans*-keto form was produced through the deactivation processes, one could observe its absorption spectra with the

absorption maximum at 430 nm and the lifetime of 7.5 μs. However, we have observed only the T-T absorption spectra under oxygen atmosphere as well as argon atmosphere in benzene at room temperature. Therefore, the deactivation of the triplet state of HBO and HBT took place to give the enol form or the *cis*-keto form: the *cis*-keto form underwent fast reverse hydrogen atom transfer within our time resolution (~20 ns) to give the enol form. Thus, the diabatic as well as adiabatic cis-trans isomerization around the double bond in the *cis*-keto form did not take place in the triplet state. These results are summarized in Figure 12 and Figure 13.

Conclusion

HBO and HBT underwent cis-to-trans isomerization followed by excited state hydrogen atom transfer in the singlet excited state to give *trans*-keto tautomer with the quantum yield of 0.2 and 0.4 for HBO and HBT, respectively. On the other hand, cis-trans isomerization did not occur in *cis*-keto form in the triplet excited state. These results indicated that intramolecular hydrogen bonding is broken in the singlet excited state, but may be present in the triplet excited state.

trans-Keto form produced by cis-trans isomerization followed by ESIPT in the ground state isomerize thermally to *cis*-keto form, which undergoes reverse hydrogen atom transfer within 20 ns. This reverse proton transfer to give enol form in the ground state was also supported by the effect of temperature on lifetime of ground state tautomer exhibiting negative activation energy of Arrhenius plot in methylcyclohexane.

In conclusion, we have revealed the potential energy surface of hydrogen atom transfer of HBO and HBT in the excited state.

References and Notes

1. M. Kasha, *J. Chem. Soc. Faraday Trans. 2*, **1986**, 82, 2379.
2. P. F. Barbara, P. K. Walsh and L. E. Brus, *J. Phys. Chem.*, **1989**, *93*, 29.
3. (a)S. J. Formosinho and L. G. Arnaut, *J. Photochem. Photobiol. A: Chem.*, **1993**, *75*, 1. (b) S. J. Formosinho and L. G. Arnaut, *J. Photochem. Photobiol. A: Chem.*, **1993**, *75*, 21.
4. M. Kasha, J. Heldt, and D. Gormin, *J. Phys. Chem.*, **1995**, *99*, 7281.
5. J. S. Stephan and K. H. Grellmann, *J. Phys. Chem.*, **1995**, *99*, 10066.
6. W. Al-Soufi, K. H. Grellmann, and B. Nickel, *Chem. Phys. Lett.*, **1990**, *174*, 609.
7. P. T. Chou, W. C. Cooper, J. H. Clements, S. L. Studer and C. P. Chang, *Chem. Phys. Lett.*, **1993**, *216*, 300.
8. P. T. Chou, M. L. Martinez, and S. L. Studer, *Chem. Phys. Lett.*, **1992**, *195*, 586.
9. S. Nagaoka, A. Itoh, K. Mukai, and U. Nagashima, *J. Phys. Chem.*, **1993**, *97*, 11385.
10. M. Itoh and Y. Fujiwara, *J. Am. Chem. Soc.*, **1985**, *107*, 1561.
11. G. Yang, F. Morelet-Savary, Z. Peng, S. Wu and J. -P, Fouassier, *Chem. Phys. Lett.*, **1996**, *256*, 536.
12. M. Ikegami and T. Arai, *Chem. Lett.*, **2000**, 996.
13. M. F. Rodriguez Prieto, B. Nickel, K. H. Grellmann, and A. Mordzinski, *Chem. Phys. Lett.*, **1988**, *146*, 387.
14. W. E. Brewer, M. L. Martinez and P. T. Chou, *J. Phys. Chem.*, **1990**, *94*, 1915.
15. P. T. Chou, S. L. Studer and M. L. Martinez, *Chem. Phys. Lett.*, **1991**, *178*, 393.

16. H. Eisenberger, B. Nickel, A. A. Ruth, W. Al-Soufi, K. H. Grellmann, and M. Novo, *J. Phys. Chem.*, **1991**, *95*, 10509.

17. A. Mordzinski and A. Grabowska, *Chem. Phys. Lett.*, **1982**, *90*, 122.

18. NBT: ^{1}H NMR(Methanol-d_4, 600 MHz) δ 4.29 (s, 3H; N-CH_3), 6.66 (m, 1H, J = 7.6 Hz; H_b), 6.86 (d, 1H, J = 8.6 Hz; H_d), 7.39 (m, 1H; H_c), 7.67 (m, 1H; H_f), 7.70 (d, 1H, J = 8.2 Hz; H_a) 7.80 (m, 1H; H_g), 8.05 (d, 1H, J = 8.5 Hz; H_h), 8.13 (d, 1H, J = 7.8 Hz; H_e) ppm.

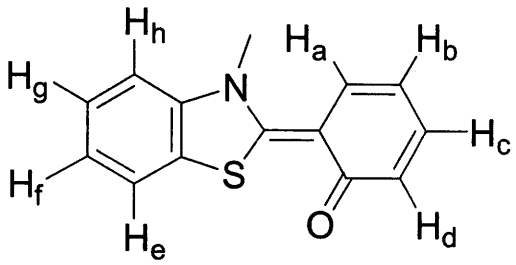

19. R. Bonneau, I. Carmichael, and G. L. Hug, *Pure & Appl. Chem.*, **1991**, *63*, 289.

20. "Handbook of Photochemistry," ed by S. L. Murov, I. Carmichal, and G. L. Hug, Macel Dekker, New York (1993).

21. (a) T. Arai and Y. Norikane, *Chem. Lett.*, **1997**, 339. (b) Y. Norikane, H. Itoh, and T. Arai, *Chem. Lett.*, **2000**, 1094. (c) Y. Norikane and T. Arai, *Chem. Lett.*, **2001**, 416.

22. T. Suzuki, Y. Kaneko, and T. Arai, *Chem. Lett.*, **2000**, 756.

23. K. Sandros, *Acta Chem. Scand.*, **1964**, *18*, 2355.

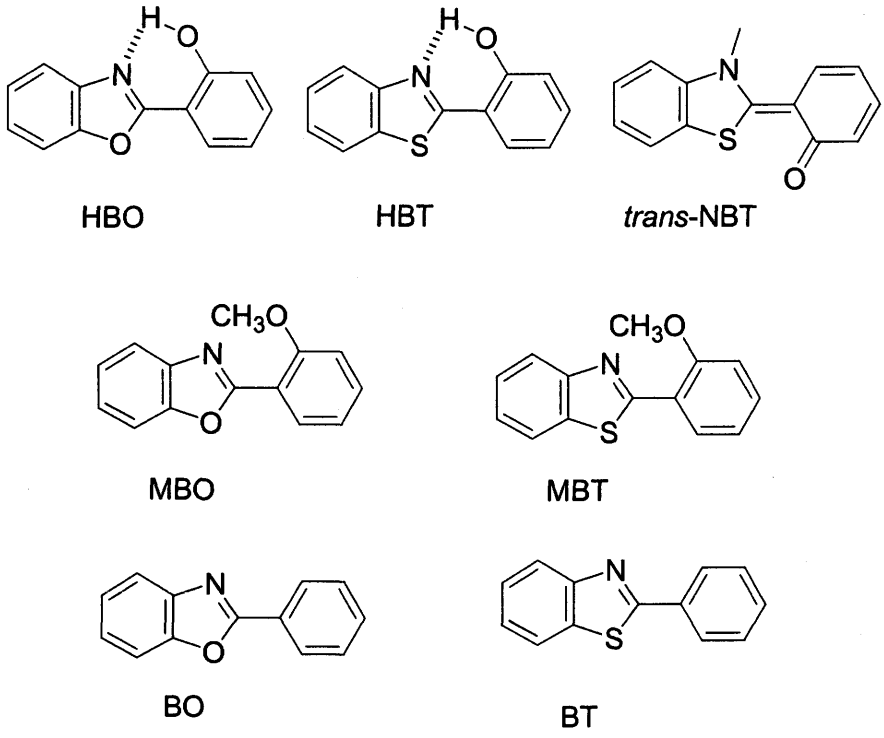

Figure 1. Compounds investigated in this study.

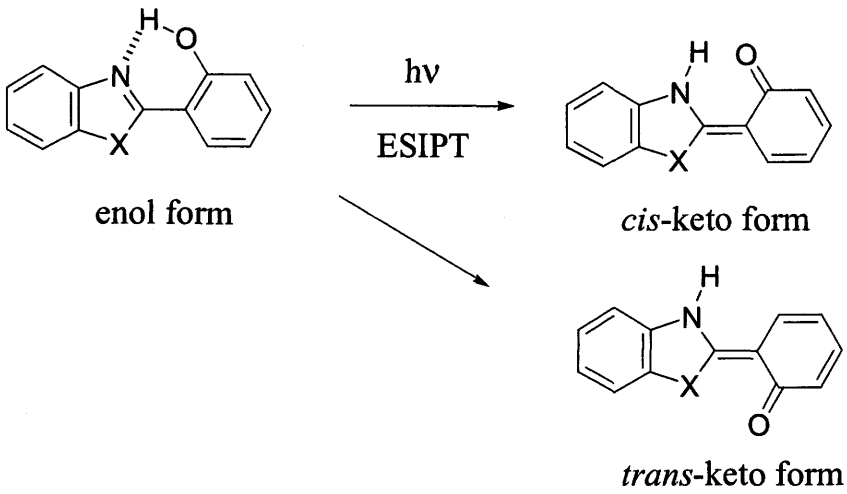

Figure 2. Excited state intramolecular hydrogen atom transfer of HBO and HBT.

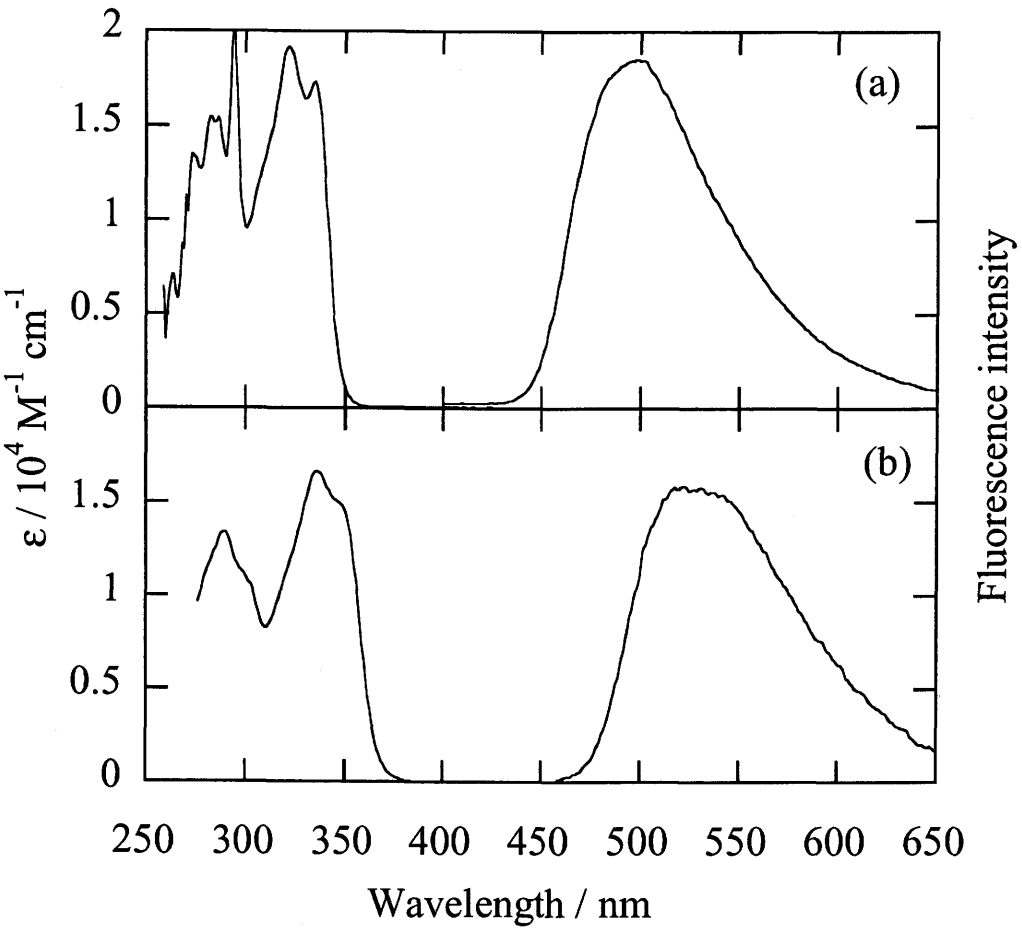

Figure 3. Absorption and fluorescence spactra of HBO (a) and HBT (b) in benzene.

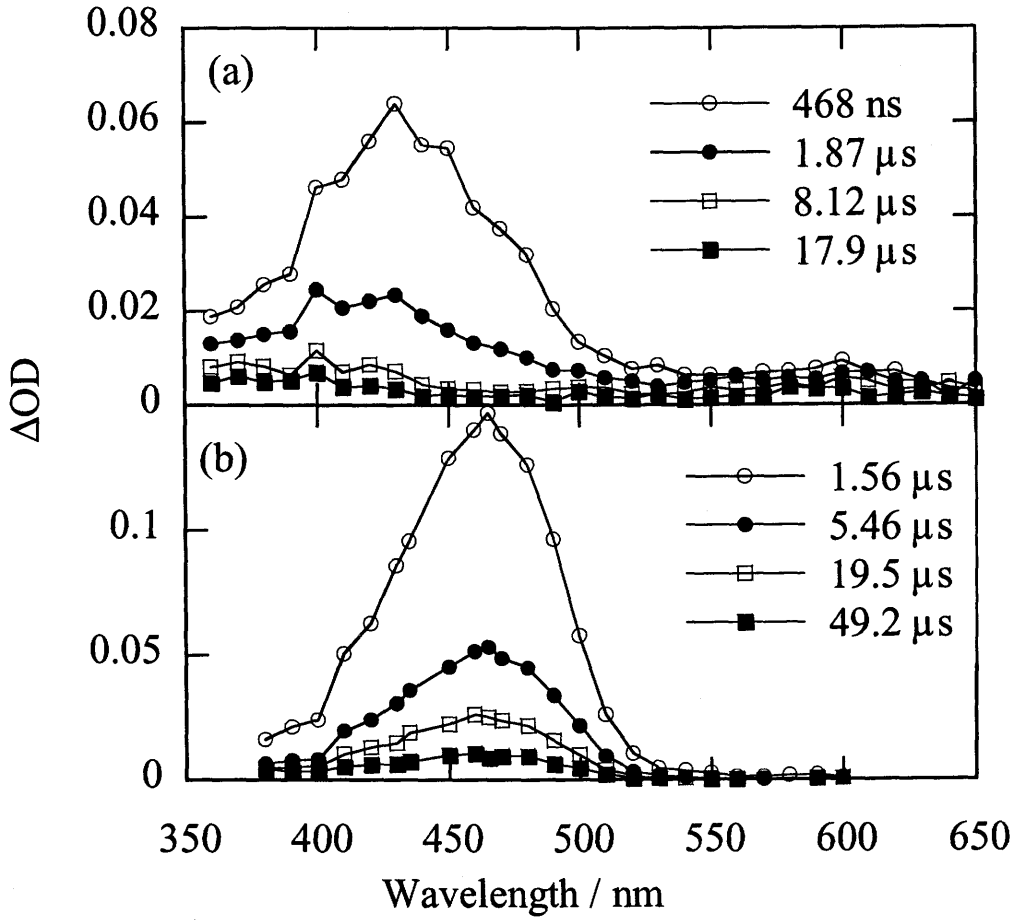

Figure 4. Transient absorption spectra of HBO (a) and HBT (b) in benzene on direct irradiation.

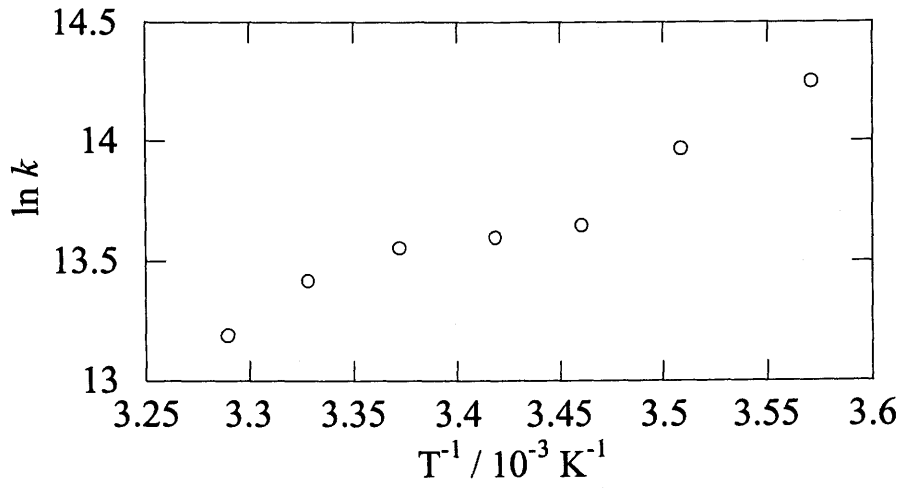

Figure 5. Arrhenius plot for decay constants of HBO tautomer in methylcyclohexane.

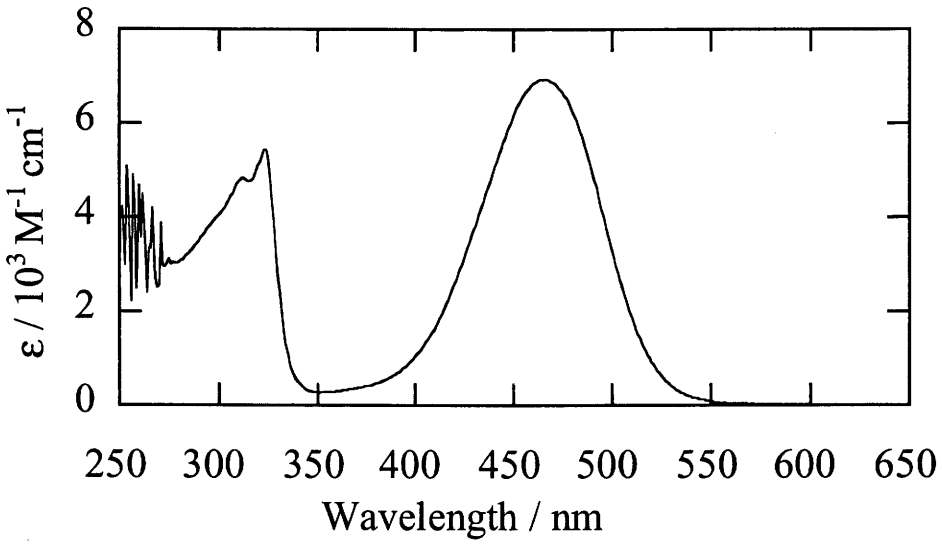

Figure 6. Absorption spectrum of *trans*-NBT in benzene at room temperature.

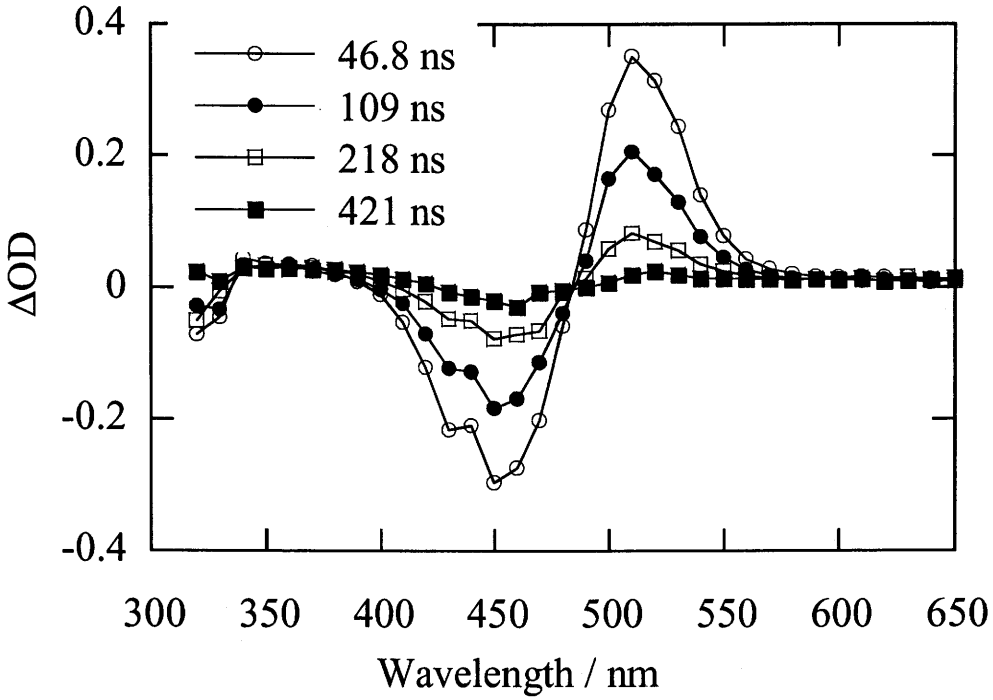

Figure 7. Transient absorption spectra of NBT in benzene at room temperature.

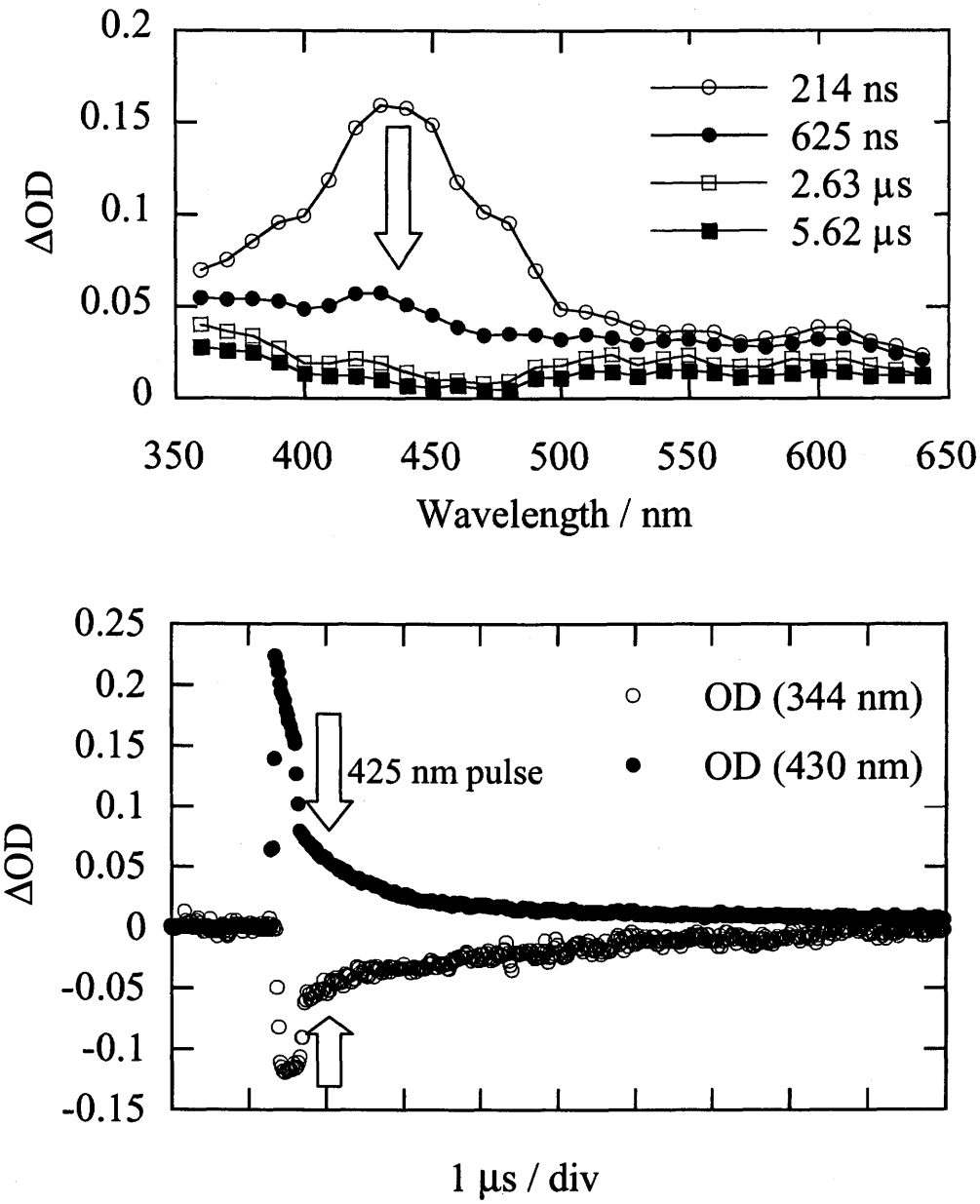

Figure 8. Time profile observed by two step laser excitation (308 and 425 nm) of HBO in benzene.

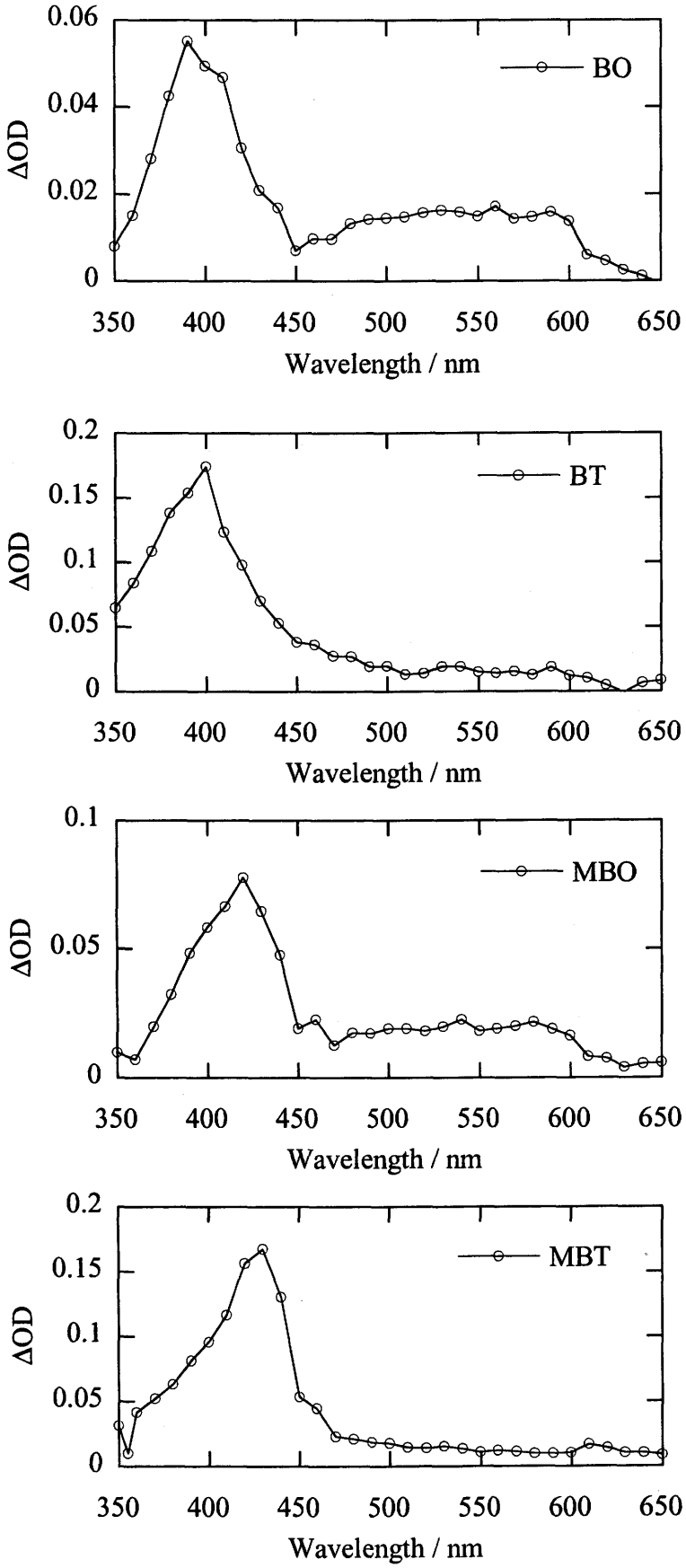

Figure 9. Transient absorption spectra of BO, BT, MBO, and MBT.

Table 1. Photochemical properties of benzoxazole derivatives at room temperature in benzene

	Φ_f [a]	τ_f /ns	Φ_{isc}	E_S [b]	E_T [b]
BO	0.66	1.5	0.13	89	(60)[d]
MBO	0.51	1.2	0.16	85	66[c]
BT	0.01		0.57	87	60[20]
MBT	0.05		0.69	83	(60)[d]
HBO	0.02		0.03	84	66[c]
HBT	5×10^{-3}			80	(60)[d]

a) 2-Phenylbenzoxazole ($\Phi_f = 0.75$ in cyclohexane)[7] used as fluorescence standard.
b) In kcal mol^{-1}.

c) From the quenching rate constant of 4,4'-bis(dimethylamino)benzophenone (**1**) (E_T = 65.8 kcal mol^{-1})[20] triplet by MBO and MBT.

d) Triplet state of 1 was quenched by BO, MBT and HBT with diffusion controlled rate constant. However, the lifetime of biacetyl triplet (E_T = 56 kcal mol^{-1}) was not affected by BO, MBO and MBT.

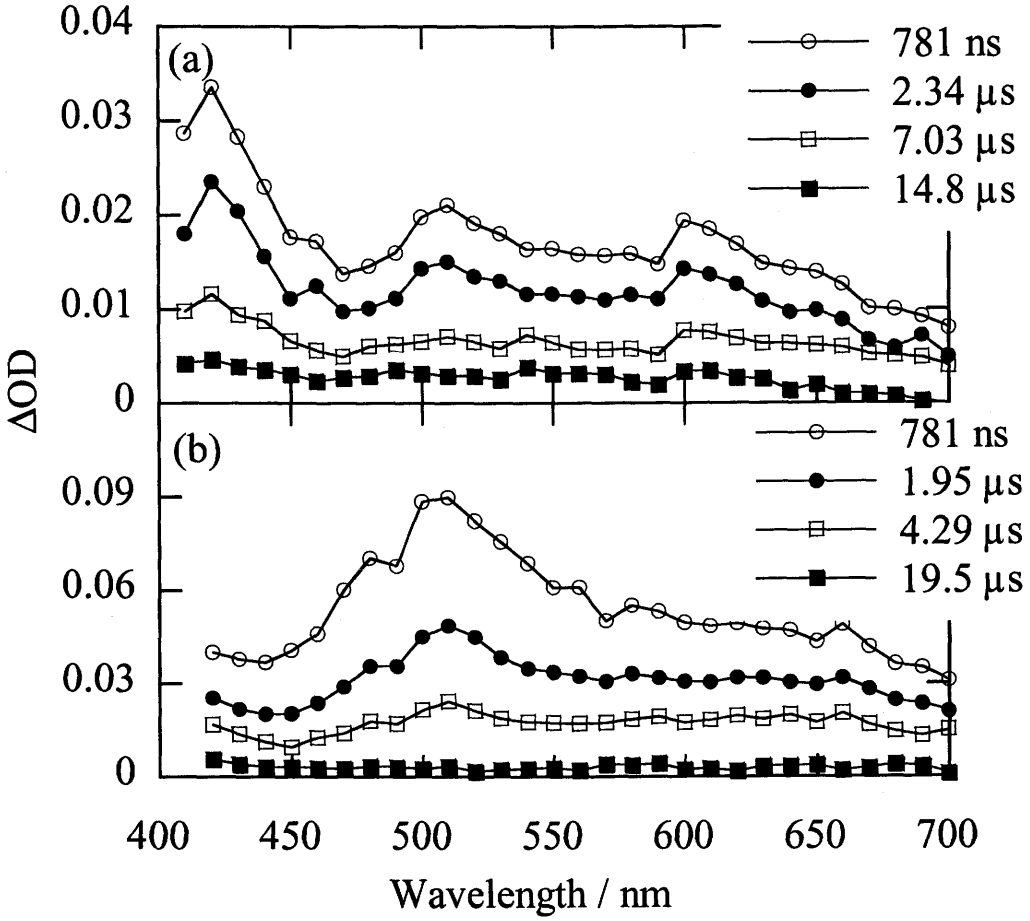

Figure 10. Transient absorption spectra of HBO and HBT on triplet sensitization in benzene.

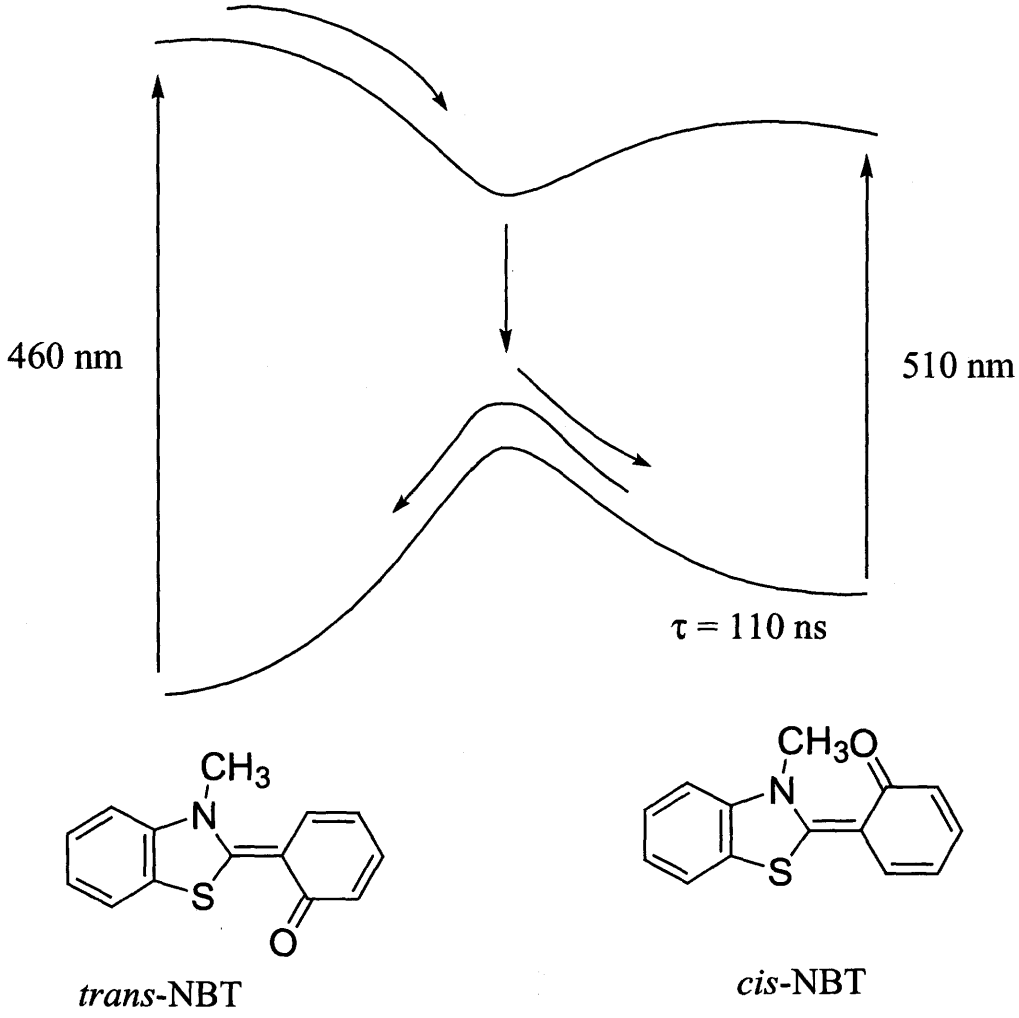

Figure 11. Potential energy surfaces of isomerization of *trans*-NBT in benzene at room temperature.

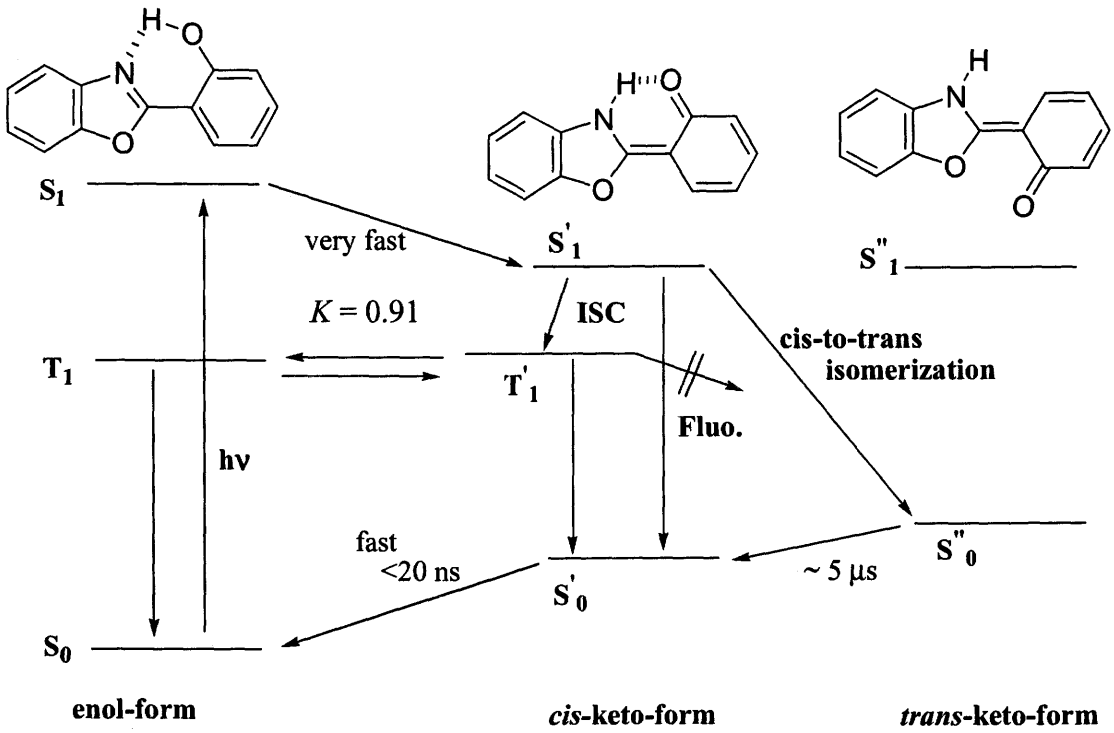

Figure 12. Energy diagram of hydrogen atom transfer of HBO.

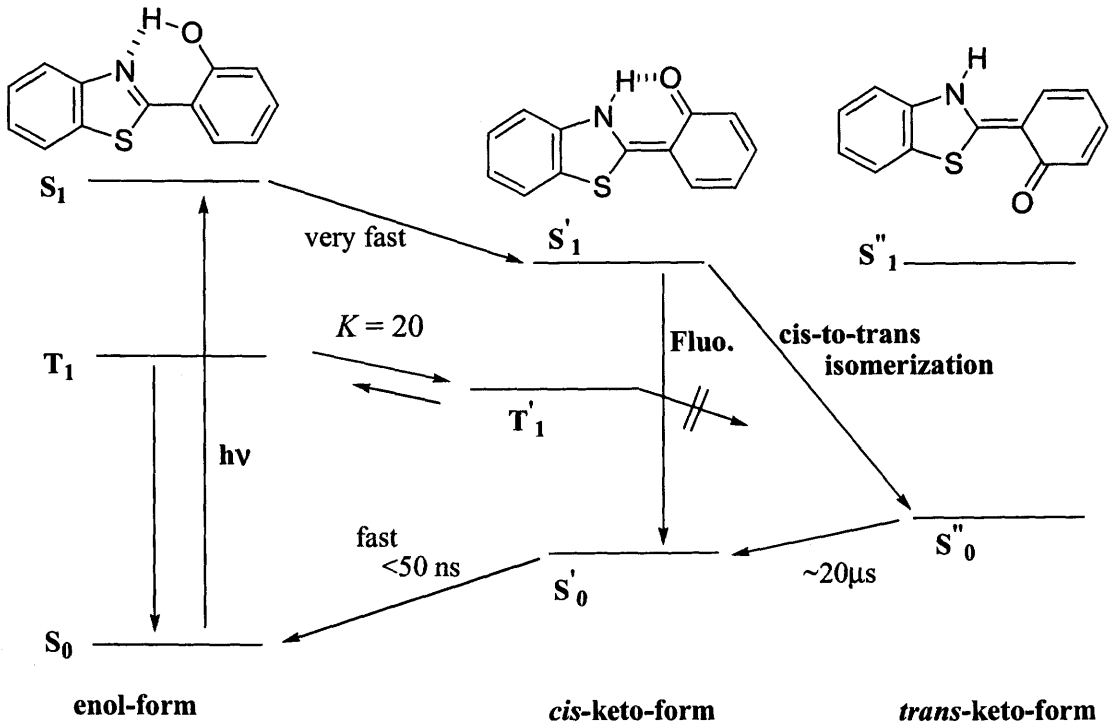

Figure 13. Energy diagram of hydrogen atom transfer of HBT.

Chapter 3

Photochromism and Thermochoromism of Hydrogen Bonded Schiff Bases

Abstract

Photochromic, thermochromic properties of 2-hydroxy-3'-methoxy -salicylideneaniline (**3**) and 2-hydroxy-4'-methoxysalicylideneaniline (**4**) were investigated. Compound **3** and **4** exhibited absorption band at longer wavelength region in methanol than in benzene and in acetonitrile. They underwent thermochromism in methanol to increase the molar extinction coefficient of longer wavelength absorption band with decreasing temperature. On the basis of the above results and the result of transient absorption spectroscopy, it was found that **3** and **4** exhibited photochromism, thermochromism and solvatochromism by hydrogen atom transfer between O atom and N atom even in solution.

Intoduction

It is well known that *N*-salicylideneaniline (**1**) exhibited photochromic and thermochromic properties in crystalline state. The photochromism and thermochromism can be explained by the tautomerization between the enol form and the keto form.[1,2] The X-ray study of the crystal have been performed and the tautomeric keto structure was observed in the colored crystal.[3-5]

2-(2-Hydroxyphenyl)benzothiazole (**2**), which has similar structure to **1**, underwent excited state hydrogen atom transfer to give the *cis*-keto form followed by the isomerization to the *trans*-keto form on photoirradiation in solution.[6] The transient photochromic properties of **2** was studied by transient absorption spectroscopies.[7] One can expect that the intramolecularly hydrogen bonded Schiff bases exhibit similar photochromic properties.[8,9]

In this study, hydrogen bonded Schiff bases, 2-hydroxy-3'-methoxysalicylideneaniline (**3**) and 2-hydroxy-4'-methoxysalicylideneaniline (**4**) were prepared and the effect of substituent on the tautomerization behavior was investigated. These molecules exhibited thermochromic, solvatochromic and transient photochromic properties.

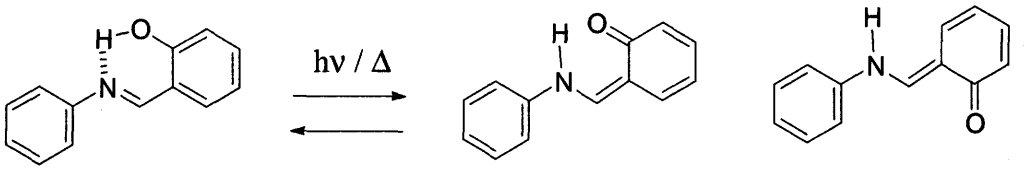

enol form *cis*-keto form *trans*-keto form

N-Salicylideneaniline (**1**)

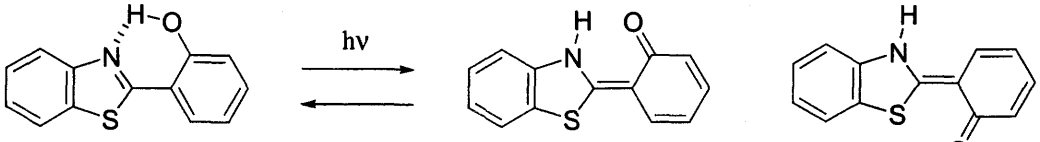

enol form *cis*-keto form *trans*-keto form

2-(2-Hydroxyphenyl)benzoxazole (**2**)

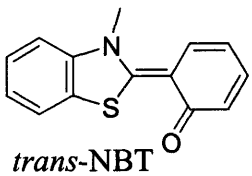

trans-NBT

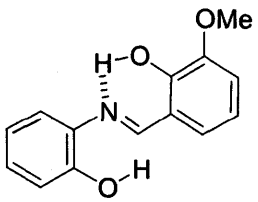

3

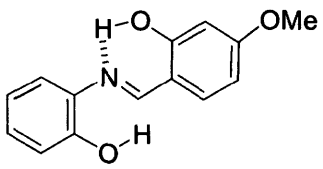

4

Experimental

Materials

The compound **3** and **4** were prepared by condensation reaction between corresponding salicyl aldehyde and *o*-aminophenol in nitrobenzene. The products were purified by recrystalization from ethanol.

2-Hydroxy-3'-methoxysalicylideneaniline (**3**): ^{1}H-NMR ($CDCl_3$, 200 MHz) δ 3.95 (3H, s; methoxy-H), 7.00 (5H, m), 7.20 (2H, m), 8.71 (1H, hydroxyl-H) ppm. Anal Calcd for $C_{14}H_{13}NO_3$: C, 69.12; H, 5.39; N, 5.76; O,

19.73%; Found C, 69.09, H, 5.46, N, 5.61. 2-Hydroxy-4'-methoxysalicylidene -aniline (**4**): ^{1}H NMR ($CDCl_3$, 200 MHz) δ 3.86 (3H, s; methoxy-H), 6.40 (2H, m), 6.98 (2H, m), 7.15 (2H, m), 7.32 (1H, m), 8.58 (1H, hydroxyl-H) ppm. mp 220 – 222 °C. Anal Calcd for $C_{14}H_{13}NO_3$: C, 69.12; H, 5.39; N, 5.76; O, 19.73%; Found C, 69.15, H, 5.47, N, 5.63.

Measurement

Absorption and fluorescence spectra were measured on a JASCO Ubest-55 and on a Hitachi F-4000 fluorescence spectrometer, respectively.

Laser flash photolysis was performed by using an eximer laser (Lambda Physik LPX-100, 308 nm, 20 ns fwhm) or excimer laser pumped dye laser (Lambda Physik LEXtra-100, 308 nm, 20 ns fwhm and Lambda Physik Scanmate; Lambda Physik LPX-100, 308 nm, 20 ns fwhm and Lambda Physik FL-4002, 10 ns fwhm). Stilbene 3 was used as a laser dye to obtaind 425 nm laser pulse. A pulsed xenon arc (Ushio UXL-159) was used as a monitoring light source.

Oxford Cryostat model DN-1704 and temperature controller ITC-4 were used for controlling the sample temperature.

Results

Absorption spectra

Absorption spectra of **3** and **4** were measured in benzene, acetonitrile and methanol and were shown in Figure 1 - 4. Compounds **3** and **4** had the intense absorption band at around 350 nm, in addition to the absorption band at 420 and

460 nm for **3** and **4**, respectively in methanol. Compound **4** has some absorbance at 420 nm even in acetonitrile.

The absorption profile at around 450 nm of **3** in methanol slightly shifted to longer wavelength region with increasing concentration from 1.0x 10^{-5} to 1.8x 10^{-4} M as shown in Figure 3(a). However, the molar extinction coefficient at 470 nm was independent of its concentration indicating that dimer was not formed in methanol and acetonitrile.

In toluene, the absorption spectra did not change at the temperature between 295 K and 200 K. On the other hand, temperature affected the absorption band at **3** and **4** in methanol as shown in Figure 5.

Fluorescence spectra

Fluorescence emission of **3** and **4** was not observed at room temperature. However, **3** and **4** exhibited fluorescence emission in methanol at 180K as shown in Figure 6. The lifetime of fluorescence at 77K in ethanol was 1.3 ns and 3.5 ns for **3** and **4**, respectively.

Transient absorption spectrum at room temperature

Transient absorption spectra of **3** and **4** were observed in benzene, acetonitrile, and methanol on 308 nm laser excitation. Compound **3** exhibited transient absorption spectra from 400 nm to 600 nm as shown in Figure 7, 8, and 9. Compound **4** exhibited transient absorption spectra from 400 nm to 550 nm as shown in Figure 10, 11, and 12. The bleaching of the absorption spectra was also observed at around 350 nm. The time constant of recovery of this band is different from that of decay at 500 nm. Since the absorption spectra of **3** and **4**

observed after laser irradiation by conventional UV spectrometer did not give any permanent change, **3** and **4** should give several transients on laser excitation. The observed transient absorption spectra were not quenched by oxygen and were assigned to the ground state intermediates.

Temperature dependence of transient absorption spectra of 4 in methanol

The transient absorption spectrum observed in toluene at 180K was slightly different from that at 295 K (τ = 10 μs) and the lifetime at 180 K (τ = ~200 μs) was longer than that at 295 K as shown in Figure 13.

Figure 14 showed the transient absorption spectra **4** at 295 K (a) and 180 K (b) in methanol. The maximum of transient absorption spectra appeared at 460 nm, in addition to the bleached band at around 350 nm at 295 K. On the other hand, the transient absorption appeared at 460 nm and the bleaching appeared at 420 nm at 180 K. These results indicate that the same transient having the absorption band at 460 nm was produced by laser excitation both at 295 K and 180 K. Therefore, the species having absorption band around 350 nm and 420 nm at 295 K and at 180 K, respectively, gave the transient absorption at 460 nm.

Two step laser excitation of 4 in benzene

Transient absorption spectroscopy of **4** in benzene was performed by using two laser pulses at 308 and 425 nm. Compound **4** exhibited transient absorption with the maximum wavelength of 440 nm on excitation of the first laser pulse of 308 nm. The transient was excited with the second laser pulse of 425 nm after appropriate delay time. The bleaching of the transient absorption at 440 nm and the recovery of the absorption at 370 nm were observed as shown

in Figure 15. The negative absorption band appeared at around 360 nm corresponded to the steady state absorption spectrum of **4** in benzene. These results indicate that the second laser excitation of transient species having absorption maximum at 440 nm efficiently gave the starting enol-form of **4** photochemically.

The steady state absorption spectrum did not change after irradiation of laser pulses. However, the intensity and time profile of the transient absorption band at 440 nm by the second laser excitation at 425 nm was different from that of the recovery at 360 nm.

Discussion

In methanol, **3** and **4** exhibited longer wavelength absorption band at 460 and 420 nm, respectively, while they showed absorption maximum at 349 nm and 354 nm in benzene, respectively. The absorbance of the longer wavelength absorption band in methanol increased with decreasing of temperature. This fact indicates that the molecular structure changed by decreasing temperature. The results of laser flash photolysis of **4** at different temperature indicate that compound **4** gave *trans*-keto form at both 298 K and 180 K, although the ground state conformation is different as revealed by thermochromic behavior (Figure 5). As to the reason of thermochromism of Schiff base in solution, the dimer formation of Schiff base was proposed in hydrocarbon solvent. In **4**, thermochromism was not observed in toluene but is observed in methanol, which can form intermolecular hydrogen bonding with hydrogen bonded Schiff base.

Solvatochromism and thermochromism of **3** and **4** in methanol can be

explained by formation of intermolecular hydrogen bonded cluster with methanol at room temperature. The contribution of intermolecular hydrogen bonding between Schiff base and methanol may increase with decreasing temperature to give *cis*-keto form. The molar extinction coefficient of *trans*-keto form and *cis*-keto form was estimated to be similar as shown in Figure 14. The result was consistent with the fact that the ε was the same between *cis*-keto form and *trans*-keto form of NBT that was model compound of keto form of **2**.[6]

Compound **2** gave the *trans*-keto form by cis-to-trans isomerization after excited state intramolecular hydrogen atom transfer, however the lifetime of *trans*-keto form become much shorter in methanol than in benzene and acetonitrile. Methanol catalyzes the reverse hydrogen atom transfer to give enol form.

However, the lifetime of *trans*-keto form of **3** and **4** was nearly the same in methanol and benzene. In addition, *cis*-keto form was observed for **3** and **4** in methanol. Therefore, it was suggested that protic solvent stabilized the NH form of Schiff base rather than OH form.

The results of two step laser excitation of **4** indicate that *trans*-keto form underwent reverse hydrogen atom transfer to give enol form followed by trans-to-cis photoisomerization and the "*cis*-enol" form was produced on excitation of **4**, which isomerized to the "*trans*-enol form" thermally with ms time scale.

On the basis of these results, the potential energy diagrams of chromism of **4** were depicted as shown in Figure 17.

On photoirradiation **4** undergoes either hydrogen atom transfer to give the *cis*-keto and *trans*-keto tautomers or isomerization around the C=N double

bond to give *Z*-isomer. The produced *Z*-isomer reverts to the *E*-isomer with the time constant of ms.

The *trans*-keto tautomer undergoes isomerization around the quasi-double bond to give the *cis*-keto form, which undergoes reverse hydrogen atom transfer to the starting *E*-isomer.

Conclusion

Compound **3** and **4** exhibited absorption band at longer wavelength region in methanol than in benzene and in acetonitrile. They showed thermochromism to give the absorption spectra at longer wavelength region with decreasing temperature.

The transient absorption spectroscopy indicates that compound **3** and **4** exhibited photochromism, thermochromism and solvatochromism by hydrogen atom transfer between O atom and N atom in solution.

References

1. "Organic Photochromic and Thremochromic Compounds," ed by J. C. Crano and R. Guglielmetti, Kluwer Academic / Plenum Press, New York (1999), Vol. 1, 2.
2. "Photochromism: Molecules and Systems," ed by H. Durr and H. Bouas-Laurent, Elsevier, Amsterdam (1990).
3. K. Ogawa, Y. Kasahara, Y. Ohtani, and J. Harada, *J. Am. Chem. Soc.*, **1998**, *120*, 7107.
4. K. Ogawa and T. Fujiwara, *Chem. Lett.*, **1999**, 657.
5. J. Harada, H. Uekusa, and Y. Ohashi, *J. Am. Chem. Soc.*, **1999**, *121*, 5809.
6. see Chapter 2.
7. J. S. Stephan and K. H. Grellmann, *J. Phys. Chem.*, **1995**, *99*, 10066 and references cited therein.
8. T. Suzuki and T. Arai, *Chem. Lett.*, **2001**, 124.
9. T. Suzuki, Y. Kaneko, and T. Arai, *Chem. Lett.*, **2000**, 756.

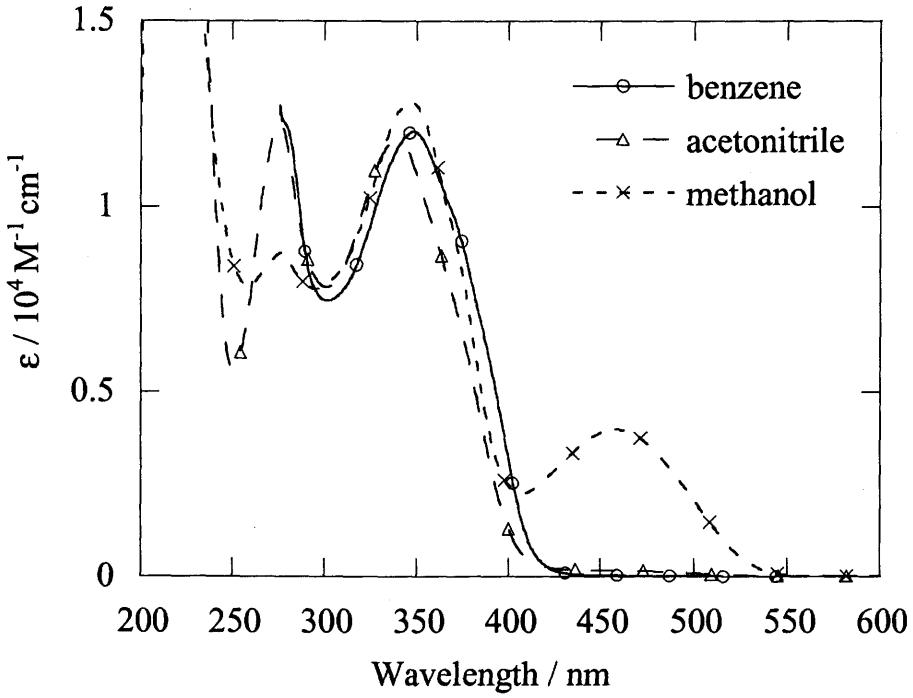

Figure 1. Absorption spectrum of **3** in benzene, acetonitrile, and methanol.

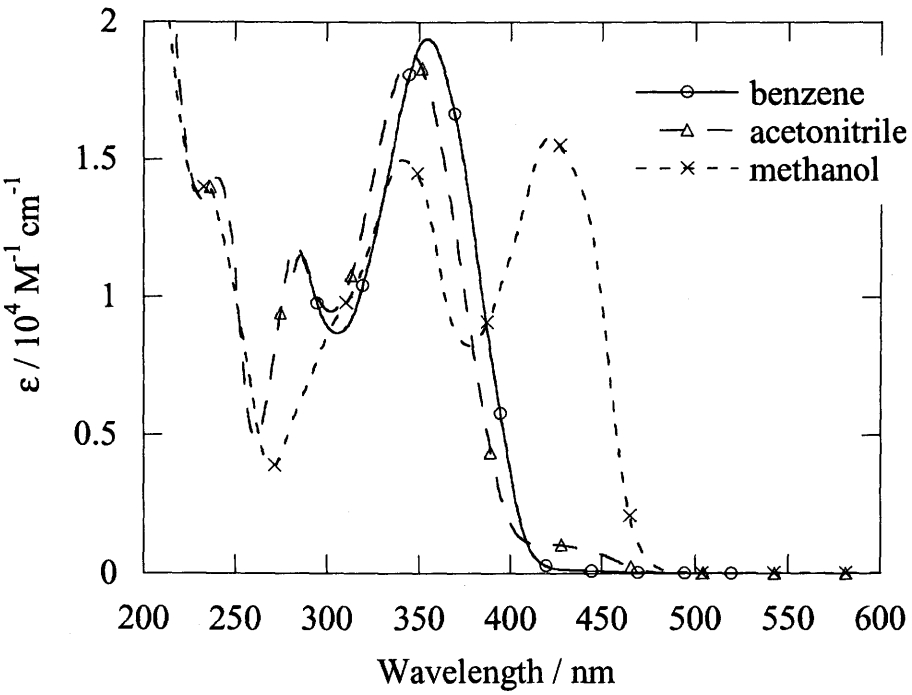

Figure 2. Absorption spectrum of **4** in benzene, acetonitrile, and methanol.

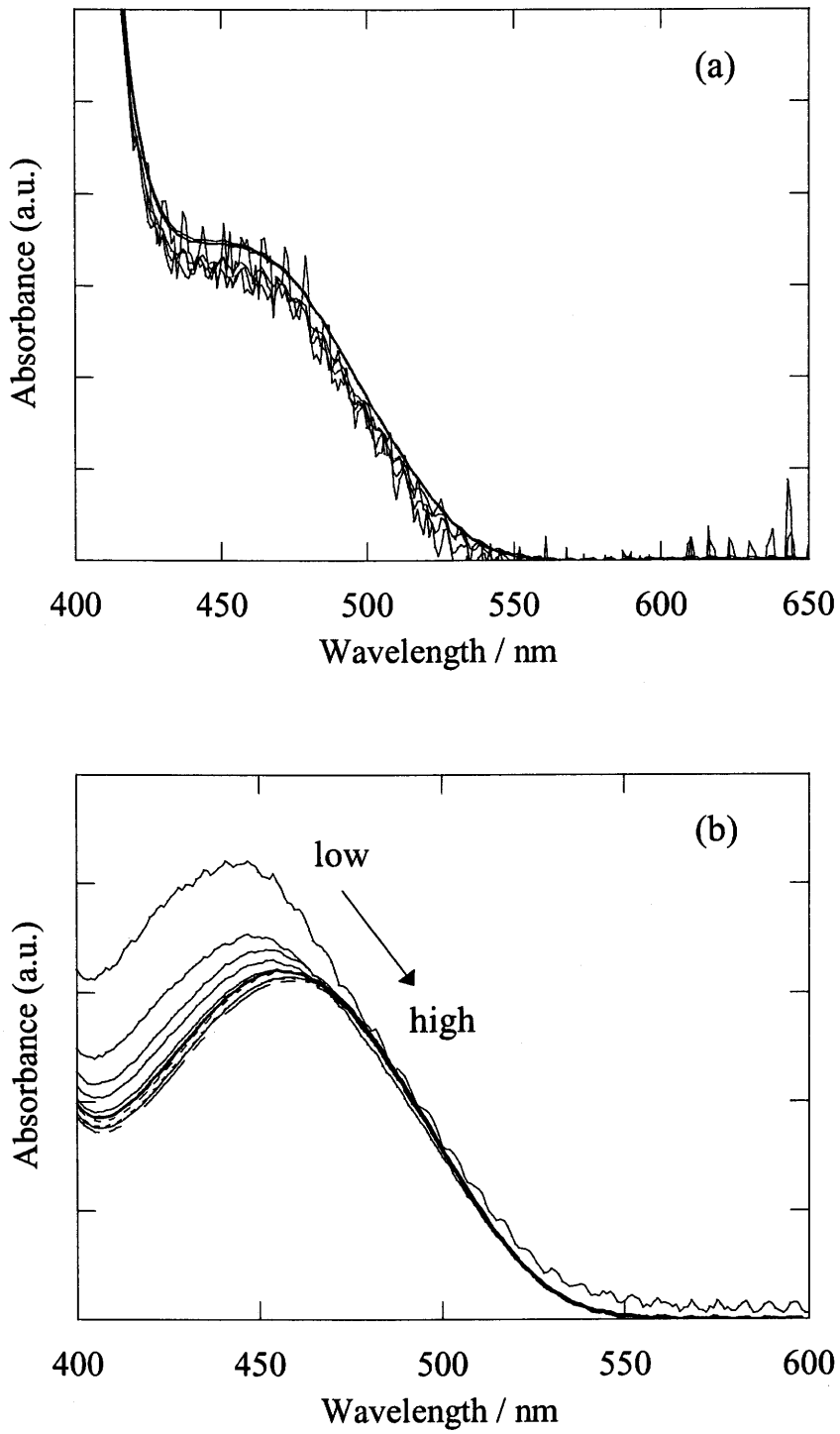

Figure 3. Concentration dependence of absorption spectrum of **3** in acetonitrile (a) and methanol (b).

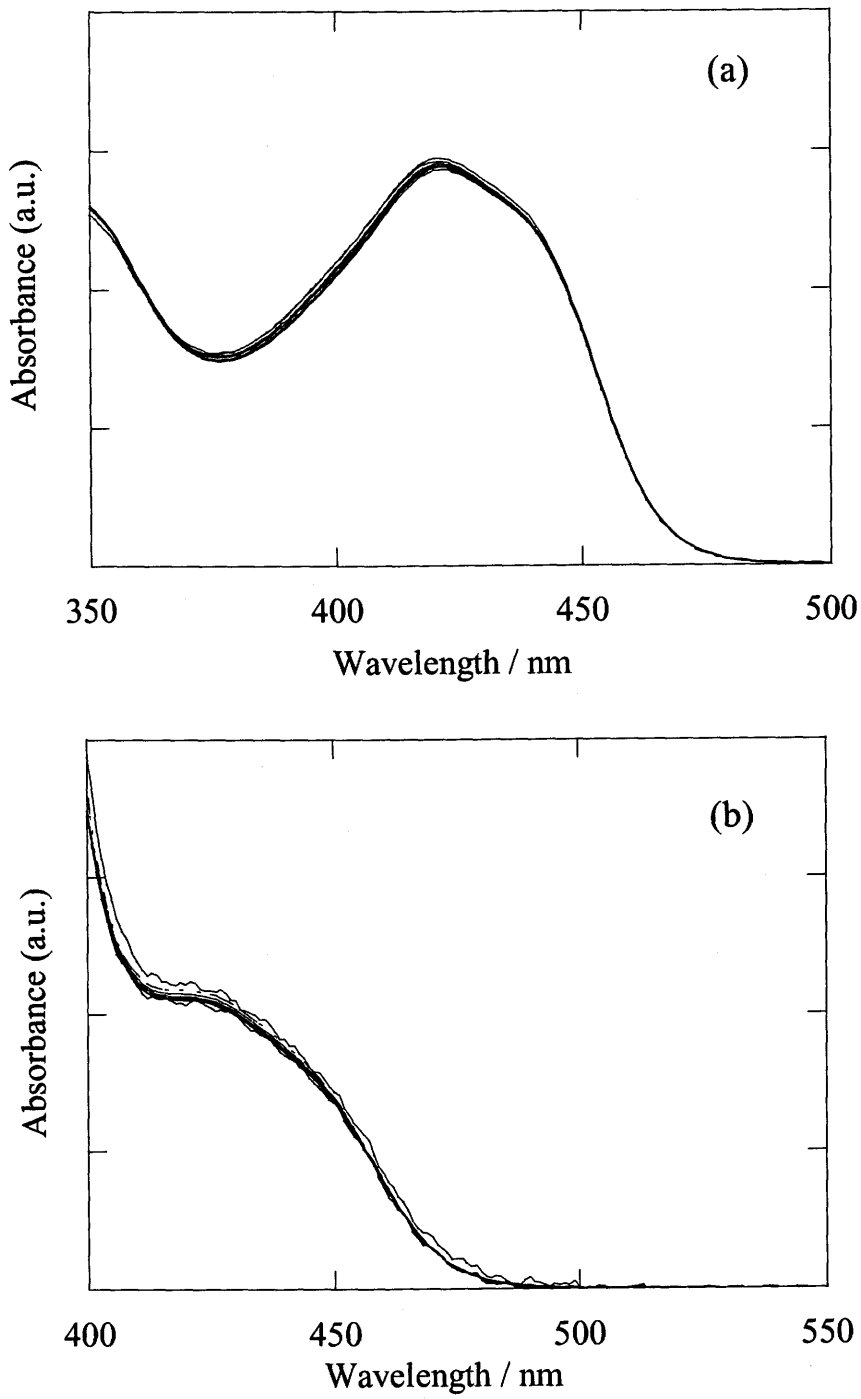

Figure 4. Concentration dependence of absorption spectrum of **4** in acetonitrile (a) and methanol (b).

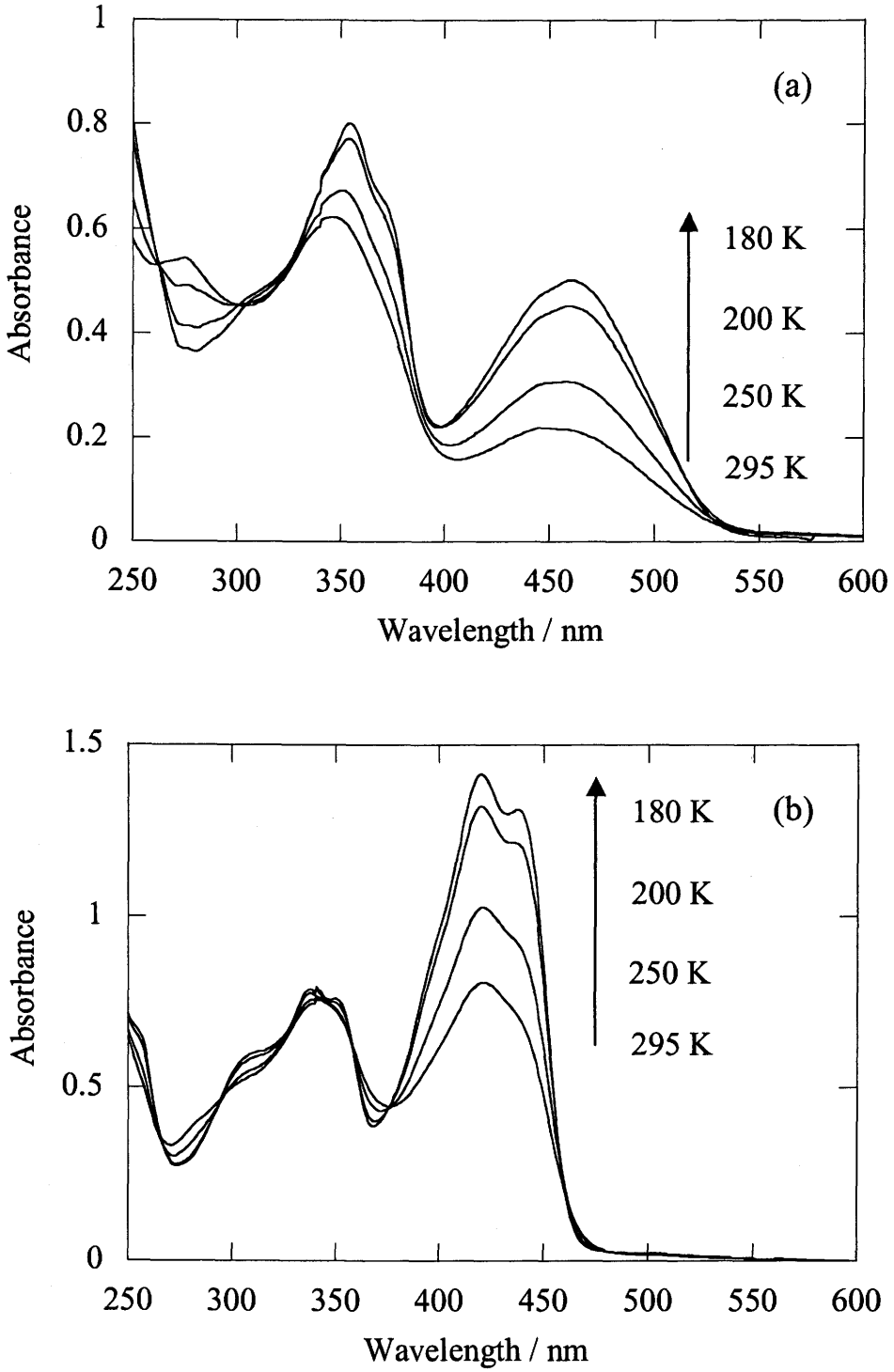

Figure 5. The temperature effect on the absorption spectrum of **3** (a) and **4** (b) in methanol.

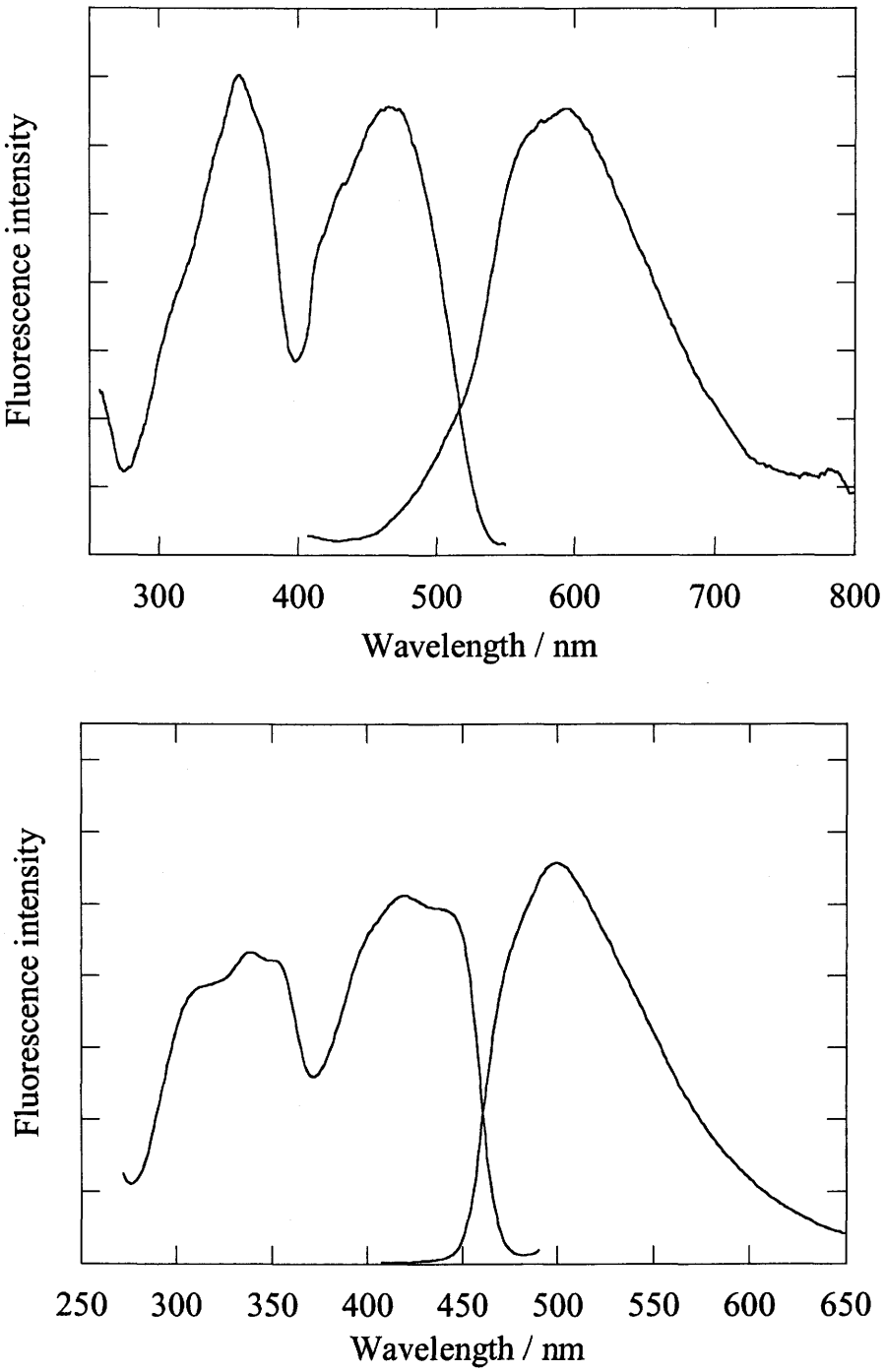

Figure 6. Fluorescence and fluorescence excitation spectra of **3** (a) and **4** (b) in methanol at 180 K.

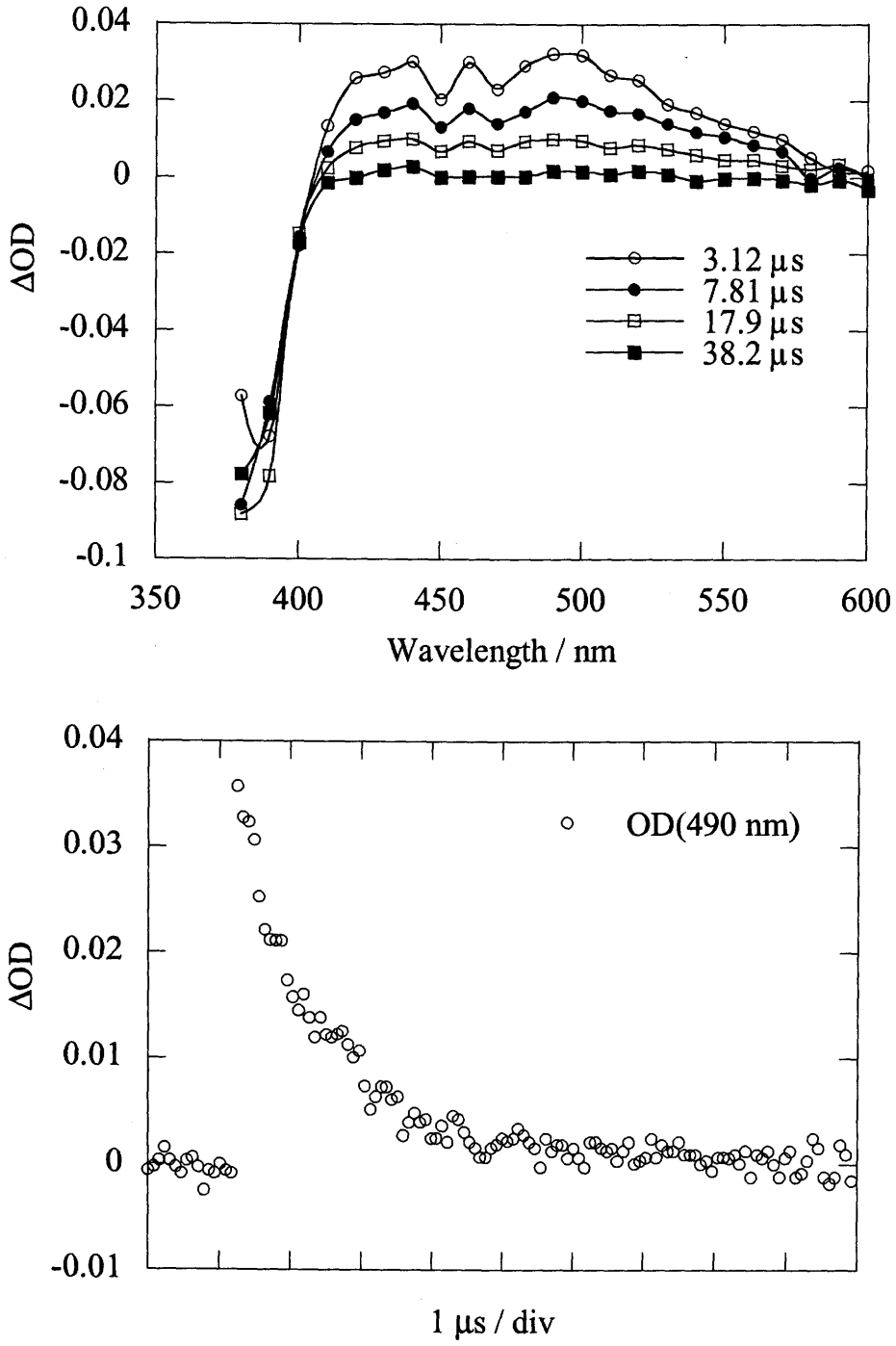

Figure 7. Transient absorption spectra of **3** in benzene at room temperature.

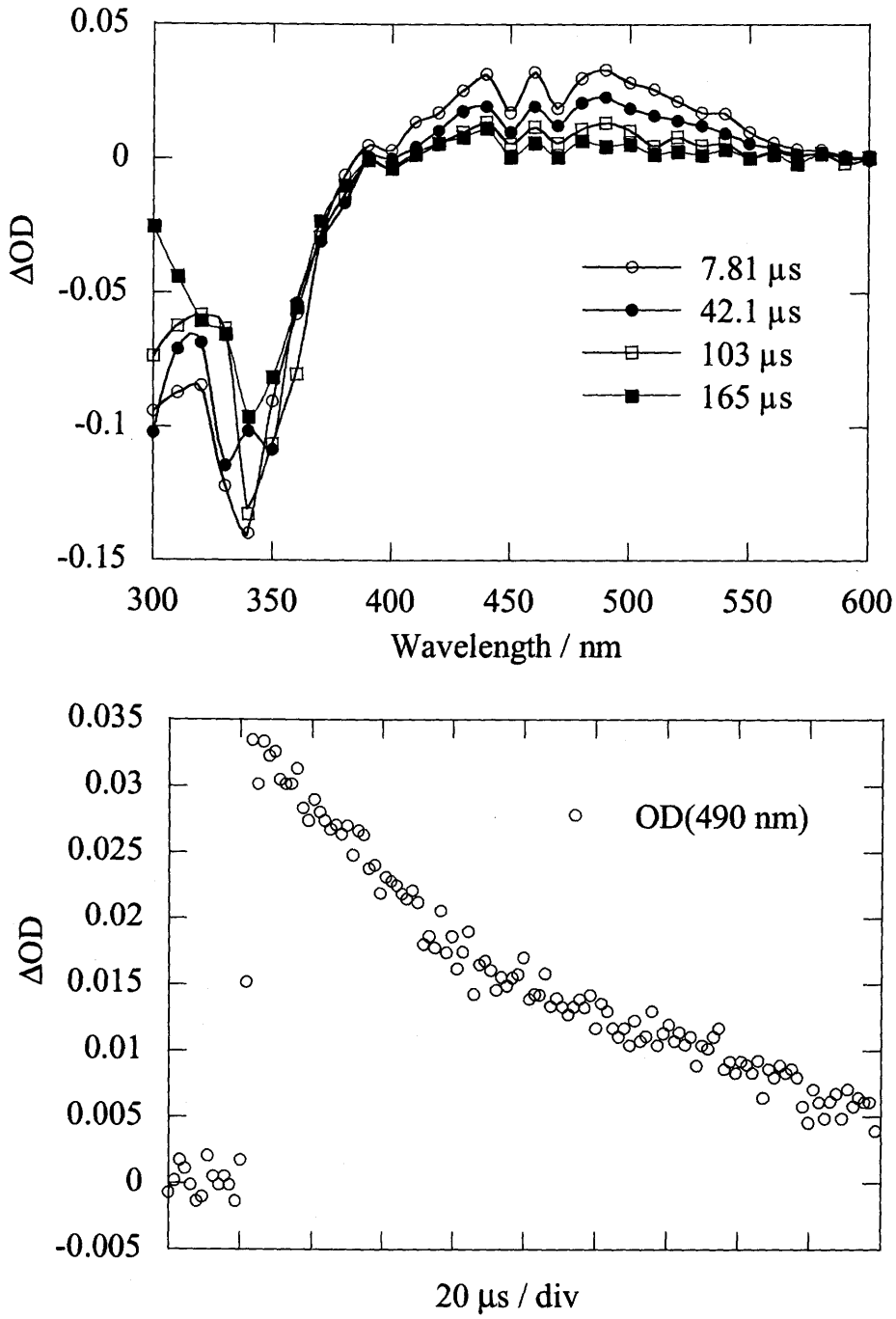

Figure 8. Transient absorption spectra of **3** in acetonitrile at room temperature.

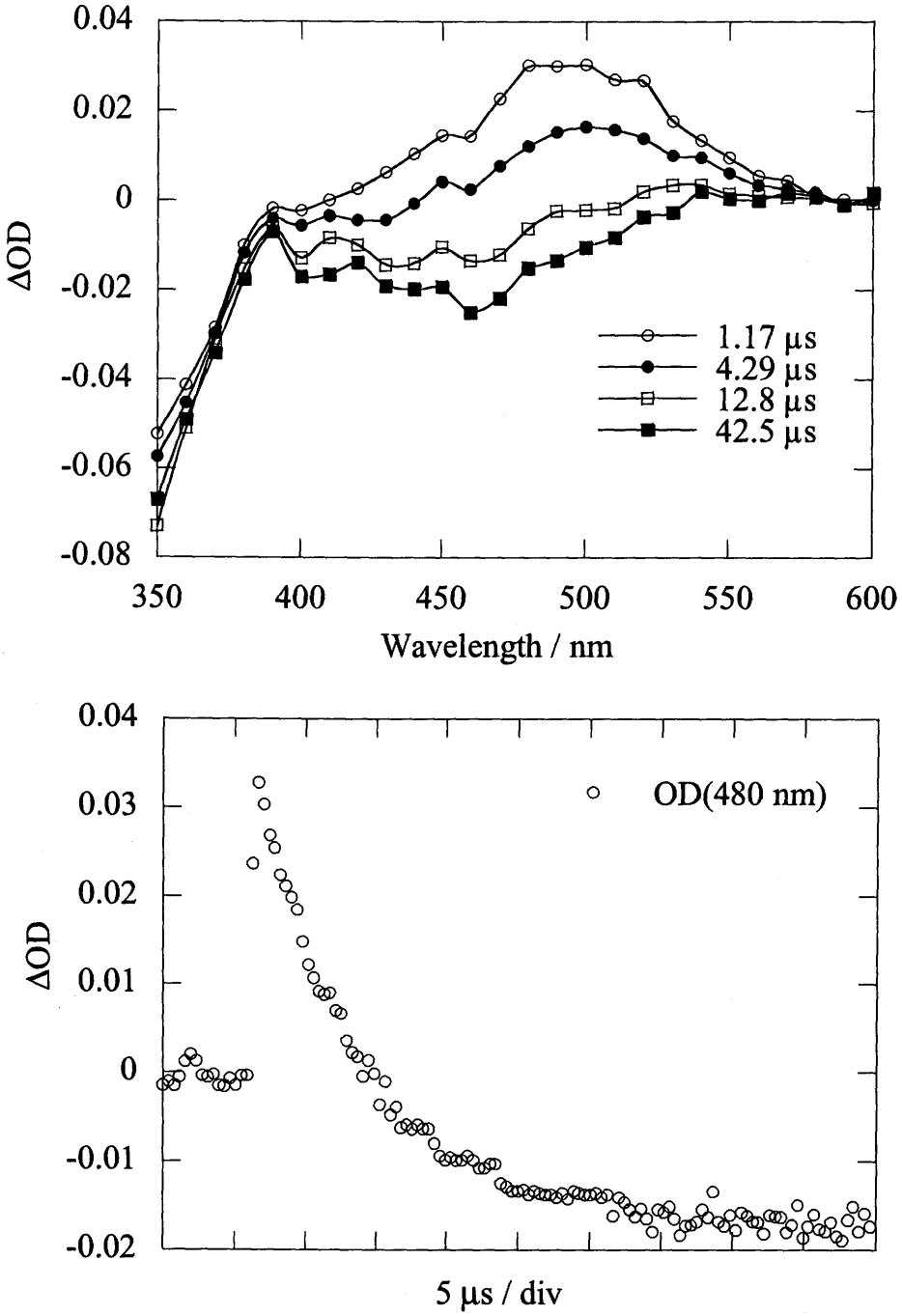

Figure 9. Transient absorption spectra of **3** in methanol at room temperature

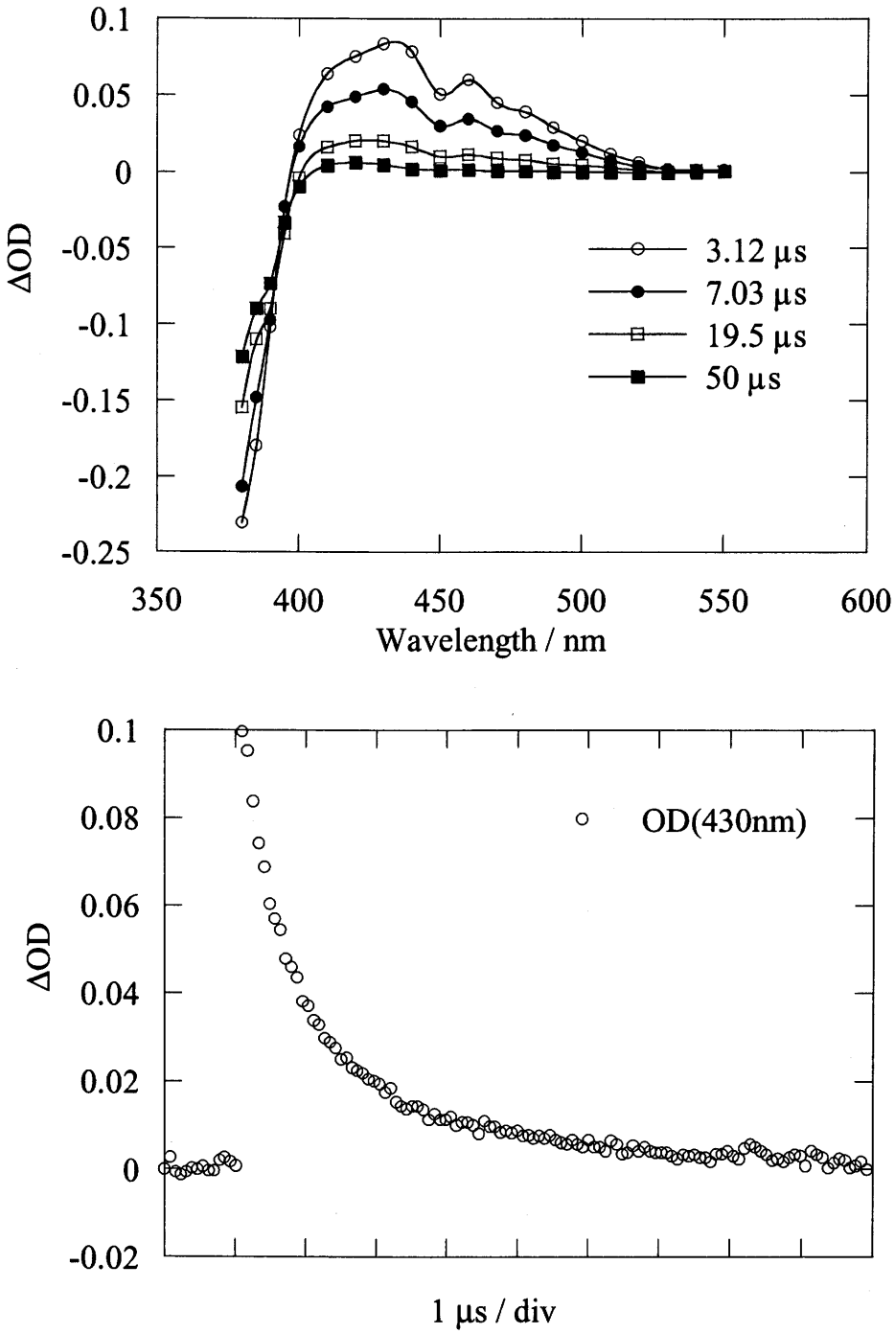

Figure 10. Transient absorption spectra of **4** in benzene at room temperature.

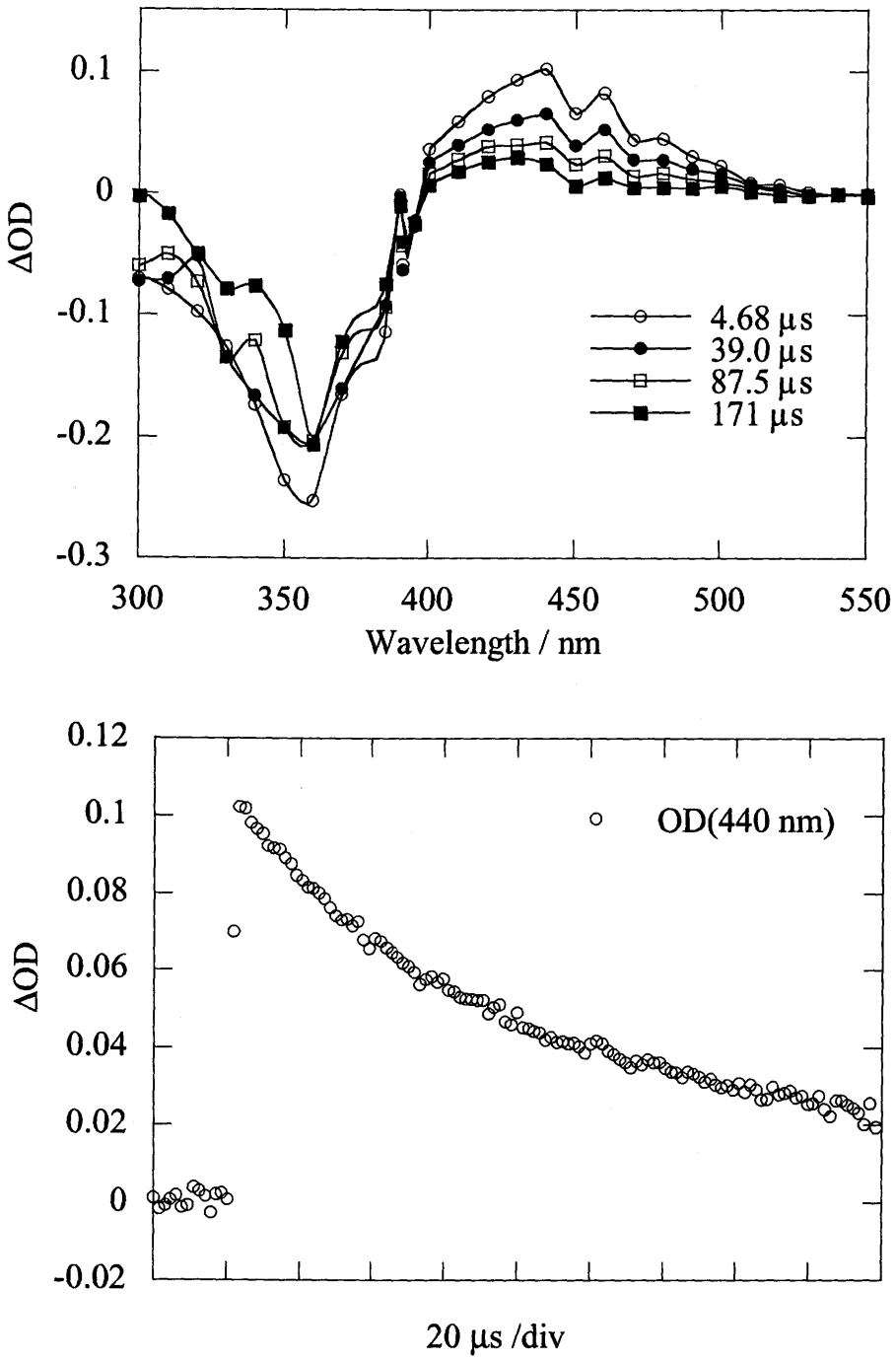

Figure 11. Transient absorption spectra of **4** in acetonitrile at room temperature.

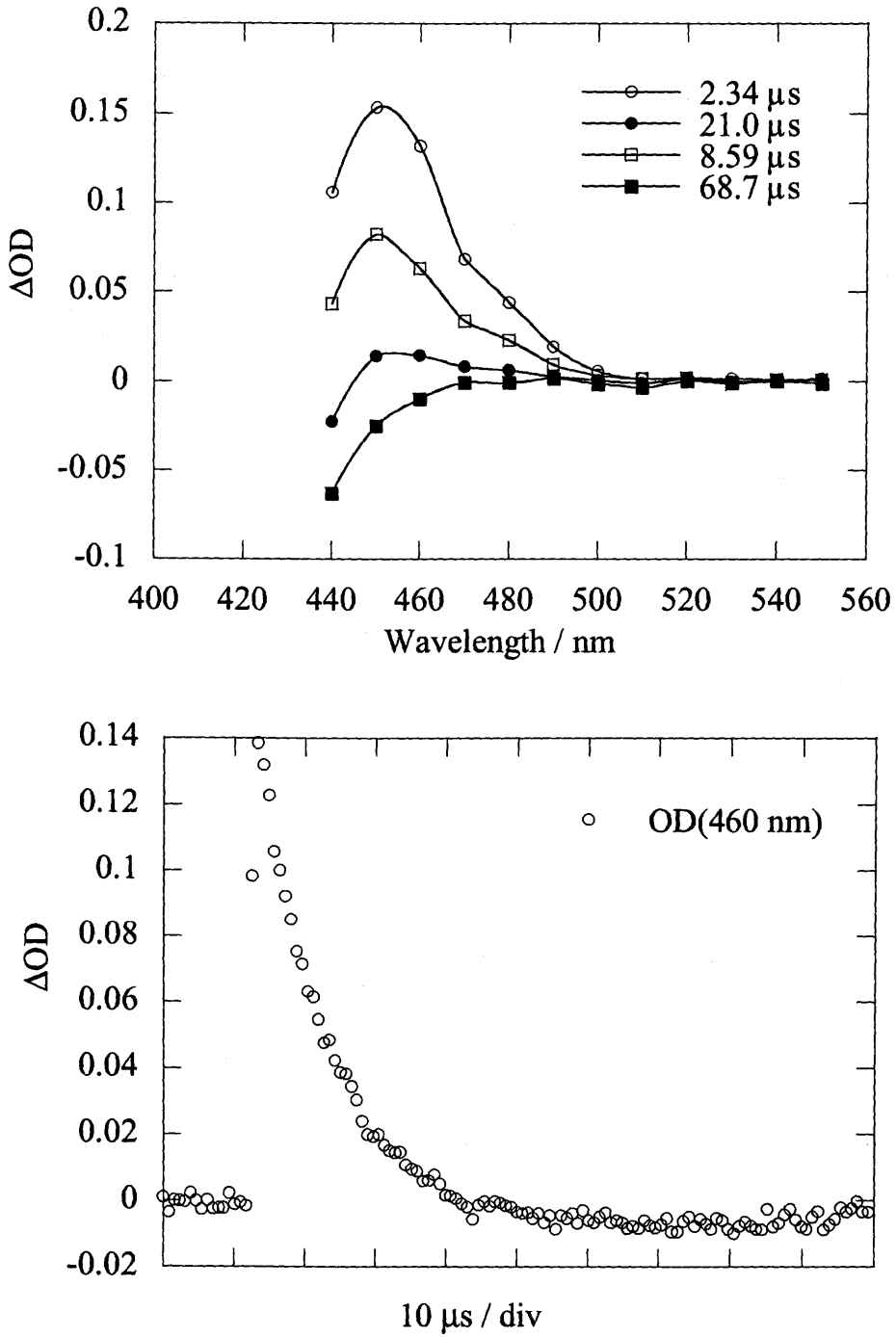

Figure 12. Transient absorption spectra of **4** in methanol at room temperature.

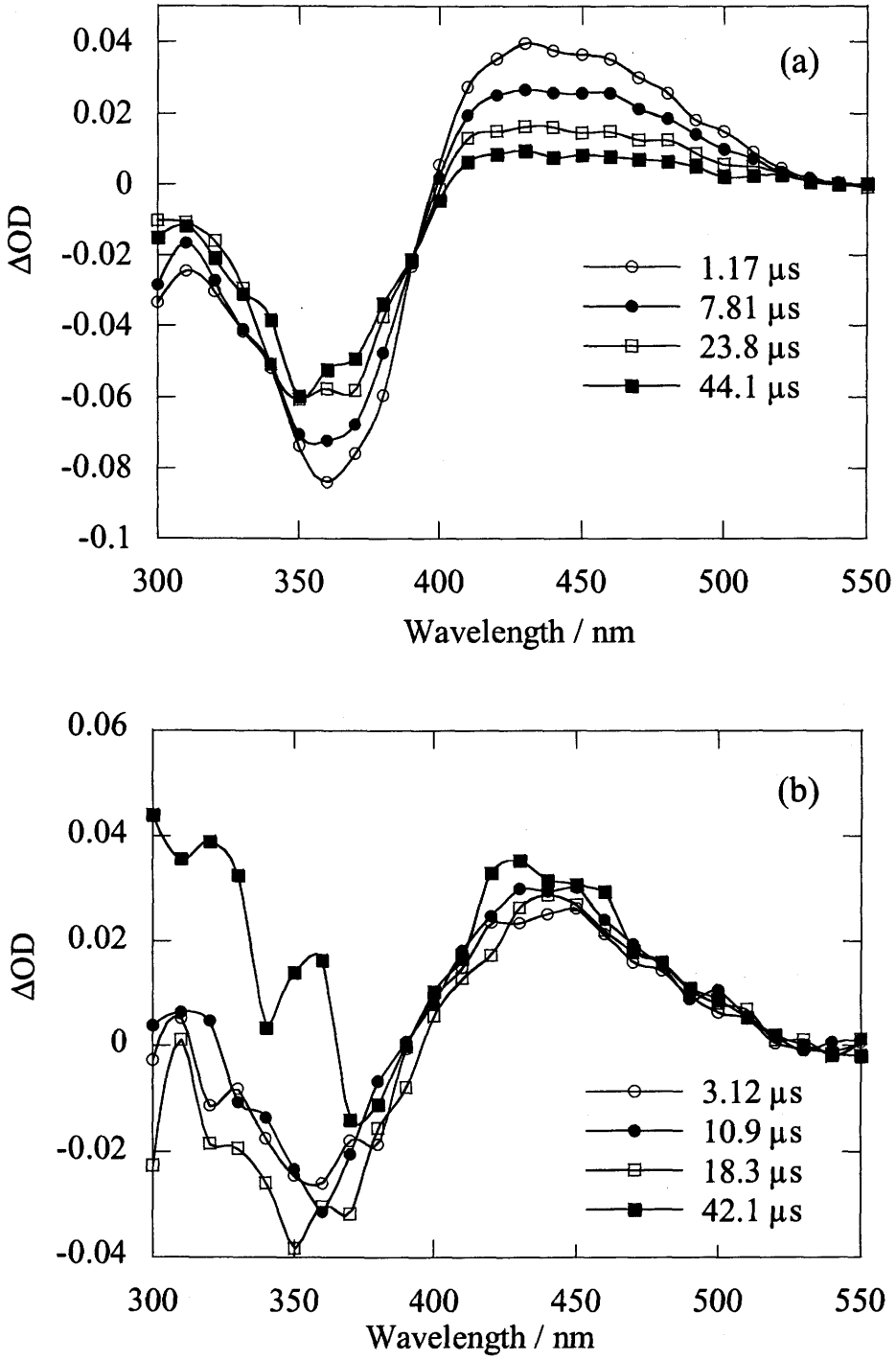

Figure 13. Transient absorption spectra of **4** in toluene at 295 K (a) and 180 K (b).

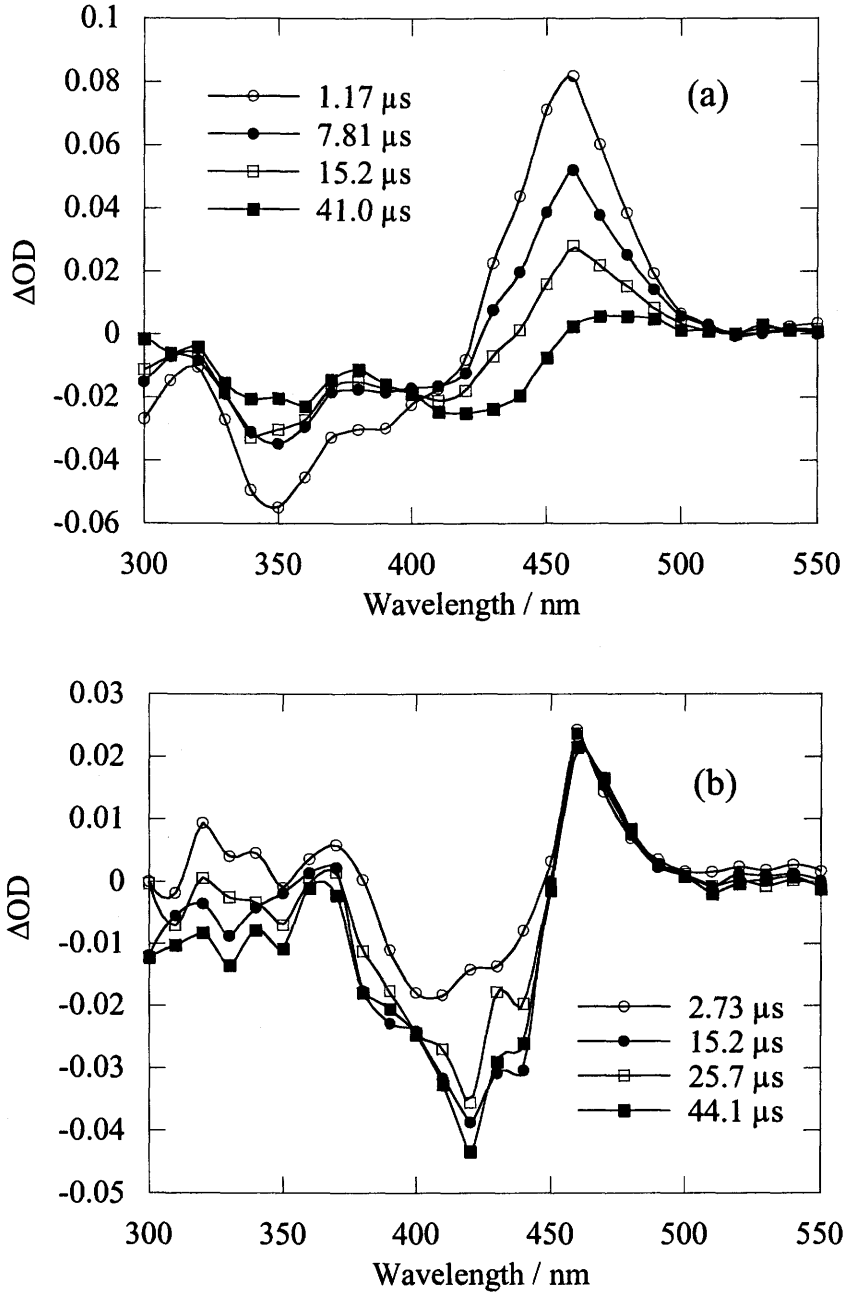

Figure 14. Transient absorption spectra of **4** in methanol at 295 K (a) and 180 K (b).

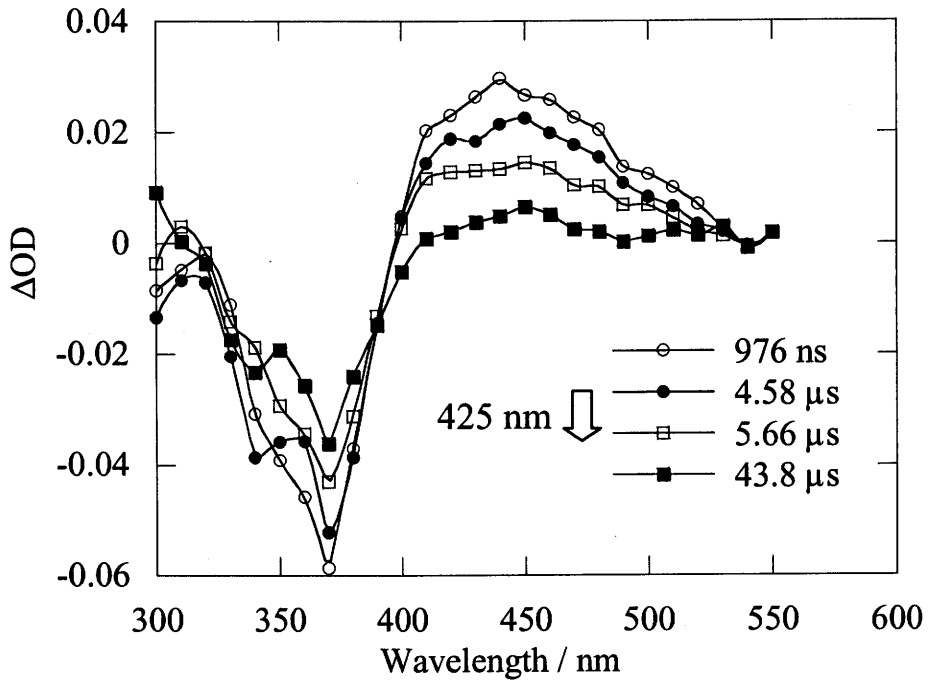

Figure 15. Transient absorption spectra of **4** on two color (308 nm and 425 nm) excitation.

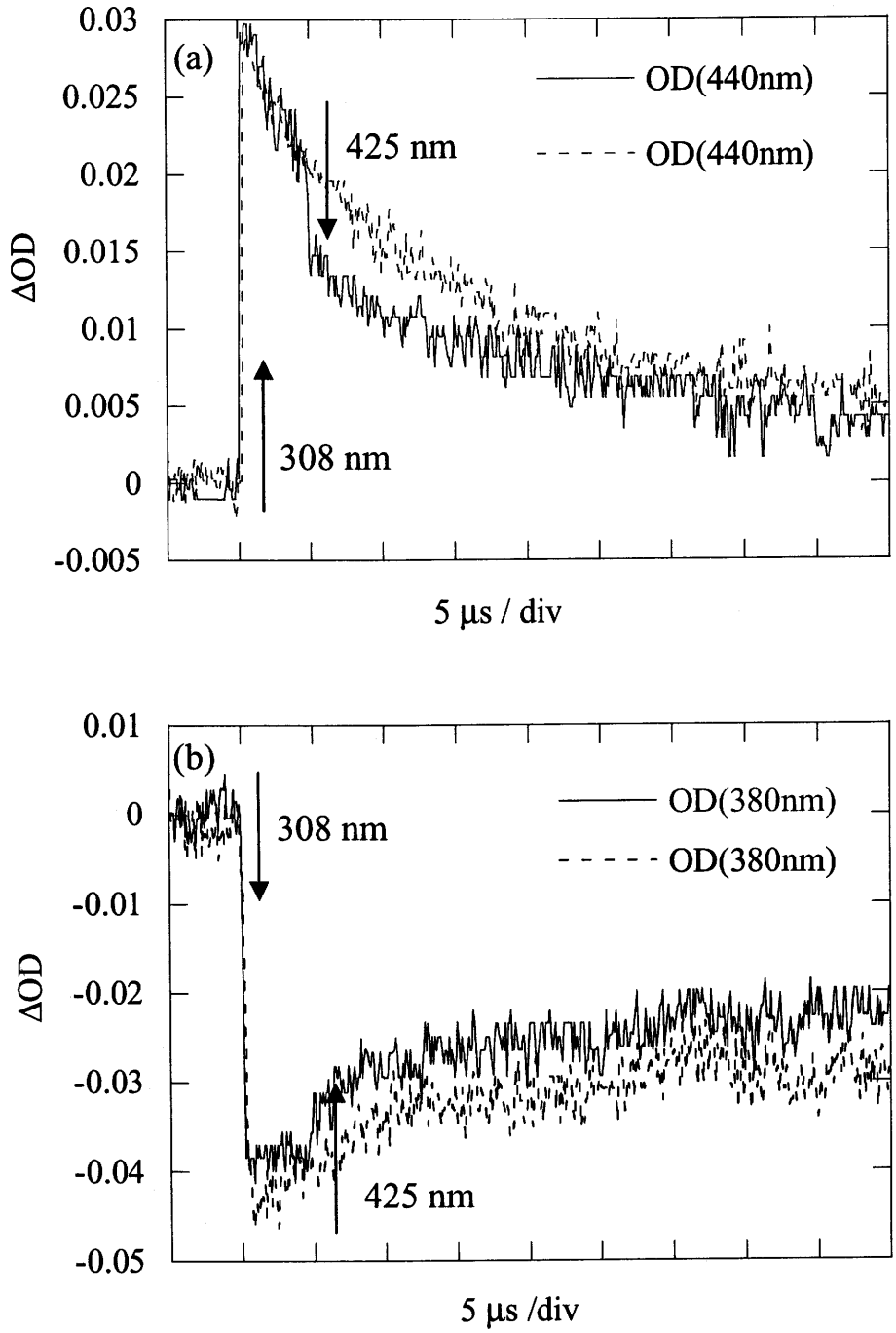

Figure 16. Time profile of transient absorption at 440 nm (a) and 380 nm (b) on two color laser excitation.

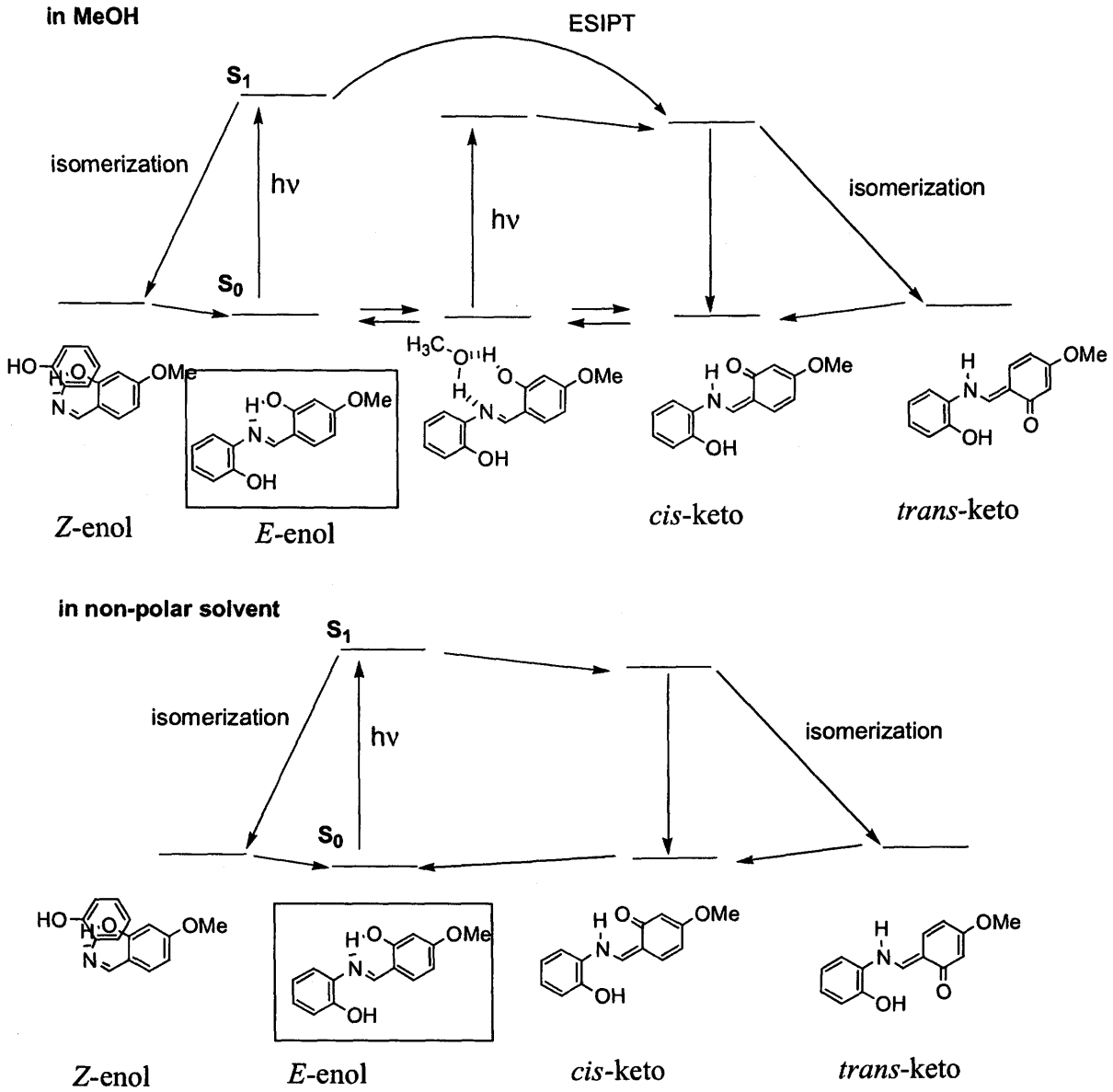

Figure 17. Energy diagram of hydrogen atom transfer of **4**.

Chapter 4

Photochromism of Hemiindigo Compounds Having Intramolecular Hydrogen Bonding

Abstract

Intramolecularly hydrogen bonded hemiindigo compounds **2** - **4** were prepared and their photochemical behavior was investigated. *Z*-**2** did not undergo isomerization, while **3** underwent isomerization mutually between *Z*-isomer and *E*-isomer in solution to exhibit color change between greenish yellow and reddish orange. Introduction of formyl group at the 2-position of pyrrole ring of **3** brought about the increase of fluorescence quantum yield and fluorescence lifetime by a factor of 10 and the decrease of quantum yield of isomerization in **4**. In addition, introduction of formyl group affects the thermal stability. The intramolecular hydrogen bonding can be used to construct a novel photochromic molecule.

Introduction

Photochromic compounds having absorption band at visible region have received considerable attention from the view point of development of photochromic memory or switching devices in recent years.[1-3] For example, Irie et al. reported a series of diarylethenes, exhibiting photochromic properties based on photochemical cyclization reaction.[4]

The intramolecular hydrogen bonding could be useful for controlling of isomerization mode and for changing the absorption maximum between *E*-isomer and *Z*-isomer. For example, an olefin with a pyrrole ring and a pyridine ring (**1**) exhibited the one-way E→Z isomerization due to the presence of an intramolecular hydrogen bonding in *Z*-isomer.[8] The *Z*-isomer in benzene exhibited an absorption maximum at longer wavelength region (λ_{max} = 372 nm) than that of *E*-isomer (λ_{max} = 347 nm).[8] However, the difference of absorption maximum between *Z*- and *E*-isomer was too small to exhibit the color change at visible region.

Some of the hydrogen bonded olefins undergo one-way photoisomerization due to the existence of fast deactivation pathway through intramolecular hydrogen bonding.[5-12] The radiationless deactivation pathway is related to the excited state dynamics and electronic structures of aromatic molecules.[9,13-14]

In this respect, we have investigated the photochemical behavior of intramolecularly hydrogen bonded hemiindigo derivatives. The absorption spectra of the hemiindigo derivatives appeared at visible region, and the isomerization around C=C double bond resulted in color change. Therefore, intramolecular hydrogen bonding can be used to construct a photochromic dye

based on isomerization of C=C double bond. Furthermore, the substituent controls their photochemical behavior.

Experiment

Materials and solvents

The hemiindigo derivatives **2**, **3**, and **4** were synthesized by aldol condensation from 3-indolylacetate and appropriate aromatic aldehyde to yield only *Z*-isomers.[15] Pyrrole-2,5-dicarboxyaldehyde was prepared by Vielsmeier reaction from pyrrole.[16] *E*-**3** was obtained by irradiation of benzene solution of *Z*-**3** at 366 nm to give photostationary mixture with high ratio of *E*-isomer. The obtained hemiindigo was purified by column chromatography and recrystalization from ethanol.

Z-2-(2-Pyridilmethylidene)indolin-3-one (*Z*-**2**): ^{1}H NMR (DMSO-d_6, 200 MHz) δ (ppm) 6.58 (1H, s; olefinic-H), 6.87 (1H, t, J = 8.0 Hz; indolin-H), 7.25 (2H, m; aromatic-H), 7.70 (4H, m; aromatic-H), 8.70 (1H, m; pyridine-H), 10.3 (1H, s; indolin-NH) mp = 153 - 154°C. Anal Calcd for $C_{14}H_{10}N_2O$, C, 75.66; H, 4.53; N, 12.61%; Found: C, 75.53, H, 4.60, N, 12.47%. *Z*-2-(2-Pyrrolylmethylidene)indolin-3-one (*Z*-**3**): ^{1}H NMR(DMSO-d_6, 200 MHz) δ (ppm) 6.31 (1H, m; pyrrole-H), 6.71 (1H, s; olefinic-H), 6.87 (2H, m; aromatic-H), 7.07 (1H, m; pyrrole-H), 7.13 (1H, d, J = 8.2 Hz; indolin-H), 7.50 (2H, m; indolin-H), 9.30 (1H, s; NH), 11.40 (1H, s; NH). mp 200-202 °C. E-3: δ (ppm) 6.34 (1H, m; pyrrole-H), 6.71 (1H, m; pyrrole-H), 6.81 (1H, s; olefinic-H), 6.87 (1H, m; indolin-H), 7.06 (1H, d, J = 8.4 Hz; indolin-H), 7.25 (1H, m; pyrrole-H), 7.47 (1H, m; pyrrole-H), 7.63 (1H, d, J = 8.4 Hz; indolin-H), 9.78 (1H, s; NH), 13.35 (1H, s; NH). mp 191-193 °C. Anal. Calcd for

$C_{13}H_{10}N_2O$: C, 74.27; H, 4.79; N, 13.32%. Found: C, 74.04; H, 4.74; N, 13.19%. *Z*-2-((2-formyl-5-pyrrolyl)methylidene)indolin-3-one (*Z*-**4**): ^{1}H-NMR (DMSO-d_6, 200 MHz) δ 6.63 (s, 1H; olefinic-H), 7.00 (s, 4H; aromatic-H), 7.53 (m, 2H; aromatic-H), 9.50 (s, 1H, formyl-H), 9.70 (br, 1H, NH), 12.4 (br, 1H, NH) ppm. mp 224-226 °C. Anal. Calcd for $C_{14}H_{10}N_2O_2$: C, 70.58; H, 4.23; N, 11.76; O, 13.43. Found: C, 70.08; H, 4.30; N, 11.59%.

In spectroscopy, Dotite Spectrosol or Luminasol were used as solvents without further purification.

Measurement

Absorption and fluorescence spectra were measured on a JASCO Ubest-55 and on a Hitachi F-4000 fluorescence spectrometer, respectively.

Laser flash photolyses were performed by using an excimer laser (Lambda Physik LPX-100, 308 nm, 20 ns fwhm) or excimer laser pumped dye laser (Lambda Physik LEXtra-100, 308 nm, 20 ns fwhm and Lambda Physik Scanmate, stilbene 3, 425 nm, or QUI, 390 nm, 10 ns fwhm) as excitation light sources and a pulsed xenon arc (Ushio UXL-159) was used as a monitoring light source. A photomultiplier (Hamamatsu R-928) and a storage oscilloscope (Iwatsu TS-8123) were used for the detection.

Fluorescence lifetimes were determined with a picosecond laser system consisting of a titanium sapphire laser (Spectra Physics 3900 "Tsunami") operated with a CW Ar^+ laser (Spectra Physic 2060), a frequency doubler (SP-390), a pulse selector (SP-3980; ≈ 2 ps fwhm) and a streak scope (Hamamatsu C4334).

Oxford Cryostat model DN-1704 and temperature controller ITC-4 were used for the low temperature experiment.

DSC measurement was performed with Seiko DSC-220 and data module SSC-5500H.

JASCO Ubsest 55 equipped with HAAKE K were used for determination of the rate constant of thermal isomerization.

Quantum yield of fluorescence was determined by using anthracene (Φ_f = 0.27)[17] as a fluorescence standard.

Quantum yield of isomerization was determined with 366 nm light from a 400 W high-pressure mercury lamp through UV-35 and U-360 filters. The sample solution was deaerated by bubbling argon and irradiated for 5 - 15 min to keep the conversion within 10%. Light intensity was determined by tris(oxalato)ferrate(III) actinometory.[18] The concentration of each isomer was determined by high performance liquid chromatography through a column (TOSO ODS-80TS) eluting with acetonitrile / water = 4 / 1.

Results

Absorption spectra

Absorption spectra of **2** and **3** were shown in Figure 1. Absorption maximum of *Z*-**2** appeared at 477, 477, and 482 nm in benzene, acetonitrile and methanol, respectively. The absorption maximum of *Z*-**2** was slightly shifted to longer wavelength region in methanol. The *Z*-isomer of **2** did not undergo isomerization to give *E*-isomer in methanol as well as in benzene on irradiation at any wavelength. In *Z*-**2**, no fluorescence spectrum was detected at room temperature.

On direct irradiation in benzene, **3** underwent isomerization mutually between *Z*-isomer and *E*-isomer. The absorption spectrum of *E*-**3** appeared at longer wavelength region than that of *Z*-**3** probably due to the presence of

intramolecular hydrogen bonding. The intramolecular hydrogen bonding may cause the increase of the conjugation through intramolecular hydrogen bonding.

The absorption spectrum of *E*-**3** slightly depended on solvent with the maximum at 524, 523, and 531 nm in benzene, acetonitrile, and methanol, respectively and giving a reddish orange color. On the other hand, absorption maximum of *Z*-**3**, which gave greenish yellow color, appeared at 495 nm in methanol and 470 nm in benzene indicating that the intermolecular hydrogen bonding between *Z*-**3** and methanol decreases the excitation energy.

Compound **4** having formyl group on 2-position of pyrrole ring of compound **3** exhibited similar absorption spectra of **3** for both *E*- and *Z*-isomer.

Intramolecular hydrogen bonding plays an important role to lower the excitation energy in intramolecularly hydrogen bonded isomer.[11] The difference of absorption maximum between *E*-form and *Z*-form of **3** and **4** seemed to be larger than that of usual aromatic ethenes. Usually, the absorption maximum of *Z*-isomer appeared at shorter wavelength than that of *E*-isomer, because of the steric hinderance in *Z*-isomer. On the other hand, *E*-isomer is almost planer form, thus π conjugation would be extended compared with *E*-isomer. For example, the absorption maximum of stilbene appeared at 282 nm and 298 nm for *Z*-isomer and *E*-isomer, respectively in benzene.

Photoisomerization

On photoirradiation, compound **3** and **4** underwent isomerization mutually between *Z*-isomer and *E*-isomer. The photostationary isomer ratio $([E]/[Z])_{pss}$ and the quantum yields of isomerization on irradiation at 366 nm were summarized in Table 1.

With irradiation at 366 nm light, **3** gave a photostationary isomer mixture

$([E]/[Z])_{pss}$ with a very high composition of *E*-form to give $([E]/[Z])_{pss}$ = 99/1 in benzene. The time development of the absorption spectrum of *Z*-**3** on irradiation at 366 nm is shown in Figure 2a. The $([E]/[Z])_{pss}$ = 99/1 value decreased in polar and protic solvent and is 95/5 and 90/10 in acetonitrile and methanol, respectively. On irradiation at 546 nm in benzene, *E*-**3** underwent isomerization to give the *Z*-isomer composition as high as 85%. The isosbestic points appeared at 366, 408, and 483 nm as shown in Figure 2.

As to the compound **3**, quantum yields of Z-to-E isomerization were 0.3 in all the solvent examined, whereas those of E-to-Z isomerization were ~0.003, 0.02 and 0.05 in benzene, acetonitrile, and methanol, respectively.

The quantum yield of isomerization of **4** was strongly dependent on solvent. Figure 3 shows the time development of Z-to-E isomerization of **4** in benzene, acetonitrile, and methanol. Thus, the change of absorbance at maximum wavelength of 546 nm, 555 nm, and 546 nm in benzene, acetonitirile and methanol, respectively were plotted against irradiation time. In benzene, the initial slope of the absorbance change was similar to that of *E*-**3** in benzene. The efficiency of isomerization decreased in acetonitrile and methanol. The quantum yield of Z-to-E isomerization of **4** was estimated to be 0.17, 0.05, and 0.009 in benzene, acetonitrile, and methanol, respectively by comparing the initial slope of the time development of isomerization.

Ground State Properties

To investigate the energetic profile in the ground state, the DSC experiments were performed at different rising temperature (2.5 - 7°C min^{-1}). Thus, the energy difference between *Z*-**3** and *E*-**3** in the ground state was determined to be 7 kcal mol^{-1}. In addition, the activation energy for Z-to-E

isomerization was calculated to be 16 kcal mol^{-1} by the similar treatment reported by Kissinger.[19]

Compound **3** isomerized thermally in methanol, 2-propanol and acetonitrile, between *Z*-isomer and *E*-isomer, while **3** was stable thermally in benzene. The rate constant of isomerization was determined from the change of absorption spectrum at constant temperature. The time development of the absorption maximum of *E*-isomer was traced and the rate constant for thermal Z-to-E isomerization was calculated by first order rate law.

In addition, the equilibrium constant between *E*-isomer and *Z*-isomer was estimated by the relationship of $K = k_{Z\rightarrow E}/k_{E\rightarrow Z}$. Furthermore, the enthalpy and the entropy difference between *Z*- and *E*-isomer were calculated by van't Hoff equation (1). The results were summarized in Table 2.

$$\ln K = -\frac{\Delta H}{RT} + \text{const.} \qquad (1)$$

Triplet state behavior

Compound **2** and **3** did not undergo intersystem crossing on direct irradiation. In addition, transient absorption spectrum was not observed in compound **4**, although it had formyl group on pyrrole ring.

To investigate the photochemical behavior in the triplet excited state, laser flash photolysis was performed in the presence of triplet sensitizer. Figure 4 shows the change of absorption spectra of *Z*-**2** (1.0×10^{-4} M) on Michler's ketone (0.06 M) sensitization. The intense band at shorter wavelength than 400 nm and the absorption at 480 nm were assigned to the

absorption spectra of Michler's ketone and *Z*-**2**, respectively. On laser excitation at 390 nm, the absorption band of 480 nm decreased, and the solution color changed from orange to pale yellow. This means that *Z*-**2** decomposed in the triplet excited state probably by hydrogen abstraction to give radical species.

Triplet sensitization experiments of *Z*-**3** and *E*-**3** were also performed. The transient absorption spectra of *Z*-**3** (6x 10^{-5} M) on Michler's ketone (1x 10^{-4} M) sensitization at 308 nm were shown in Figure 5. Immediately after laser excitation, the decrease of absorption of *Z*-**3** was observed at 470 nm and absorbance at 530 nm corresponding to the absorption of *E*-**3** was gradually increased. The change of transient absorption spectrum indicates that the Z-to-E isomerization occurred in the triplet excited state. Actually, the composition of *E*-isomer after laser excitation in the presence of Michler's ketone was larger than that in the absence of Michler's ketone.

On the other hand, *E*-**3** (5x 10^{-4} M) gave the transient absorption spectra with the maximum wavelength at 600 and 620 nm on biacetyl (0.14 M) sensitization (Figure 6) with 425 nm laser pulse. Oxygen quenched the transient species appeared at 600 nm, which was assigned to the triplet excited state. The other transient species can be assigned to the radical, which was produced by hydrogen abstraction reaction of carbonyl group. The absorption spectrum of *E*-**3** decreased after the irradiation with triplet sensitizer as shown in Figure 7 as similar to the case of *Z*-**2**. Energy diagram of **3** in the triplet excited state was shown in Figure 8.

The rate constant of triplet quenching from benzil (E_T = 53 kcal mol^{-1}) to *E*-**3** in benzene was determined to be 7.4x 10^9 M^{-1} s^{-1}. Both compound **2** and **3** did not exhibit phosphorescence spectra at 77K. Thus, the triplet energies of **2** and **3** could not be determined.

Fluorescence properties

Fluorescence and fluorescence excitation spectra of **3** and **4** in toluene were shown in Figure 9 and 10. The singlet energies are almost the same for **3** and **4** and fluorescence excitation spectra are similar to the absorption spectra.

Quantum yield of fluorescence and fluorescence lifetime of compound **3** and **4** were measured in toluene and the results were summarized in Table 3.

Fluorescence lifetime of **4** were ca. 10 times longer than that of **3** and the quantum yield of fluorescence of **4** were 10 times larger than that of **3**. The rate constant of fluorescence emission was calculated by equation 2. In this equation, k_f, τ_f, and Φ_f stand for the rate constant of natural fluorescence decay, fluorescence lifetime and quantum yield of fluorescence, respectively.

$$k_f = \Phi_f / \tau_f \qquad (2)$$

Thus, k_f was estimated to be 2.8x 10^7 s^{-1} and 6.6x 10^7 s^{-1}, respectively for *E*-**3** and *Z*-**3** and to be 1.9x 10^7 s^{-1} and 5.9x 10^7 s^{-1}, respectively for *E*-**4** and *Z*-**4**. The value of k_f was nearly the same for **3** and **4**. These results indicate that the rate constant of non-radiative deactivation pathway decreased as a result of introduction of formyl substituent to the pyrrole ring.

Temperature effect on fluorescence emission

The intensity and lifetime of fluorescence emission of **3** and **4** increased with decreasing temperature.

Since quantum yield of isomerizaiton of *Z*-**3** was estimated to be as low as 0.05, the rate constant of non-radiative deactivation from S_1 state to S_0 state in

E-**3** should be affected by temperature. Comparing the fluorescence intensity at 77K with that at room temperature, the quantum yield of fluorescence emission (Φ_f) at 77K was estimated to be 0.1 both for *Z*-**3** and *E*-**3** as shown in Figure 11; at room temperature Φ_f was 6x 10^{-4} and 6x 10^{-4} for *Z*-**3** and *E*-**3** in ethanol.

The maximum wavelength of fluorescence excitation spectra of *Z*-**3** and *E*-**3** at 77K was the same as that at room temperature as shown in Figure 12. The maximum wavelength of fluorescence spectrum of *Z*-**3** at 77K was also the same with that at room temperature. On the other hand, that of *E*-**3** was shifted from 578 nm to 565 nm with decrease of temperature from 165K to 77K as shown in Figure 13, though the maximum wavelength at 165K was identical to that at 295K.

The temperature dependence of fluorescence lifetime in toluene was observed from 298K to 185K. The fluorescence lifetime of *E*-**3** increased from 210 ps to 2.9 ns with decreasing temperature from 295K to 185K. The fluorescence lifetime of *E*-**4** also increased from 4.6 ns to 8.1 ns with decreasing temperature from 295K to 185K.

Discussion

Energetic Profile in the Ground State

The difference of enthalpy between *Z*-**3** and *E*-**3** was estimated to be 7 kcal mol^{-1} from the result of DSC experiment. On the other hand, *Z*-**3** was more stable than *E*-**3** by 0.85 kcal mol^{-1} in methanol. These results indicate that the intermolecular hydrogen bonding between *Z*-**3** and methanol stabilizes the ground state of *Z*-**3**. The negative value of the entropy difference observed for

Z-to-E isomerization, -1.4 cal mol^{-1} K^{-1}, could be explained by the existence of intermolecular hydrogen bonding between *Z*-**3** and methanol. In 2-propanol, the enthalpy difference between *Z*-**3** and *E*-**3** was smaller than that in methanol probably because more bulky alkyl group of 2-propanol than that of methanol may prevent from forming intermolecular hydrogen bonding.

The activation energy (E_a) for isomerization in methanol, 2-propanol and acetonitrile was calculated by Arrhenius equation. The rate constant of thermal isomerization increased with increasing temperature. The E_a and the frequency factor (A) for Z-to-E isomerization were calculated to be 23.4 kcal mol^{-1} and 4.4x 10^{11} s^{-1}, respectively in methanol and 24.9 kcal mol^{-1} and 1.2x 10^{12} s^{-1}, respectively in 2-propanol. In acetonitrile, E_a and A for Z-to-E isomerization were calculated to be 17.6 kcal mol^{-1} and 9.4x 10^8 s^{-1}, respectively.

Although, compound **3** underwent isomerization mutually between *E*-isomer and *Z*-isomer thermally, compound **4** was stable even in methanol. Introduction of formyl group increases the thermal stability for isomerization around C=C double bond in protic solvent.

Effects of formyl group on the fluorescence emission and isomerization

Both *Z*- and *E*-**3** exhibited fluorescence emission with the quantum yield of 0.023 and 5.9x 10^{-3}, respectively in benzene. The introduction of formyl group at the 5-position of pyrrole ring of **3** brought about large increase of fluorescence quantum yield and fluorescence lifetime by a factor of 10. It was reported that quantum yield of fluorescence of **1** increased by a factor of 100 as a result of introduction of formyl group at 5-position of pyrrole ring.[9]

Introduction of formyl group to the compound **3** may increase the efficiency of the intersystem crossing. However, compound **4** did not exhibit

transient absorption spectrum on laser flash photolysis experiment at room temperature. In addition, compound **4** underwent isomerization mutually between *Z*-isomer and *E*-isomer without decomposition. As mentioned above, *E*-**3** having intramolecular hydrogen bonding underwent decomposition in the triplet excited state. Therefore, it was estimated that the efficiency of intersystem crossing of compound **4** is almost negligible.

On the basis of fluorescence quantum yield and lifetime as shown in Table 2, it was found that the increase of quantum yield by introduction of formyl group was attributed to the decrease of non-radiative decay constant.

Generally, it is considered that hydrogen bonding accelerates the rate constants of non-radiative deactivation due to the high frequency vibrational motion. Inoue et al. reported that fluorescence quantum yield of aminoanthraquinone or aminofluorenone derivatives decreased in the alcoholic solvents by intermolecular hydrogen bonding interaction.[13,14]

The proximity effect can explain the acceleration of non-radiative deactivation.[20] When the energy differences between excited $n\pi^*$ state and $\pi\pi^*$ state was small, non-radiative decactivation can be accelerated by its proximity. For example, the results that quantum yield of fluorescence of *trans*-2-styrylpyridine and *trans*-4-styrylpyridine is smaller than that of *trans*-stilbene can be attributed to perturbation of the $\pi\pi^*$ state by a nearly isoenergetic $n\pi^*$ state, resulting in greatly enhanced non-radiative decay.[21]

In the hemiindigo compounds, the rate constant of non-radiative deactivation decreased by introduction of formyl group, and the explanation of this mechanism needs further investigation.

Introduction of formyl group affect the fluorescence as well as the isomerization behavior. In acetonitrile and methanol, fluorescence emission

was strongly quenched. It was considered that in methanol, intermolecular hydrogen bonding between methanol and **4** would accelerate the non-radiative deactivation much more than that in benzene by a factor of 100. As a result, both fluorescence and isomerization efficiencies were lowered. As mentioned above, quantum yields of Z-to-E isomerization of **3** were 0.3 in all the solvent examined. However, the quantum yield of Z-to-E isomerization of **4** was strongly dependent on the solvent and was estimated to be 0.17, 0.05 and 0.009 in benzene, acetonitrile and methanol, respectively.

Polar solvent and protic solvent accelerate the non-radiative deactivation of **4**. Probably solvent polarity and intermolecular hydrogen bonding interaction brings about the decrease of the interaction between formyl group and NH group in pyrrole ring. As a result of that, frequency factor of the non-radiative deactivation become large, and the rate constant of non-radiative deactivation increases with concomitant decrease of quantum efficiency of isomerization and fluorescence.

Deactivation processes

It was considered that the intramolecular hydrogen bonding accelerate the deactivation pathway, thus quantum yield of fluorescence emission was smaller than that of corresponding compound without hydrogen bonding in ordinary hydrogen bonded system. We have reported that quantum yield of fluorescence of the isomer having intramolecular hydrogen bonding is lower than that of the other isomer.

The fluorescence lifetime of *E*-**3** (τ_s = 210 ps) is shorter than that of *Z*-**3** (τ_s = 350 ps), since the intramolecular hydrogen bonding in *E*-**3** plays an important role in the deactivation from the excited singlet state. As to *Z*-**2**

having intramolecular hydrogen bonding, fluorescence emission was not observed at room temperature. In addition, Z-to-E isomerization did not occur in *Z*-**2** on photoirradiation, indicating that *Z*-**2** undergoes ultra fast deactivation from the excited singlet state through the intramolecular hydrogen bonding. However, at 77 K in ethanol glass, *Z*-**2** exhibited the fluorescence emission with maximum at 520 nm and the lifetime of ca. 8 ns indicating that the deactivation through the intramolecular hydrogen bonding is suppressed with decreasing temperature.

These results indicate that the intramolecular hydrogen bonding would play an important role in the deactivation from the singlet excited state in *Z*-**2** and *E*-**3**. The intramolecular hydrogen bonding suppresses the rotation around C=C double bond in *Z*-**2**.

The quantum yield of isomerization of *Z*-**3** was 0.3 at room temperature. Therefore, one can expect that the decrease of temperature may suppress the isomerization in the singlet excited state and increase the fluorescence emission. However, the intensity was still increasing with decreasing temperature under freezing point of ethanol to indicate the existence of non-radiative deactivation pathway other than E-to-Z isomerization. Fluorescence intensity of *E*-**3** having intramolecular hydrogen bonding also increased with decreasing temperature, although the quantum yield of isomerization was as low as 0.05 in ethanol.

Furthermore it was found that the shape of fluorescence spectra of *E*-**3** changed as a result of decrease of temperature in ethanol as shown in Figure 13. The shift of fluorescence emission maximum indicated the existence of two emissive states in the singlet excited state of *E*-**3** in ethanol. *E*-**3** was excited to the Franck-Condon state, followed by deactivation to the lower energy state and exhibited fluorescence at 578 nm. However, when the temperature was lower

than 165K, the internal conversion to lower emissive state scarcely occurred and at 77K the emission of 565 nm was observed. The temperature effect on the fluorescence spectrum and lifetime indicated the presence of activation barrier for deactivation pathway through the intramolecular hydrogen bonding. On the basis of these findings, energy diagram of **3** in the singlet excited state in ethanol was proposed as shown in Figure 14.

Ethanol can affect the deactivation pathway of *E*-**3** by forming intermolecular hydrogen bonding. Thus, we observed the temperature effect on fluorescence spectrum in toluene. The result showed that the maximum wavelength of fluorescence spectrum did not change in the temperature range between 295K and 185K. The fluorescence intensity also increased with decreasing temperature in toluene.

As described above, quantum yields of E-to-Z isomerization of *E*-**3** and *E*-**4** were estimated to be less than 0.01 in toluene. In addition, the intersystem crossing process was negligible. Therefore, we can postulate that the singlet lifetime (τ_f) of *E*-form was explained by equation 3.

$$\tau_f = 1 / (k_f + k_{nr}) \qquad (3)$$

It was considered that only k_{nr} is dependent on temperature. The fluorescence lifetime in toluene was observed from 298K to 185K. The fluorescence lifetime of *E*-**3** increased from 210 ps to 2.9 ns with decreasing temperature from 295K to 185K. τ_f of *E*-**4** increased from 4.6 ns to 8.1 ns with decreasing temperature from 295K to 185K. From these observations, the activation energy and frequency factor for k_{nr} was calculated to be 2.7 kcal mol^{-1} and 5.2x 10^{11} s^{-1}, respectively for *E*-**3**, 1.4 kcal mol^{-1} and 2.2x 10^{9} s^{-1}

respectively for *E*-**4** from equation 3.

$$\ln (k_{nr}) = \ln (1/\tau_f - k_f) = \ln A - E_a / RT \qquad (3)$$

The fluorescence lifetime of *E*-**4** become constant to be 8.0 ns under 140K, therefore the values from 295K to 250K were used for the calculation of activation parameter. As to *E*-**3**, the fluorescence lifetime was 9.0 ns at 77K in ethanol glass solvent.

The frequency factor of non-radiative deactivation for *E*-**4** was smaller than that of *E*-**3** by a factor of 100. This result indicates that the frequency of vibrational mode attributed to non-radiative deactivation was lowered by introduction of formyl group due to the inductive effect of formyl group or hydrogen bonding interaction between formyl group and NH group in pyrrole ring.

Photochromic properties

The isomer composition of **3** at the photostationary state was dependent on the irradiation wavelength as shown in Figure 2.

Thus, **3** exhibited almost one-way Z-to-E isomerization on irradiation with 366 nm light, where both *Z*-isomer and *E*-isomer have similar absorption coefficient. The considerably large difference between $\Phi_{Z\rightarrow E}$ and $\Phi_{E\rightarrow Z}$ is the reason for almost one-way isomerization. However, a very high ratio of *Z*-**3** to *E*-**3** as 85:15 was observed on irradiation at 546 nm, where the *E*-**3** has much higher absorption coefficient than *Z*-**3**. Therefore, the irradiation wavelength

affected the photostationary state isomer composition to give ~99% of the *E*-isomer and ~85% of the *Z*-isomer with irradiation at 366 nm and 546 nm, respectively. The repetition characteristics of absorption spectrum by alternate irradiation between 366 nm and 546 nm was shown in Figure 16.

Conclusion

Compound **3** exhibited almost one-way Z-to-E isomerization on irradiation with 366 nm light, where both *Z*-**3** and *E*-**3** have similar absorption coefficient, due to the considerably large difference between $\Phi_{Z\rightarrow E}$ and $\Phi_{E\rightarrow Z}$. However, **3** gives a photostationary mixture with a very high ratio of Z-isomer to E-isomer as 85:15 on irradiation at 546 nm where the *E*-**4** has much higher absorption coefficient than *Z*-**3**.

Introduction of formyl group to pyrrole ring of **3** improves thermal stability in solvent. The quantum yield of isomerizaiton of **4** in methanol was lowered by a factor of 100 than that in benzene, while the quantum yield of isomerization of **3** was almost the same in methanol and benzene. Introduction of formyl group resulted in the increase of quantum yield of fluorescence and fluorescence lifetime.

On the basis of the these findings, it was found that the intramolecular hydrogen bonding could play an important role for constructing photochromic compounds having absorption band at visible region and the substituent and solvent could affect their photochromic properties.

References

1. "Organic Photochromic and Thremochromic Compounds," ed by J. C. Crano and R. Guglielmetti, Kluwer Academic / Plenum Press, New York (1999), Vol. 1, 2.
2. "Photochromism: Molecules and Systems," ed by H. Durr and H. Bouas-Laurent, Elsevier, Amsterdam (1990).
3. M. Irie, *Chem. Rev.*, **2000**, *100*, 1683.
4. M. Irie and K. Uchida, *Bull. Chem. Soc. Jpn.*, **1998**, *71*, 985.
5. F. D. Lewis, B. A. Yoon, T. Arai, T. Iwasaki, and K. Tokumaru, *J. Am. Chem. Soc.*, **1994**, *116*, 3171.
6. T. Arai, M. Obi, T. Iwasaki, K. Tokumaru, and F. D. Lewis, *J. Photochem. Photobiol. A: Chem.*, **1995**, *96*, 65.
7. T. Arai, M. Moriyama, and K. Tokumaru, *J. Am. Chem. Soc.*, **1994**, *116*, 3171.
8. M. Obi, H. Sakuragi, and T. Arai, *Chem. Lett.*, **1998**, 169.
9. T. Arai and Y. Hozumi, *Chem. Lett.*, **1998**, 1153.
10. Y. Yang and T. Arai, *Tetrahedron, Lett.*, **1998**, *39*, 2617.
11. T. Arai and M. Ikegami, *Chem. Lett.*, **1999**, 965.
12. M. Ikegami and T. Arai, *J. Chem. Soc. Perkin Trans. 2*, in press.
13. T. Yatsuhashi and H. Inoue, *J. Phys. Chem. A*, **1997**, *101*, 8166.
14. T. Yatsuhashi, Y. Nakajima, T. Shimada, and H. Inoue, *J. Phys. Chem. A*, **1998**, *102*, 3018.
15. A. R. Katrinzky, Q. L. Li and W. Q. Fan, *J. Heterocyclic Chem.*, **1988**, *25*, 1287.
16. J. Bergman, *Tetrahedron Lett.*, **1972**, *46*, 4723.
17. D. F. Eaton, *Pure & Appl. Chem.*, **1988**, *60*, 1107.

18. "Handbook of Photochemistry," ed. By S. L. Murov, I. Carmichal and G. L. Hug, Marcel Dekker, New York (1993).
19. H. E. Kissinger, *Anal. Chem.*, **1957**, *29*, 1702.
20. E. C. Lim, *J. Phys. Chem.*, **1986**, *90*, 6770.
21. F. D. Lewis, R. S. Kalgutkar, and J. -S. Yang, *J. Am. Chem. Soc.*, **2001**, *123*, 3878.

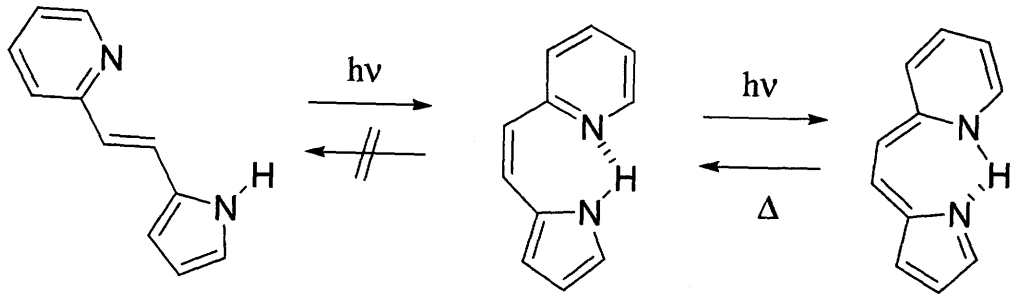

E-1 *Z*-1 *Z*-1'

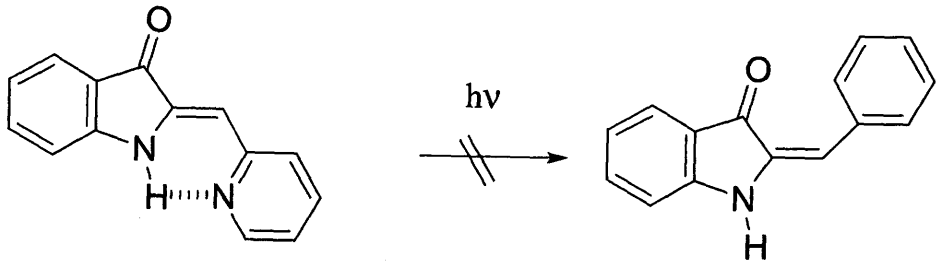

Z-2 *E*-2

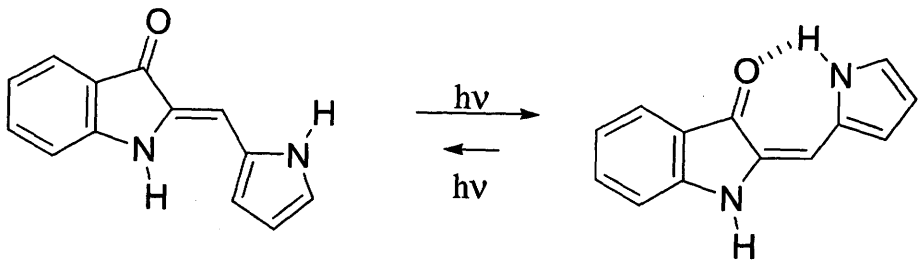

Z-3 *E*-3

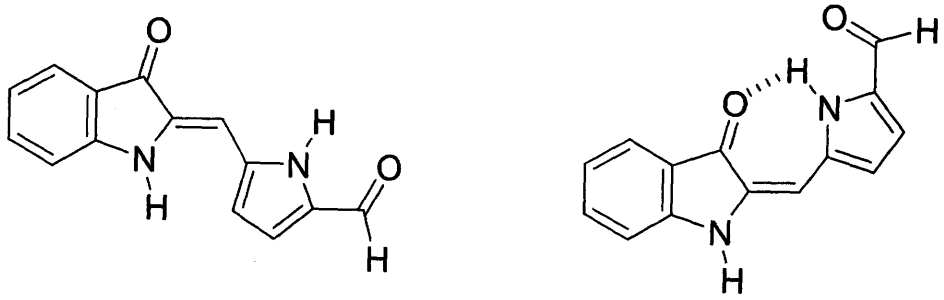

Z-4 *E*-4

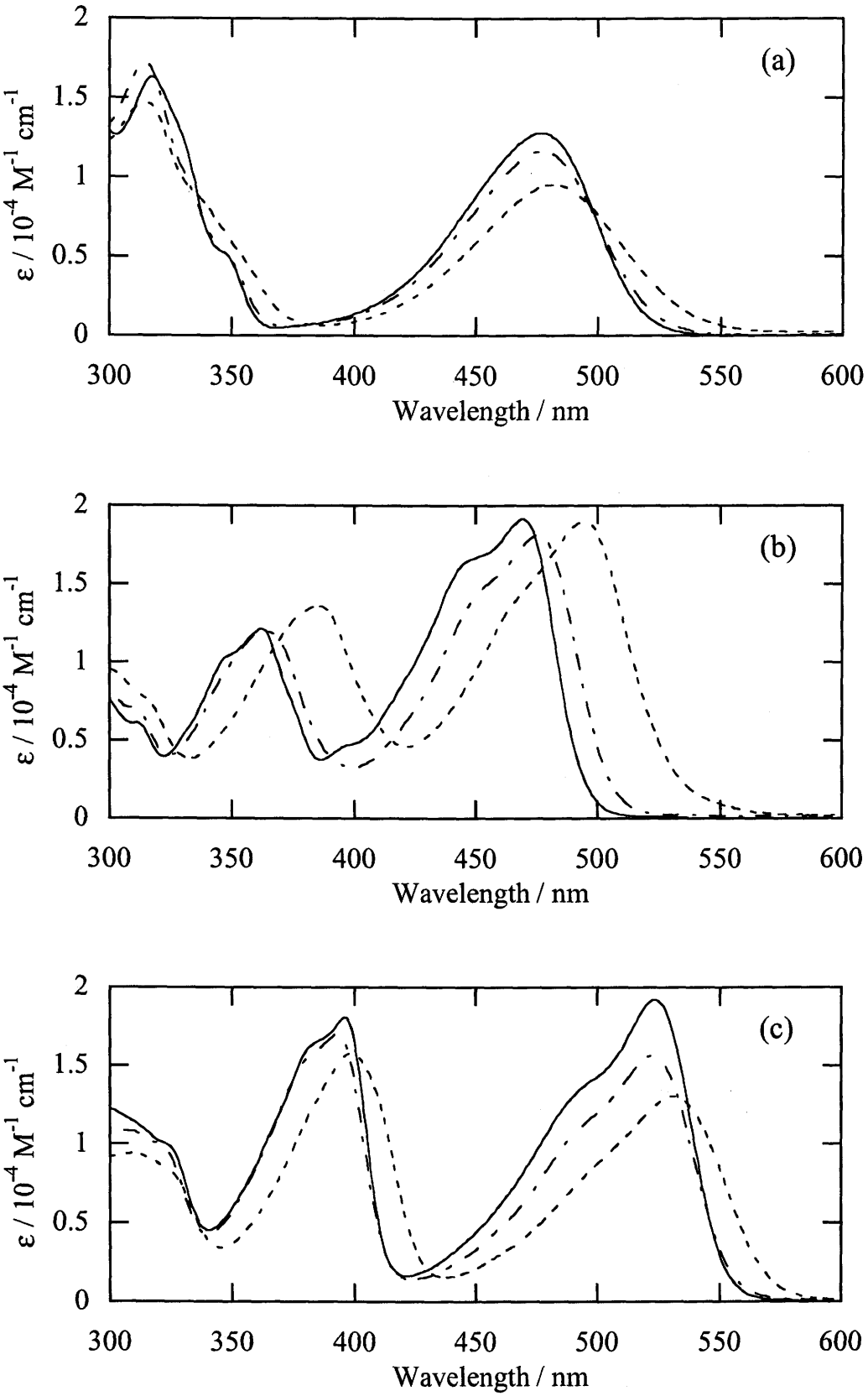

Figure 1. Absorption spectra of *Z*-**2** (a), *Z*-**3** (b) and *E*-**3** (c) in benzene (solid line), acetonitrile (dashed line) and methanol (dotted line).

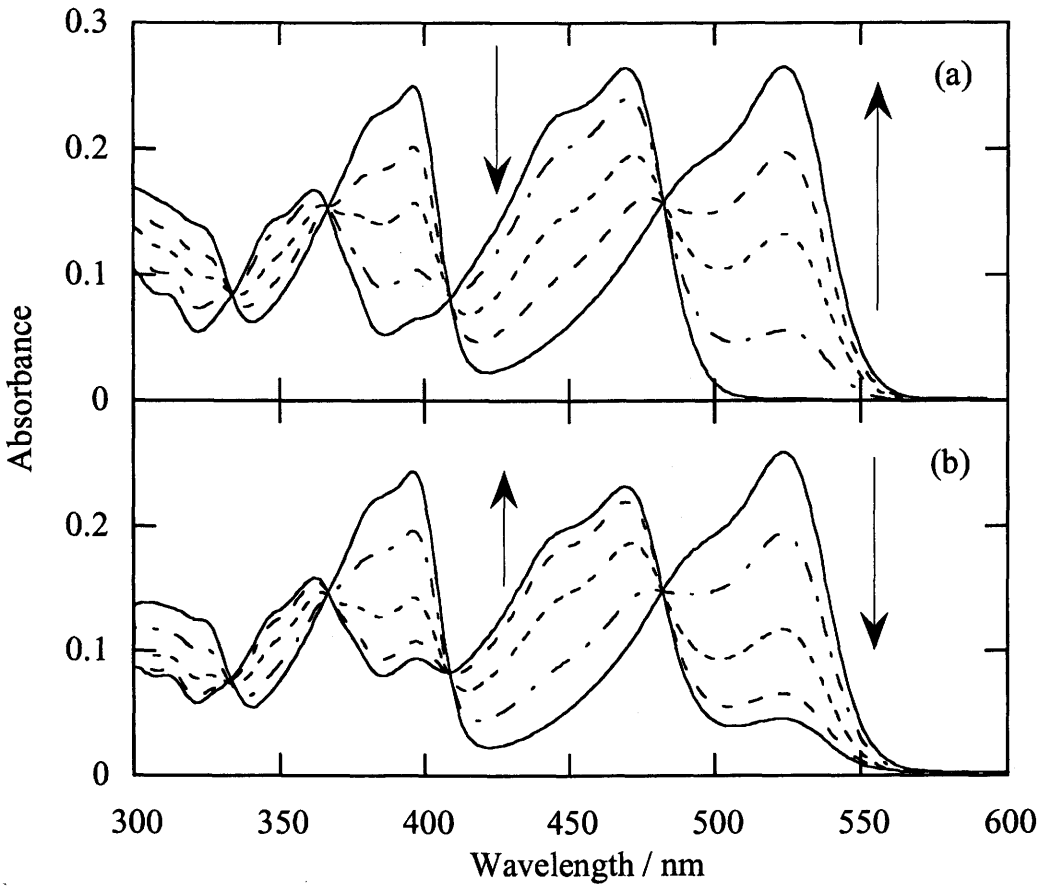

Figure 2. Change of absorption spectrum of *Z*-**3** (a) and *E*-**3** (b) on irradiation at 366 nm 546 nm, respectively in benzene under argon.

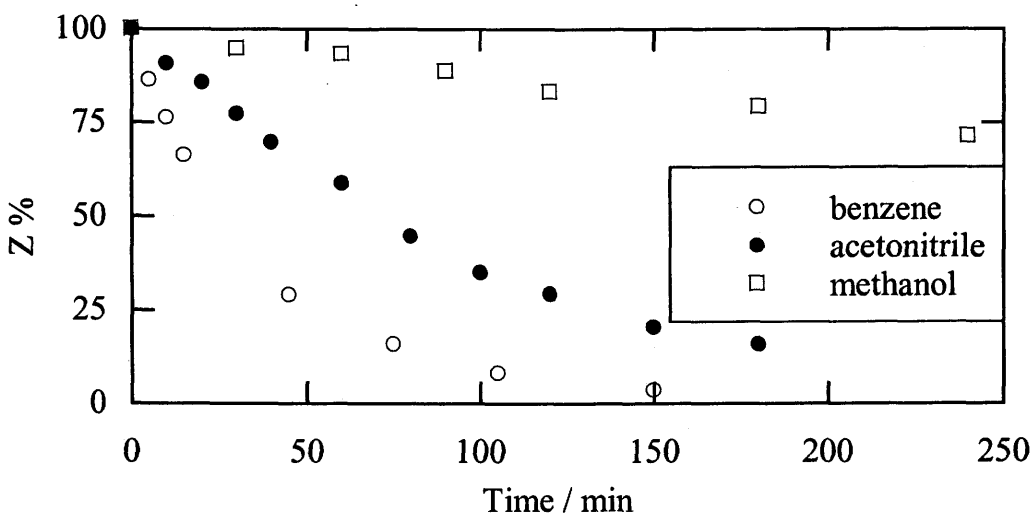

Figure 3. Time development for Z-to-E isomerizaion of *Z*-**4** on irradiation at 350 nm in benzene, acetonitrile, and methanol.

Table 1. Quantum yields of isomerization and isomer ratio at photostationary state on irradiation at 366 nm for **3** and **4**

	Compound **3**			Compound **4**	
	$\Phi_{Z\rightarrow E}$	$\Phi_{E\rightarrow Z}$	$([E]/[Z])_{pss}$	$\Phi_{Z\rightarrow E}$	$([E]/[Z])_{pss}$
Benzene	0.31	0.003	99 / 1	0.17	99 / 4
Acetonitrile	0.32	0.02	99 / 5	0.05	93 / 7
Methanol	0.33	0.05	89 / 11	0.009	90 / 10

Table 2. Rate constants of isomerization and thermodynamic parameters for Z-to-E isomerizaiton of **3**

		A / s^{-1}	E_a / kcal mol^{-1}	ΔH / kcal mol^{-1}	ΔS / cal mol^{-1} K^{-1}	[E]/[Z] at 298K
Methanol	Z→E	4.4×10^{11}	23.4	-0.85	1.4	27 / 73
	E→Z	2.2×10^{11}	22.5			
2-Propanol	Z→E	1.2×10^{12}	24.9	-0.4	1.3	50 / 50
	E→Z	6.4×10^{11}	24.5			
Acetonitrile	Z→E	9.4×10^{6}	17.6	1.4	-3.4	65 / 35
	E→Z	5.3×10^{7}	19.0			
Solid (DSC)	Z→E		16	7		

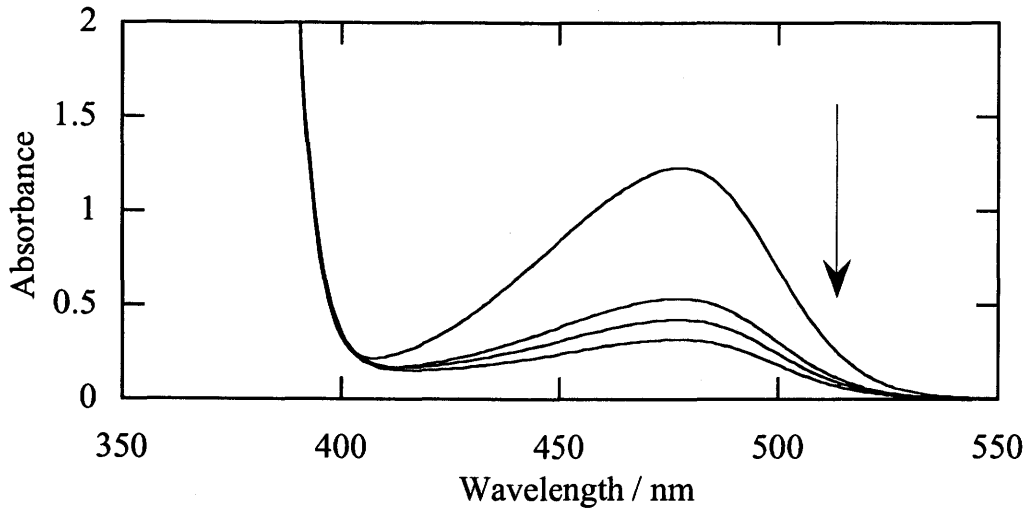

Figure 4. Absorption spectrum change of *Z*-**2** on Michler's ketone sensitization with 390 nm light.

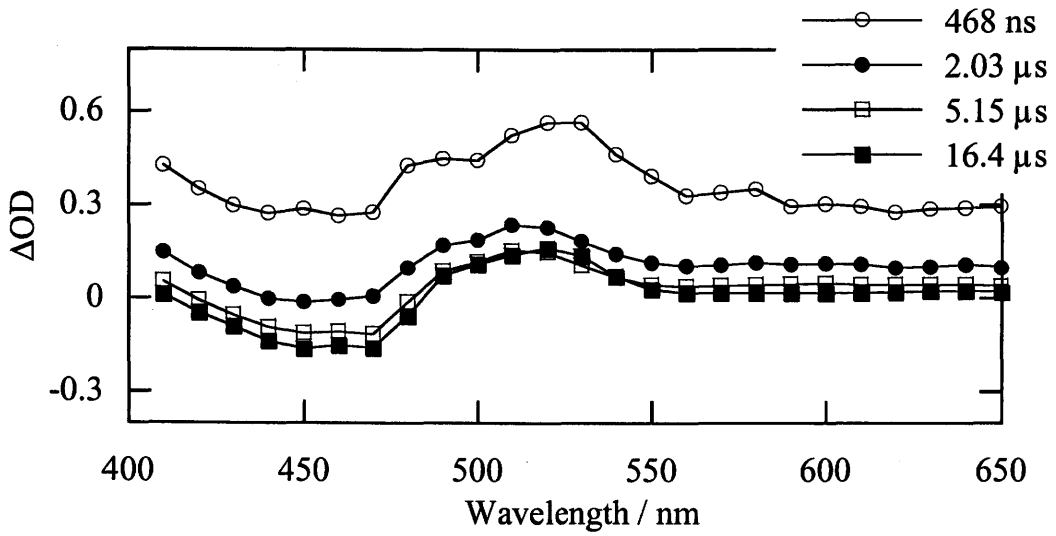

Figure 5. Transient absorption spectra of *Z*-**3** on Michler's ketone sensitization in benzene.

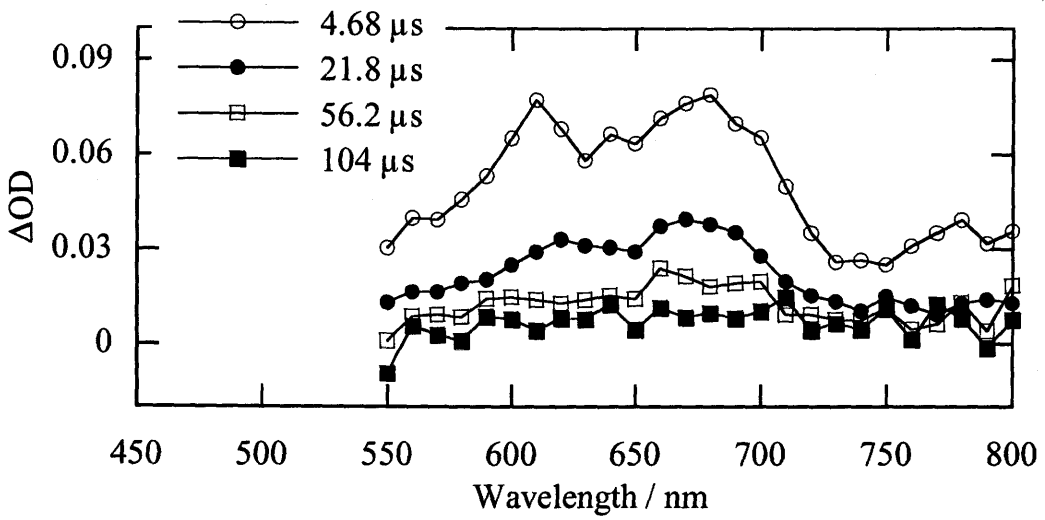

Figure 6. Transient absorption spectra of *E*-**3** on biacetyl sensitization in benzene.

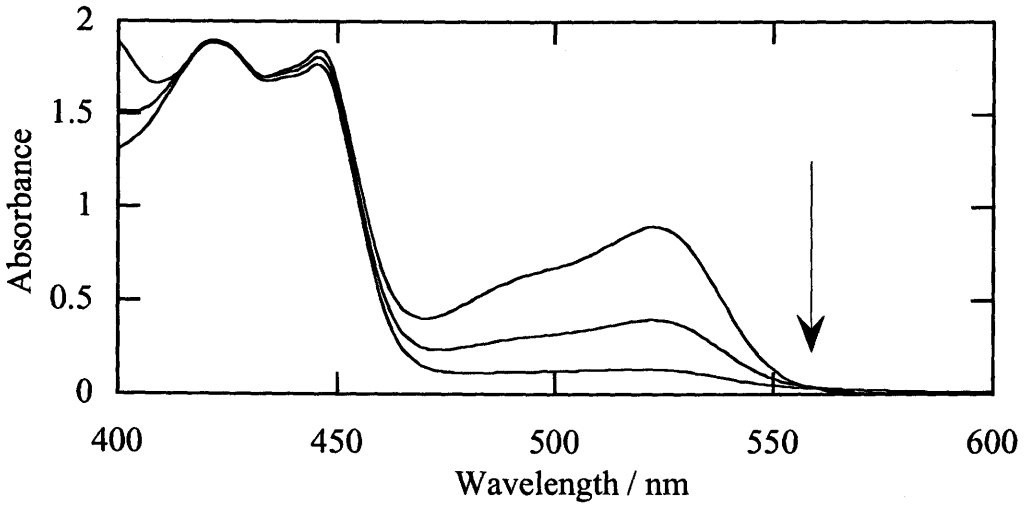

Figure 7. Absorption spectrum change of *E*-**3** on biacetyl sensitization with 425 nm light.

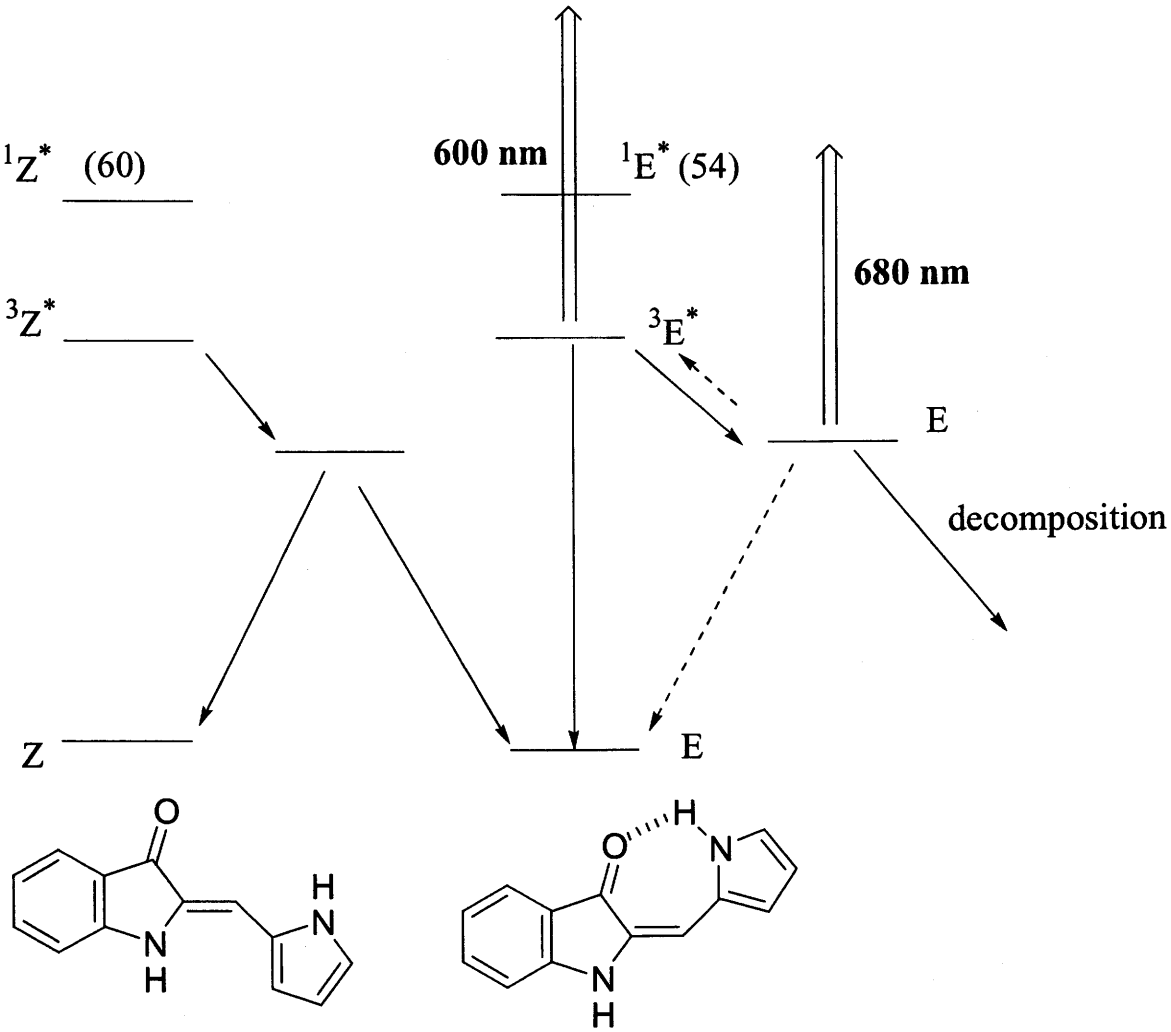

Figure 8. Energy diagram of **3** in the triplet excited state.

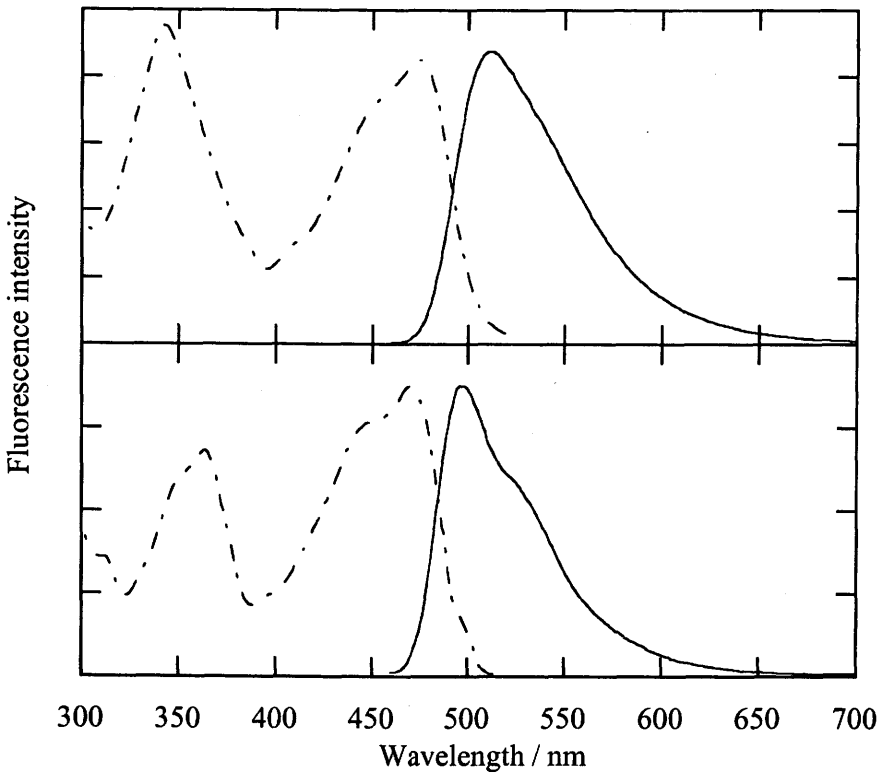

Figure 9. Fluorescence and fluorescence excitation spectra of *Z*-**3** and *Z*-**4** in toluene at 295 K.

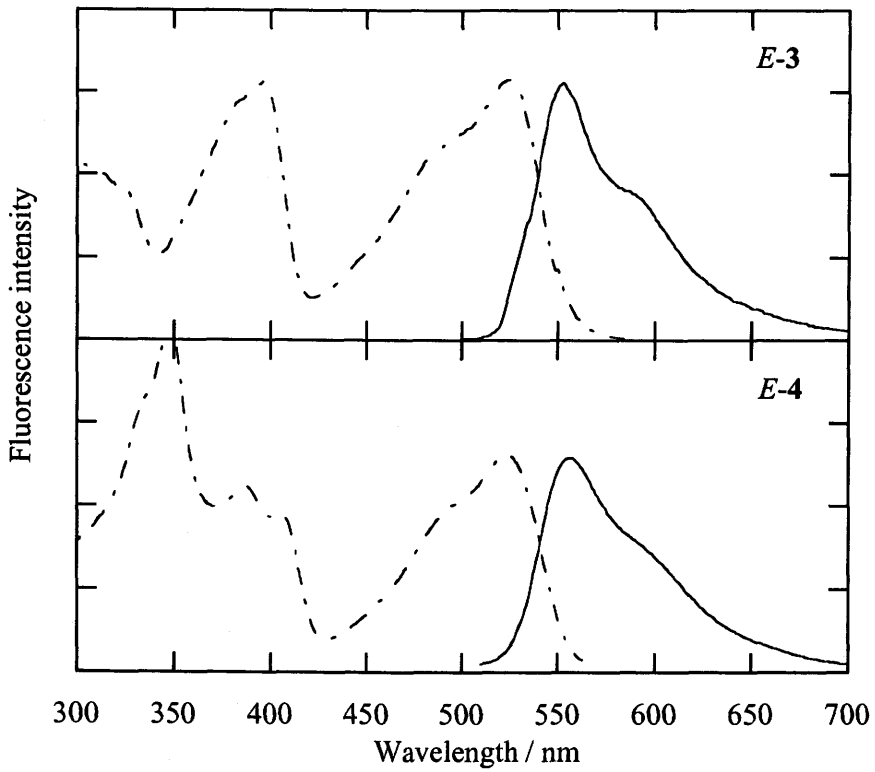

Figure 10. Fluorescence and fluorescence excitation spectra of *E*-**3** and *E*-**4** in toluene at 295 K.

Table 3. Spectroscopic parameters for fluorescence of **3** and **4** at 295K

			λ_{max} / nm		E_s [a]	Φ_f	τ_f / ns	k_f [b]
			Abs.	Fluo.				
3	Benzene	Z	470	500	59.0	0.023	0.35	6.6
		E	524	554	53.1	5.9×10^{-3}	0.21	2.8
	Toluene	Z	470	498	58.8	0.025	0.35	7.1
		E	525	553	53.1	5.2×10^{-3}	0.21	2.5
	Acetonitrile	Z	477	514	57.6	2.6×10^{-3}		
		E	523	560	52.6	2.1×10^{-3}		
	Methanol	Z	494	533	55.9	5.9×10^{-4}		
		E	531	574	51.6	6.4×10^{-4}		
	Chloroform	Z	476	514	57.6	2.0×10^{-3}		
		E	524	560	52.6	1.8×10^{-3}		
4	Toluene	Z	475	511	58.1	0.29	4.9	5.9
		E	524	556	52.8	0.086	4.6	1.9
	Acetonitrile	Z	482	543	56.4	0.04		
		E	528	590	51.7	4×10^{-3}		
	Methanol	Z	491	585	54.5	8×10^{-4}		
		E	534	630	50.7	3×10^{-5}		

a) in kcal mol^{-1} b) in 10^7 s^{-1}

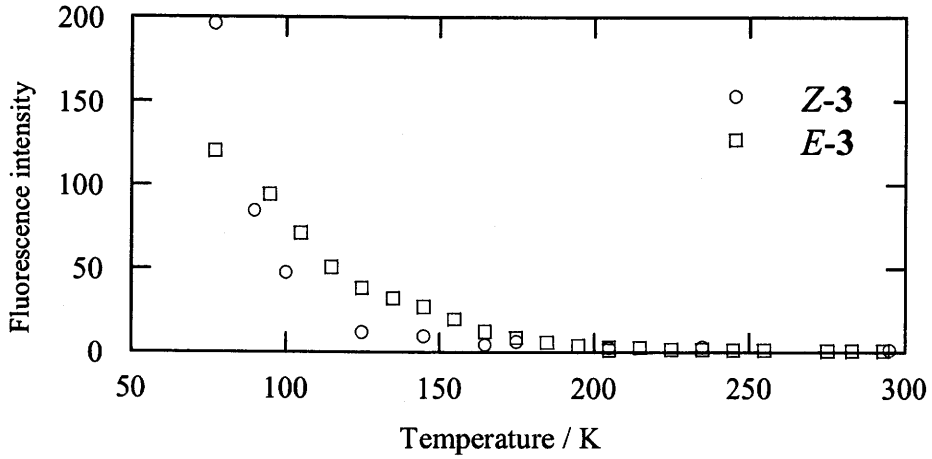

Figure 11. Temperature dependence of fluorescence intensity of *Z*-**3** (circle) and *E*-**3** (square) in ethanol.

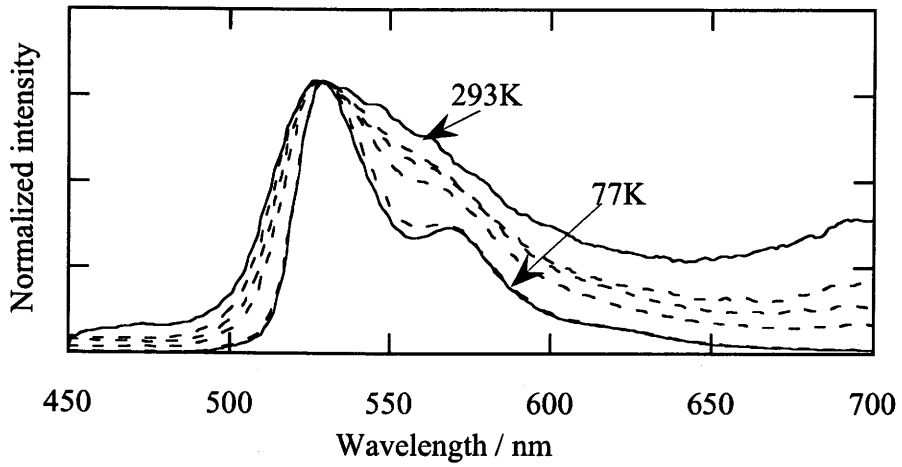

Figure 12. Temperature dependence of fluorescence spectrum of *Z*-**3** in ethanol between 293K and 77K.

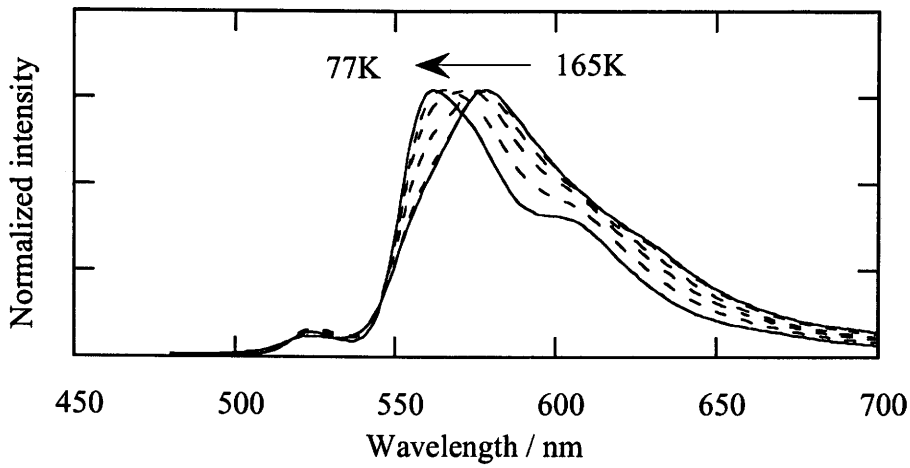

Figure 13. Temperature dependence of fluorescence spectrum of *E*-**3** in ethanol between 165K and 77K.

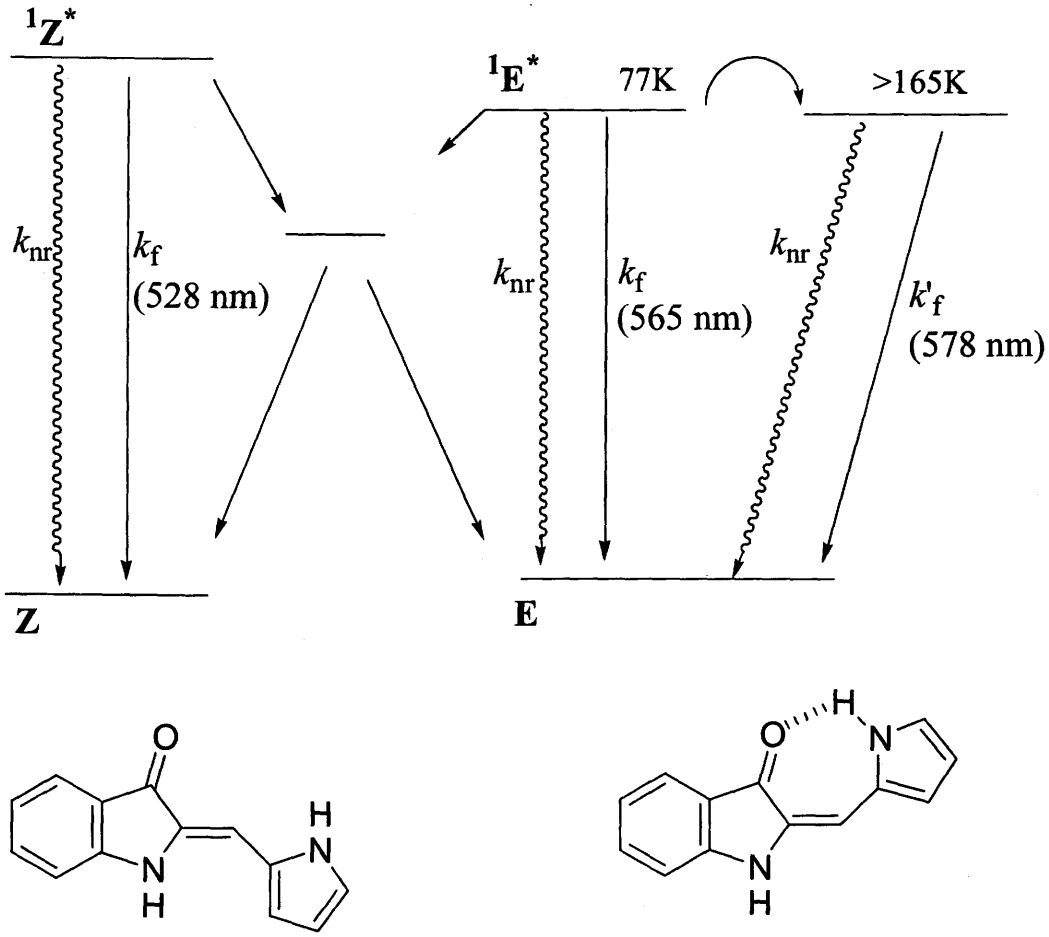

Figure 14. Energy diagram of **3** in the singlet excited state in ethanol.

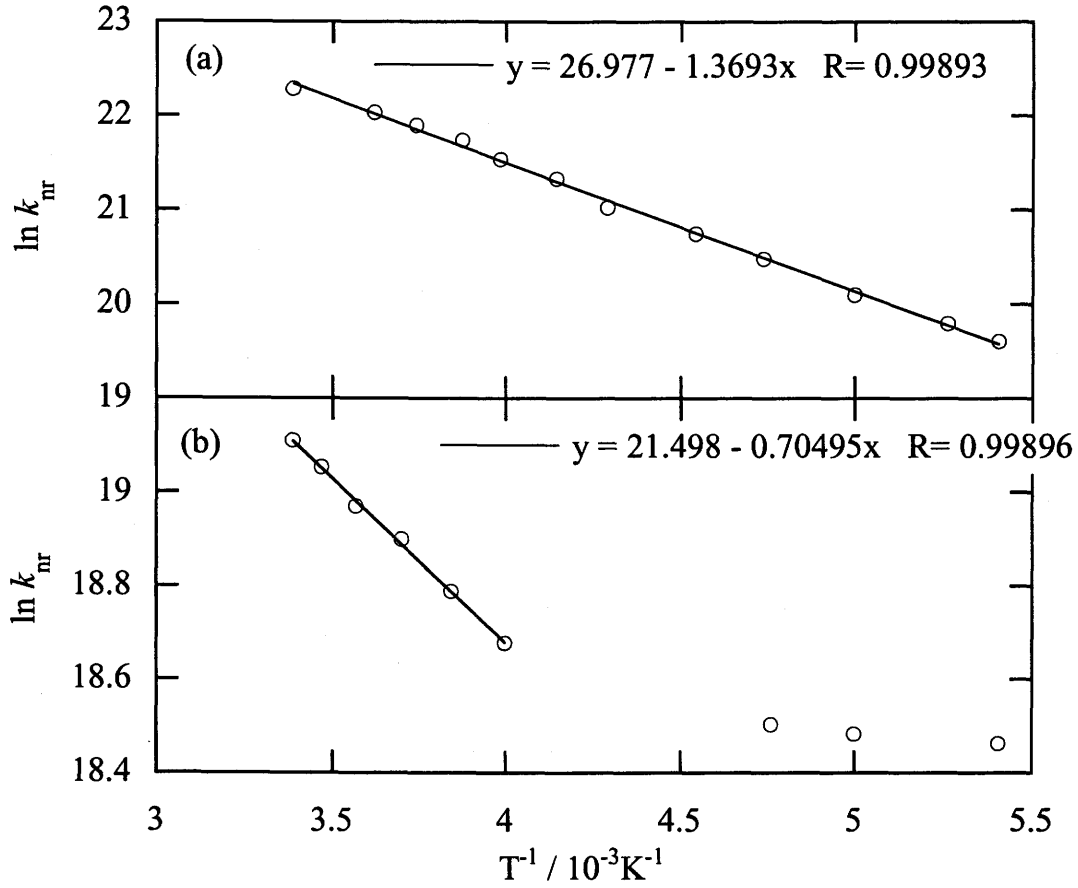

Figure 15. Arrhenius plot for non-radiative deactivation form singlet excited state of *E*-**3** and *E*-**4** in toluene.

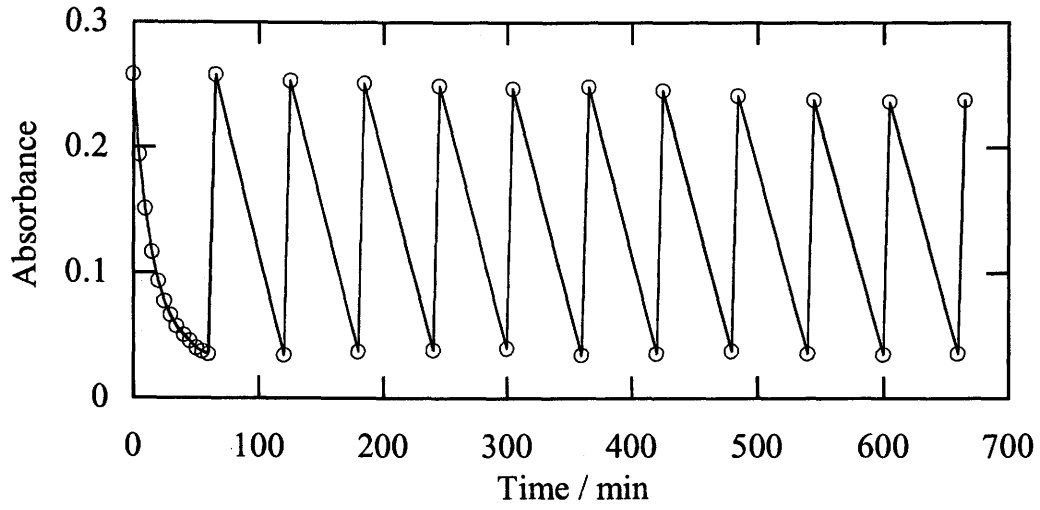

Figure 16. Repetition characteristics of **3** by alternate irradiation at 366 nm and 546 nm of high pressure mercury lamp in benzene under argon monitored at 524 nm.

Chapter 5

Study on Triplet State Behaviors of Pyrrole-2-carboxyaldehyde and Its Related Compounds

Abstract

Triplet state behaviors of pyrrole-2-carboxyaldehyde (**1**) and its related compounds were investigated by means of nano-second laser flash photolysis. Compound **1** did not exhibit fluorescence emission, but underwent intersystem crossing to the triplet state with the efficiency of 0.80 in benzene. The lifetime of **1** triplet depended on its concentration. The rate constant of self-quenching was determined to be 1.6×10^{8} M^{-1} s^{-1} in benzene. Taking into account photochemical behavior of the related compounds, intermolecular hydrogen bonding between triplet state of **1** and ground state of **1** seemed to play an important role in the self-quenching process.

Introduction

Photochemical reactions of aromatic carbonyl compounds were well studied because of their interesting spectroscopic and photochemical properties. The carbonyl compounds undergoes intersystem crossing to give the triplet excited state with high quantum yield due to the $n\pi^*$ character of excited state. Therefore, most of the photochemical reaction of these compounds occurred in the triplet excited state; triplet energy transfer, cycloaddition, hydrogen abstraction, photocleavage reaction and so on.[1,2]

In the course of our study on the effects of inter- or intramolecular hydrogen bonding on the photochemical behavior of aromatic olefins, we come to pay attention to pyrrole-2-carboxyaldehyde (**1**).[3-10] We have reported that the quantum yield of fluorescence of an olefin having pyrrole ring and pyridine ring increased with introduction of formyl group on the 5-position of pyrrole ring by a factor of 100.[5,6] This effect of formyl group on the fluorescence emission was very interesting, since one can usually expect that introduction of formyl group results in the increase of quantum yield of intersystem crossing by spin-orbit interaction.

Since **1** have both hydrogen bonded accepter (NH proton) and donor (carbonyl oxygen) in a molecule, one can think that **1** forms dimer by intermolecular hydrogen bonding like 7-azoindole or 2-hydroxypyridine (2-pyridone) as shown in Scheme 1.[11,12] In addition, **1** have a carbonyl group inducing the intersystem crossing. Thus, the effect of hydrogen bonding on the triplet state of **1** was very interested.

We have prepared **1**, *N*-methylpyrrole-2-carboxyaldehyde (**2**), 2-acetylpyrrole (**3**), *N*-methyl-2-acetylpyrrole (**4**), and 2,5-diformylpyrrole (**5**), and the triplet state behaviors of these compounds were investigated by means

of laser flash photolysis.

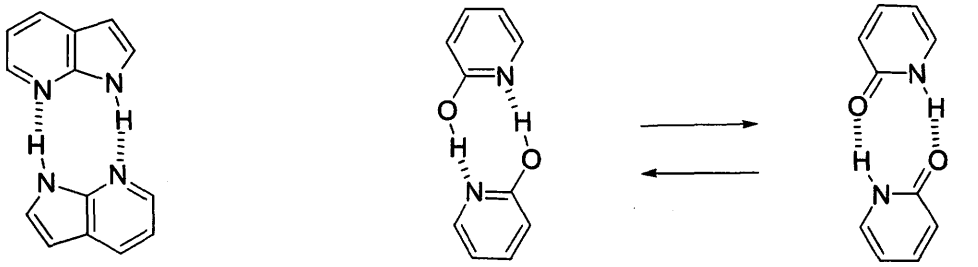

7-azaindole 2-hydroxypyridine 2-pyridone

Scheme 1.

1 **2** **3** **4**

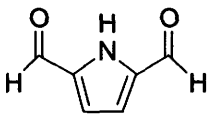

5

Scheme 2. Pyrroles investigated in this study.

Experiment

Materials and Solvents

Compound **1** and **3** were purchased from Aldrich and purified by recrystallization from hexane. Compound **2** and **4** were purchased from Aldrich and purified by distillation under reduced pressure. Compound **5** was prepared by Vielsmeier reaction from pyrrole.[13] The purity was checked by ^{1}H NMR and HPLC analysis.

In spectroscopy, Dotite Spectrosol or Luminasol was used as solvents without further purification except for ethanol. Ethanol was purified by distillation over calcium hydride.

Measurement

Absorption and fluorescence spectra were measured on a Shimadzu UV-1600 and on a Hitachi F-4000 fluorescence spectrometer, respectively. Phosphorescence spectra were measured on a Hitachi F-4000 equipped with the accessory unit for phosphorescence.

Laser flash photolyses were performed by using an excimer laser (Lambda Physik LPX-100, 308 nm, 20 ns fwhm) or excimer laser pumped dye laser Lambda Physik Scanmate, (DMQ, 360 nm, 10 ns fwhm) as excitation light sources and a pulsed xenon arc (Ushio UXL-159) was used as a monitoring light source. A photomultiplier (Hamamatsu R-928) and a storage oscilloscope (Iwatsu TS-8123) were used for the detection.

Results

Absorption spectra

Absorption spectra of **1**, **2**, **3**, and **4** in methylcyclohexane, benzene, acetonitrile and methanol were shown in Figure 1. The intense band at around 280 nm was shifted to longer wavelength with increase solvent polarity from 279 nm in methylcyclohexane to 288 nm in methanol, and was assigned to $\pi\pi^*$ transition. The absorption band at longer than 320 nm with the ε value of 40 at 340 nm was assigned to the $n\pi^*$ transition in methylcyclohexane.

Absorption spectrum of **5** was also observed in hexane appeared at 306 nm ($\varepsilon = 2.0 \times 10^4$ M^{-1} cm^{-1}) and 350 nm ($\varepsilon = 150$ M^{-1} cm^{-1}), which were assigned to the $\pi\pi^*$ and $n\pi^*$ transition, respectively.

Concentration dependence of absorption spectrum of **1** was explored in methylcyclohexane at the concentration from 6.5×10^{-5} to 1.1×10^{-2} M (Figure 3). The ε value was the same in the concentration examined, indicating that the dimer formation or aggregation did not occur in **1**.

The concentration dependence of absorption spectrum of **5** was also studied and the result was shown in Figure 4. Compound **5** did not give dimer or aggregate even in hexane.

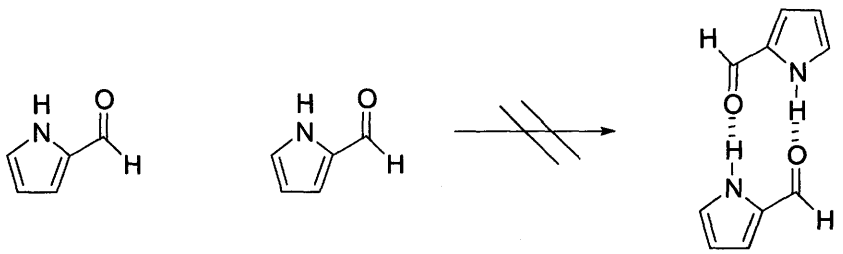

Phosphorescence spectra

Compounds **1-5** did not exhibit fluorescence and phosphorescence emission at room temperature. The phosphorescence spectra of these compounds were observed in methylcyclohexane and ethanol at 77K and those of **1** and **5** were shown in Figure 5 and 6. The vibrational structure was observed in the phosphorescence spectrum of **1** in methylcyclohexane with 1400 cm^{-1}, but broad spectrum was observed in ethanol. On the other hand, phosphorescence spectrum of **5** in ethanol was similar to that in methylcyclohexane.

Laser Photolysis with 308 nm pulse

On laser excitation at 308 nm, **1** - **5** gave fluorescent products. Figure 7 shows absorption spectrum of **1** after 600 times laser pulse excitation (~20 mJ $pulse^{-1}$) in methylcyclohexane and the absorption attributed to the photolysis product appeared at 390 nm with vibrational structure of 1400 cm^{-1}. The vibrational structure of 1400 cm^{-1} was also observed in fluorescence spectrum of the product (Figure 7). The fluorescence excitation spectrum corresponded to the absorption spectrum as shown in Figure 7.

The change of absorption spectrum of **5** on irradiation at 308 nm laser pulse (~20 mJ $pulse^{-1}$) was shown in Figure 8. The absorption band at 300 nm of **5** decreased with irradiation time and a new band appeared at 400 nm with isosbestic point at 324 nm. After laser irradiation with 1000 pulses, the fluorescence and fluorescence excitation spectra of photolysis products were observed. The maximum of fluorescence spectrum appeared at 385 nm with vibrational structure of 1400 cm^{-1}. Comparing the absorption and fluorescence spectra, we can conclude that **1** and **5** underwent similar photochemical process to give fluorescence products and the efficiency was higher for **5** than **1**. The fluorescence efficiency of photolysis product of **5** in benzene was roughly estimated to be 0.15 by using anthracnene as a fluorescence standard. The assignment of photolysis products were not finished

Triplet energies

Triplet energies of these compounds were calculated from 0-0 band of phosphorescence spectrum and are summarized in Table 1. Furthermore, the

triplet energies were estimated from the quenching rate constant of benzophenone triplet by **1**, **2**, **3**, and **4** by using Sandros equation (eq 1).[14] The values are in good agreement with those estimated from 0-0 band of phosphorescence spectra.

$$k_q = k_{diff} \exp(-\Delta E_a/RT)/[1+\exp(-\Delta E_a/RT)] \qquad (1)$$

k_q: triplet quenching rate constant

k_{diff}: diffusion controlled rate constant

R: gas constant

T: temperature

ΔE_a: difference of triplet enegy

Transient absorption spectra and triplet lifetime

Compound **1** - **5** exhibited transient absorption spectra on irradiation at 308 nm laser pulse in benzene. The absorption maximum appeared at around 340 nm for **1**, **2**, **3** and **4** (Figure 9) and at 380 and 580 nm for **5** (Figure 10).

The triplet lifetime of **1** in benzene was dependent on concentration of **1** from 5.5 μs to 3.4 μs ranging in concentration from 4.5x 10^{-4} M to 1.2x 10^{-3} M. Furthermore, the triplet lifetime becomes 430 ns at the concentration of 0.01 M in the presence of acetophenone as a triplet sensitizer on irradiation at 360 nm in benzene. Concentration dependence of the decay curve of the triplet state of **1** (^{3}(**1**)*) observed at 340 nm in benzene under argon was shown in Figure 11. On the other hand, the triplet lifetime of **2** was independent on its concentration. In this experimental condition, the contribution of triplet-triplet annihilation can

be ruled out.

Thus, the rate constant of the self-quenching (k_{sq}) and the intrinsic triplet lifetime (τ_T^0) were evaluated from the slope and the intercept of the linear plot of equation 2, respectively, as listed in Table 2.

$$^3(\mathbf{1})^* + {}^1(\mathbf{1}) \xrightarrow{k_{sq}} {}^1(\mathbf{1}) + {}^1(\mathbf{1})$$

$$1/\tau_T = 1/\tau_T^0 + k_{sq}[\mathbf{1}] \qquad (2)$$

Triplet quenching

On addition of triplet quenchers (Q), the triplet state of **1** - **5** were quenched and the second-order rate constants (k_q) were calculated from pseudo-first order plots (equation 3) as summarized in Table 3. The value τ_T is the triplet lifetime of **1** at a certain concentration in the absence of quencher.

$$1/\tau'_T = 1/\tau_T + k_q[Q] \qquad (3)$$

Quantum yield of intersystem crossing (Φ_T) and extinction coefficient (ε_T)

The quantum yield of intersystem crossing was estimated by energy transfer from the triplet state of the pyrrole derivatives to β-carotene by using 308 nm excitation. Benzophenone (BP) was used as a standard (Φ_T =1).[18] For example, the optically matched benzene solution of **1** and BP were prepared, whose absorbance at 308 nm was 0.50. The rate constant of triplet energy

transfer to β-carotene observed at 540 nm were measured in the presence of β-carotene (2.1x 10^{-5} M, 4.2x 10^{-5} M, and 6.3x 10^{-5} M). β-Carotene did not exhibit transient absorption on direct irradiation. Time profiles at 540 nm (triplet state of β-carotene) obtained by laser photolysis on irradiation at 308 nm in benzene was shown in Figure 12. The quantum yield of intersystem crossing was estimated from the following equation[15] and the calculated values were summarized in Table 4.

$$\Delta OD = \frac{k_1}{k_1 - k_2} A[\exp(-k_2 t) - \exp(-k_1 t)] \quad (4)$$

$$\Phi_T = \Phi_T^{BP} \frac{A}{A^{BP}} \frac{k_1}{k_1 - k_0} \frac{k_1^{BP} - k_0^{BP}}{k_1^{BP}} \quad (5)$$

A : constant

k_0 : decay constant of triplet state pyrrole derivatives in the absence of β-carotene

k_1 : pseudo-first order rate constant of triplet energy transfer to β-carotene

k_2 : decay rate constant of triplet state of β-carotene

The extinction coefficients (ε_T) of T-T absorption spectra of **1** - **5** were estimated by using benzophenone as a standard (ε_T = 7220 M^{-1} cm^{-1})[16] by equation 6.[16]

$$\varepsilon = \frac{\Delta OD\ \Phi_{isc}}{\Delta OD_{std}\ \Phi_{isc.std}} \varepsilon_{std} \quad (6)$$

Discussion

Possibility of Dimer formation by intermolecular hydrogen bonding in the ground state

Compound **1** has two parts of hydrogen bonding in a molecule, NH proton and carbonyl oxygen. Thus, **1** can form dimer by intermolecular hydrogen bonding. 7-Azaindole and 2-hydroxypyridine (2-pyridone) have similar structure and are well known to form hydrogen bonded dimer in non-polar solvent and underwent intermolecular hydrogen atom transfer on photoirradiation.[11,12] It is reported that the absorption spectrum of hydrogen bonded dimer appeared at longer wavelength region than that of monomer, and the equilibrium constants for dimer formation can be determined by observation of the spectral change at red edge of the absorption band on its concentration.[11,12]

The results of concentration dependence of absorption spectrum of **1 - 5** indicated that hydrogen bonded dimer was not formed even in methylcyclohexane or hexane, since the molar extinction coefficient at high concentration was identical to that at low concentration.

Triplet state properties

The quantum yield of intersystem crossing of **1- 5** was determined by the observation of triplet energy transfer to β-carotene to be as high as 0.8 in benzene. The high quantum yield of intersystem crossing and the lack of fluorescence emission are caused by the high spin-orbit coupling of carbonyl group.

The vibrational structure in phosphorescence spectrum of **1** in

methylcyclohexane showed energy difference of 1390 cm^{-1}. If the triplet state had $n\pi^*$ character, the vibrational structre with ~1700 cm^{-1} assigned to the stretching mode of carbonyl group would appeared in the phosphorescence spectrum.[1] This result indicates that the triplet state of **1** has $\pi\pi^*$ character. In ethanol, the vibrational structure disappeared and the broad spectrum was observed.

On the other hand, **5** gave similar phosphorescence spectrum in both methylcyclohexane and ethanol with the vibrational structure of 1430 cm^{-1}.

Hydrogen abstraction reaction of aromatic carbonyl compounds in the triplet excited state is well known.[1,2] Among the compounds investigated in this study, **2** and **4** have a γ-hydrogen atom for carbonyl oxygen, but a radical species due to the occurrence of hydrogen abstraction was not observed in the laser flash photolysis experiment in benzene.

On irradiation with laser pulse at 308 nm, **1** - **5** gave fluorescent products. Thus, hydrogen abstraction in the triplet excited state may occurr although the efficiency was quite low.

These results indicate that the reactivity of hydrogen abstraction reaction in the tripet excited state of **1** - **5** was less than that of benzophenone or acetophenone, because the triplet state of **1** - **5** has $\pi\pi^*$ character.

The rate constant of energy transfer from triplet state **1** - **5** to the quencher (Table 3) was nearly the diffusion controlled rate constant and the results were consistent with the estimated triplet energies.

The quenching rate constant of triplet state of **1** - **5** by oxygen was about 6×10^9 M^{-1} s^{-1}. The triplet quenching rate constant by energy transfer process to oxygen was estimated to be $(2 - 3) \times 10^9$ M^{-1} s^{-1}, which was 1/9 of the diffusion controlled rate constant. The observed quenching rate constant by molecular

oxygen seemed to be large, indicating a role of charge transfer interaction in the quenching process of **1** - **4** by oxygen.

The triplet energy of **5** was estimated to be 59.2 kcal mol^{-1}, and therefore energy transfer to oxygen (E_S = 22.5 kcal mol^{-1}) could occur by diffusion controlled process. However, the quenching rate constant of **5** by oxygen was 8.4x 10^8 M^{-1} s^{-1}, which was smaller than that of **1** by a factor of 10.

Self-quenching of triplet state of 1

The lifetime of triplet state of **1** was dependent on its concentration. The plot of the inverse of triplet lifetime ($1/\tau_T$) versus the concentration of **1** in benzene gave a straight line. From the slope, the rate constant of self-quenching (k_{sq}) was determined to be 1.6x 10^8 M^{-1} s^{-1}. When the concentration of **1** was 0.01 M, the triplet lifetime of **1** was 430 ns on acetopheneone sensitization, which is in agreement with the calculated k_{sq} value. The triplet lifetime of **1** at infinite dilution (τ_T^0) was calculated from the intercept of the plot to be 10.1 μs. On the other hand, the triplet lifetime of **2** was 10.0 μs, which was independent of its concentration from 4.5x 10^{-4} M to 1.2x 10^{-3} M. Since the intrinsic triplet lifetimes of **1** (τ_T^0 = 10.1 μs) and **2** (τ_T^0 = 10.0 μs) were the same, triplet character of **1** and **2** was considered to be similar. In acetonitrile, k_{sq} and τ_T^0 for **1** were determined to be 1.4x 10^8 M^{-1} s^{-1} and 10.0 μs, respectively.

Compound **1** can form hydrogen bonded dimer between NH group and carbonyl oxygen, while **2** could not form dimer. Therefore, the occurrence of self-quenching in **1** was explained by the intermolecular hydrogen bonding interaction between triplet state of **1** and ground state of **1**.

The above self-quenching reaction would not occur or be suppressed in protic solvent such as methanol. However, the self-quenching was observed even in methanol, and the rate constant of self-quenching of **1** was estimated to be 1.6×10^8 M^{-1} s^{-1} (τ_0 = 12.7 μs) in methanol.

The mechanism of self-quenching of **1** can be explained as follows. The electronic interactions would bring about self-quenching of **1** as suggested for thiones.[15] In the first step of self-quenching of $^3(\mathbf{1})^*$ by the ground state of **1**, $^3(\mathbf{1})^*$ should come close to $^1(\mathbf{1})$ to form intermolecular hydrogen bonding. The observed self-quenching rate constants were lower than the diffusion controlled rate constant by a factor of 100.

The triplet lifetime of **5** was 5 μs both at 5×10^{-5} M and at 1×10^{-2} M on irradiation at 308 nm and 360 nm, respectively, indicating that self-quenching did not occur in **5**. Considering dimer formation by intermolecular hydrogen bonding, the orientation of the hydrogen bonding between hydrogen bonded donor (D) and accepter (A) was important for the stability of the dimer. Compound **5** have a ADA array of hydrogen bonding. In the dimer, D-A interaction was "attractive" and A-A or D-D interaction was "repulsive". As shown in Figure 13, the number of arrow of "attractive" and "repulsive" interaction was 2 and 4, respectively indicating that "repulsive" interaction was dominant interaction. Therefore, hydrogen bonded dimer formation was unfavorable in the **5**.

The repulsive force in **1** is smaller than that in **5** and therefore, the interaction by intermolecular hydrogen bonding would play an important role in non-radiative deactivation of **1**.

Conclusion

Pyrroles **1** - **5** underwent intersystem crossing with the quantum yield as high as 0.8 in benzene. No fluorescence emission was observed at room temperature. From the results of phosphorescence spectra, the triplet state of these compounds was assigned to $\pi\pi^*$ triplet state. In addition, it was found that triplet self-quenching occurs in **1** and **3** by intermolecular hydrogen bonding between NH proton and carbonyl oxygen.

Concentration dependence of absorption spectrum of these compounds clearly showed that the hydrogen bonded dimer can not be formed in the ground state, but hydrogen bonding interaction between ^{3}(**1**)* and ^{1}(**1**) seemed to play an important role in the deactivation pathway from the triplet excited state.

References

1. N. J. Turro, "Modern Molecular Photochemistry," University Science Books (1991).
2. A. Gilbert and J. Baggott, "Essentials of Molecular Photochemistry," Blackwell Scientific Publications (1991).
3. F. D. Lewis, B. A. Yoon, T. Arai, T. Iwasaki and K. Tokumaru, *J. Am. Chem. Soc.*, **1994**, *116*, 3171.
4. T. Arai, M. Obi, T. Iwasaki, K. Tokumaru and F. D. Lewis, *J. Photochem. Photobiol. A: Chem.*, **1995**, *96*, 65.
5. T. Arai, M. Moriyama and K. Tokumaru, *J. Am. Chem. Soc.*, **1994**, *116*, 3171
6. M. Obi, H. Sakuragi and T. Arai, *Chem. Lett.*, **1998**, 169.
7. T. Arai and Y. Hozumi, *Chem. Lett.*, **1998**, 1153.
8. Y. Yang and T. Arai, *Tetrahedron, Lett.*, **1998**, *39*, 2617.
9. T. Arai and M. Ikegami, *Chem. Lett.*, **1999**, 965.
10. M. Ikegami and T. Arai, *J. Chem. Soc. Perkin Trans. 2*, in press.
11. P. T. Chou, C. Y. Wei and F. T. Hung, *J. Phys. Chem. B* **1997**, *101*, 9119 and references cited therein.
12. P. T. Chou, W. S. Yu, Y. C. Chen, C. Y. Wei and S. S. Martinez, *J. Am. Chem. Soc.*, **1998**, *120*, 12927 and references cited therein.
13. J. Bergman, *Tetrahedron Lett.*, **1972**, *46*, 4723.
14. K. Sandros, *Acta Chem. Scand.*, **1964**, *18*, 2355.
15. C. V. Kumar, L. Qin and P. K. Das, *J. Chem. Soc., Faraday Trans. 2*, **1984**, *80*, 783.
16. R. Bonneau, I. Carmichael and G. L. Hug, *Pure & Appl. Chem.*, **1991**, *63*, 289.

17. C. Lambert and R. W. Redmond, *Chem. Phys. Lett.*, **1994**, *228*, 495.

18. "Handbook of Photochemistry," ed by S. L. Murov, I. Carmichal, and G. L. Hug, Macel Dekker, New York (1993).

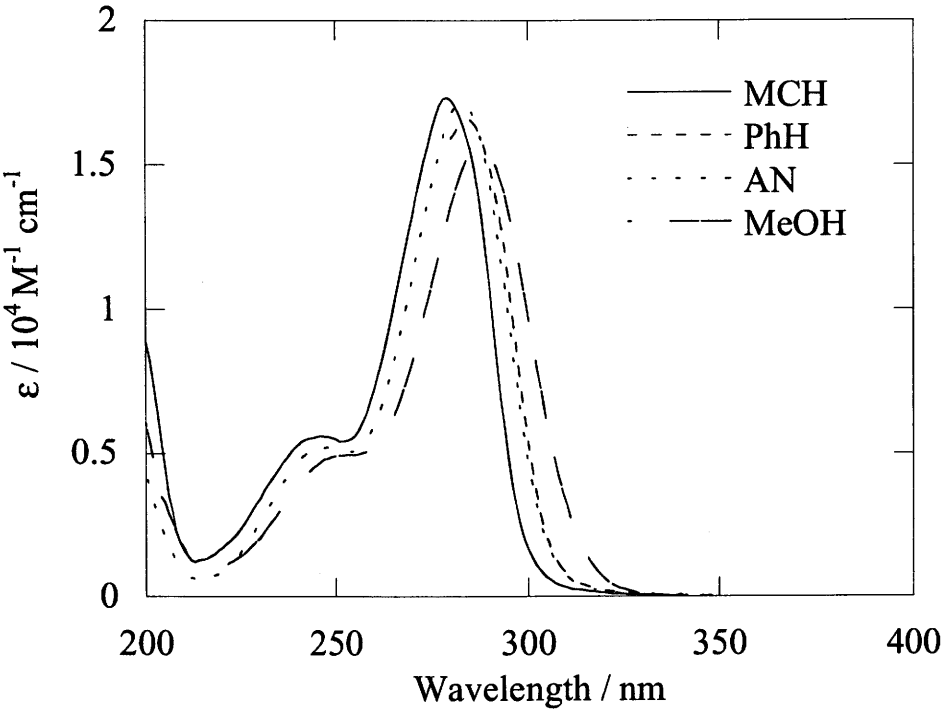

Figure 1-1. Absorption spectra of **1** in methylcyclohexane, benzene, acetonitrile, and methanol.

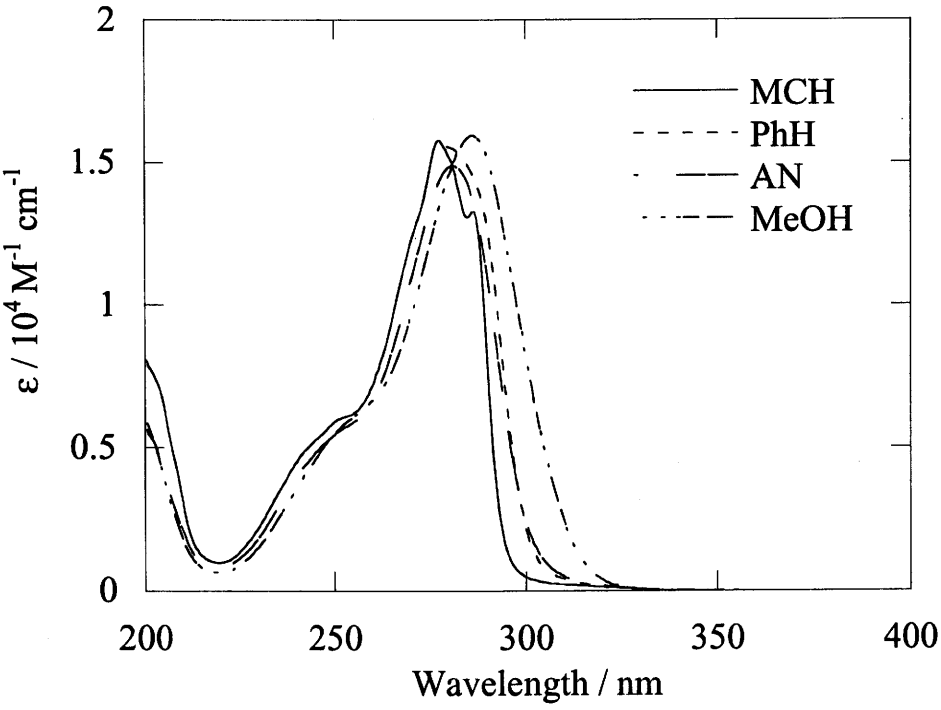

Figure 1-2. Absorption spectra of **2** in methylcyclohexane, benzene, acetonitrile, and methanol.

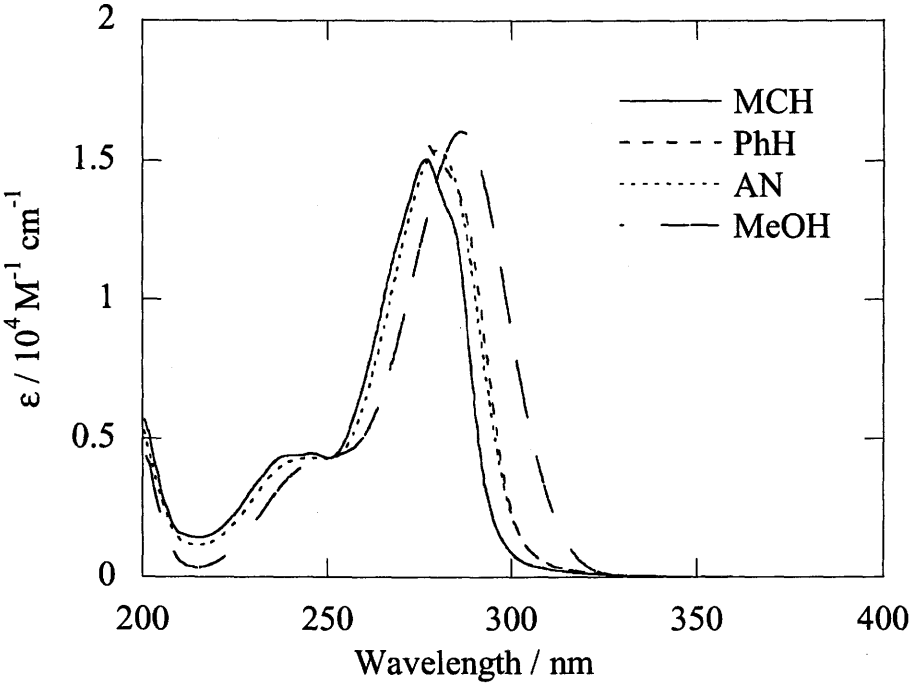

Figure 1-3. Absorption spectra of **3** in methylcyclohexane, benzene, acetonitrile, and methanol.

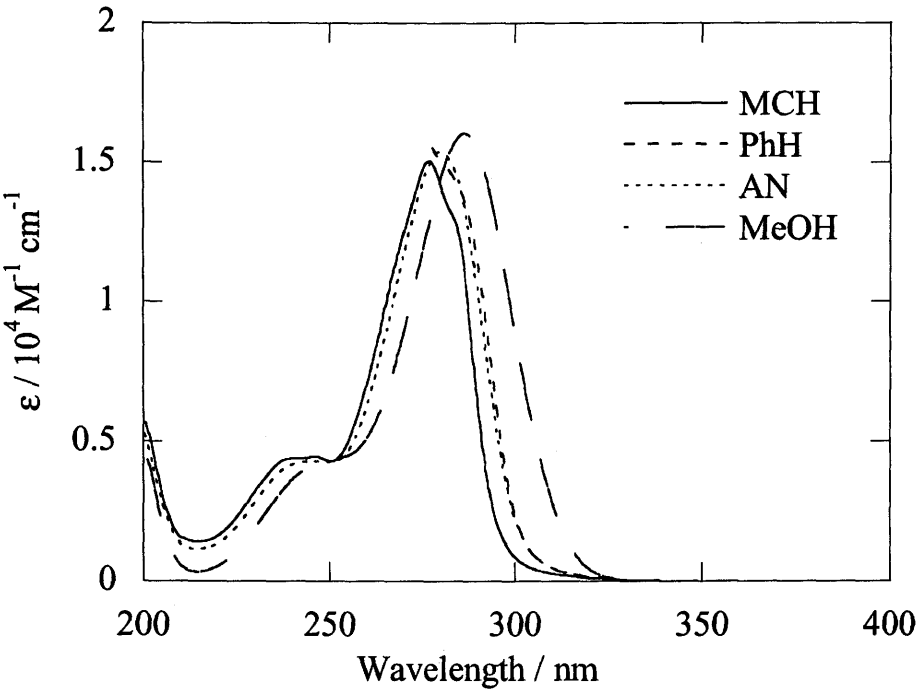

Figure 1-4. Absorption spectra of **4** in methylcyclohexane, benzene, acetonitrile, and methanol.

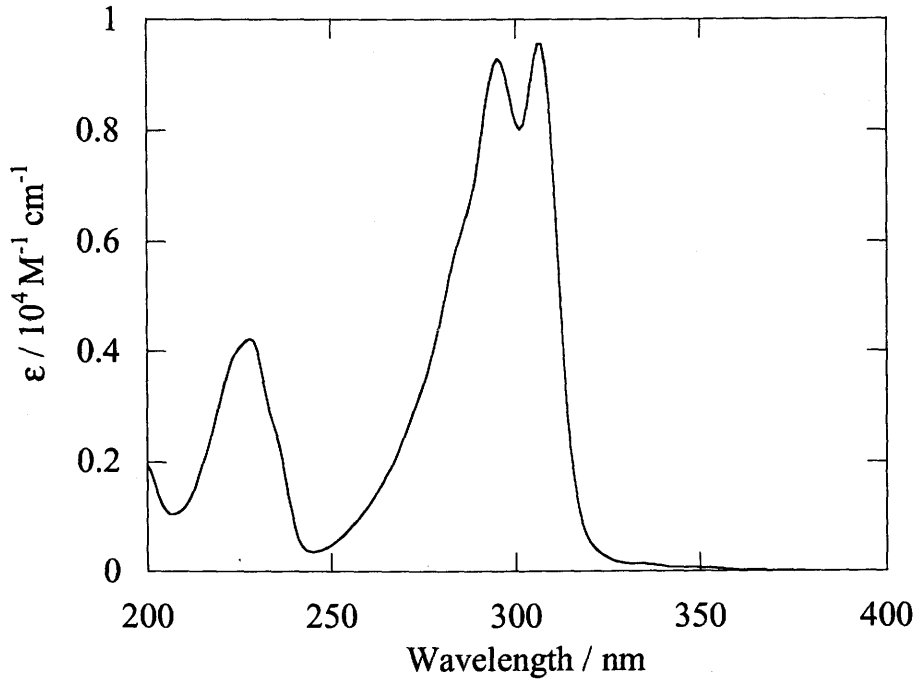

Figure 2. Absorption spectrum of **5** in hexane.

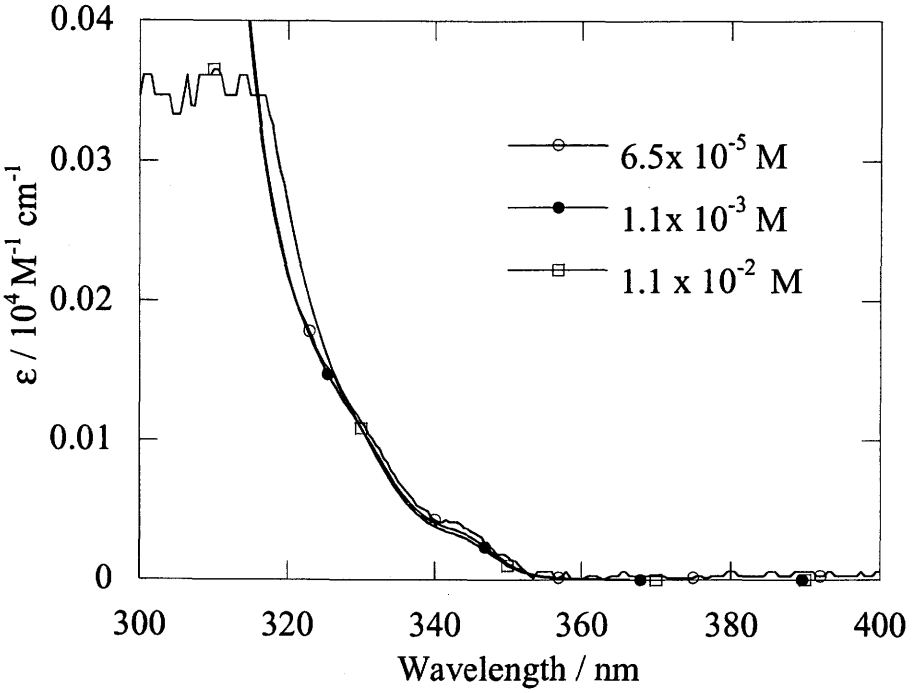

Figure 3. Concentration dependence of absorption spectrum of **1** in methylcyclohexane.

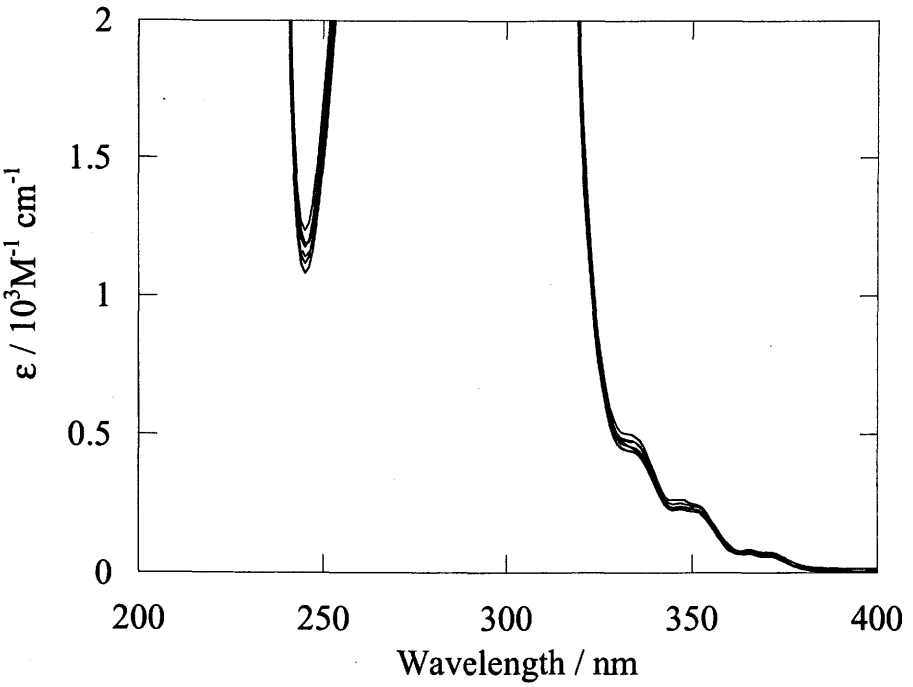

Figure 4. Concentration dependence of absorption spectrum of **5** in hexane.

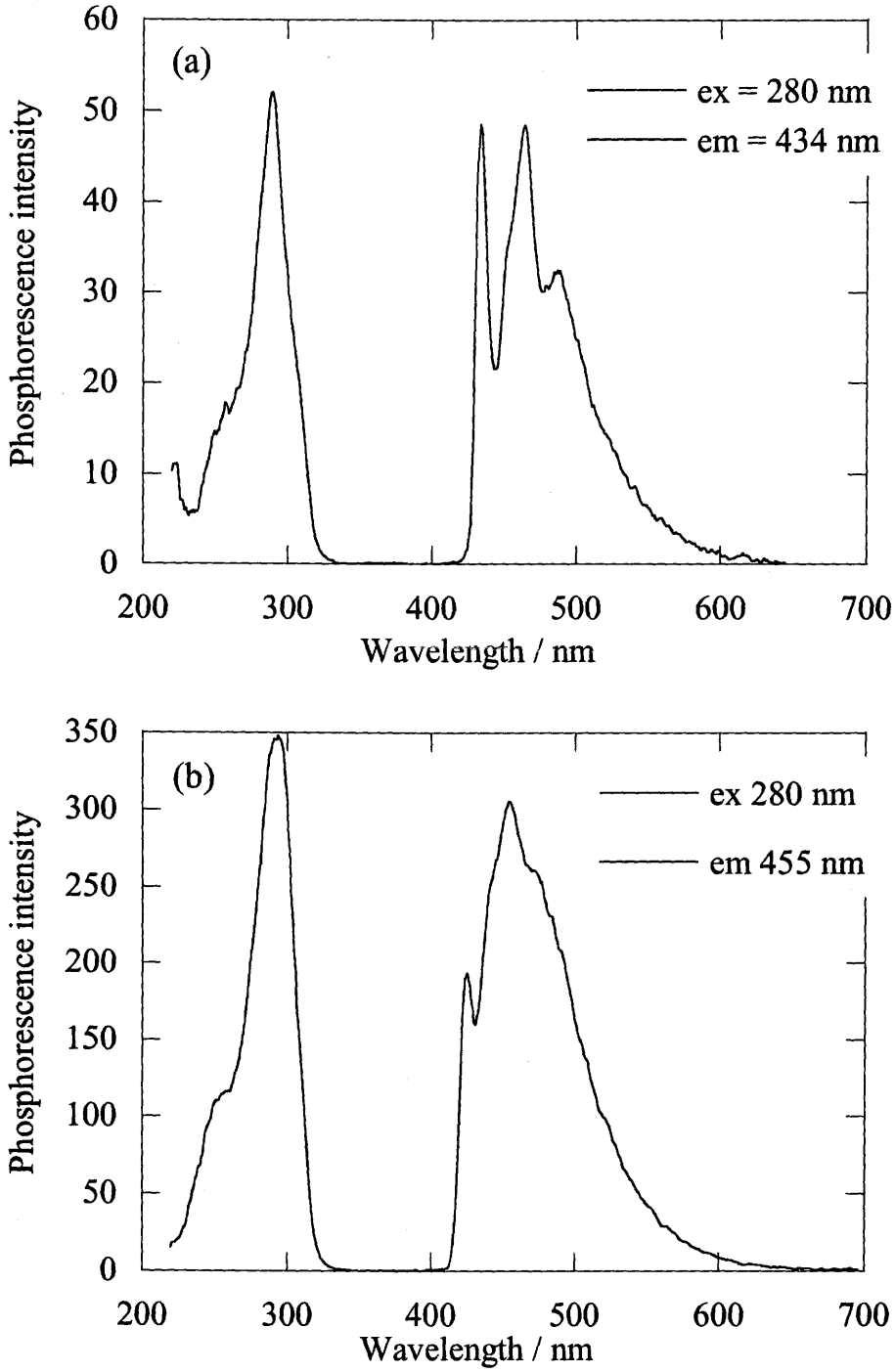

Figure 5. Phosphorescence and phosphorescence excitation spectra of **1** in methylcyclohexane (a) and ethanol (b) at 77K.

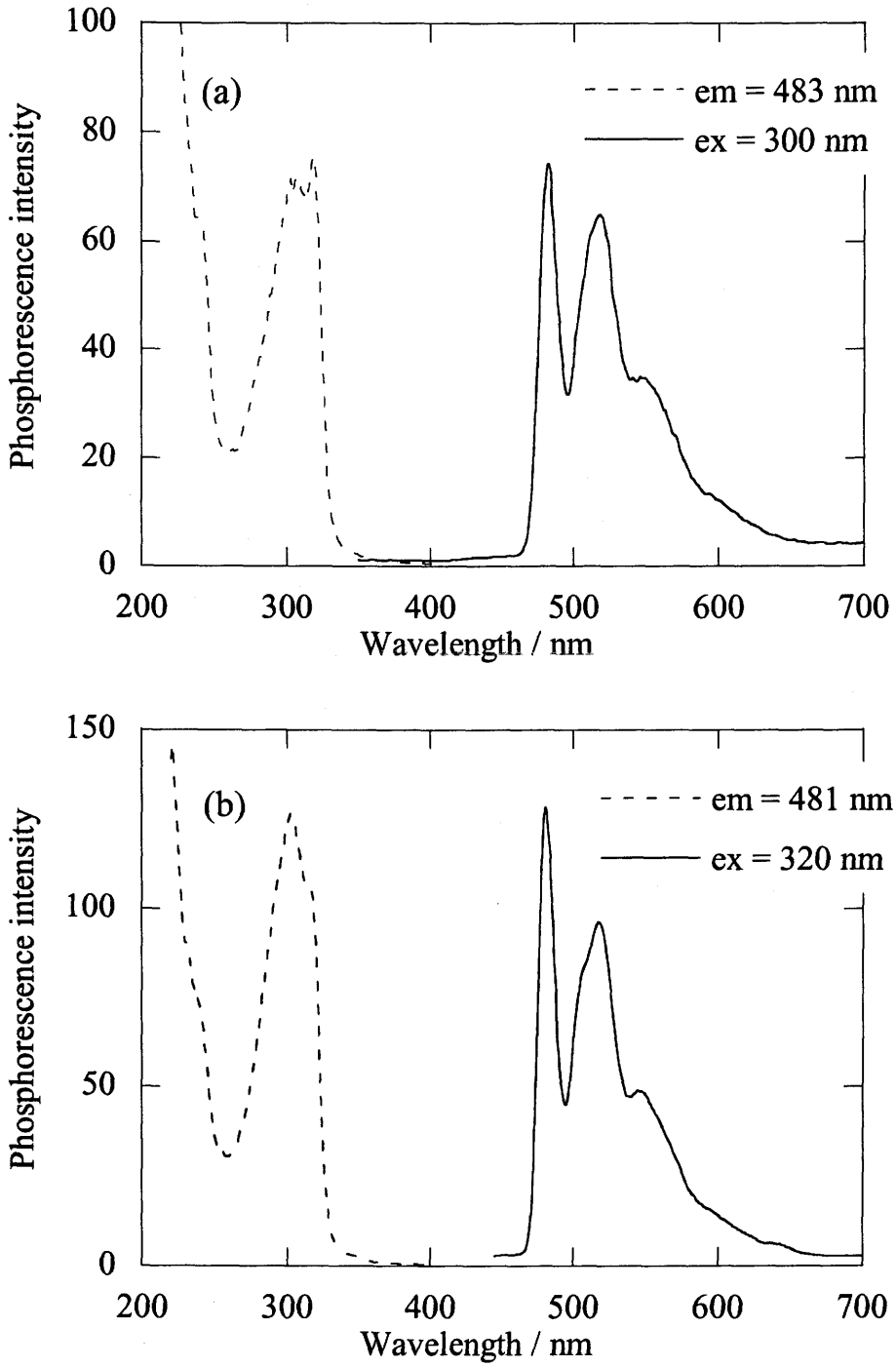

Figure 6. Phosphorescence and phosphorescence excitation spectra of **5** in methylcyclohexane (a) and ethanol (b) at 77K.

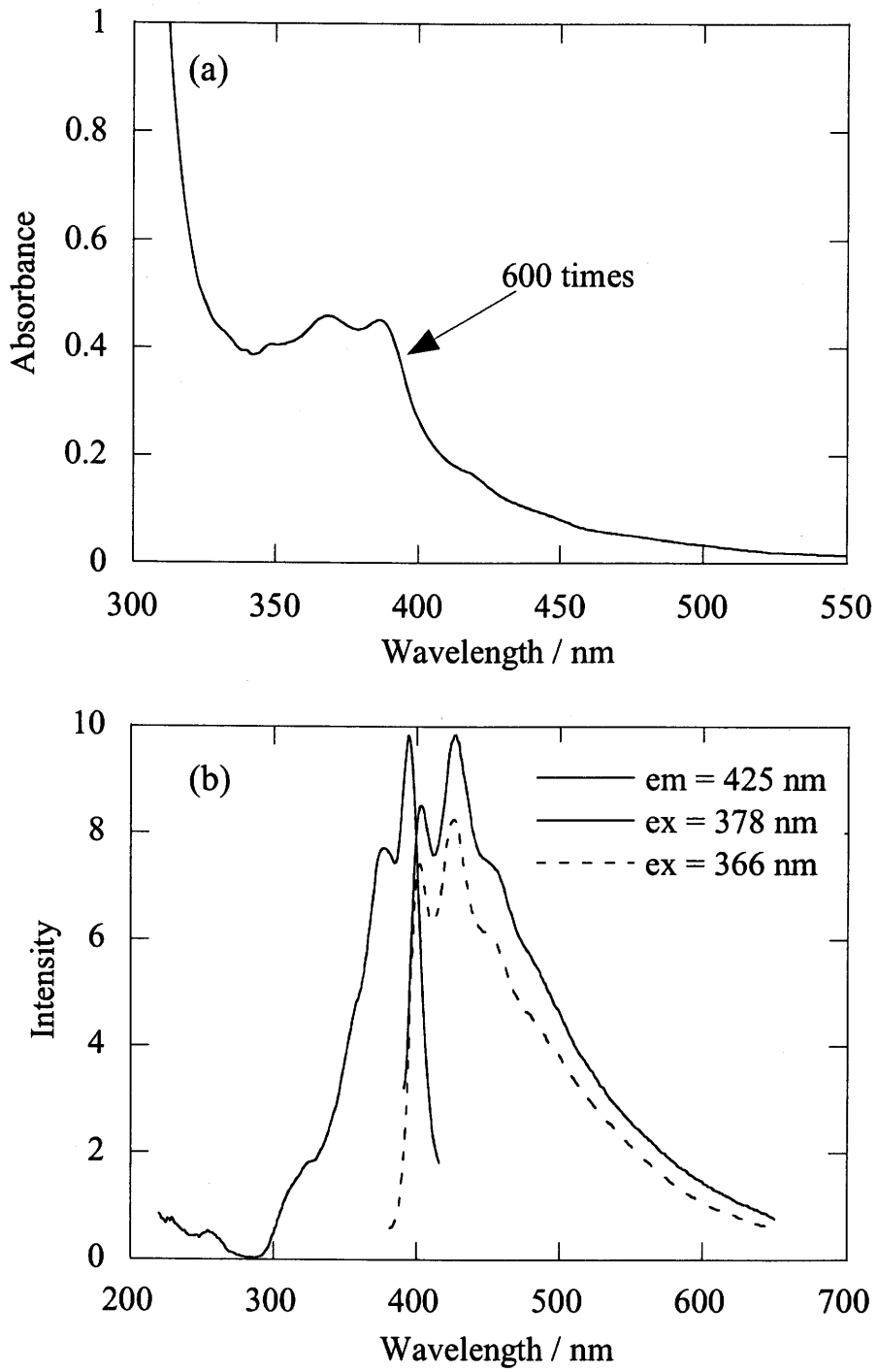

Figure 7. Absorption spectrum of **1** after laser irradiation of 600 shots of 308 nm pulse in methylcyclohexane (a); Fluorescence and fluorescence excitation spectra of photolysis product of **1** (b).

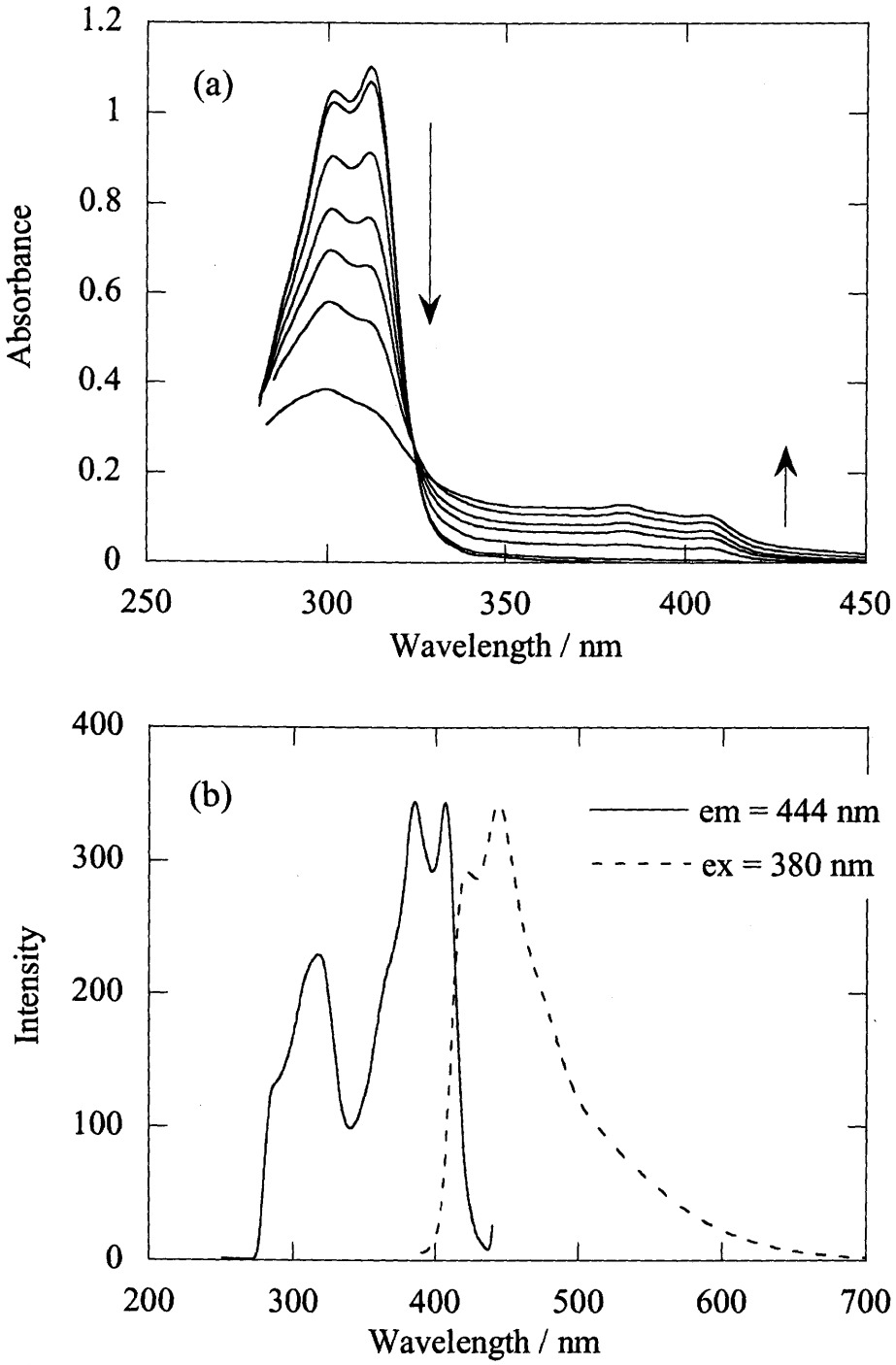

Figure 8. Change of absorption spectrum of **5** on irradiation of laser pulse at 308 nm in benzene (a); Fluorescence and fluorescence excitation spectra of photolysis product of **5** (b).

Table 1. Triplet energies of **1** - **5**

	PhH[a)]	MeCN[a)]	MCH[b)]	EtOH[b)]
1	68.6	69.2	65.9	67.3
2	70.2	71.7	68.4	67.6
3	69.7	68.9	68.2	67.3
4			70.2	67.3
5			59.2	59.4

a) estimated from quenching rate constant of benzophenone triplet
b) calculated from 0-0 band of phosphorescence spectra

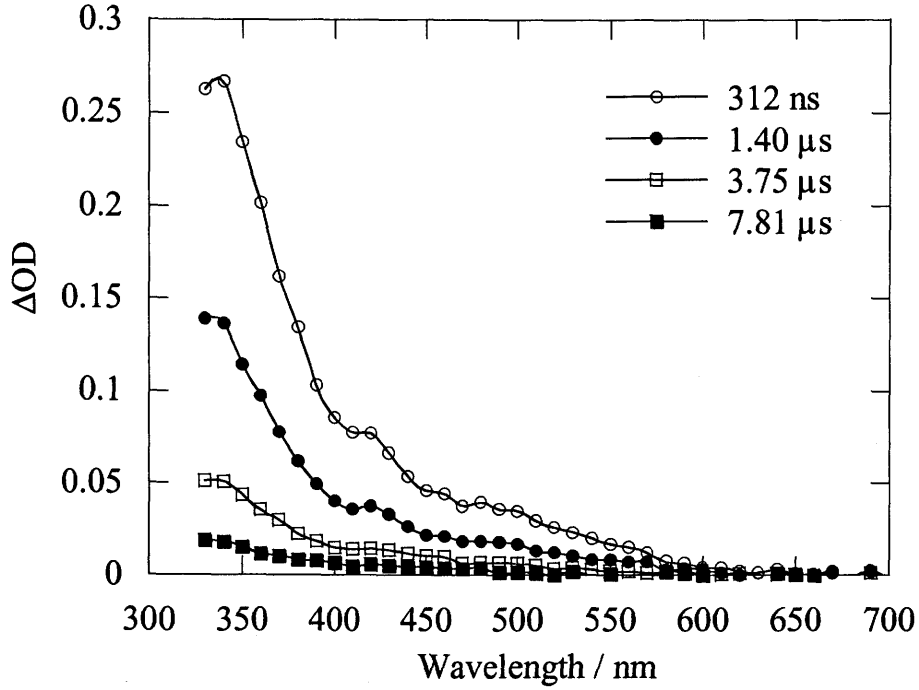

Figure 9-1. Transient absorption spectra of **1** in benzene under argon on irradiation at 308 nm.

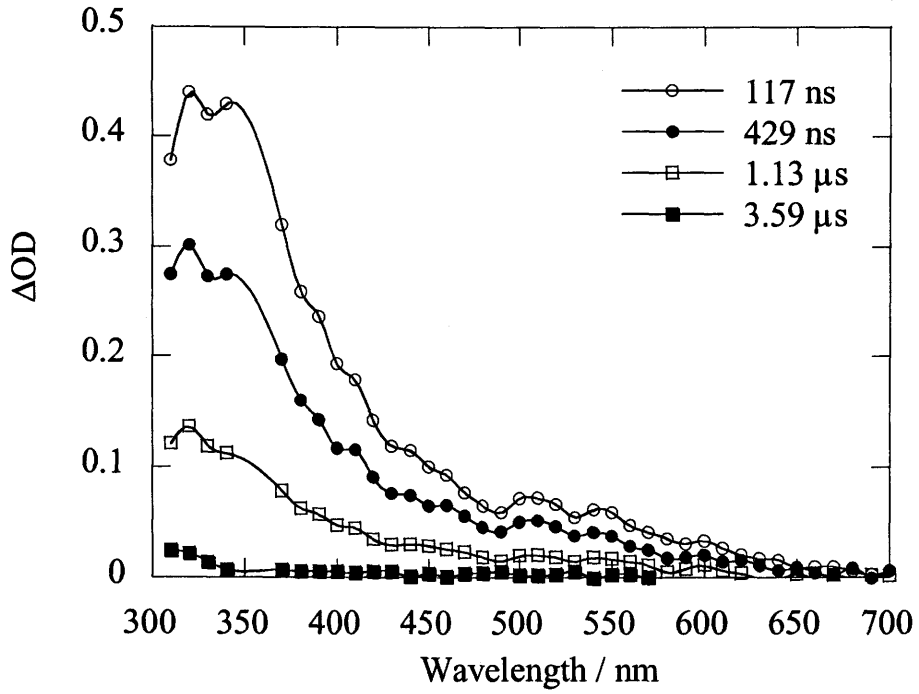

Figure 9-2. Transient absorption spectra of **2** in benzene under argon on irradiation at 308 nm.

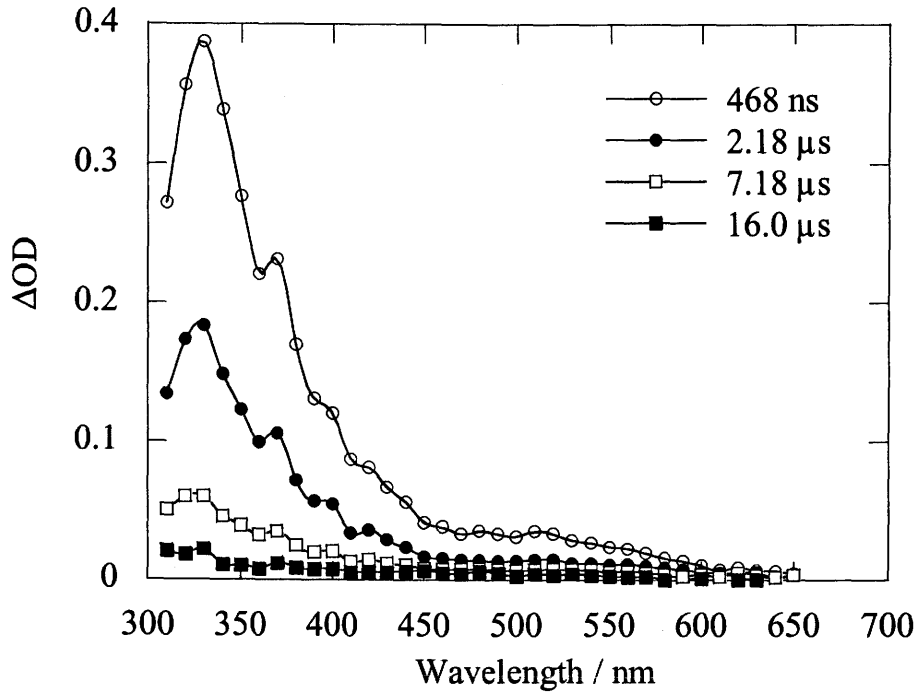

Figure 9-3. Transient absorption spectra of **3** in benzene under argon on irradiation at 308 nm.

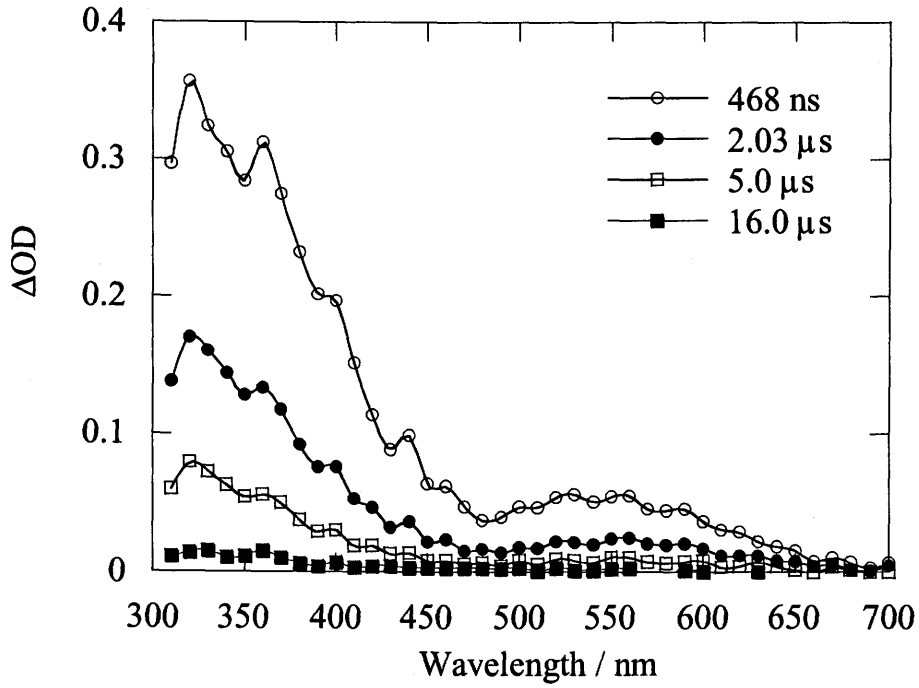

Figure 9-4. Transient absorption spectra of **4** in benzene under argon on irradiation at 308 nm.

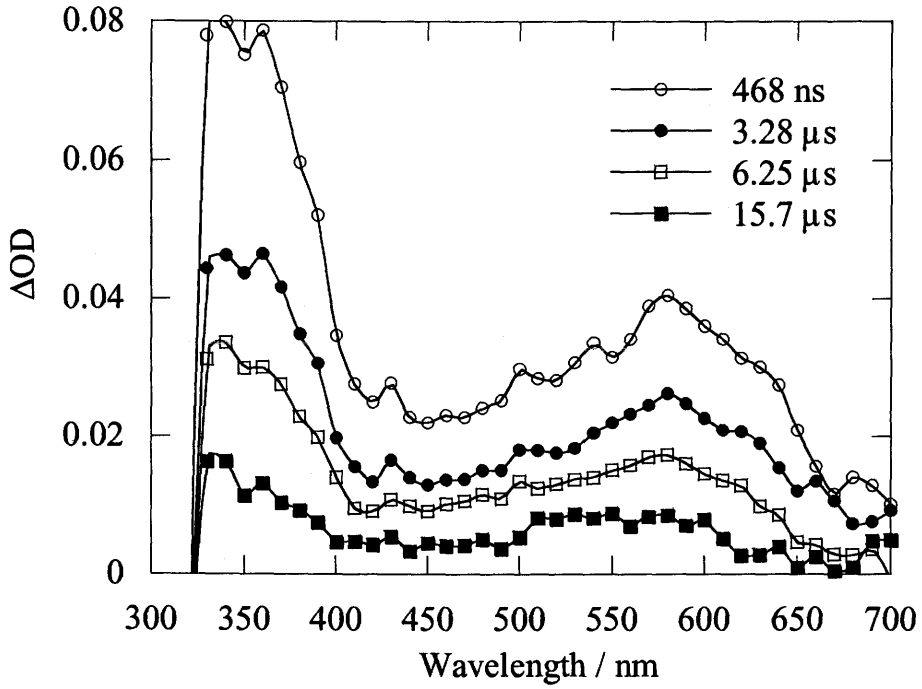

Figure 10. Transient absorption spectra of **5** in benzene under argon on irradiation at 308 nm.

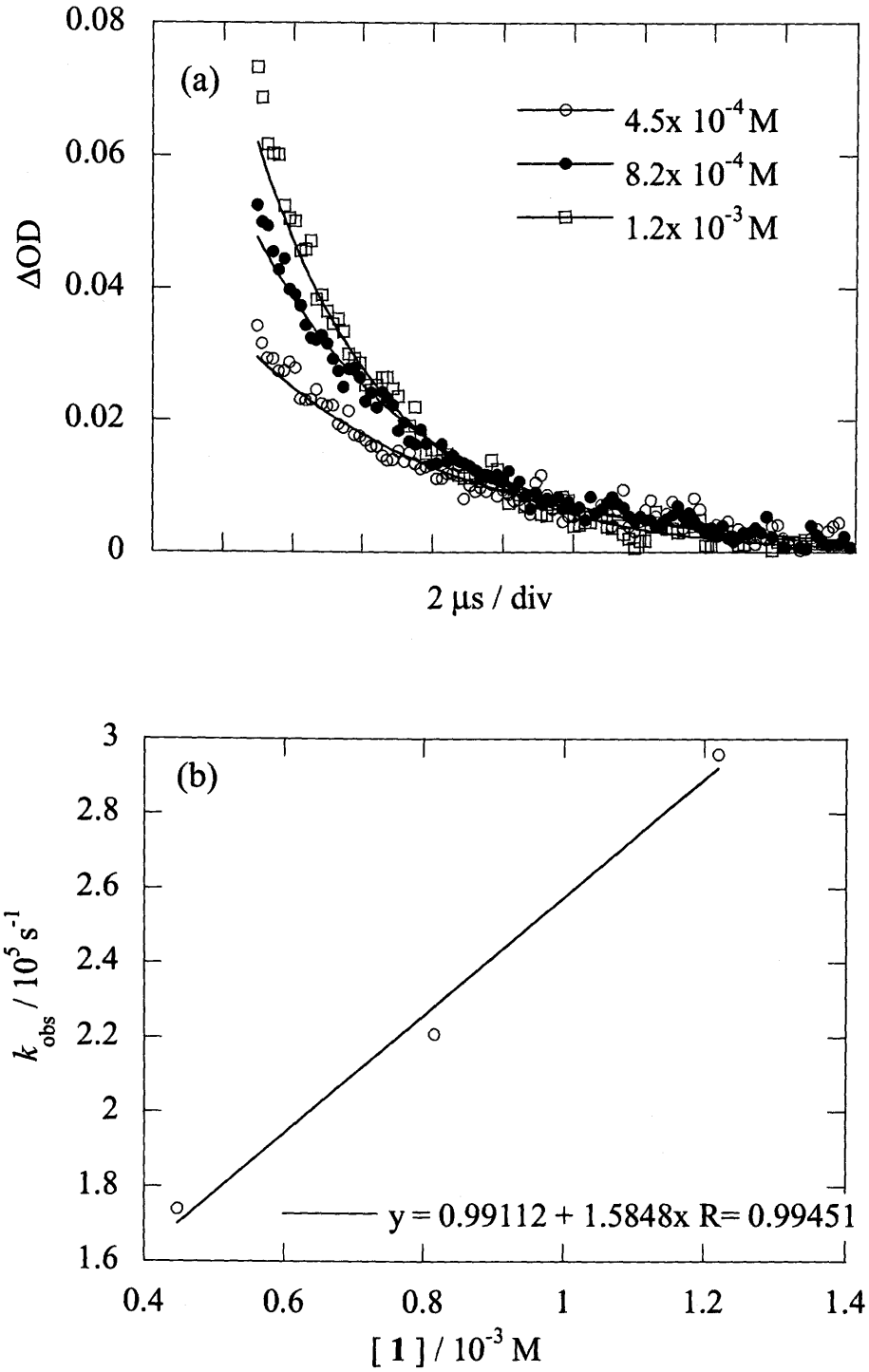

Figure 11. Concentration dependence of decay constants of **1** (a) and first-order plots for the decay constant (b) in benzene.

Table 2. Rate constant of self-quenching for **1** - **4**

Solvent		**1**	**2**	**3**	**4**
benzene	k_{sq} / M^{-1} s^{-1}	1.6x 10^8	--	4.3x 10^8	--
	τ_0 / μs	10.1	10.0	3.8	7.7
acetonitrile	k_{sq} / M^{-1} s^{-1}	1.4x 10^8	--	1.9x 10^8	--
	τ_0 / μs	10.0	7.7	7.7	5.9
methanol	k_{sq} / M^{-1} s^{-1}	1.6x 10^8	--	2.9x 10^8	--
	τ_0 / μs	12.7	9.1	7.1	6.7
methylcyclohexane	k_{sq} / M^{-1} s^{-1}	5.0x 10^8	--	--	--
	τ_0 / μs	11.1	(~ 300 ns)	(~ 300 ns)	(~ 300 ns)

Table 3. Quenching rate constant of triplet excited state of **1** - **5**

	k_q / $M^{-1}s^{-1}$				
Quencher	**1**	**2**	**3**	**4**	**5**
β-Catrotene (19.5 kcal mol^{-1})[17]	1.1x 10^{10}	8.9x 10^9	9.8x 10^9	8.3x 10^9	9.9x 10^9
Biacetyl (56 kcal mol^{-1})[18]	8.4x 10^9	8.2x 10^9	8.9x 10^9	7.6x 10^9	5.2x 10^9
Ferrocene (38 kcal mol^{-1})[18]	---	---	---	---	1.3x 10^{10}
Oxygen (22.5 kcal mol^{-1})[18]	6.2x 10^9	6.9x 10^9	6.6x 10^9	5.7x 10^9	8.4x 10^8

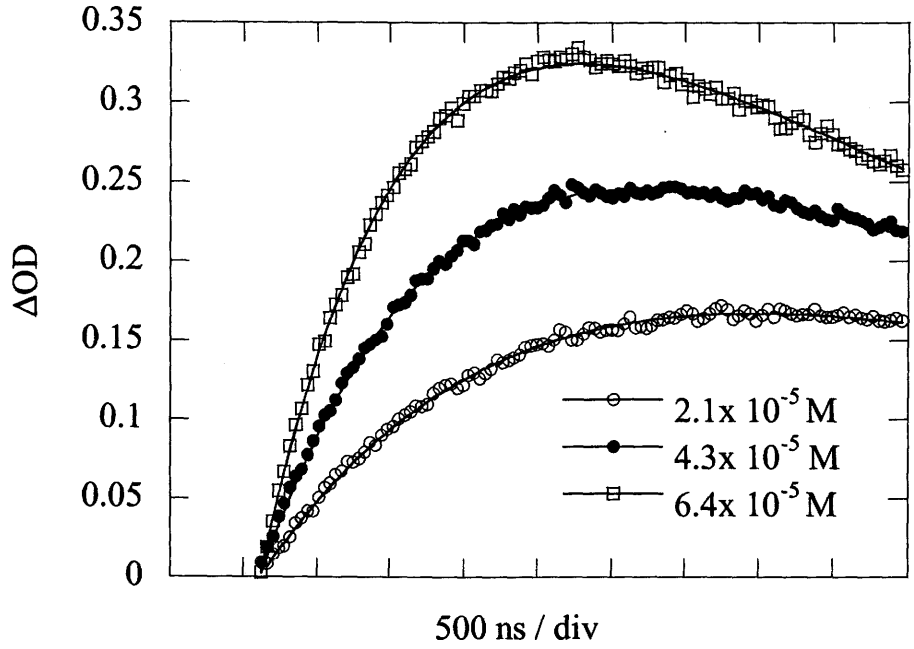

Figure 12. Time profiles at 540 nm of ^{3}(β-carotene)* obtained by laser photolysis of **1** (OD_{308} = 0.50) in benzene under argon.

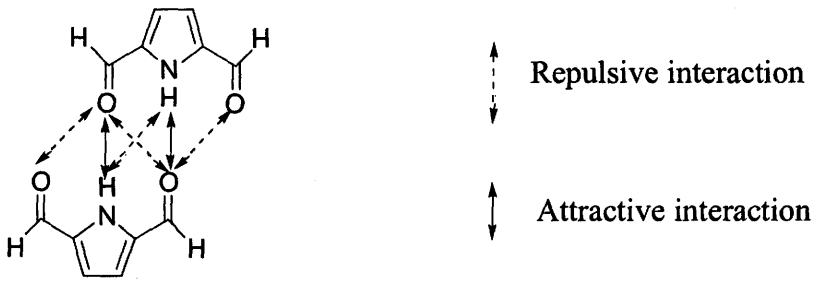

Figure 13. Intermolecular hydrogen bonding interaction in dimer of **5**.

Chapter 6

Excimer or Exciplex Formation and Energy Transfer of Aromatic Compounds Linked by Intermolecular Quadruple Hydrogen Bonding

Abstract

2-Ureido-4[*1H*]-pyrimidinone (UPy) derivatives having pyrene ring, anthracence ring, naphthalene ring, *N,N*-dimethylaniline ring and azobenzene group were prepared and their photochemical behavior was investigated. Exciplex emission between pyrene ring and *N,N*-dimethylaniline ring was observed in chloroform, and energy transfer was observed from naphthalene to anthracene even when the concentration of both compounds was as low as 1x 10^{-5} M, due to the formation of hydrogen bonded dimer of UPy. These results show that one can construct molecular assemblies exhibiting efficient charge transfer or energy transfer interaction by taking advantage of quadruple intermolecular hydrogen bonding.

Introduction

In recent years, the construction of the self-organized molecular system by intermolecular hydrogen bonding has received much attention.[1] Hydrogen bonding is expected to be useful in construction of supramolecular structure because of its association character of directional and selective way. Practically, the molecular systems having multiple hydrogen bond can be used as building blocks for supramolecular structure.[2-14] In addition, it is expected that hydrogen bonding can be formed and be broken by external stimulation such as temperature, light, pH and so on, since hydrogen bonding is weak interaction different from covalent bond. In this respect, photoinduced processes to control the molecular weight of the assemblies constructed by hydrogen bond have received much attention to apply for photolithography, gel reagent, memory devices and so on.[8,14] In hydrogen bonded polymer system, photochemical reactions can control the polymerization or depolymelization of polymer by the change of molecular structure.[8,14] The change in the chemical structure of the materials can change the properties like solubility and viscosity.[8]

In a series of the building blocks of self-organized structure by hydrogen bonding, the dimers with double or triple hydrogen bond are well known in DNA base pairs.[15] Therefore, numerous triply hydrogen bonded molecules have been prepared and the association behavior has been investigated.[2-13] However, the association constant of usual hydrogen bonded system is small; for example, the association constant of adenine-thymine and guanine-cytosine dimer is in the range of 10^2 to 10^3 M^{-1} and 10^4 to 10^5 M^{-1}, respectively in chloroform.[16,17]

Recently, Meijer et al. introduced the concept of using quadruple intermolecular hydrogen bonding to prepare the reversible supramolecular

polymers.[7] Linear polymers are formed by the self-assembly of two 2-ureido-4[*1H*]-pyrimidinone (UPy) units, which dimerize strongly in solvent like $CHCl_3$ with the dimerization constant as high as $>10^6$ M^{-1}.[9,11] They also reported on the photo-initiated generation of chain stopper. The viscosity of solution of supramolecular hydrogen bonded polymer decreases by using photochemical reaction.[8] Because of its high dimerization constant, one can use UPy group to construct supramolecular systems having photoresponsive chromophore.[18,19]

Photoinduced electron transfer reaction has received much attention not only in solution chemistry, but also in heterogeneous systems such as photosynthetic reaction centers and solid state photoresponsive materials.[20] For example, the electron donor and acceptor binary molecules linked by a non-absorbing spacer such as flexible polymethylene chain or rigid steroid group have been extensively investigated.[20] These systems are also of great values in the studies of the interaction between two chromophores in dilute solution to explore the fundamental mechanism of photoinduced electron transfer or charge transfer reaction. However, the electron transfer reaction in the macromolecules connected not by covalent bonds but by weak interaction such as intermolecular hydrogen bonding[21] was scarcely investigated because the dimerization constant was not enough in almost all the cases. High dimerization constants of UPy make these molecules very interesting building blocks not only for supramolecular chemistry but also for photochemical systems.[22]

We wish to report here the preparation of the UPy derivatives having electon donor or acceptor and energy donor or acceptor, and the photochemical reactions of these compounds. We have revealed that excimer or exciplex

formation and singlet energy transfer occur efficiently in dilute solution as low as 10^{-5} M by utilizing quadruple intermolecular hydrogen bonding.

These results show that we can construct molecular assemblies exhibiting efficient electron transfer, charge transfer or energy transfer interaction by taking advantage of quadruple intermolecular hydrogen bonding of UPy.

Scheme 1. General Scheme for the Synthesis of Ureidopyrimidinone Dereivatives

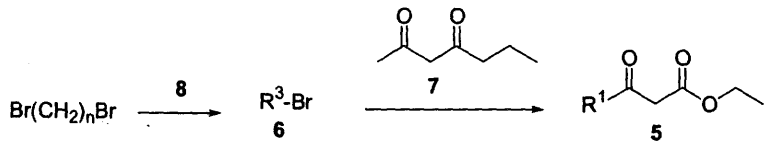

8c: 4-(Azo)OH
8d: 9-(Ant)CH_2OH
8e: 1-(Py)CH_2OH
8f: 3-(DMA)OH

6b: R^3= $C_{12}H_{25}$
6c: R^3=4-(Azo)OC_4H_8
6d: R^3=9-(Ant)$CH_2OC_4H_8$
6e: R^3=1-(Py)$CH_2OC_4H_8$
6f: R^3=3-(DMA)OC_2H_4
6g: R^3=3-(DMA)OC_3H_6
6h: R^3=3-(DMA)OC_4H_8
6i: R^3=3-(DMA)OC_5H_{10}

5b: R^1=n-$C_{13}H_{27}$
5c: R^1=4-(Azo)OC_5H_{10}
5d: R^1=9-(Ant)$CH_2OC_5H_{10}$
5e: R^1=1-(Py)$CH_2OC_5H_{10}$
5f: R^1=3-(DMA)OC_3H_6
5g: R^1=3-(DMA)OC_4H_8
5h: R^1=3-(DMA)OC_5H_{10}
5i: R^1=3-(DMA)OC_6H_{12}

Azo = Azobenzene
Ant = Anthracene
Py = Pyrene
DMA = *N,N*-Dimethylaniline
Nap = Naphthalene

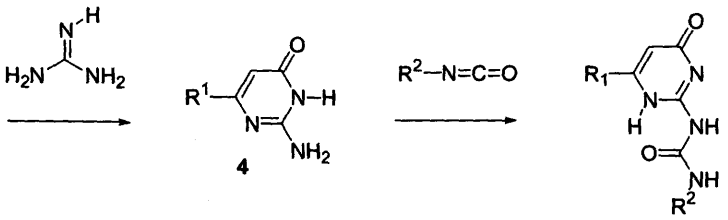

4a: R^1=CH_3
4b: R^1=n-$C_{13}H_{27}$
4c: R^1=4-(Azo)OC_5H_{10}
4d: R^1=9-(Ant)$CH_2OC_5H_{10}$
4e: R^1=1-(Py)$CH_2OC_5H_{10}$
4f: R^1=3-(DMA)OC_3H_6
4g: R^1=3-(DMA)OC_4H_8
4h: R^1=3-(DMA)OC_5H_{10}
4i: R^1=3-(DMA)OC_6H_{12}

1a: R^1=CH_3, R^2=n-C_4H_9
1b: R^1=n-$C_{13}H_{27}$, R^2=n-C_4H_9
1c: R^1=4-(Azo)OC_5H_{10}, R^2=n-C_4H_9
1d: R^1=9-(Ant)$CH_2OC_5H_{10}$, R^2=n-C_4H_9
1e: R^1=1-(Py)$CH_2OC_5H_{10}$, R^2=n-C_4H_9
2a: R^1=3-(DMA)OC_3H_6, R^2=n-C_4H_9
2b: R^1=3-(DMA)OC_4H_8, R^2=n-C_4H_9
2c: R^1=3-(DMA)OC_5H_{10}, R^2=n-C_4H_9
2d: R^1=3-(DMA)OC_6H_{12}, R^2=n-C_4H_9
3aR: R^1=n-$C_{13}H_{27}$
R^2=1-(*R*)-(Nap)(CH_3)CH
3aS: R^1=n-$C_{13}H_{27}$
R^2=1-(*S*)-(Nap)(CH_3)CH
3bR: R^1=9-(Ant)$CH_2OC_5H_{10}$
R^2=1-(*R*)-(Nap)(CH_3)CH
3bS: R^1=9-(Ant)$CH_2OC_5H_{10}$
R^2=1-(*S*)-(Nap)(CH_3)CH

Scheme 2. 2-Ureido-4[*1H*]-pyrimidinone Derivatives and Model Compounds Investigated in This Study

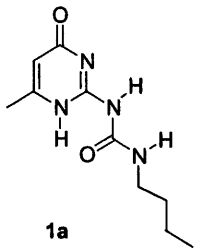

1a

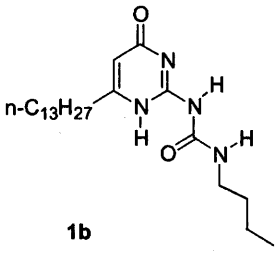

1b

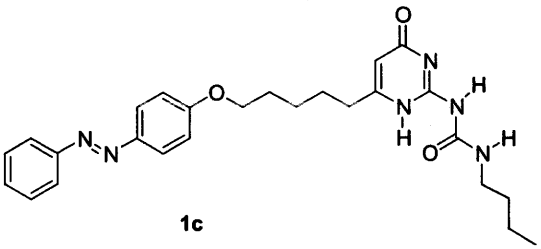

1c

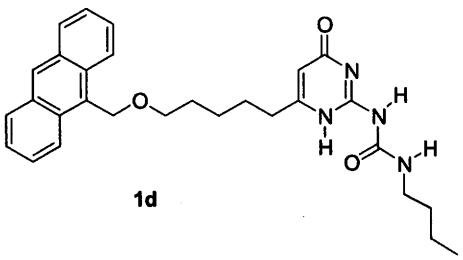

1d

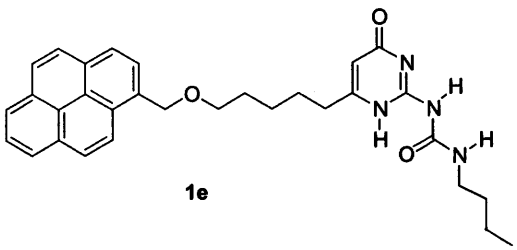

1e

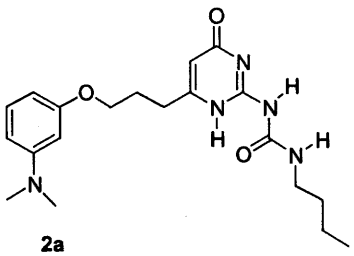

2a

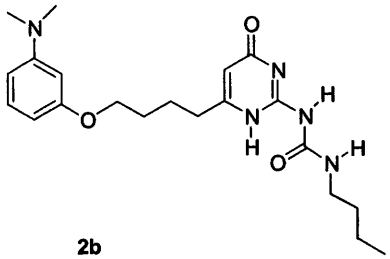

2b

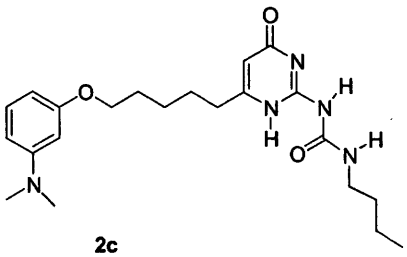

2c

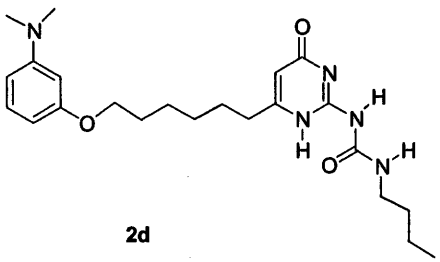

2d

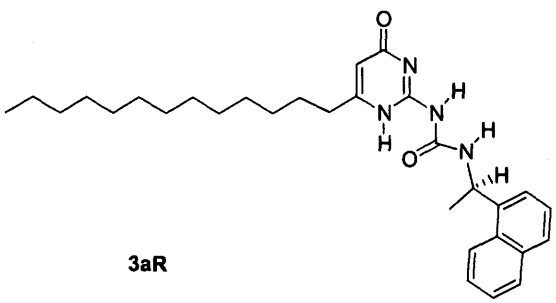

3aR

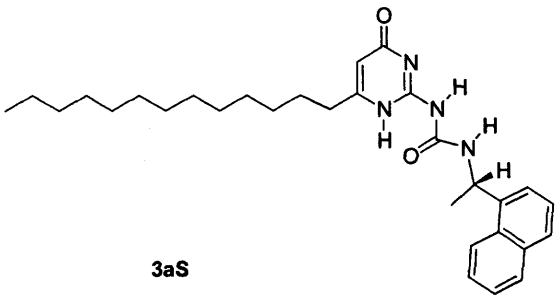

3aS

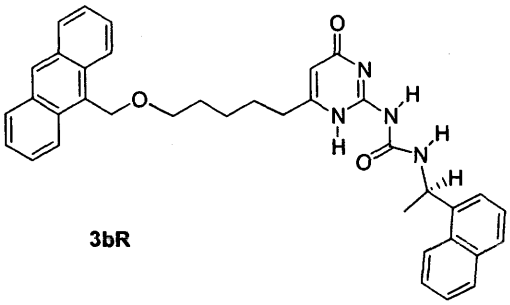

3bR

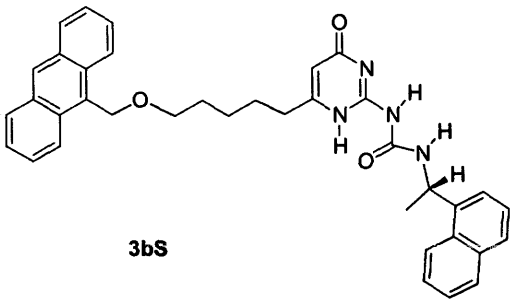

3bS

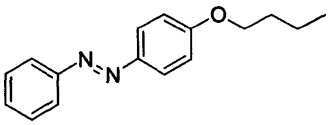

9

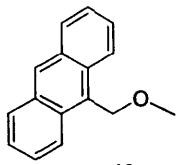

10

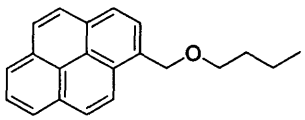

11

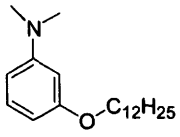

12

Results

^{1}H NMR spectroscopy

The signal of NH proton of all the UPy derivatives appeared at 10, 12 and 13 ppm in ^{1}H NMR spectrum in chloroform-d. The assignment of the signal was summarized in the experimental section. This unusual downfield shift of NH proton signal was due to the formation of quadruple intermolecular hydrogen bonding.[9]

ESI-MS spectroscopy

The results of ESI-MS spectroscopy of **1d**, **1e**, and **2c** were shown in Figure 1. The sample solution, which contained 1 mg of **1d**, **1e**,or **2c** dissolved in 1 ml of chloroform, was diluted with methanol by a factor of 200. In the spectra, the peaks of monomer, dimer and trimer were observed. The dimer peak was the main peak for **1d**, **1e**, and **2c**. This result strongly indicates that UPy forms dimer by quadruple intermolecular hydrogen bonding in solution.

Absorption spectrum of 1a

Absorption spectrum of **1a** in chloroform appeared at shorter wavelength than 320 nm. Figure 2 shows the concentration dependence of absorption spectrum of **1a**. The molar extinction coefficient (ε) at 280 nm - 310 nm region decreased with increasing of the concentration. This change of absorption spectra corresponded to the tautomerization or dimerization of UPy unit.[11] Considering that the ε value of the keto-form was smaller than that of the enol-form, this result indicates that enol-form was predominant at low concentration and the composition of keto-form increased at high concentration.

Neither fluorescence emission nor transient absorption spectrum was

observed in chloroform at room temperature on direct irradiation of **1a**

Cyclic Voltammetry

Neither oxidation peak nor reduction peak of **1a** was not observed in dichloromethane solution in the presence of 0.1 M tetrabutylammonium hexafluorophospate as an electrolyte with Ag/Ag^+ electrode as a reference. In addition, the reduction potential of **10** was –2.2 V vs. Ag/Ag^+ and the oxidation potential of *N,N*-dimethylaniline and 3-dodecyloxy-*N,N*-dimethylaniline (**12**) was 0.41 V and 0.37 V, respectively, vs. Ag/Ag^+ in acetonitrile solution in the presence of 0.1 M tetrabutylammonium perechrolate as a electrolyte.

Excimer formation of 1e

1e exhibited excimer emission with the maximum at 485 nm in addition to the normal emission around 400 nm even at very low concentration ($1.0x\ 10^{-5}$ M) as shown in Figure 3a. The lifetime of the excimer was determined to be 60 ns at 500 nm. Contrary to this observation, 1-(butoxymethyl)pyrene (**11**) ($1.0x\ 10^{-5}$ M) without UPy unit, exhibited only the monomer fluorescence (Figure 3b). These results clearly indicate the importance of quadruple intermolecular hydrogen bonding for the formation of pyrene excimer.

This excimer formation was prevented by addition of **1a**. Figure 4 showed the change of fluorescence spectrum of **1e** ($1.0x\ 10^{-6}$ M) by addition of **1a**. The maximum of pyrene excimer at 485 nm decreased with increasing concentration of **1a**, and the intensity become just half as that in the absence of **1a** when the concentration of both **1a** and **1e** was $1.0x\ 10^{-5}$ M.

Figure 5 shows a 3D structure of **1e** optimized by MD calculation in Chem3D. The distance between two pyrene ring is 33 Å when the dimer takes

a extended conformation. Since the methylene spacer was flexible, thus two pyrene ring could be brought so close together up to 3 Å that their π orbitals overlap each other. The thermodynamic study of excimer formation of pyrene showed that the excimer adopt a sandwich structure, with the distances between the planes of the aromatic rings of the order of 3 - 4 Å.[23] As a result, **1e** exhibited efficient excimer emission.

Absorption and fluorescence spectra of 1d

The absorption spectrum of **1d** was identical to the sum of absorption of the model compound 9-(methoxymethyl)anthracene (**10**) and **1a** as shown in Figure 6. In addition, fluorescence spectra of **1d** at the concentration of 1.0x 10^{-5} M were almost the same as **10** (Figure 7). Furthermore, the fluorescence lifetimes of **1d** and **10** were almost the same as 2.6 and 2.5 ns, respectively. The quantum yield of fluorescence emission was 0.15 for both **1d** and **10** in chloroform under argon atmosphere at room temperature. These results showed that UPy unit did not affect the excited singlet state behavior of anthracene ring.

Transient absorption spectra of 1d

Transient absorption spectrum of **1d** (1.0x 10^{-4} M) was observed in chloroform on irradiation with 360 nm laser pulse as shown in Figure 8. Transient absorption maximum appeared at 430 nm under argon atmosphere with the lifetime of 10 μs, which was assigned to the triplet state of anthracene ring. The transient spectrum was very similar to that of **10**, indicating that UPy unit did not quench the triplet state of anthracene ring.

Exciplex formation between 1 and 2c

The fluorescence intensity of **1d** decreased by addition of **2c** and the weak fluorescence at 550 nm assigned to the exciplex emission between anthracene group and *N,N*-dimethylaniline group was observed as shown in Figure 9. The lifetime of the exciplex emission was determined to be 40 ns by nano-second laser photolysis under argon atmosphere at the concentration of both **1d** and **2c** in 1.0x 10^{-5} M.

When we added **2c** as an electron donor to the solution of **1e** (1.0x 10^{-5} M), the fluorescence intensities of both monomer and excimer of pyrene at 400 nm and 485 nm, respectively, were decreased and the fluorescence maximum shifted to the longer wavelength region to give λ_{max} = 488 nm at the concentration of both **1e** and **2c** to be 1.0x 10^{-5} M. Further addition of **2c** shifted emission peak to λ_{max} = 505 nm in the presence of **2c** to be 1.0x 10^{-4} M as shown in Figure 10. The change of fluorescence spectrum can be explained by the formation of the hetero dimers between **1e** and **2c** instead of the homo dimer of **1e**, since the final concentration of **2c** (1.0x 10^{-4} M) is 10 times higher than that of **1e**; in this case at least 95% of **1e** forms the hetero dimer with **2c**. The lifetime of the exciplex emission was determined to be 50 ns at 500 nm.

The chain length dependence on the exciplex formation between 1e and 2

Compounds **2a**, **2b**, **2c**, and **2d**, were prepared and the chain length dependence on the exciplex formation between **1e** and **2** was studied. The maximum wavelength of the exciplex emission between pyrene ring and *N,N*-dimethylaniline ring was slightly dependent on the chain length of **2** and was appeared at 492, 500, 502, and 501 nm for **2a**, **2b**, **2c**, and **2d**, respectively in the presence of **1e** and **2** at 1.0x 10^{-5} M and 1.0x 10^{-4} M, respectively. **2c**

quenched fluorescence of pyrene monomer more efficiently than **2a**, **2b** and **2d** as shown in Figure 11.

Solvent effect on the excimer formation of 1e

Fluorescence spectrum of **1e** was strongly dependent on the solvent polarity and hydrogen bonded character of the solvent. In chloroform, **1e** exhibited excimer emission with the maximum at 485 nm in addition to the normal emission around 400 nm at 1.0x 10^{-5} M as shown in Figure 12. The intensity of monomer emission (397 nm) increased and the intensity of excimer emission (485 nm) decreased with increasing the ratio of acetonitrile in chloroform. The dependence of the fluorescence intensity at 397 nm and 485 nm on the concentration of acetonitrile was plotted in Figure 13.

The quantum yield of fluorescence of 1-(butoxymethyl)pyrene (**11**) was 0.3, 0.7, and 0.7 in chloroform, acetonitrile and methanol, respectively. Thus the addition of acetonitrile or methanol to chloroform solution would result in the increase of the intensity of monomer emission of **1e**.

The fluorescence spectral change on addition of methanol in chloroform is different from that on addition of acetonitrile. Thus, the intensity at 485 nm decreased rapidly by the addition of methanol and remained constant at the concentration of 5 M. The intensity at 400 nm increased rapidly by the addition of methanol up to 5 M and increased with increasing concentration of methanol more than 5 M as shown in Figure 13.

These results strongly indicate that the formation of hydrogen bonded dimer by quadruple intermolecular hydrogen bonding was prevented by the addition of methanol.

The change of the exciplex emission between 1e and 2c by addition of acetonitrile

The exciplex emission was observed in the system of quadruple intermolecular hydrogen bonded dimer between **1e** and **2c**. Figure 14 shows the change of fluorescence spectrum of **1e** (1.0×10^{-5} M) in the presence of **2c** (1.0×10^{-4} M) by the addition of acetonitrile in chloroform. The exciplex emission band at 485 nm shifted to 490 nm and the intensity decreased with increasing the ratio of acetonitrile up to 40% v/v. These results indicate that the exciplex was stabilized by the increase of solvent polarity. On the other hand, the increase of solvent polarity increase the electron transfer reaction to produce the cation radical and the anion radical and decreased the intensity of the exciplex emission.

Magnetic field effect on the exciplex emission between 1e and 2c

The intensity of the exciplex emission between **1e** and **2c** in chloroform-acetonitrile binary solution (acetonitrile 40% v/v) increased by the application of magnetic field. Figure 15 shows the decay curve of exciplex emission monitored with 0.4 T (dashed line) and with 0 T (solid line). Since the emission intensity corresponds to the integral of the decay curve, the emission intensity with 0.4 T was larger than that with 0 T.

The magnetic field effect on the exciplex emission was not observed when the composition of acetonitrile was less than 30% and more than 50%. This means that the equilibrium between radical ions and exciplex was established only in the solvent with ca. 40% acetonitrile v/v in chloroform.

Absorption and fluorescence spectra of UPy having naphthalene ring liked

by chiral spacer

The UPy derivatives having naphthalene ring linked by chiral spacer, **3aR**, **3aS**, **3bR**, and **3bS** were prepared and absorption spectra and fluorescence spectra were measured. Absorption spectrum of **3aR** and **3aS** was similar to the sum of 1-methylnaphthalene and **1a** as shown in Figure 16. In addition, absorption spectrum of **3bR** and **3bS** was similar to the sum of **3aR** or **3aS** and 9-(methoxymethyl)anthracene (**10**) as shown in Figure 17.

The fluorescence spectrum of **3bR** on excitation at 293 nm, where molar extinction coefficient of naphthalene ring was much larger than that of anthracene ring, was shown in Figure 18. The fluorescence intensity of naphthalene ring at 340 nm was smaller than that of anthracene ring at 415 nm.

The fluorescence excitation spectrum of **3bR** was similar to the absorption spectrum indicating that intramolecular energy transfer form naphthalene ring to anthracene ring occurs with high quantum efficiency.

Fluorescence spectra of **1d** (1.0×10^{-5} M) were observed on excitation at 293 nm in the absence or in the presence of **3aR** (1.0×10^{-5} M). The molar extinction coefficient of naphthalene ring was much larger than that of anthracene ring at 293 nm. Although fluorescence intensity of anthracene ring increased by addition of **3aR**, that of naphthalene ring decreased as shown in Figure 19. These results indicate that intermolecular energy transfer from naphthalene ring to anthracene ring occurs with the aid of formation of quadruple hydrogen bonded dimer.

The intensity of fluorescence emission from anthracene ring of **3bR** (5.0×10^{-6} M) increased by the addition of **3aR** as shown in Figure 20. This result also indicates that intermolecular energy transfer occurs from naphthalene ring of **3aR** to anthracene ring of **3bR**.

It was interesting to study whether the efficiency of energy transfer from naphthalene ring to anthracene ring was different in the compounds with a chiral substituent. However, fluorescence and fluorescence excitation spectra of **3bR** (5.0×10^{-6} M) in the presence of **3aR** (2.0×10^{-5} M) was identical with that in the presence of **3bS** (2.0×10^{-5} M). In this experimental condition, 80% of **3bR** forms hetero dimer with **3aR** or **3bS**.

Absorption and fluorescence spectra of **3aR** (5.0×10^{-6} M) were observed in methylcyclohexane with decreasing temperature (Figure 21). Broad fluorescence spectrum was observed at 180 K, while the fluorescence excitation spectra was similar to that at room temperature. The absorption spectrum are broadened with decreasing temperature.

Photoisomerization and thermal isomerization of 1c

It is well known that azobenzene undergoes trans-cis photoisomerization and azobenzene derivatives are widely used in photoresponsive supramolecular systems.[24,25] We expect that azobenzene is useful to construct a photoresponsive supramolecular hydrogen bonded polymer used by UPy unit as well. In this respect, **1c** was prepared and the effect of UPy unit on the cis-trans isomerization of azobenzene was studied.

Absorption spectrum of **1c** in chloroform was shown in Figure 22. The spectrum of **1c** was the same as that of 4-butoxyazobenzene (**9**) in the wavelength region longer than 300 nm. On irradiation at 366 nm light, absorption band at 350 nm decreased with concomitant increase of absorbance at 440 nm. This spectrum change showed that trans-to-cis photoisomerization of **1c** occurred with the same efficiency with that of **9**.

The rate constants of cis-to-trans thermal isomerization of **1c** increased

from 7.7x 10^{-6} s^{-1} to 4.4x 10^{-5} s^{-1} and that of **9** increased from 8.9x 10^{-7} s^{-1} to 4.6x 10^{-6} s^{-1} in the temperature range from 303 K to 316 K. The Arrhenius plot for cis-to-trans isomerization of **1c** and **9** was shown in Figure 23. The frequency factor and activation energy for the isomerization of **1c** were determined to be 8.2x 10^{13} s^{-1} and 26.4 kcal mol^{-1} kcal mol^{-1}, respectively in chloroform. The values for **9** were similar to those of **1c** and were 1.0x 10^{12} s^{-1} and 23.6 kcal mol^{-1}, respectively.

These results indicate that **1e** undergoes the isomerization similar to azobenzene.[26]

Discussion

The dimer formation by utilizing quadruple hydrogen bonding of UPy in dilute solution

UPy unit can form hydrogen bonded dimer by DDAA array of hydrogen bonding with dimerization constant as high as 10^7 M^{-1}.[9,11] In addition, the result of ESI-MS spectroscopy strongly indicates formation of dimer by intermolecular quadruple hydrogen bonding.

Pyrene excimer was observed for **1e** even at low concentration of 1.0x 10^{-5} M. However, model compound 1-(butoxymethyl)pyrene (**11**) did not exhibit excimer emission at this concentration. This result showed that UPy can form dimer even at low concentration as low as 10^{-5} M.

As to the hetero dimers, photoinduced electron transfer reaction may take place. The oxidation and reduction potential of the compounds were determined by cyclic voltammetry. From these results, ΔG value of photoinduced electron transfer form *N,N*-dimethylaniline (DMA) to **10** was estimated to be –0.57 eV ($\Delta G = E_{ox} - E_{red} + E_{0\text{-}0}$; $E_{0\text{-}0} = 3.2$ eV, where E_{ox} and E_{red}

are the oxidation and reduction potential, respectively and $E_{0\text{-}0}$ is the excitation energy for **10**). Thus, the photoinduced electron transfer reaction to produce $Ant^{\bullet -}$ and $DMA^{\bullet +}$ occurred in exothermic and diffusion controlled process.

The plot of the observed fluorescence intensity vs. the concentration of DMA gave the Stern-Volmer constant $k_q\tau_s$ to be 22.8 and 25.1 for **1d** and **10**, respectively as shown in Figure 24. By using the fluorescence lifetime of **1d** and **10** in the absence of DMA, the quenching rate constants of the singlet excited states of **1d** and **10** by DMA (k_q) were determined to be 9.1x 10^9 M^{-1} s^{-1} and 1.0x 10^{10} M^{-1} s^{-1}, respectively in chloroform. The exciplex emission was not observed when the concentration of **1d** and DMA was 1.0x 10^{-5} M and 1.0x 10^{-4} M, respectively. However, the exciplex emission was observed in hydrogen bonded dimer even at the concentration as low as 10^{-5} M.

Excimer emission of **1e** was quenched by addition of **1a**, and the intensity of excimer emission became just half as that in absence of **1a** when the concentration of both **1a** and **1e** was 1.0x 10^{-5} M. This result indicated that homo dimer and hetero dimer existed at the ratio of [**1a-1a**] : [**1a-1e**] : [**1e-1e**] = 1 : 2: 1 when [**1a**] = [**1e**].

Estimation of the efficiency of intermolecular energy transfer from 3aR to 3bR

The efficiency of energy transfer from **3aR** to **3bR** was estimated from the fluorescence spectroscopic experiments of **3bR** in the presence of **3aR** (Figure 20).

The concentration of homo dimer and hetero dimer in the mixture of UPy's was estimated by the following equation, where A and B mean the

different UPy and a and b are their concentrations.

$$A : B = a : b$$

$$AA : AB : BB = a^2 : 2ab : b^2 \qquad (1)$$

Thus, the ratio of hetero dimer and homo dimer at a certain concentration can be calculated by eq. 1. For example, when A and B exist at the ratio of 1 : 1, the ratio of AA : AB : BB can be estimated to be 1 : 2 : 1.

In the solution containing both **3aR** and **3bR**, the concentration of homo dimer and hetero dimer was calculated as summarized in Table 1. The fluorescence intensity of anthracene ring at 415 nm (I_{hetero}) on excitation of naphthalene ring at 293 nm can be estimated from the values in Table 1 by using eq. 2. The molar extinction coefficient of naphthalene ring at 293 nm is much larger than that of anthracene ring. The concentration of **3bR** was kept constant at 5.0x 10^{-6} M. Figure 24 shows the plot for I_{hetero} vs. **[3aR-3bR]** to give a straight line. The value of I_{hetero} at any concentration of hetero dimer (**3aR-3bR**) can be calculated from Figure 25. Thus, I_{hetero} was estimated to be 37 at the concentration of **[3aR-3bR]** = 5.0x 10^{-6} M on excitation at 293 nm.

$$I_{hetero} = I_{obs} - I^0 \cdot 2 \cdot [\mathbf{3bR\text{-}3bR}] / 5.0\text{x } 10^{-6} \qquad (2)$$

I_{hetero} Fluorescence intensity of anthracene ring at 415 nm of hetero dimer on excitation at 293 nm

I_{obs} Fluorescence intensity of anthracene ring at 415 nm in the presence of **3aR**

I^0 Fluorescence intensity of anthracene ring at 415 nm in the absence of **3aR**

[**3bR-3bR**] Concentration of homo dimer of **3bR** in the presence of **3aR**

Efficiency of singlet energy transfer in hetero dimer between **3aR** and **3bR** was estimated by the following way. As described above, fluorescence intensity of anthracene ring observed on excitation at 293 nm at the concentration of 5.0x 10^{-6} M was estimated to be 37, where the absorbance of hetero dimer at 293 nm was 0.058 (Figure 17). The fluorescence intensity at 415 nm and the absorbance at 293 nm of **3bR** in the absence of **3aR** was 24 and 0.030, respectively. If the energy transfer did not occur from **3aR** to **3bR**, the fluorescence intensity at the concentration of [**3aR**] = [**3bR**] = 5.0x 10^{-6} M (I_{hetero} = 37) should be the same with that in the absence of **3aR** (I^0 = 24). These results indicate the occurrence of energy transfer from **3aR** to **3bR** in hetero dimer.

From these results, the efficiency of intramolecular energy transfer from naphthalene ring of **3aR** to anthracene ring of **3bR** was estimated to be $\{(37/0.058)/(24/0.030) - 0.5\}x\ 2 = 0.6$

The solvent effect on dimer formation of UPy

The formation of hydrogen bonded dimer was strongly affected by solvent. Actually, the addition of methanol brings about the breaking of hydrogen bonding in the dimer. The quantum yield of fluorescence of 1-(butoxymethyl)pyrene (**11**) was 0.3, 0.7, and 0.7 in chloroform, acetonitirile, and methanol, respectively. The addition of acetonitrile or methanol to

chloroform solution also increased the fluorescence intensity of pyrene monomer emission. As shown in Figure 12, **1e** exhibited excimer emission with the maximum at 485 nm in addition to the normal emission around 400 nm at 1.0x 10^{-5} M in chloroform and the intensity of monomer emission (397 nm) increased and the intensity of excimer emission (485 nm) decreased with increasing of the ratio of acetonitrile in chloroform. On the other hand, the intensity at 485 nm decreased and that at 400 nm increased rapidly by the addition of methanol up to 5 M. These results strongly indicate that the formation of hydrogen bonded dimer by quadruple intermolecular hydrogen bonding was prevented by the addition of methanol.

If we assume that the intensity of excimer emission was only dependent on the concentration of the dimer in chloroform-methanol binary solution, the ratio of excimer emission in the absence (I_0) and the presence (I) of methanol was plotted against the concentration of methanol in chloroform as shown in Figure 26. The concentration dependence of excimer emission intensity fitted the following equation.

$$\frac{I_0}{I} = 1 + A\,[MeOH]^B \qquad (3)$$

A : 2.2
B : 1.8

The result indicates that the 2 mol of methanol was expected to participate in the dissociation of the intermolecular hydrogen bonding in the dimer by quadruple hydrogen bonding.

Conclusion

Absorption spectra of UPy derivatives having aromatic group were quite similar to the sum of absorption spectrum of **1a** and the corresponding aromatic molecule, indicating that UPy group and the aromatic group did not interact in the ground state. Furthermore, from the results of fluoresecence and transient absorption spectroscopy, it was found that energy transfer and electron transfer between UPy and aromatic group could not occur. The efficiency of cis-to-trans isomerization of azobenzene was not affected by UPy group.

On the basis of the results of fluorescence studies, it was revealed that the electron transfer and the energy transfer efficiently occurred between the aromatic molecules linked by intermolecular quadruple hydrogen bonding. The formation of hydrogen bonded dimer of UPy was affected by solvent. Almost all the hydrogen bonded dimer was dissociated to the monomer by the addition of 5 M of methanol in chloroform.

Further studies on this line by connecting appropriate donor and acceptor molecules may open the way to construct macromolecules formed by weak interaction capable to induce efficient electron transfer and energy transfer reaction.

Experiment

Measurement

Absorption and fluorescence spectra were measured on a Shimadzu UV-1600 and on a Hitachi F-4000 fluorescence spectrometer, respectively. Fluorescence lifetimes were determined with a time resolved spectrofluorometer, Horiba NAES 1100. The lifetimes of exciplex and excimer emission were also measured by nano-second laser photolysis on excitation at 308 nm (Lamda

Phisik LPX-100) or 355 nm (Spectra Physics GCR-3). The oxidation and the reduction potentials of aromatic ring were determined with a cyclic voltammety apparatus, BAS CV-50W. Oxford Cryostat model DN-1704 and temperature controller ITC-4 were used for the low temperature experiment.

Laser flash photolyses were performed by using excimer laser pumped dye laser (Lambda Physik LPX-100, 308 nm, 20 ns fwhm and Lambda Physik FL-4002, DMQ, 360 nm, 10 ns fwhm) and a pulsed xenon arc (Ushio UXL-159) was used as a monitoring light source. A photomultiplier (Hamamatsu R-928) and a storage oscilloscope (Iwatsu TS-8123) were used for the detection.

ESI-MS spectroscopy was performed by FT-ICRMS (Buruker APEX II 70e) in National Food Research Institute (NFRI).

Synthesis

Ureidopyrimidinone (UPy) derivatives were synthesized by the similar procedure previously reported by Meijer et al.[9]

***N*-[(Butylamino)carbonyl]-6-methylisocytosine (1a).** A suspension of 6-methyl-isocytosine **4a** (0.025 mol) and butyl isocyanate (0.045 mol) in pyridine dried over molecular sieves 4A was heated under reflux for 2 h to give clear solution. After cooling, the white precipitate was washed with acetone. Recrystallization from ethanol/chloroform 9:1 v/v gave pure **1a** (99%). ^{1}H NMR ($CDCl_3$, 200 MHz): δ 0.94 (t, 3H, J = 7.2 Hz), 1.2-1.8 (m, 4H), 2.23 (s, 3H), 3.24 (m, 2H), 5.83 (s, 1H), 10.14 (s, 1H), 11.86 (s, 1H), 13.15 (s, 1H) ppm.

***N*-[(Butylamino)carbonyl]-6-tridecylisocytosine (1b).** A solution of 6-tridecylisocytosine **4b** (5.4 mmol) and butyl isocyanate (9.0 mmol) in pyridine dried over molecular sieves 4A was heated under reflux for 2 h. After cooling, product was precipitated by addition of acetone and was filtrated.

Recrystallization form ethanol/chloroform 8:2 v/v gave pure **1b** (35%). ^{1}H NMR ($CDCl_3$, 200 MHz): δ 0.90 -1.0 (m, 6H), 1.2-1.8 (m, 28H), 2.46 (t, 3H, J = 7.6 Hz), 24 (m, 2H), 5.83 (s, 1H), 10.14 (s, 1H), 11.86 (s, 1H), 13.15 (s, 1H) ppm.

***N*-[(Butylamino)carbonyl]-6-[5-(4-phenylazophenoxy)pentyl] -isocytosine (1c).** A solution of **4c** (500 mg, 1.37 mmol) and butyl isocyanate (0.5 ml) in pyridine (10 ml) dried over molecular sieves 4A was heated under reflux for 2 h. After cooling, product was precipitated by addition of acetone and was filtrated. Recrystallization form ethanol/chloroform 8:2 v/v gave pure **1c** (324 mg, 51%). ^{1}H NMR ($CDCl_3$, 200 MHz): δ 0.94 (t, 3H, J = 7.2 Hz, CH_3), 1.60 (m, 10H, CH_2), 3.26 (m, 2H, CH_2), 4.05 (t, 2H, J = 6.0 Hz, -CH_2O-), 5.84 (s, 1H, isocytosine-H), 7.00 (m, 2H, Ar-H), 7.46 (m, 3H, Ar-H), 7.89 (m, 4H, Ar-H), 10.2 (br, 1H, NH), 11.9 (br, 1H, NH), 13.2 (br, 1H, NH) ppm. mp 165 –167 °C. Anal Calcd for $C_{26}H_{34}N_6O_3$: C, 65.25; H, 7.16; O, 17.56. Found: C, 65.15; H, 6.96; O, 17.21.

***N*-[(Butylamino)carbonyl]-6-[5-(9-anthrylmethoxy)pentyl] -isocytosine (1d).** A solution of **4d** (1.79 g, 4.62 mmol) and butyl isocianate (1.0 ml) in pyridine (10 ml) dried over molecular sieves 4A was heated under reflux for 2 h. After cooling, the reaction mixture was extracted by dichloromethane and washed with water. After the oil layer was dried with $MgSO_4$, solvent was removed by evaporation. On addition of acetone to the residue, the product was precipitated and was filtrated. The precipitate was purified by silica-gel column chromatography (eluent: chloroform 100%) and the fraction, which was eluted by chloroform, was collected and evaporated to dryness. The residue was recrystallized from ethanol/chloroform 8:2 v/v gave pure **1d** (284 mg, 13%). ^{1}H NMR ($CDCl_3$, 400 MHz), δ 0.91 (3H, t, J = 7.2

Hz; -CH_3), 1.2 - 1.7 (10H), 2.34 (2H, t, J = 7.6 Hz; CH_2CH_2-Ar), 3.21 (2H, m; $NHCH_2$), 3.63 (2H, t, J = 6.4 Hz; $ArCH_2OCH_2$), 5.45 (2H, s; $ArCH_2O$), 5.73 (1H, s; Ar-H), 7.45 (2H, m; Ar-H), 7.53 (2H, m; Ar-H) 7.98 (2H, m; Ar-H), 8.36 (2H, d, J = 9.2 Hz; Ar-H), 8.43 (1H, s; Ar-H) 10.1 (1H, s; NH), 11.8 (1H, s; NH), 13.1 (1H, s; NH) ppm. mp 144-145°C. ESI-MS calcld for $C_{29}H_{34}N_4O_3$ $[M+H]^+$ = 487.2709 found: 487.2714.

***N*-[(Butylamino)carbonyl]-6-[5-(1-pyrenylmethoxy)pentyl] -isocytosine (1e).** A suspension of **5e** (1.20 g, 2.88 mmol) and guanidine carbonate (0.585 g,1.68 mmol) in ethanol (10 ml) dried over molecular sieves 4A was heated under reflux for 12 h. After cooling, ethanol was removed by evaporation, further dried in vacuo with rotary pump to give **4e**. A solution of **4e** and butyl isocyanate (1.0 ml) in pyridine (10 ml) dried over molecular sieves 4A was heated under reflux for 2 h. After cooling, the reaction mixture was extracted by dichloromethane and washed with water. After the oil layer was dried with $MgSO_4$, solvent was removed by evaporation. On addition of acetone to the residue, the product was precipitated and was filtrated. The precipitate was purified by silica-gel column chromatography (eluent: chloroform 100%) and the fraction, which was eluted by chloroform, was collected and evaporated to dryness. The product was dissolved in hot chloroform and crystallized in refrigerator (35%). ^1H NMR ($CDCl_3$, 400 MHz), δ 0.91 (3H, t, J = 7.2 Hz; -CH_3), 1.2 - 1.8 (10H), 2.36 (2H, t, J = 7.6 Hz; CH_2CH_2-Ar), 3.24 (2H, m; $NHCH_2$), 3.59 (2H, t, J = 6.2 Hz; $ArCH_2OCH_2$), 5.19 (2H, s; $ArCH_2O$), 5.69 (1H, s; Ar-H), 7.98 (4H, m; Ar-H), 8.15 (4H, m; Ar-H), 8.34 (1H, d, J = 9.2 Hz; Ar-H), 10.1 (1H, s; NH), 11.7 (1H, s; NH), 13.1 (1H, s; NH). mp 174-175°C. ESI-MS calcld for $C_{31}H_{34}N_4O_3$ $[M+H]^+$ = 511.2709 found: 511.2760.

***N*-[(Butylamino)carbonyl]-6-[3-(3-*N*,*N*-dimethylaminophenoxy)pro -pyl]isocytosine (2a).** A suspension of **5f** (3.15 g, 10.8 mmol) and guanidine carbonate (1.14 g, 6.38 mmol) in ethanol (15 ml) dried over molecular sieves 4A was heated under reflux for 12 h. After cooling, ethanol was removed by evaporation, further dried in vacuo with rotary pump to give **4f**. Then, 15 ml of pyridine and 3 ml of butyl isocyanate were added and was heated under reflux for 4 h. After cooling, 50 ml of water was added and the product was precipitated. The precipitate was filtrated and washed with water and acetone. Then it was dissolved in chloroform and purified with silica-gel column chromatography (eluent: chloroform). The fraction, which was eluted by chloroform, was collected and the solvent was removed by evaporation. Acetone was added to the residue, the product was precipitated and filtrated. Recrystallization from ethanol gave **2a** (780 mg, 20%). ^{1}H NMR ($CDCl_3$, 200 MHz) δ 0.94 (3H, t, J = 7.0Hz), 1.40 (2H, m), 1.60 (2H, m), 2.12 (2H, m), 2.71 (2H, t, J = 7.2 Hz), 2.93 (6H, s, NCH_3), 3.26 (2H, m, $NHCH_2$), 4.02 (2H, t, J = 6.0 Hz, OCH_2), 5.89 (1H, s), 6.20-6.45 (3H, m), 7.13 (1H, m), 10.14 (1H, br), 11.89 (1H, s), 13.29 (1H, s). mp 133 - 134°C. Anal Calcd for $C_{20}H_{29}N_5O_3$: C, 62.00; H, 7.54; N, 18.07. Found: C, 61.45; H, 7.69; N, 17.60.

***N*-[(Butylamino)carbonyl]-6-[4-(3-*N*,*N*-dimethylaminophenoxy)butyl]isocytosine (2b).** A suspension of **5g** (3.17 g, 10.3 mmol) and guanidine carbonate (1.10 g, 6.38 mmol) in ethanol (15 ml) dried over molecular sieves 4A was heated under reflux for 4 h. After cooling, ethanol was removed by evaporation. And dried in vacuo with rotary pump to give **4g**. In this flask, 15 ml of pyridine and 3 ml of butyl isocyanate were added and was heated under reflux for 4 h. After cooling, 50 ml of water was added and the product was

precipitated. The precipitate was filtrated and washed with water and acetone. Then it was dissolved in chloroform and purified with silica-gel column chromatography (eluent: chloroform). The fraction, which was eluted by chloroform, was collected and the solvent was removed by evaporation. Acetone was added to the residue, the product was precipitated and filtrated. Recrystallization from ethanol gave **2b** (1.21 g, 29%). ^{1}H NMR ($CDCl_3$, 200 MHz) δ 0.94 (3H, t, J = 7.0Hz), 1.40 (2H, m), 1.60 (2H, m), 1.86 (4H, m), 2.56 (m, 2H), 2.93 (6H, s, NCH_3), 3.25 (2H, m, $NHCH_2$), 3.99 (m, 2H, OCH_2), 5.86 (1H, s), 6.20-6.45 (3H, m), 7.13 (1H, m), 10.15 (1H, br), 11.88 (1H, s), 13.26 (1H, s). mp 150 – 152 °C. Anal Calcd for $C_{21}H_{31}N_5O_3$: C, 62.82; H, 7.78; N, 17.44. Found: C, 62.74; H, 7.97; N, 17.22.

***N*-[(Butylamino)carbonyl]-6-[5-(3-*N*,*N*-dimethylaminophenoxy)pen -tyl]isocytosine (2c).** A suspension of **4h** (1.09 g, 3.44 mmol) and 1 ml of butyl isocyanate in 15 ml of pyridine dried over added and solvent reflux for 4 h. After cooling, the reaction mixture was extracted with dichloromethane and water. The oil layer was removed by evaporation after dried over $MgSO_4$. The residue was purified with silica-gel column chromatography (eluent: chloroform). Recrystallization from ethanol gave pure **2c**. ^{1}H NMR ($CDCl_3$, 400 MHz), δ 0.92 (3H, t, J = 7.2 Hz; $-CH_3$), 1.2 – 2.0 (10H), 2.48 (2H, t, J = 7.6 Hz; CH_2CH_2-Ar), 2.91 (6H, s; NCH_3), 3.24 (2H, m; $CONHCH_2CH_2$), 3.94 (2H, t, J = 6.2 Hz; ArO-CH_2), 5.81 (1H, s; Ar-H), 6.25 (2H, m; Ar-H), 6.34 (1H, m; Ar-H), 7.10 (1H, m; Ar-H), 10.2 (1H, s; NH), 11.8 (1H, s; NH), 13.2 (1H, s; NH) ppm. mp 121-122°C. ESI-MS calcld for $C_{22}H_{33}N_5O_3$ $[M+H]^+$ = 416.2661 found: 416.2641. Anal Calcd for $C_{22}H_{33}N_5O_3$: C, 63.59; H, 8.00; N, 16.85. Found: C, 63.73; H, 8.27; N, 16.43.

***N*-[(Butylamino)carbonyl]-6-[6-(3-*N*,*N*-dimethylaminophenoxy)hexyl**

]isocytosine (2d). A suspension of **5i** (3.47 g, 10.3 mmol) and guanidine carbonate (1.15 g, 6.38 mmol) in ethanol (15 ml) dried over molecular sieves 4A was heated under reflux for 6 h. After cooling, ethanol was removed by evaporation, further dried in vacuo with rotary pump to give **4h**. Then, 15 ml of pyridine and 3 ml of butyl isocyanate were added and was heated under reflux for 4 h. After cooling, 100 ml of water was added and the product was precipitated. The precipitate was filtrated and washed with water and acetone. Then it was dissolved in chloroform and purified with silica-gel column chromatography (eluent: chloroform). The fraction, which was eluted by chloroform, was collected and the solvent was removed by evaporation. Acetone was added to the residue, the product was precipitated and filtrated. Recrystallization from ethanol gave **2d** (1.65 g, 37%). ^{1}H NMR ($CDCl_3$, 200 MHz) δ 0.94 (t, 3H, J = 7.0Hz), 1.3-1.8 (12H, m), 2.48 (t, 2H, J = 7.4 Hz), 2.93 (s, 6H, NCH_3), 3.26 (m, 2H, $NHCH_2$), 3.95 (t, 2H, J = 6.0 Hz, OCH_2), 5.83 (1H, s), 6.20-6.45 (3H, m), 7.13 (1H, m), 10.14 (1H, br), 11.89 (1H, s), 13.29 (1H, s). mp 107 - 109°C. Anal Calcd for $C_{23}H_{35}N_5O_3$: C, 64.31; H, 8.21; N, 16.30. Found: C, 64.92; H, 8.48; N, 15.76.

6-Tridecyl-2-(3-(1-(1-naphtyl)ethyl)ureido)-4[*1H*]-pyrimidinone (3a). A suspension of **4b** (500 mg, 1.70 mmol) and 1-(1-isocyanatoethyl)naphthalene (400mg, 2.0 mmol) in dry pyridine (10 ml) was heated under reflux for 2 h. The reaction mixture was extracted with chloroform and water, then the solvent was removed by evaporation after dried over $MgSO_4$. The residue was purified with silica-gel column chromatography, and recrystallization from ethanol gave pure **3a** (**3aR**, 34%; **3aS**, 80%). ^{1}H NMR ($CDCl_3$, 400MHz) d (ppm) 0.87 (3H, t, J = 6.4 Hz; $-CH_3$), 1.15-1.35 (20H, m; $-CH_2-$), 1.57 (2H, m; $ArCH_2CH_2-$), 1.71 (3H, d, J = 6.8 ppm; CH_3C^*-), 2.38 (2H, t, J = 7.8 Hz; $ArCH_2-$), 5.80 (1H, m;

C*H), 5.86 (1H, s; Ar-H), 7.50 (2H, m; Nap), 7.54 (1H, m; Nap), 7.64 (1H, d, J = 7.6 Hz; Nap), 7.73 (1H, d, J = 8.4 Hz; Nap), 7.85 (1H, d, J = 8.0 Hz; Nap), 8.18 (1H, d, J = 8.8 Hz; Nap), 10.87 (1H, br; NH), 12.16 (1H, br), 13.02 (1H, br). Anal calcd for $C_{30}H_{42}N_4O_2$; C 73.47, H 8.63, N 11.26%; found C 73.27, H 8.72, N 11.26% for **3aR** and C 73.44, H 8.84, N 11.16% for **3aS**.

6-(5-(9-Anthrylmethoxy)pentyl)-2-(3-(1-(1-naphtyl)ethyl)ureido) -4[*1H*]-pyrimidinone (3b). A suspension of **4b** (500 mg, 1.70 mmol) and 1-(1-isocyanatoethyl)naphthalene (400 mg, 2.0 mmol) in dry pyridine (10 ml) was heated under reflux for 2 h. The reaction mixture was extracted with chloroform and washed with water, then the solvent was removed by evaporation after dried over $MgSO_4$. The residue was purified with silica-gel column chromatography, and recrystallization from ethanol gave pure **3a** (**3aR**, 34%; **3aS**, 80%). ^{1}H NMR ($CDCl_3$, 400MHz) δ (ppm) 1.33 (2H, m; -CH_2-), 1.48 (2H, m; -CH_2-), 1.58 (2H, m; -CH_2-), 1.72 (3H, d, J = 6.8 Hz; CH_3C*), 2.28 (2H, t, J = 7.8 Hz; ArCH_2-), 3.58 (2H, t, J = 6.4 Hz; -CH_2-O), 5.40 (2H, s; Ar-CH_2-O-), 5.77 (1H, s; Ar-H), 5.80 (1H, m; C*H), 7.44 (4H, m), 7.51 (3H, m), 7.66 (1H, d, J = 6.8 Hz), 7.71 (1H, d, J = 8.0 Hz), 7.82 (1H, d, J = 8.0 Hz), 7.96 (2H, d, J = 8.4 Hz), 8.17 (1H, d, J = 8.4 Hz), 8.33 (2H, d, J = 8.8 Hz), 8.41 (1H, s), 10.88 (1H, br), 12.13 (1H, br), 12.98 (1H, br).

3-Oxo-heptadecanoic acid ethyl ester (5b). A THF solution of ethylacetoacetate (**7**) (6.5 g, 0.050 mol) was added dropwise to a suspension of sodium hydrate (60%, 2 g, 0.055 mol) at 0 °C under nitrogen atmosphere. The solution color turned to yellow. After 15 min, 1.6 M n-butyllithium in hexane (33 ml; 0.050 mol) was added to the reaction mixture with syringe, and stirred for 15 min. The solution color changed from yellow to dark orange. Then, dodecyl boromide (27.6 g, 0.11 mol) was added to the reaction mixture with

syringe, and warmed to room temperature for 30 min. When the reaction mixture was poured into acidified ice-water (2 ml of conc. HCl, and 200 ml of ice-water), the color of the reaction mixture changed from orange to yellow. The mixture was extracted with diethylether and was washed with water. The solvent was removed by evaporation to give the product **5b** (12 g, 84%).

3-Oxo-8-(4-phenylazophenoxy)octanoic acid ethyl ester (5c). A THF solution of ethylacetoacetate (**7**) (0.010 mol) was added dropwise to a suspension of sodium hydrate (0.011 mol) at 0 °C under nitrogen atmosphere. The solution color turned to yellow. After 15 min, 1.6 M n-butyllithium in hexane (0.010 mol) was added to the reaction mixture with syringe, and stirred for 15 min, the solution color changed from yellow to dark orange. Then, **6c** (0.011 mol) was added to the reaction mixture with syringe, and warmed to room temperature and stirred for 2 h. The reaction mixture was poured into acidified ice-water (2 ml of conc. HCl, and 200 ml of ice-water). The color of the reaction mixture changed from orange to yellow. The mixture was extracted with diethylether and was washed with water. After the solvent was removed, the residue was purified by silica-gel column chromatography (eluent: ethylacetete/ hexane = 1/11) to give **5c** (78%). ^{1}H NMR ($CDCl_3$, 200 MHz) δ 1.28 (t, 3H, J = 7.2 Hz, CH_3CH_2O-), 1.60 (m, 4H), 2.60 (t, 2H, J = 7.4 Hz), 3.44 (s, 2H), 4.04 (t, 2H. J = 6.4 Hz), 4.22 (q, 2H, J = 7.2 Hz), 6.99 (m, 2H, aromatic-H), 7.49 (m, 3H, aromatic-H), 7.89 (m, 4H, aromatic-H) ppm.

3-Oxo-8-(9-anthrylmethoxy-octanoic acid ethyl ester (5d) A THF solution of ethylacetoacetate (**7**) (1.95 g, 15 mmol) was added dropwise fo 15 min to a suspension of sodium hydrate (15.5 mmol) in 30 ml of dry THF at 0 °C under nitrogen atomosphere. The solution color turned to yellow. After 15 min, 12 ml of 1.6 M n-butyllithium in hexane was added to the reaction mixture

with syringe and was stirred for 15 min. The solution color changed from yellow to dark orange. Then, **6d** (5.00 g, 14.6 mmol) was added to the reaction mixture with syringe, and warmed to room temperature and stirred for 2 h. The reaction mixture was poured into acidified ice-water (1 ml of conc. HCl, and 100 ml of ice-water). The color of the reaction mixture changed from orange to yellow. The mixture was extracted with diethylether and was washed with water. After the solvent was removed, the residue was purified by silica-gel column chromatography (eluent: ethylacetete/ hexane = 1/5) to give **5d** (2.79 g, 49%). ^{1}H NMR (200 MHz, $CDCl_3$) δ 1.28 (t, 3H, J = 7.2 Hz), 1.3-1.7 (6H), 2.45 (t, 2H, J = 7.2 Hz), 3.36(s, 2H), 3.65 (t, 2H, J =7.2 Hz)、4.16 (q, 2H, 7.2 Hz), 5.45 (s, 2H), 7.3 - 7.6 (4H), 8.0 (2H), 8.3 - 8.5 (3H).

3-Oxo-8-(1-pyrenylmethoxy-octanoic acid ethyl ester (5e) A THF solution of ethylacetoacetate (7) (2.01 g, 15.5 mmol) was added dropwise fo 15 min to a suspension of sodium hydrate (0.618 g, 60%) in 5 ml of dry THF at 0 °C under nitrogen atmosphere. The solution color turned to yellow. After 15 min, 6.3 ml of 2.47 M n-butyllithium in hexane was added to the reaction mixture with syringe and was stirred for 15 min. The solution color changed from yellow to dark orange. Then, **6e** (2.27 g, 6.18 mmol) in 10 ml of THF was added to the reaction mixture with syringe and warmed to room temperature and stirred for 2 h. The reaction mixture was poured into acidified ice-water (1 ml of conc. HCl, and 150 ml of ice-water). The color of the reaction mixture changed from orange to yellow. The mixture was extracted with diethylether and was washed with water. After the solvent removed, the residue was purified by silica-gel column chromatography (eluent: ethylacetete/ hexane = 1/5) to give **5d** (1.21 g, 47%). ^{1}H NMR ($CDCl_3$, 200MHz) δ 1.2 - 1.9 (9H), 2.46 (2H, t, J = 7.2 Hz; $COCH_2CH_2$), 3.34 (2H, s; $COCH_2CO$), 3.60 (2H, t, J =

6.3 Hz; $ArCH_2OCH_2$), 4.16 (2H, q, J = 7.0 Hz; CO-O-CH_2), 5.20 (2H, s; $ArCH_2O$), 7.8-8.5 (9H) ppm.

6-(3-*N*,*N*-Dimethylamino-phenoxy)-3-oxo-hexanoic acid ethyl ester (5f), 5g, 5h, and 5i A THF solution of ethylacetoacetate (7) (5.27 g, 40.5 mmol) in 5 ml of THF was added dropwise for 15 min to a suspension of sodium hydrate (1.62 g, 60%) in 5 ml of dry THF at 0 °C under nitrogen atmosphere. The solution color turned to yellow. After 15 min, 16.5 ml of 2.46 M n-butyllithium in hexane was added to the reaction mixture with syringe and was stirred for 15 min. The solution color changed from yellow to dark orange. Then, **6f** (3.94 g, 13.4 mmol) in 10 ml of THF was added to the reaction mixture with syringe, and warmed to room temperature and was stirred for 2 h. The reaction mixture was poured into acidified ice-water (1 ml of conc. HCl, and 150 ml of ice-water). The color of the reaction mixture changed from orange to yellow. The mixture was extracted with diethylether and wash with water. After the solvent was removed, the residue was purified by silica-gel column chromatography (eluent: ethylacetete/ hexane = 1/5) to give **5f** (3.16 g, 56%). ^{1}H NMR ($CDCl_3$, 200 MHz) δ 1.26 (3H, t, J =7.2 Hz), 2.12 (2H, t, J = 7.0 Hz; CH_2O), 2.93 (6H, s; NCH_3), 3.47 (2H, s; $COCH_2CO$), 3.98 (2H, t, J = 6.0 Hz; OCH_2), 4.19 (2H, q, J = 7.2 Hz), 6.05 – 6.20 (3H, m), 7.13 (1H, m). **5g** (43%). ^{1}H NMR ($CDCl_3$, 200 MHz) δ 1.27 (3H, t, J = 7.2 Hz), 2.12 (2H, m), 2.7 (2H, t, J = 7.0 Hz; CH_2O), 2.93 (6H, s; NCH_3), 3.44 (2H, s; $COCH_2CO$), 3.95 (2H, t, J = 6.0 Hz; OCH_2), 4.19 (2H, q, J = 7.2 Hz), 6.20 – 6.40 (3H, m), 7.13 (1H, m). **5h** (56%). ^{1}H NMR ($CDCl_3$, 200 MHz) δ 1.28 (3H, t, J = 7.0 Hz), 1.4 – 1.9 (6H, m), 2.58 (2H, t, J = 7.2 Hz), 2.93 (6H, s; NCH_3), 3.43 (2H, s), 3.95 (2H, t, J = 6.3 Hz), 4.20 (2H, q, J = 7.0 Hz), 6.26 (3H, m), 7.13 (1H, m) ppm. **5i** (58%). ^{1}H NMR ($CDCl_3$, 200 MHz) δ 1.26 (3H, t, J = 7.2 Hz), 2.12

(2H, m), 1.4 –1.8 (8H), 2.55 (2H, t, J = 7.2 Hz; CH_2O), 2.93 (6H, s; NCH_3), 3.94 (2H, m; OCH_2), 4.19 (2H, q, J =7.2 Hz), 6.20 –6.40 (3H, m), 7.13 (1H, m).

4-(4-Bromobutoxy)azobenzene (6c). A solution of 4-hydroxy-azobenzene (**8c**) (25 mmol) and 1,4-dibromobutane (50 mmol) in 2-butanone (75 ml) was heated under reflux in the presence of potassium carbonate (50 mmol) for 2.5 h. The reaction mixture was filtrated to remove potassium carbonate and the solvent was reduced by evaporation. The mixture was extracted with diethyl ether and washed with water, and solvent was evaporated. The residue was separated by silica-gel column chromatography (eluent hexane/ethylacetate =5/1) and recrystallization from hexane gave **6c** (4.2g, 50%). ^{1}H NMR ($CDCl_3$, 200 MHz) δ 2.03 (m, 4H), 3.51 (t, 2H, J = 6.4 Hz), 4.09 (t, 2H, J =5.6 Hz), 7.02 (m, 2H, aromatic-H), 7.49 (m, 3H, aromatic-H), 7.90 (m, 4H, aromatic-H) ppm.

9-(4-Bromobutoxymethyl)anthracene (6d). A solution of 10.0 g of **8d** (4.8 mmol) and 20.7 g of 1,4-dibromobutane (9.6 mmol) in THF (200 ml) was heated under reflux in the presence of NaH(60%, 2.0g) for 6 h. The reaction mixture was poured into ice-water, and was extracted with diethyl ether and was washed with water. The solvent was evaporated and the residue was separated by silica-gel column chromatography (eluent hexane/ethylacetate = 11/1) to give **6d** (4.1g, 25%). ^{1}H NMR ($CDCl_3$, 200 MHz) δ 1.6-2.0 (4H), 3.33 (t, 2H, J = 6.5 Hz), 3.65 (t, 2H, J = 6.0 Hz), 5.43 (s, 2H), 7.3 - 7.6 (4H), 8.0 (m. 2H), 8.3 - 8.5 (3H) ppm.

References

1. J. M. Lehn, "Supramolecular Chemistry," VCH, Weinheim (1995).
2. N. Zimmerman, J. S. Moore and S. C. Zimmerman, *Chemistry & Industry*, **1998**, 604.
3. P. Terech and R. G. Weiss, *Chem. Rev.*, **1997**, *97*, 3133.
4. N. Kimizuka, T. Kawasaki, K. Hirata and T. Kunitake, *J. Am. Chem. Soc.*, **1998**, *120*, 4094.
5. C. He, A. M. Donald, A. C. Griffin, T. Waigh and A. H. Windle, *J. Polym. Sci., Part B: Polym. Phys.*, **1998**, *36*, 1617.
6. H. Kihara, T. Kato, T. Uryu and J. M. J. Frechet, *Chem. Mater.*, **1998**, *120*, 6761.
7. R. P. Sijbesma, F. H. Beijer, L. Brunsveld, B. J. B. Folmer, J. H. K. Hirschberg, R. G. M. Lange, J. K. L. Lowe and E. W. Meijer, *Science*, **1997**, 1601.
8. B. J. B. Folmer, E. Cavini, R. P. Sijbesma and E. W. Meijer, *Chem. Commun.*, **1998**, 1847.
9. F. H. Beijer, R. P. Sijbesma, H. Koojiman, A. L. Spek and E. W. Meijer, *J. Am. Chem. Soc.*, **1998**, *120*, 6761.
10. B. J. B. Folmer, R. P. Sijbesma, H. Kooijman, A. L. Spek, and E. W. Meijer, *J. Am. Chem. Soc.*, **1999**, *121*, 9001.
11. S. H. M. Söntjens, R. P. Sijbesma, M. H. P. van Genderen and E. W. Meijer, *J. Am. Chem. Soc.*, **2000**, *122*, 7487.
12. A, P. H. J. Schenning, P. Jonkheijm, E. Peeters, and E. W. Meijer, *J. Am. Chem. Soc.*, **2001**, *123*, 409.
13. S. H. M. Sontjens, R. P. Sijbesma, M. H. P. van Genderen, and E. W. Meijer, *Macromolecules*, **2001**, *34*, 3815.
14. M. S. Vollmer, T. D. Clark, C. Steinem, and M. R. Ghadiri., *Angew. Chem.*

Int. Ed., **1999**, *38*, 1598.

15. D. Voet and J. G. Voet , "Biochemistry," John Wiley & Sons (1995).
16. S. C. Zimmerman and G. J. Bridges, *J. Am. Chem. Soc.*, **1989**, *111*, 3744.
17. Y. Kyogoku, R. C. Lord and A. Rich, *Biochim. Biophys. Acta*, **1969**, *179*, 10.
18. M. T. Rispens, L. Sánchez, J. Knol, and J. C. Hummelen, *Chem. Commun.*, **2001**, 161.
19. J. J. González, S. González, E. M. Priego, C. Luo, D. M. Guldi, J. de Mendoza, and N. Martin, *Chem. Commun.*, **2001**, 163.
20. G. J. Kavaronos, "Fundamentals of Photoinduced Electron Transfer", VCH Publishers (1993); G. L. Kavarnos and N. J. Turro, *Chem. Rev.*, **1986**, *86*, 401.
21. J. L. Sessler, M. Sathiosatham, C. T. Brown, T. A. Rhodes, and G. Wiederrecht, *J. Am. Chem. Soc.*, **2001**, *123*, 3655.
22. M. Ikegami and T. Arai, *Chem. Lett.*, **2001**, 694.
23. J. B. Birks, "Photophysics of Aromatic Molecules," Wiley-Interscience (1970).
24. K. Ichimura, S. K. Oh, and M. Nakagawa, *Science*, **2000**, *288*, 5471.
25. D. M. Junge and D. V. McGrath, *Chem. Commun.*, **1997**, 857.
26. T. Asano, T. Okada, S. Shinkai, K. Shigematsu, Y. Kosano, and O. Manabe, *J. Am. Chem. Soc.*, **1981**, *103*, 5161.

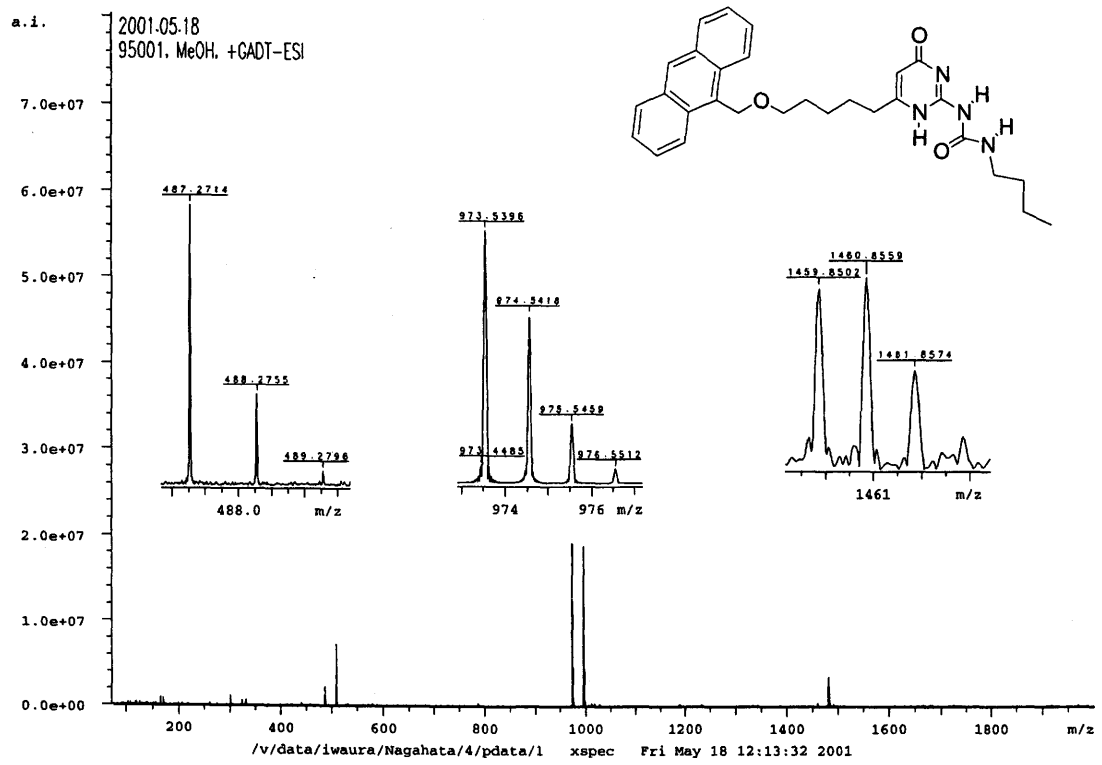

Figure 1a. ESI-MS spectrum of **1d**.

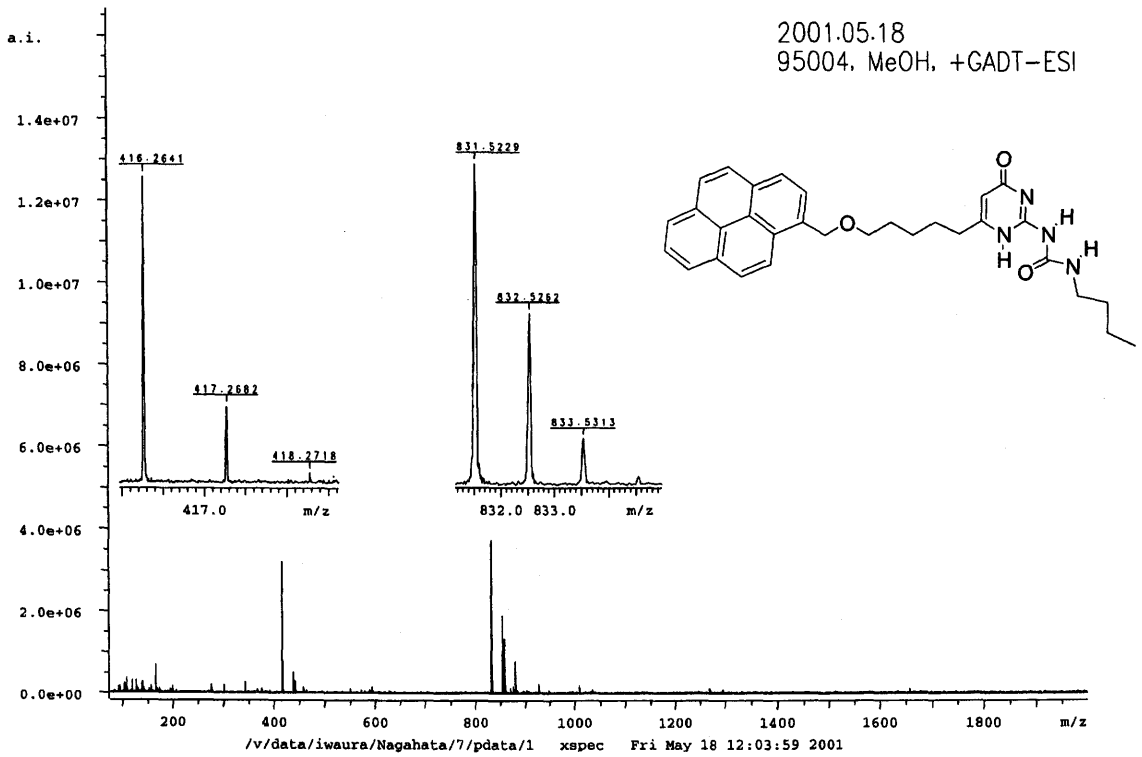

Figure 1b. ESI-MS spectrum of **1e**.

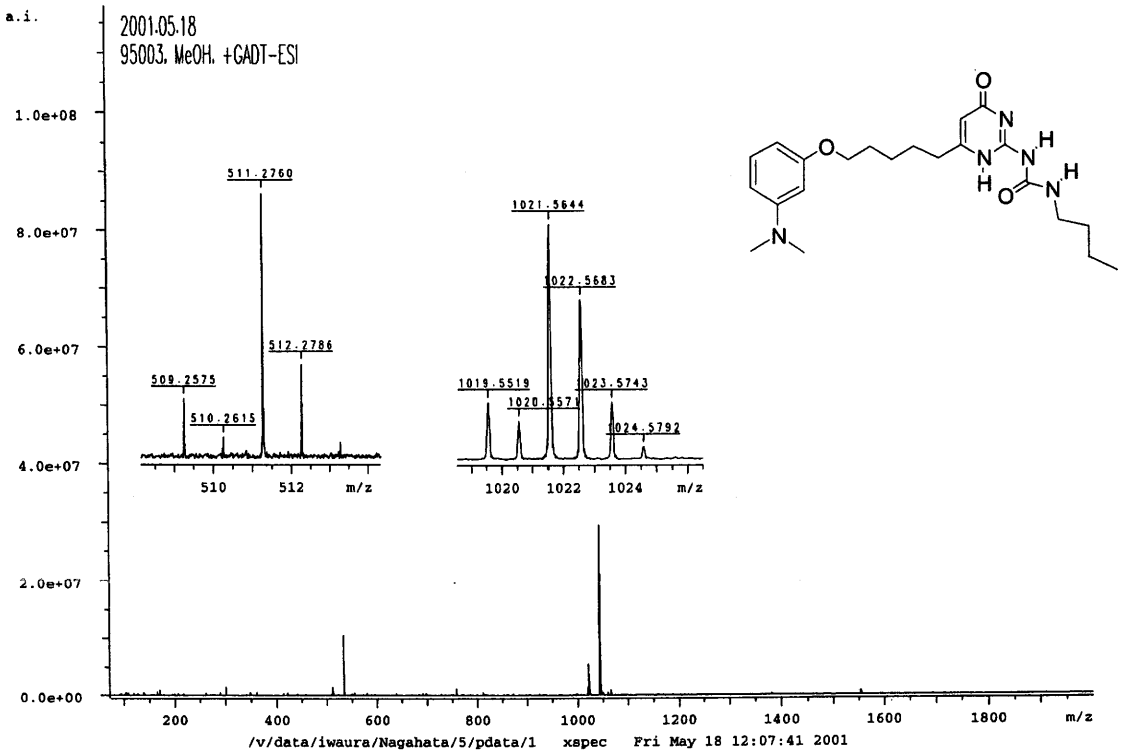

Figure 1c. ESI-MS spectrum of **2c**.

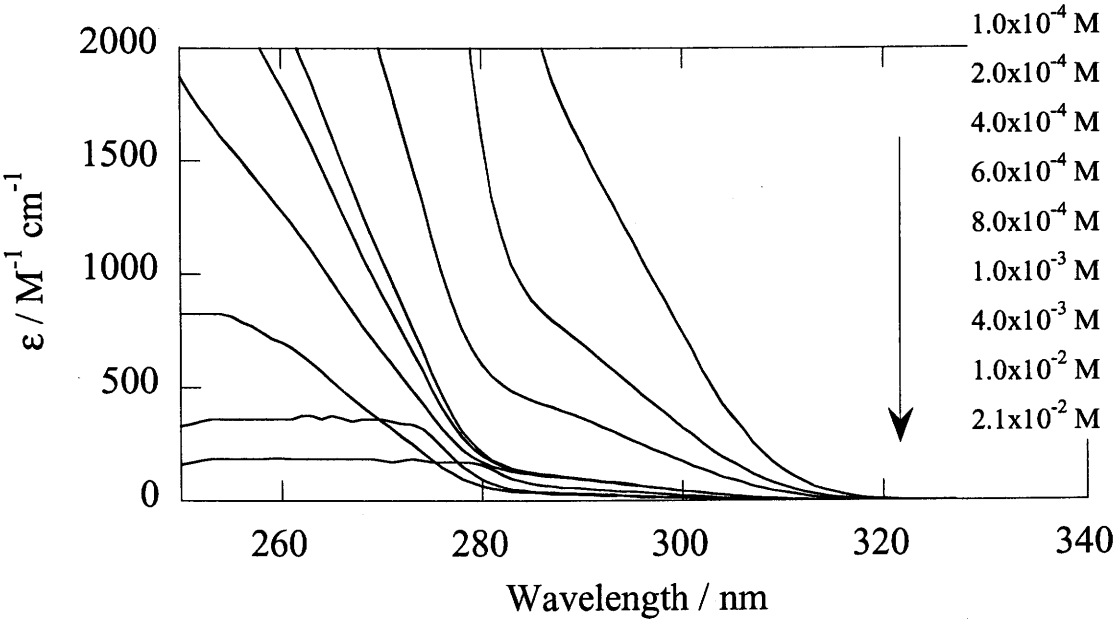

Figure 2. The concentration dependence of absorption spectrum of **1a**.

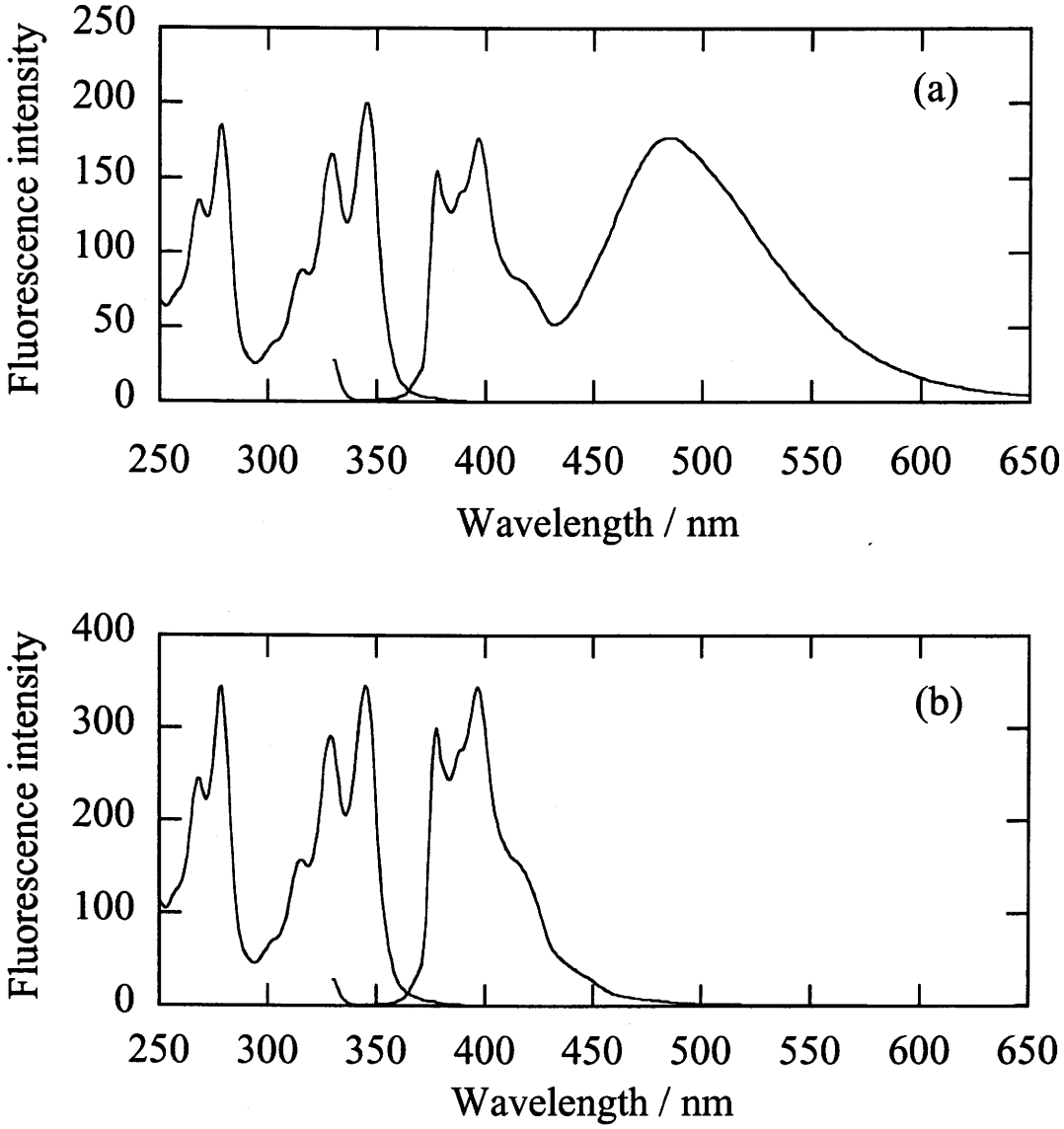

Figure 3. Fluorescence spectra of **1e** (a) and **11** (b) in chloroform at the concentration of 1.0x 10^{-5} M.

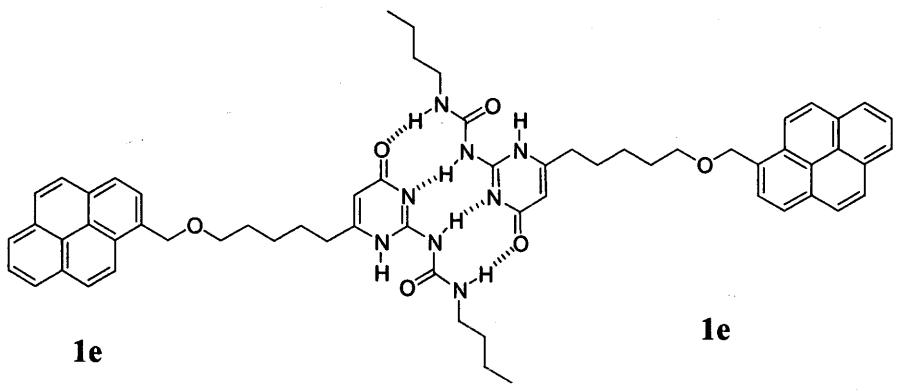

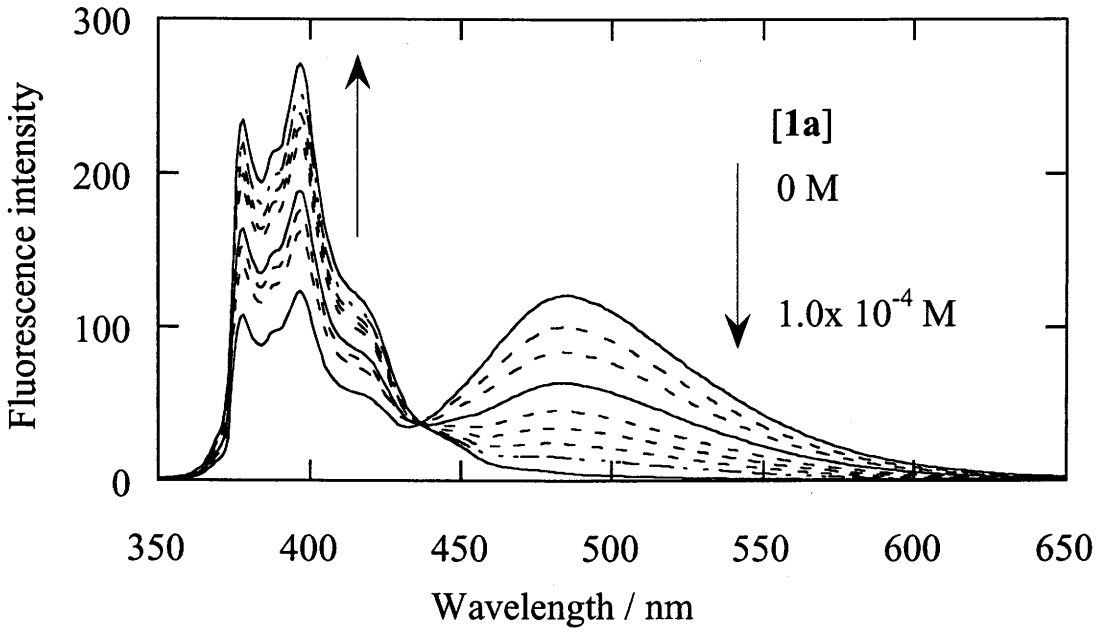

Figure 4. Fluorescence spectrum of **1e** (1.0×10^{-5} M) in the presence of various concentrations of **1a**.

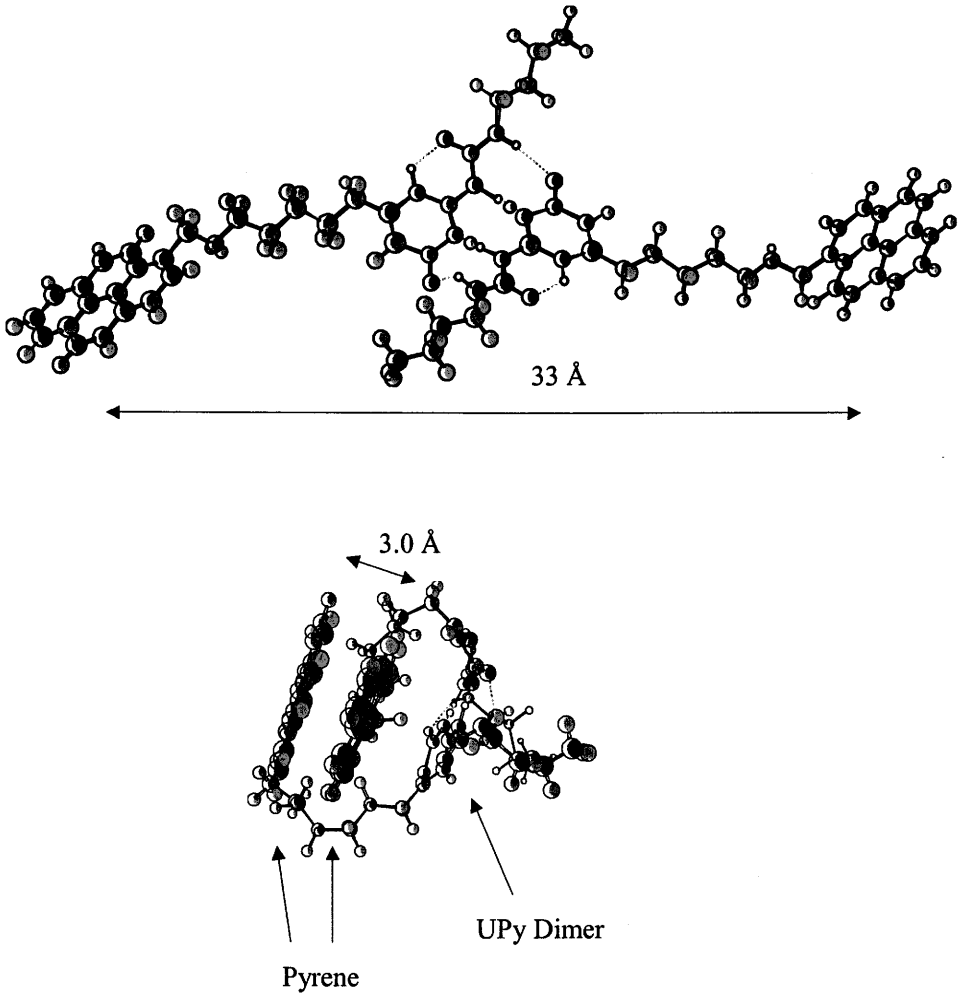

Figure 5. 3D structures of **1e** dimer. top: extended form. bottom: congested form.

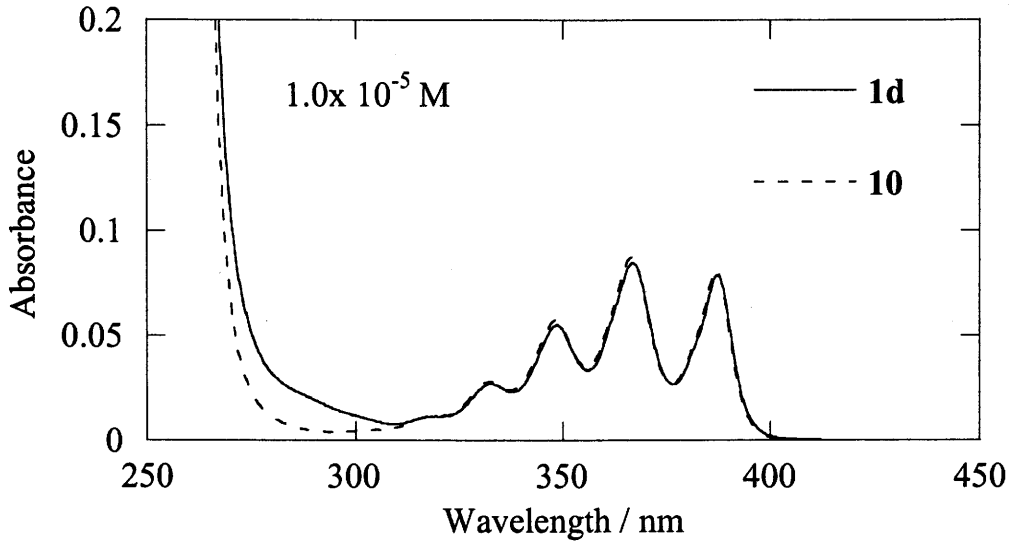

Figure 6. Absorption spectra of **1d** and **10** at the concentration of 1.0x 10^{-5} M in chloroform.

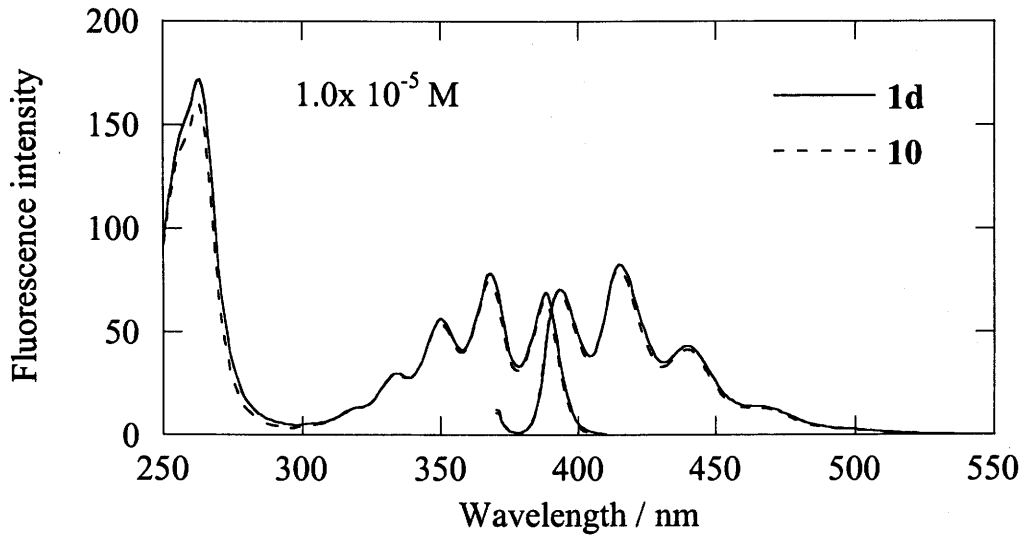

Figure 7. Fluorescence and fluorescence excitation spectra of **1d** and **10** in chloroform.

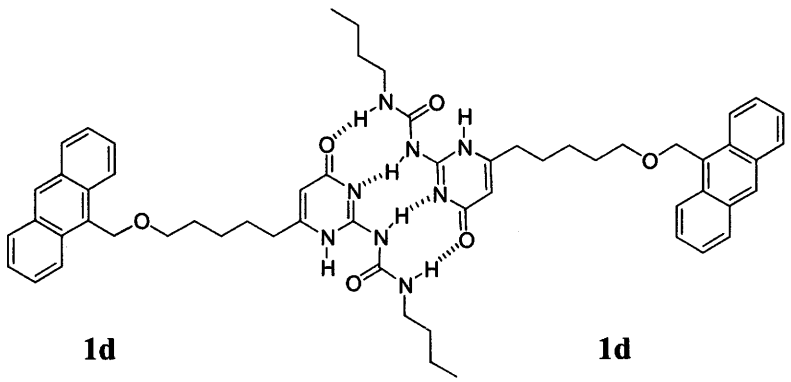

1d **1d**

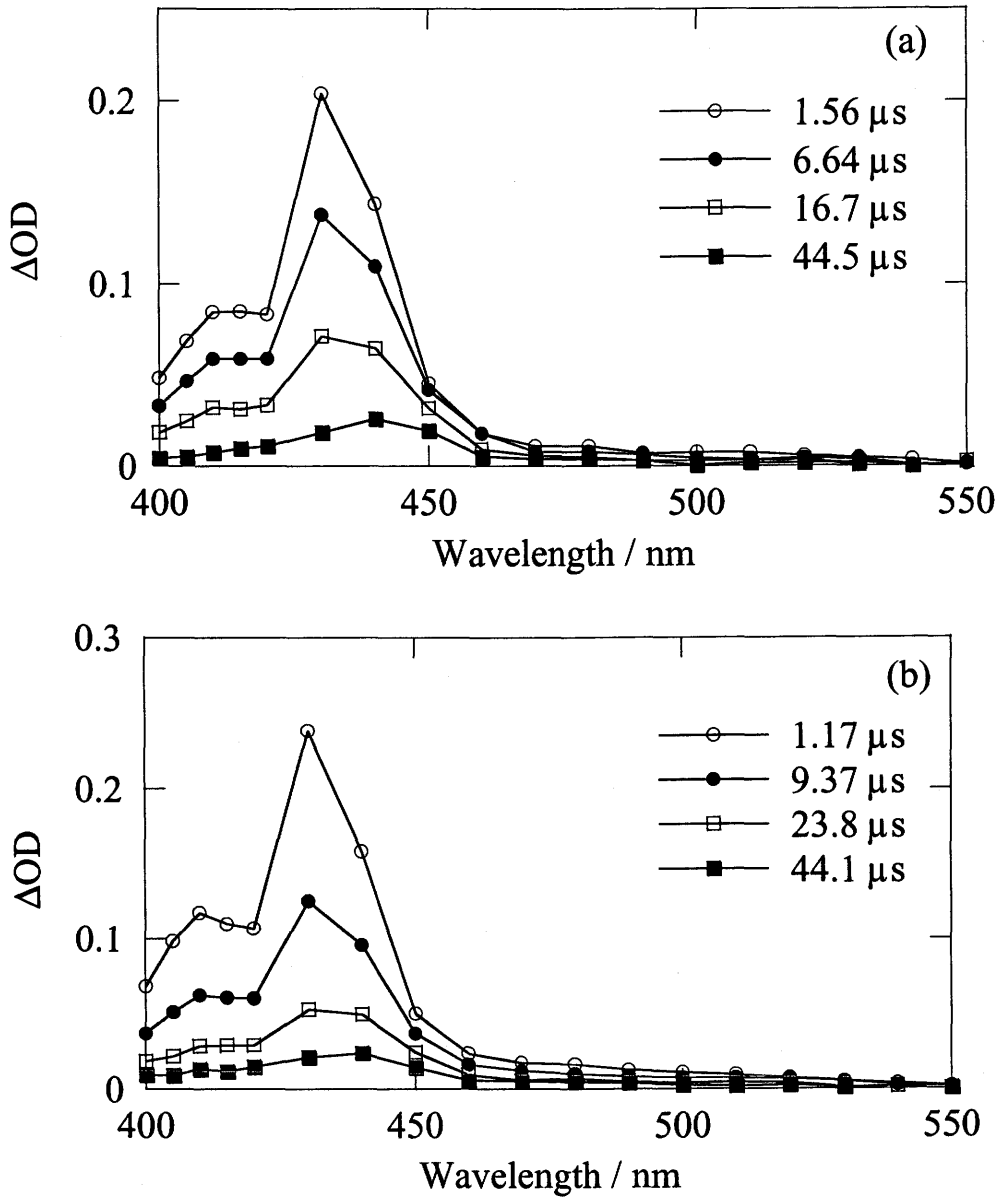

Figure 8. Transient absorption spectra of **10** (1.0x 10^{-4} M) (a) and **1d** (1.0x 10^{-4} M) (b) in chloroform under argon.

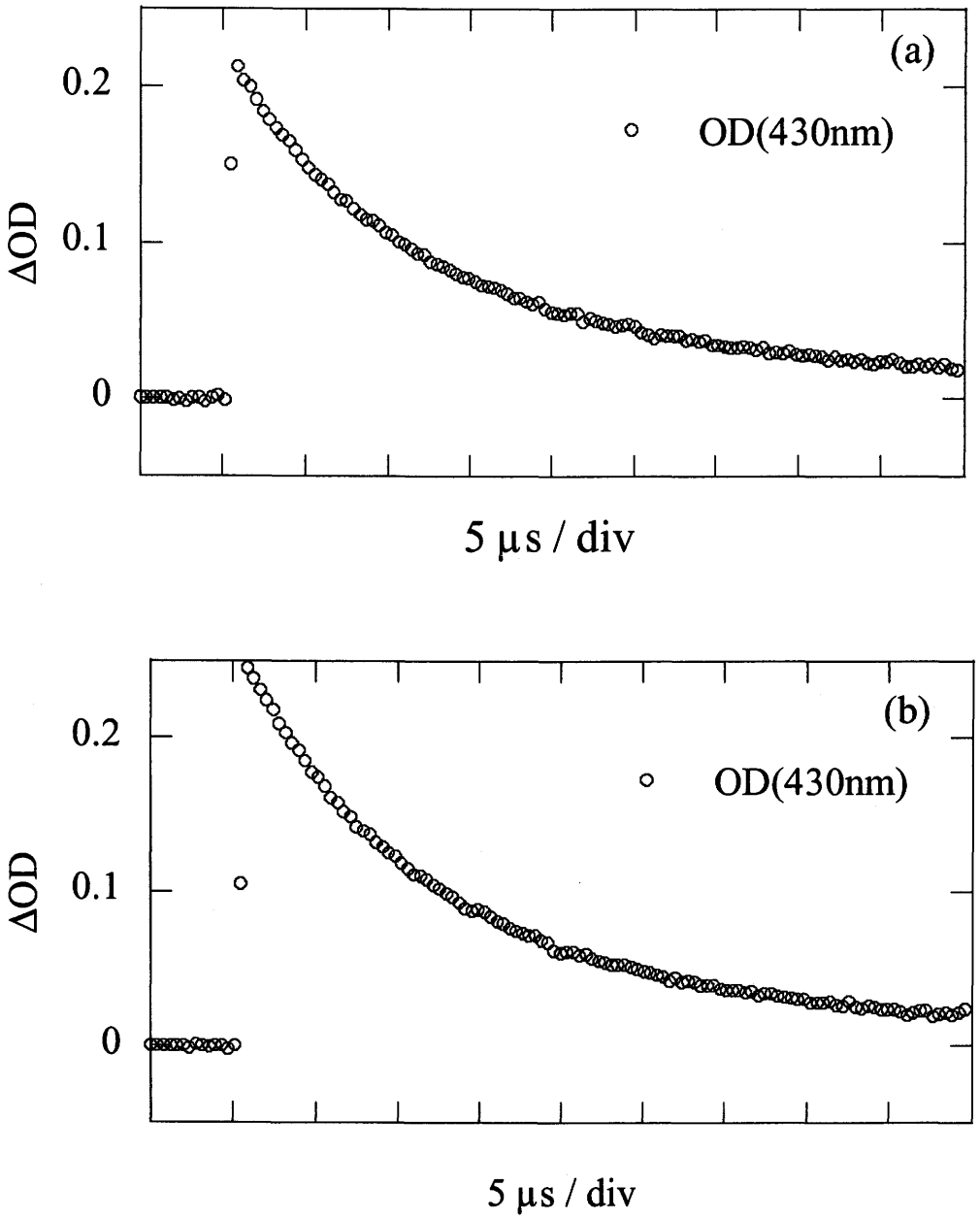

Figure 8-2. Decay profiles at 430 nm of the transient absorption spectra of **10** (1.0×10^{-4} M) (a) and **1d** (1.0×10^{-4} M) (b).

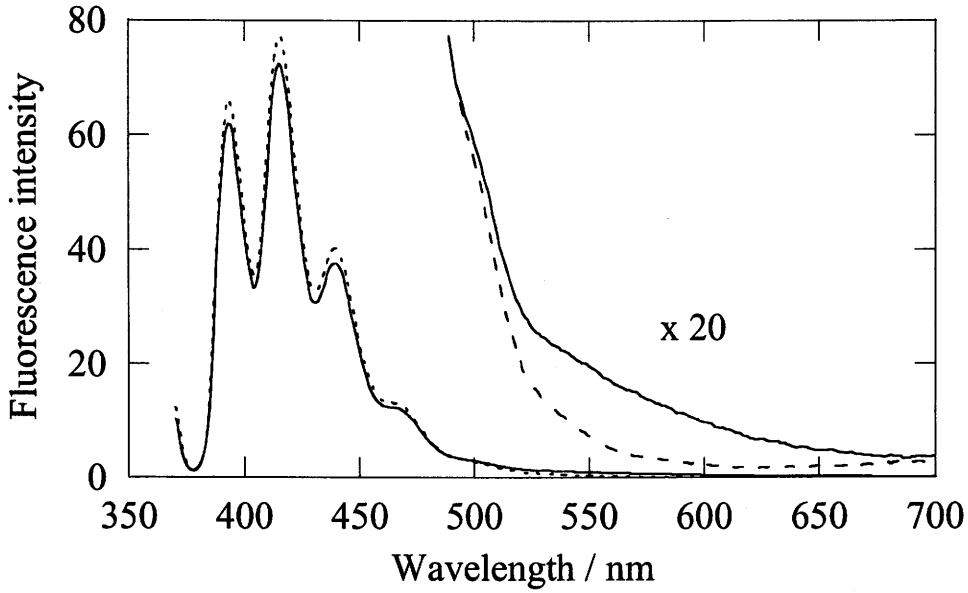

Figure 9. Fluorescence spectra of **1d** (1.0×10^{-5} M) in the absence of **2c** (dashed line) and in the presence of **2c** (1.0×10^{-5} M) (solid line).

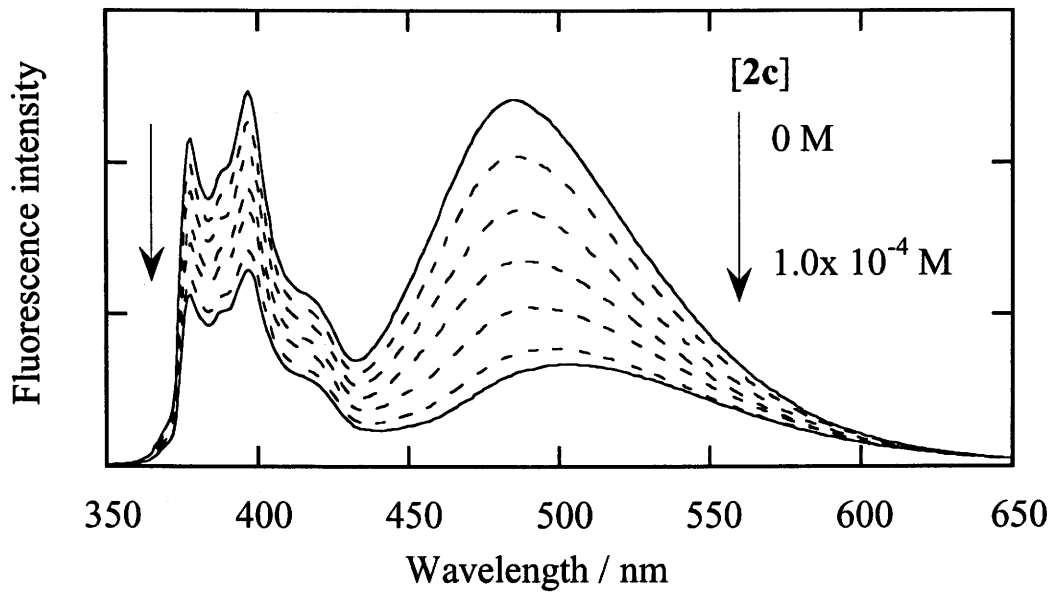

Figure 10. The change of fluorescence spectrum of **1e** (1.0×10^{-5} M) by the addition of **2c** from 0 M to 1.0×10^{-4} M on excitation at 335 nm.

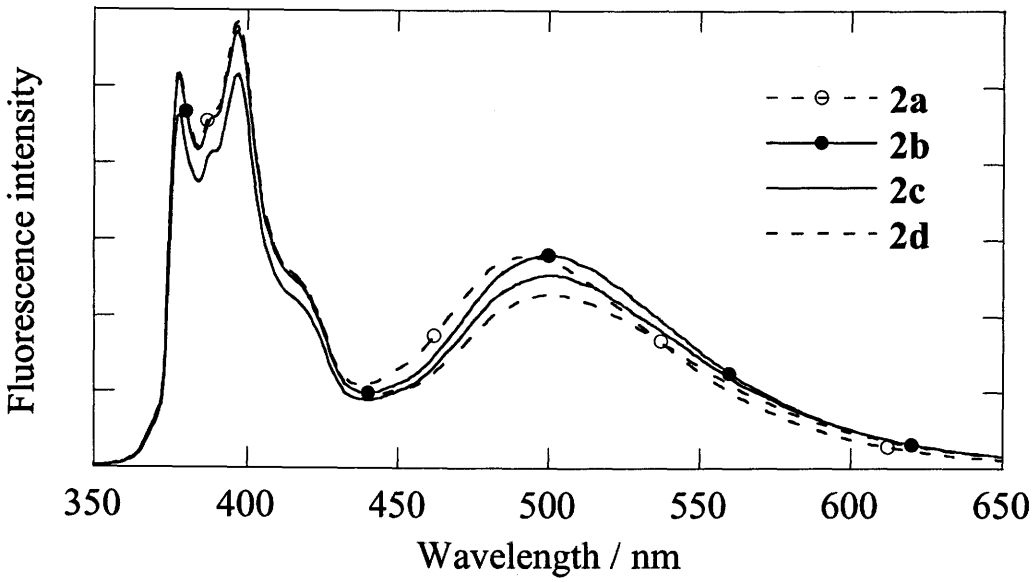

Figure 11. The chain length dependence of the exciplex emission between **1e** (1.0×10^{-5} M) and **2** (1.0×10^{-4} M) on excitation at 335 nm.

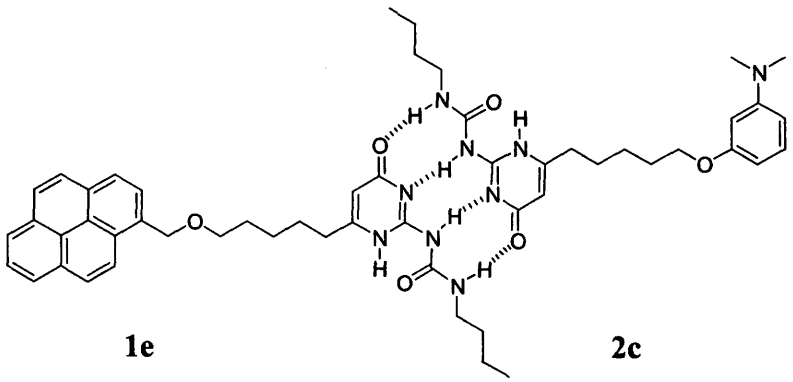

1e **2c**

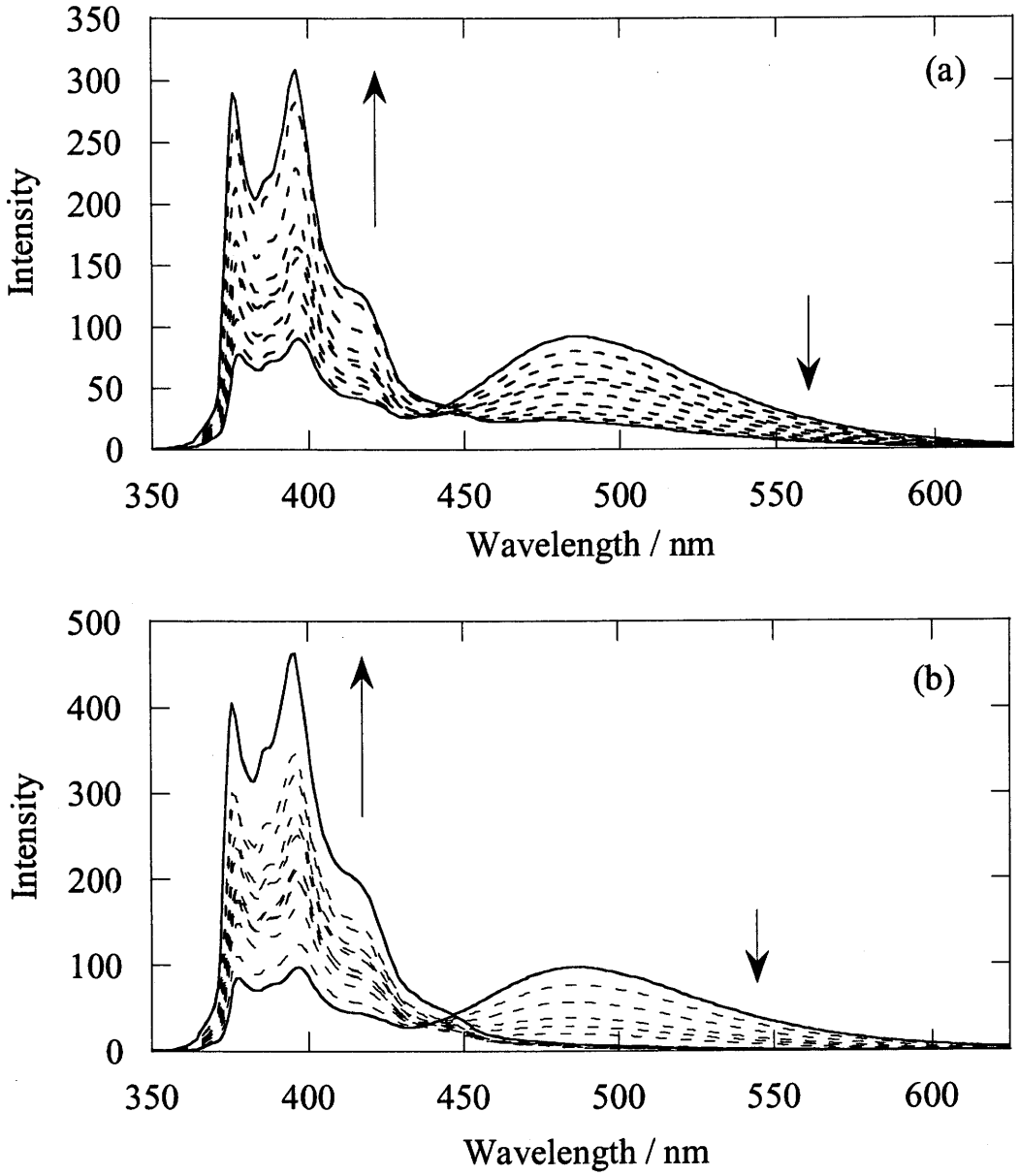

Figure 12. The change of fluorescence spectrum of **1e** (1.0×10^{-5} M) by the addition of acetonitrile (a) or methanol (b) in chloroform.

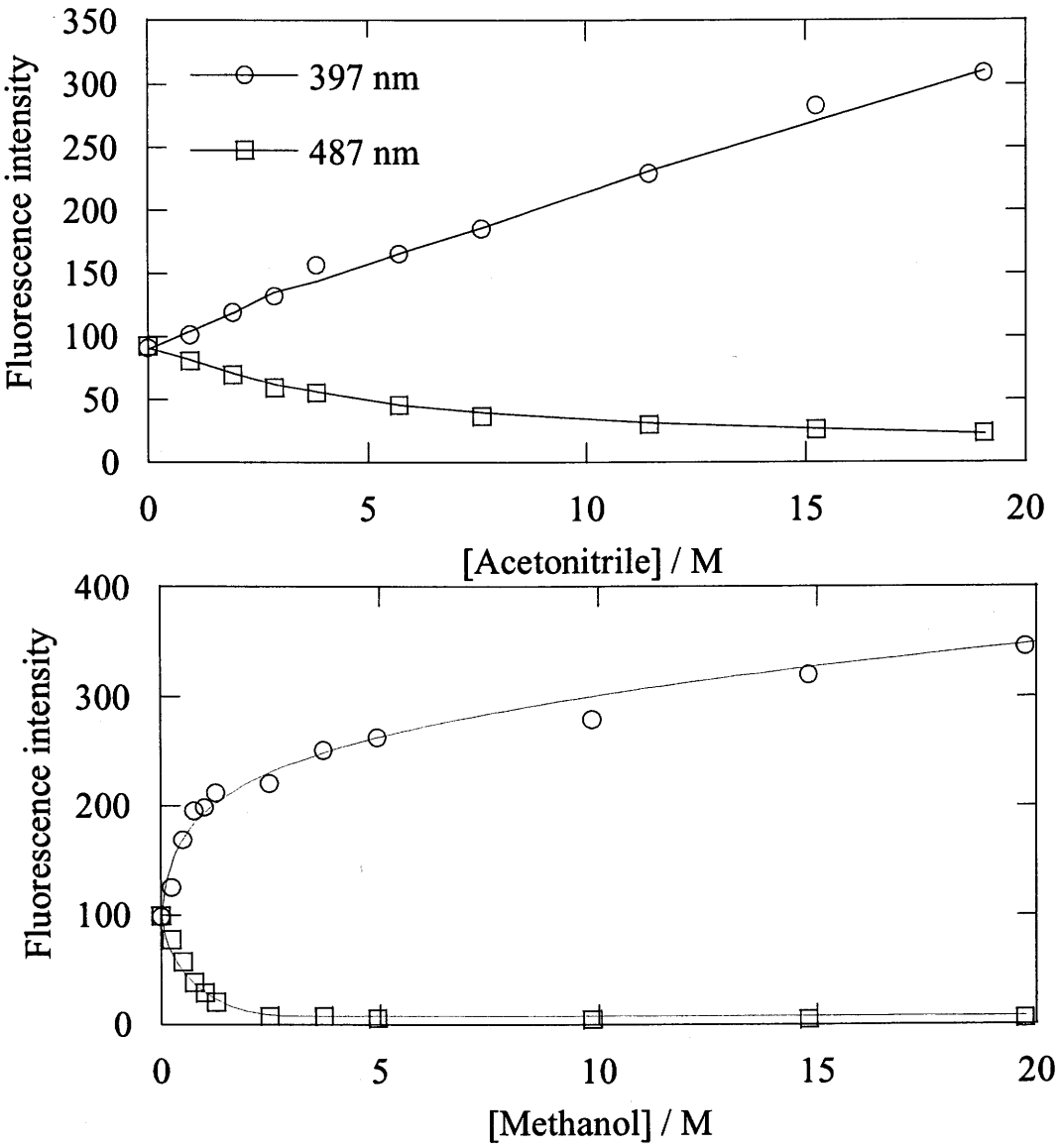

Figure 13. The change of fluorescence intensity of **1e** (1.0×10^{-5} M) at 397 nm and 487 nm dependent on the concentration of acetonitrile (up) and methanol (bottom) in chloroform.

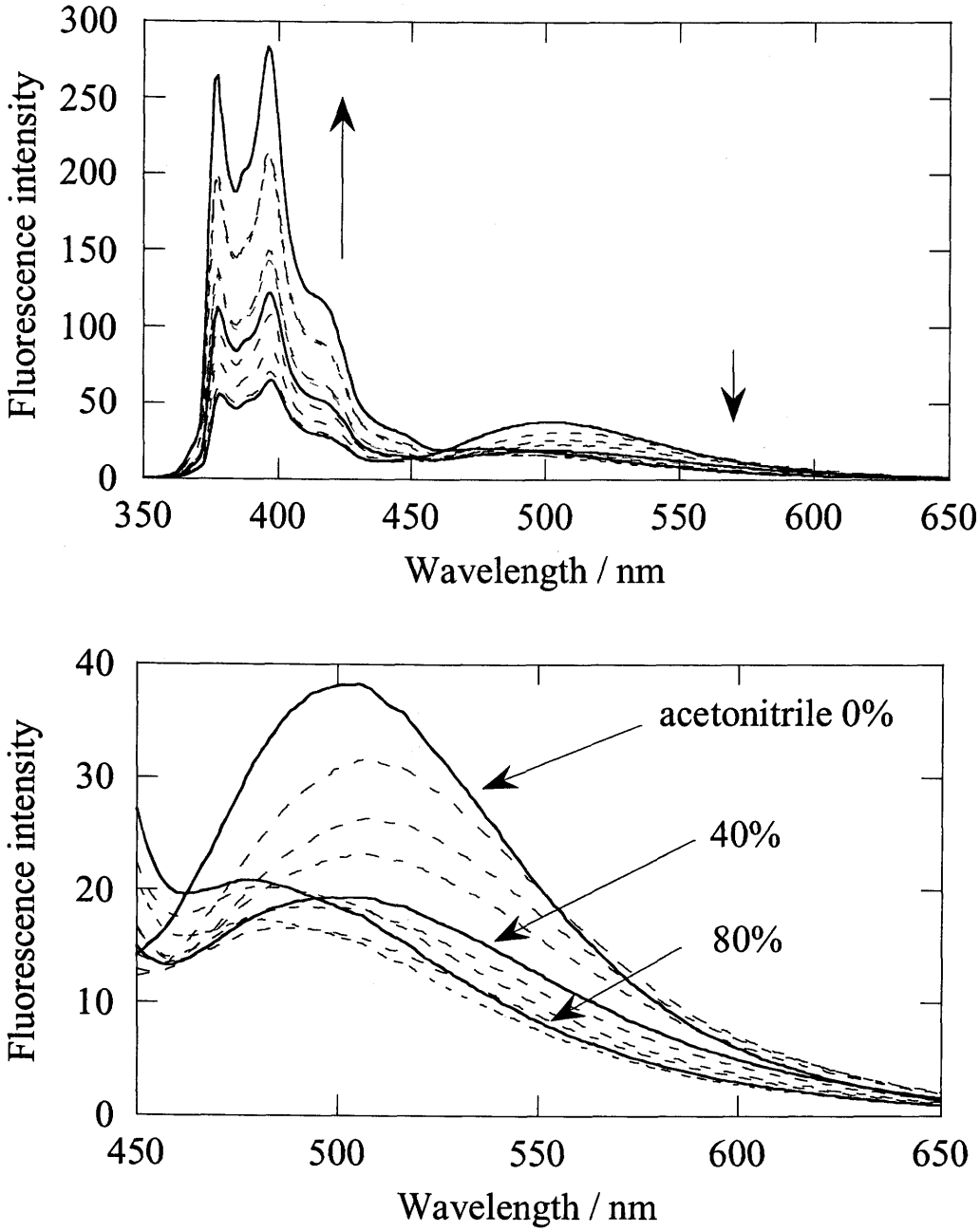

Figure 14. The change of fluorescence spectrum of **1e** (1.0×10^{-5} M) in the presence of **2c** (1.0×10^{-4} M) by the addition of acetonitrile in chloroform.

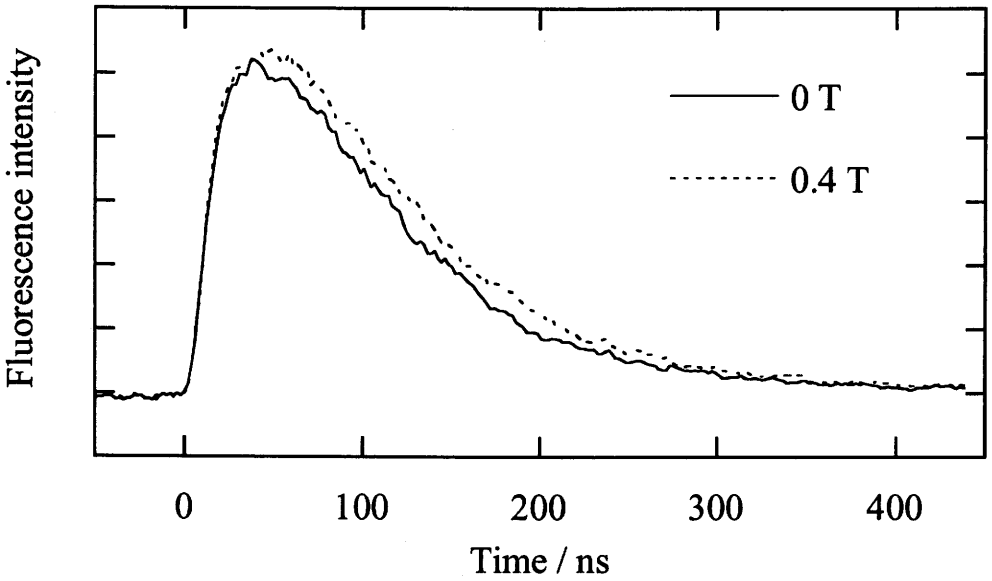

Figure 15. Magnetic field effect on the decay curve of exciplex emission observed at 550 nm between **1e** (1.0×10^{-5} M) and **2c** (1.0×10^{-4} M) in a 60/40 (v/v) mixture of chloroform and acetonitrile.

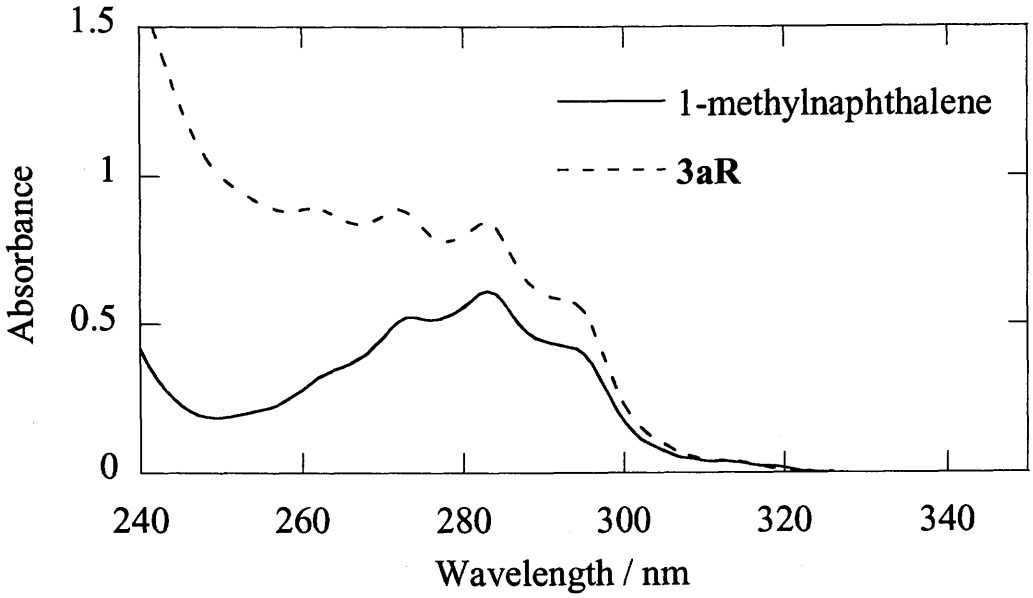

Figure 16. Absorption spectra of 1-methylnaphthalene and **3aR** at the concentration of 1.0x 10^{-4} M in chloroform.

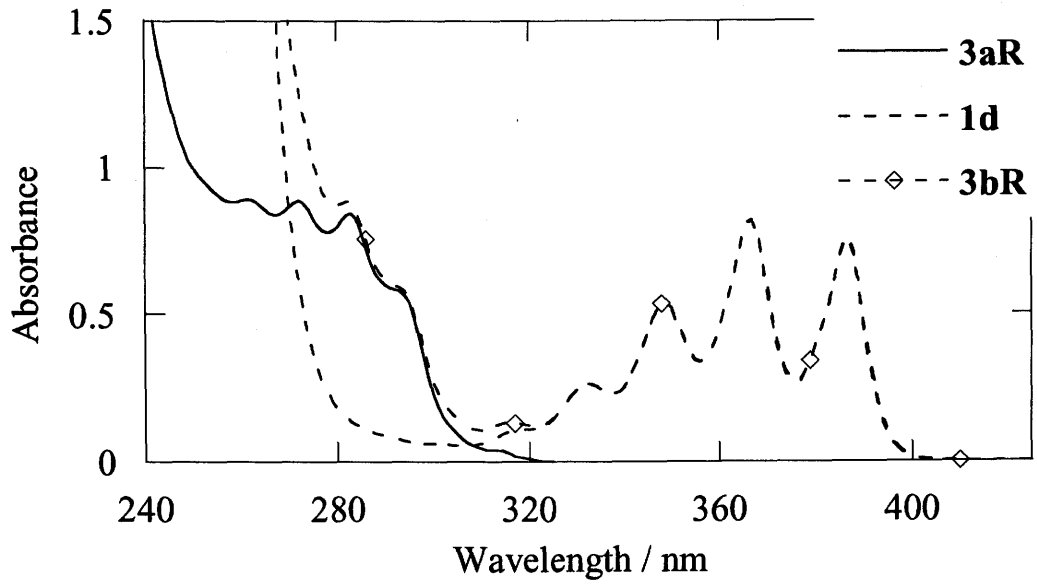

Figure 17. Absorption spectra of **3aR**, **1d** and **3bR** at the concentration of 1.0x 10^{-4} M in chloroform.

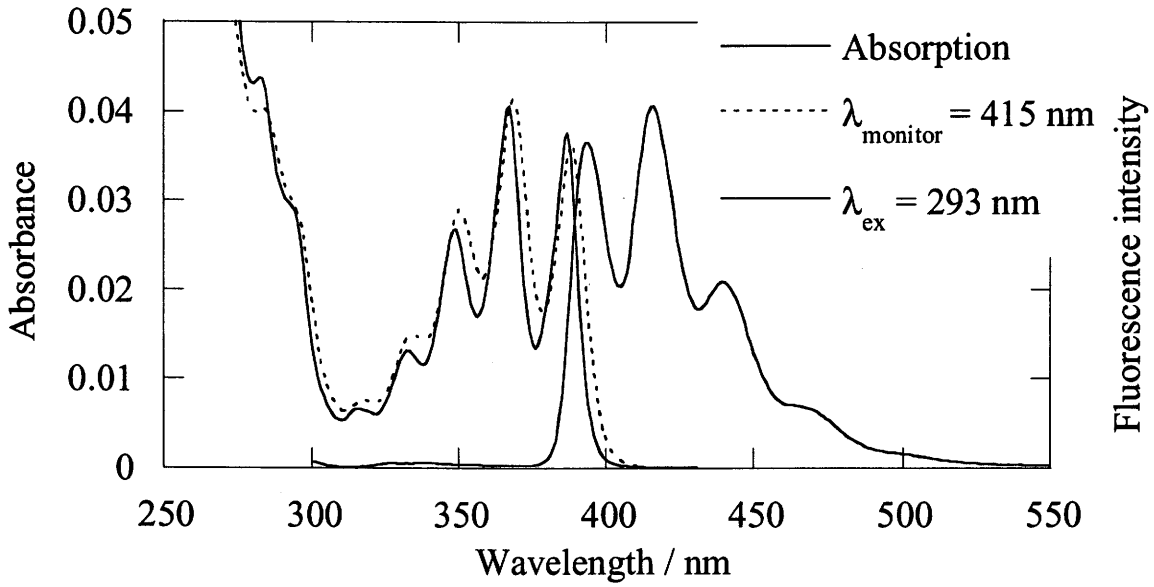

Figure 18. Absorption, fluorescence and fluorescence excitation spectra of **3bR** in chloroform.

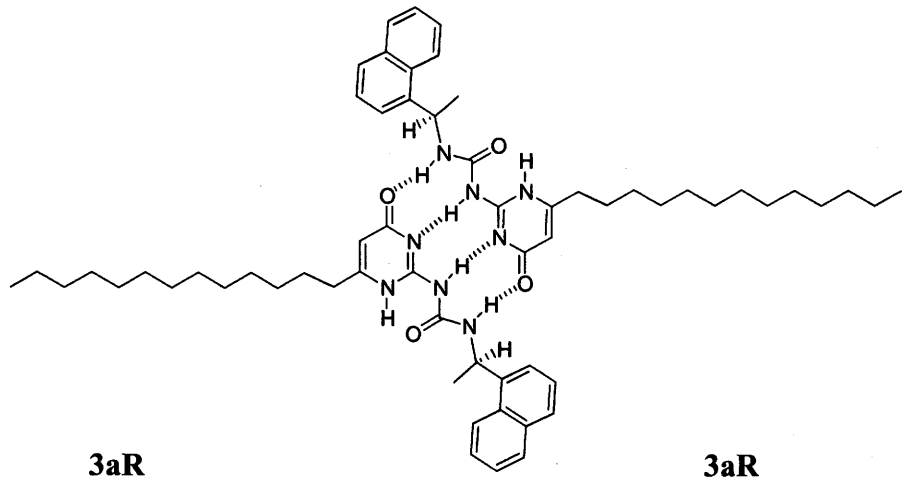

3aR **3aR**

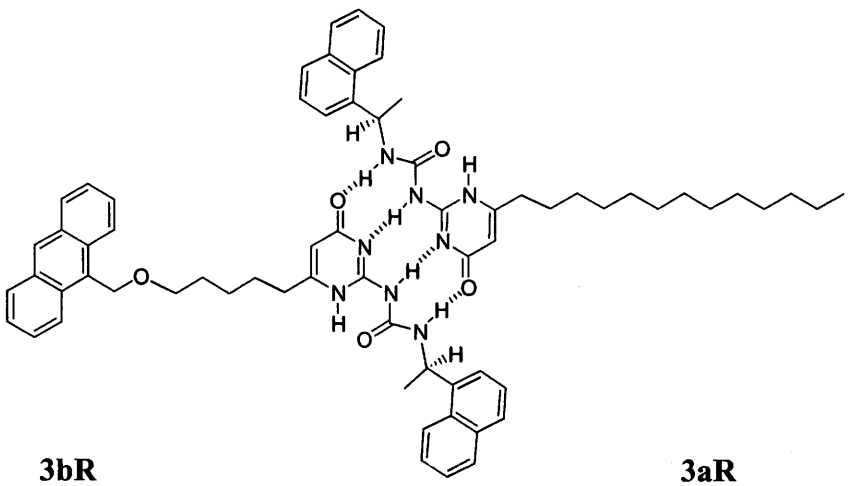

3bR **3aR**

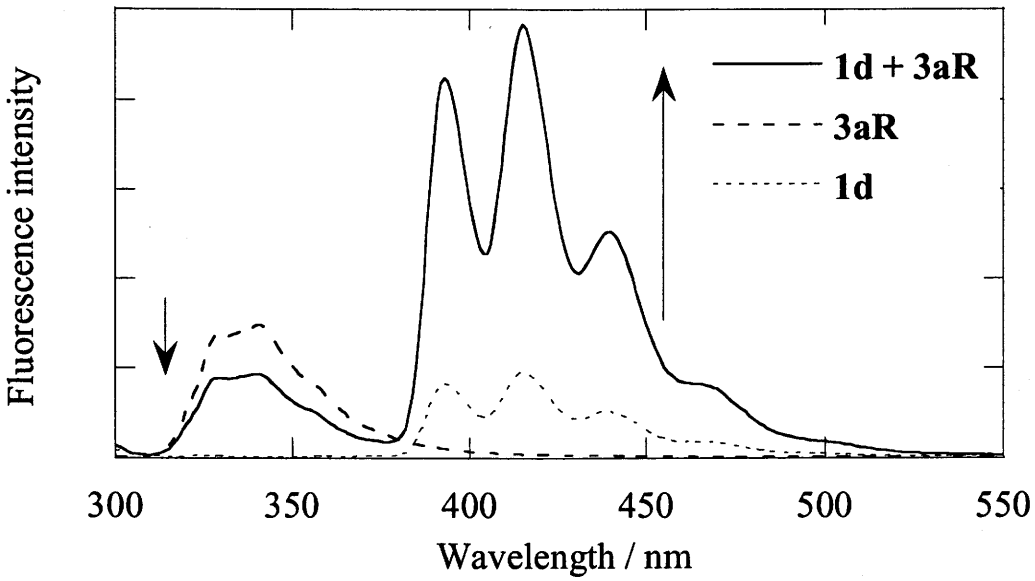

Figure 19. Fluorescence spectrum of **1d** (1.0x 10^{-5} M) in the absence of (dotted line) and in the presence of **3aR** (1.0x 10^{-5} M) (solid line) and fluorescence spectrum of **3aR** (1.0x 10^{-5} M) (dashed line) in chloroform on excitation at 293 nm.

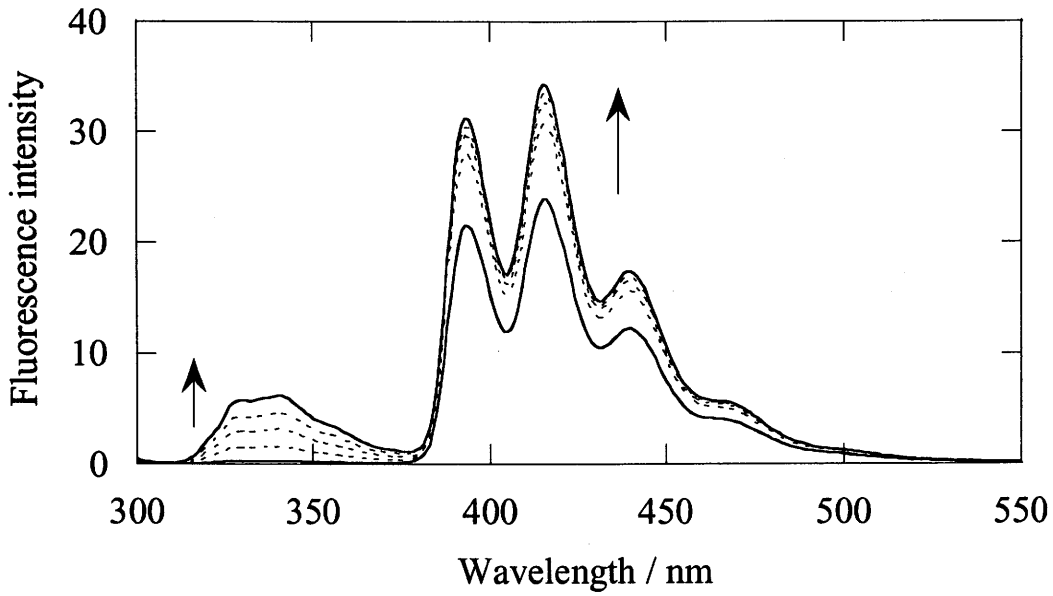

Figure 20. The change of fluorescence spectrum of **3bR** (1.0x 10^{-5} M) by the addition of **3aR** (0, 5.0x 10^{-6}, 1.0x 10^{-5}, 1.5x 10^{-5}, and 2.0x 10^{-5} M) on excitation at 293 nm.

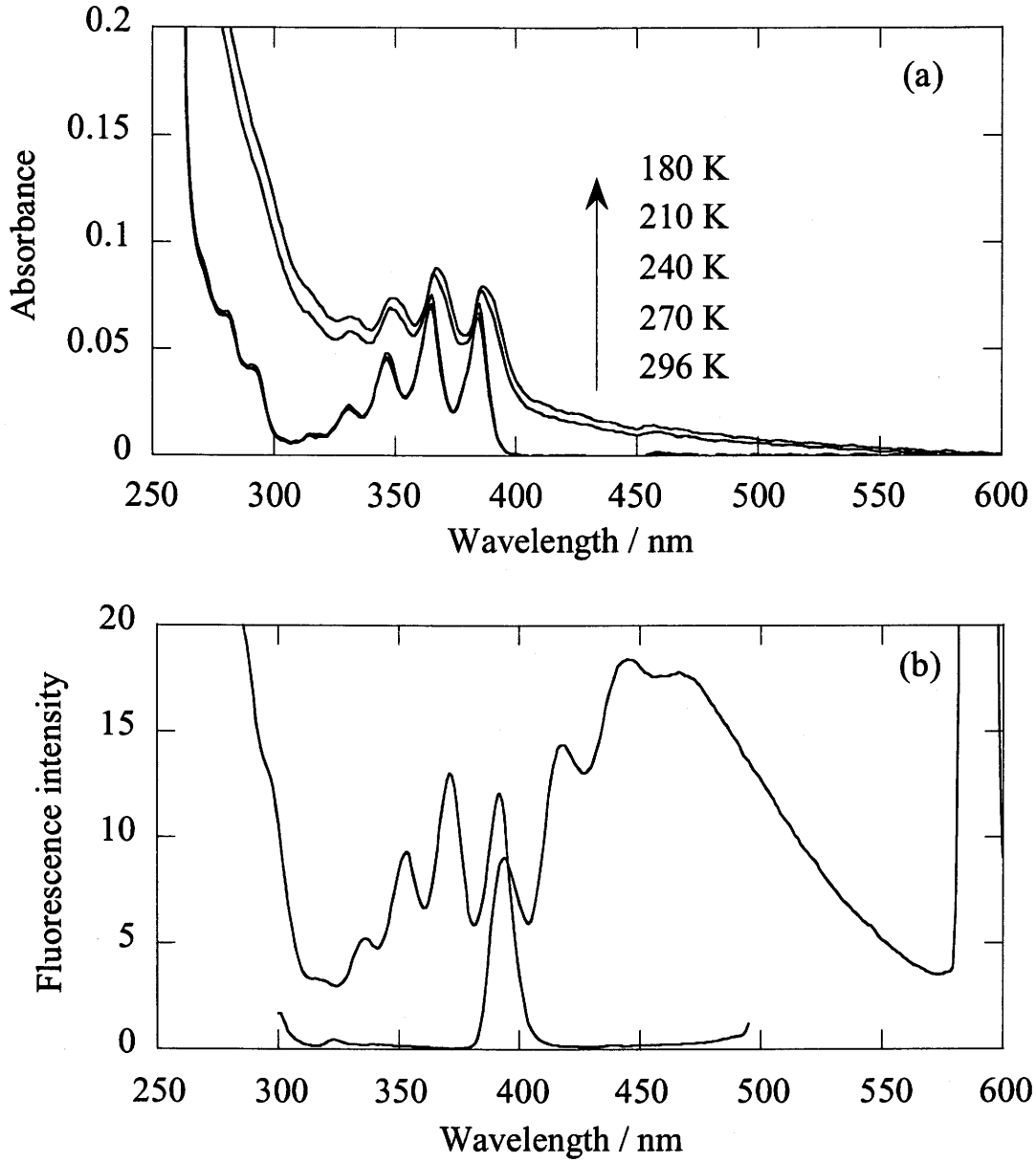

Figure 21. (a) Temperature dependence of absorption spectrum of **3bR** (5.0x 10^{-6} M) in methylcyclohexane. (b) Fluorescence (λ_{ex} = 293 nm) and fluorescence excitation ($\lambda_{monitor}$ = 500 nm) spectra of **3bR** in methylcyclohexane at 180 K.

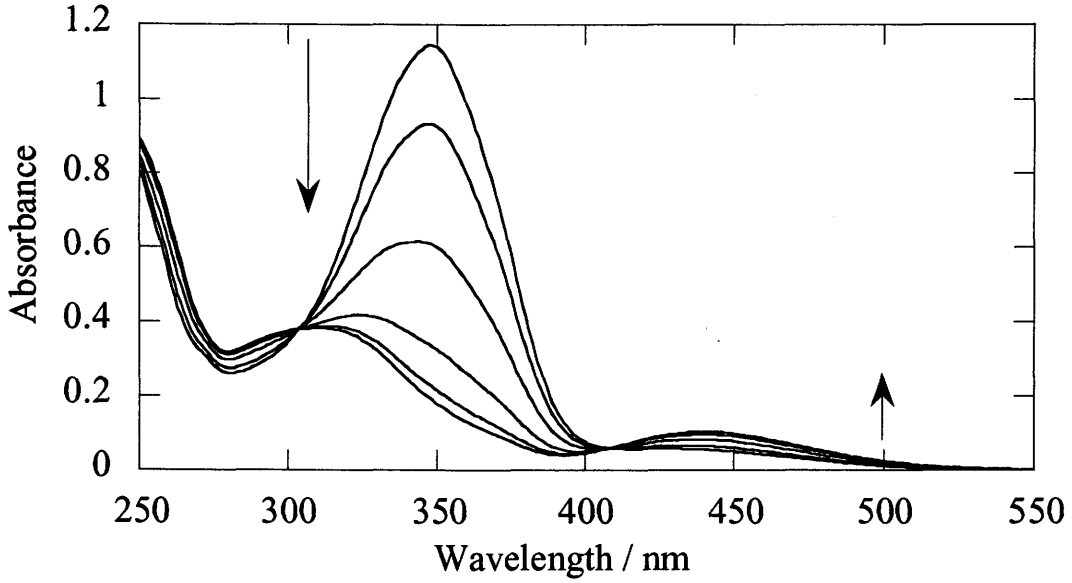

Figure 22. The change of absorption spectrum of **1c** (5x 10^{-4} M) on irradiation at 366 nm in chloroform.

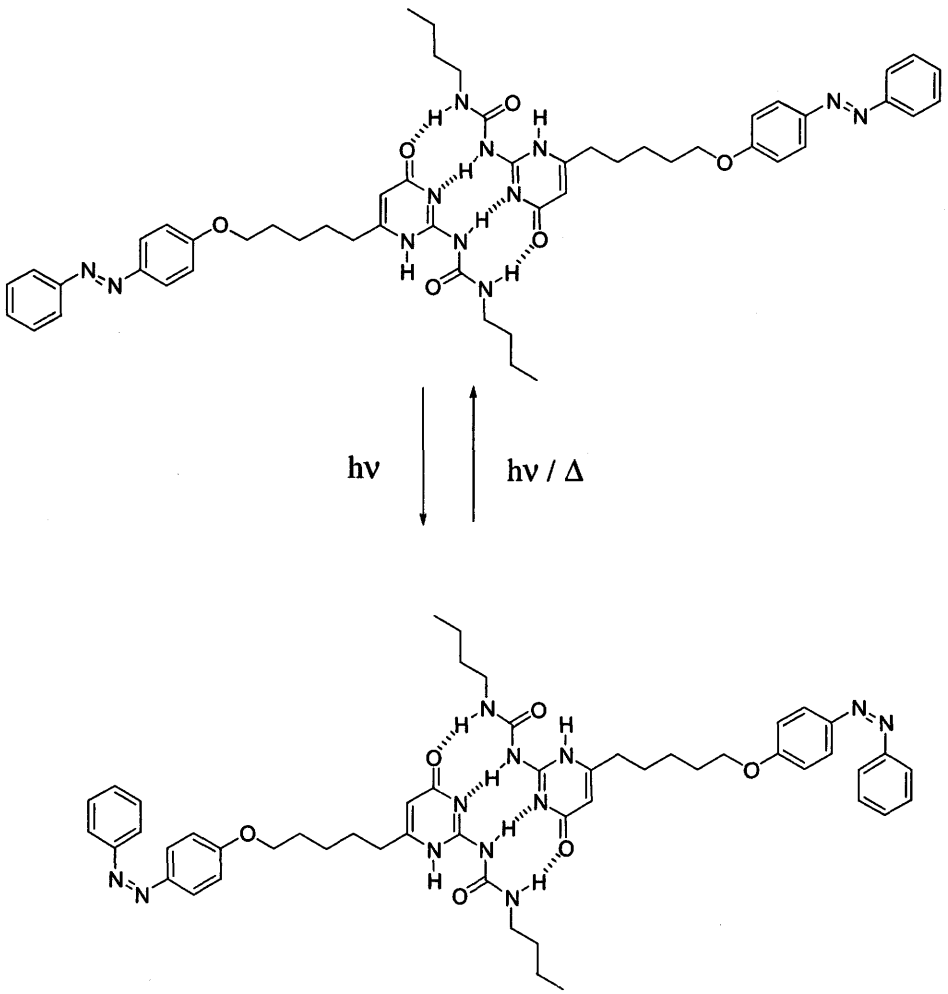

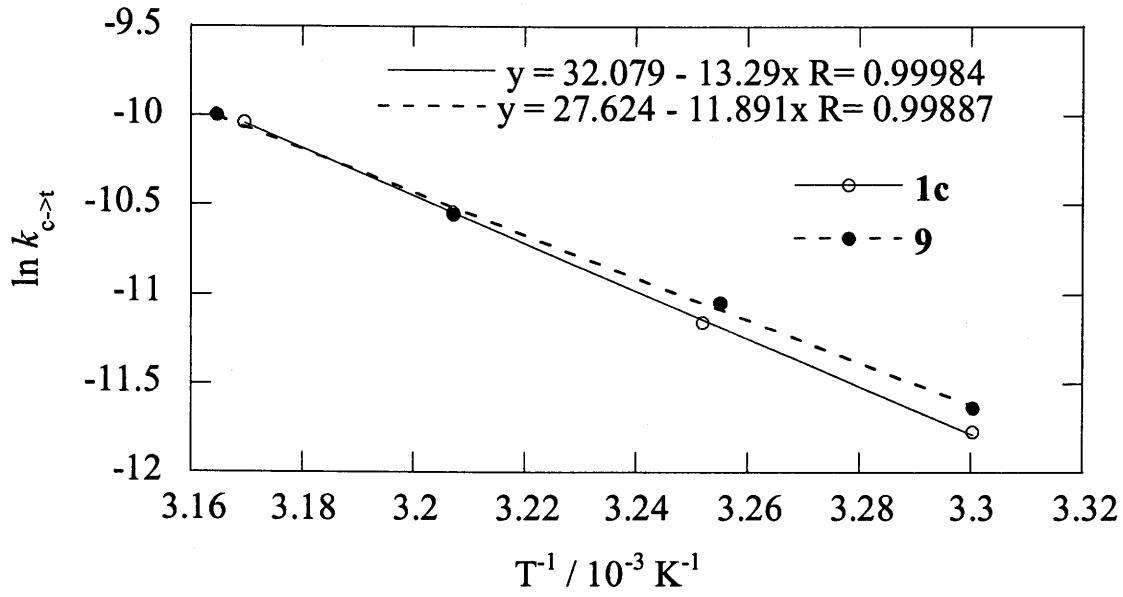

Figure 23. Arrhenius plot for cis-to-trans isomerization of **1c** and **9** in chloroform.

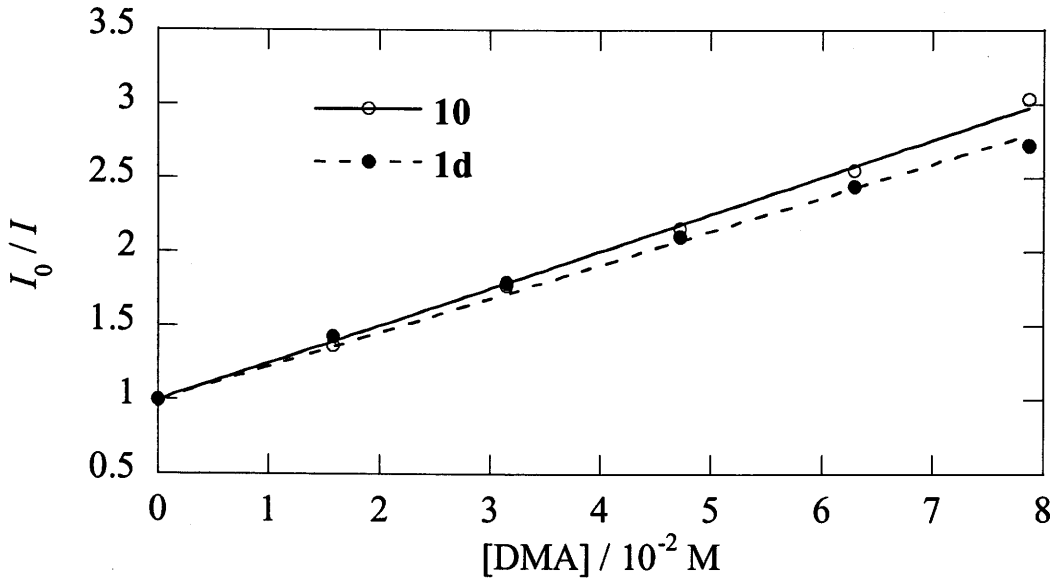

Figure 24. Stern-Volmer plot for the fluorescence quenching of **1d** and **10** by *N,N*-dimethylaniline (DMA).

Table 1. Concentrations of homo dimer (**3bR-3bR**) and hetero dimer (**3aR-3bR**) in the binary solution of **3aR** and **3bR** and fluorescence intensity at 415 nm on excitation at 293 nm (I_{obs}) and fluorescence intensity derived from hetero dimer (I_{hetero})

[3aR][a)]	[3bR-3bR][a),c)]	[3aR-3bR][a),c)]	I_{obs}	I_{hetero}[d)]
0	2.50	0	23.9(= I^0)	0
2.5	1.67	1.67	28.2	12.3
5.0	1.25	2.50	30.7	18.8
10	0.83	3.33	32.6	24.7
15	0.63	3.75	33.5	27.5
20	0.50	4.00	34.3	29.6

a) in 10^{-6} M b) The concentration of **3bR** was kept constant at 5.0x 10^{-6} M.
c) calculated from eq. 1. d) calculated from eq. 2.

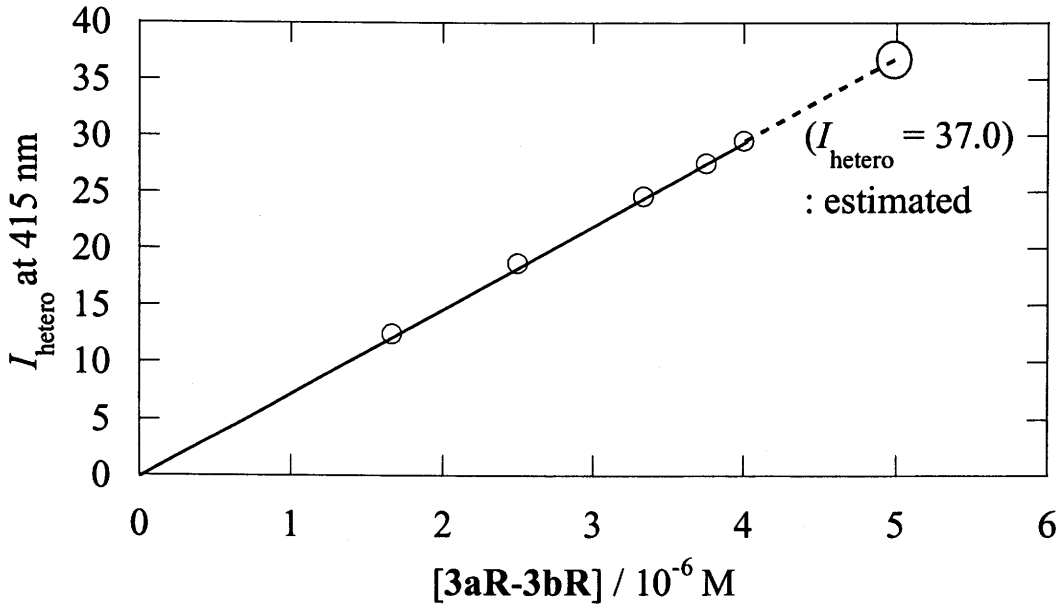

Figure 25. The plot for fluorescence intensity at 415 nm vs. the concentration of hetero dimer, **3aR-3bR**, calculated from equation 1 and 2.

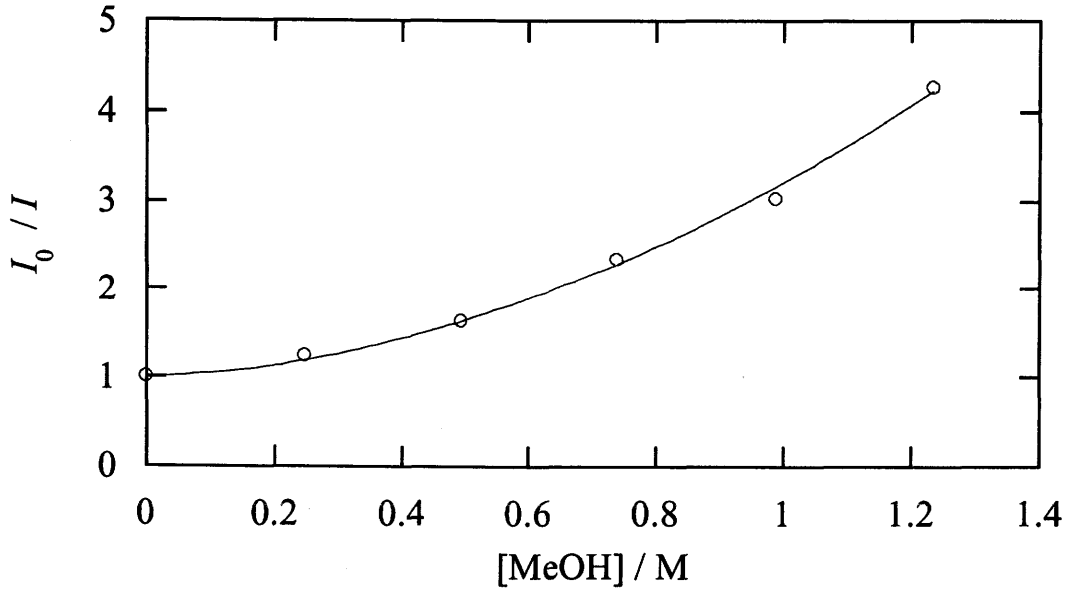

Figure 26. The plot for the inverse of the ratio of exicmer emission quenching vs. the concentrations of methanol.